LEVEL II

12

TECHNICAL REPORT S-78-7

PREDICTING POTENTIAL HEAVE AND HEAVE WITH TIME IN SWELLING FOUNDATION SOILS

by

Lawrence D. Johnson

Geotechnical Laboratory
U. S. Army Engineer Waterways Experiment Station
P. O. Box 631, Vicksburg, Miss. 39180

July 1978
Final Report

Prepared for Office, Chief of Engineers, U. S. Army
Washington, D. C. 20314

Destroy this report when no longer needed. Do not return it to the originator.

Unclassified

SECURITY CLASSIFICATION OF THIS PAGE (When Data Entered)

REPORT DOCUMENTATION PAGE

READ INSTRUCTIONS BEFORE COMPLETING FORM

1. REPORT NUMBER: Technical Report S-78-7

2. GOVT ACCESSION NO.:

3. RECIPIENT'S CATALOG NUMBER:

4. TITLE (and Subtitle): (6) PREDICTING POTENTIAL HEAVE AND HEAVE WITH TIME IN SWELLING FOUNDATION SOILS

5. TYPE OF REPORT & PERIOD COVERED: (9) Final report

6. PERFORMING ORG. REPORT NUMBER:

7. AUTHOR(s): (10) Lawrence D. Johnson

8. CONTRACT OR GRANT NUMBER(s):

9. PERFORMING ORGANIZATION NAME AND ADDRESS:
U. S. Army Engineer Waterways Experiment Station
Geotechnical Laboratory
P. O. Box 631, Vicksburg, Miss. 39180

10. PROGRAM ELEMENT, PROJECT, TASK AREA & WORK UNIT NUMBERS:

11. CONTROLLING OFFICE NAME AND ADDRESS:
Office, Chief of Engineers, U. S. Army
Washington, D. C. 20314

12. REPORT DATE: (11) July 1978

13. NUMBER OF PAGES: 194

14. MONITORING AGENCY NAME & ADDRESS (if different from Controlling Office): (14) WES-TR-S-78-7

15. SECURITY CLASS. (of this report): Unclassified

15a. DECLASSIFICATION/DOWNGRADING SCHEDULE:

16. DISTRIBUTION STATEMENT (of this Report):
Approved for public release; distribution unlimited. (12) 194 p.

17. DISTRIBUTION STATEMENT (of the abstract entered in Block 20, if different from Report):

18. SUPPLEMENTARY NOTES:

19. KEY WORDS (Continue on reverse side if necessary and identify by block number):
Computer programs
Heaving
Permeability (Soils)
Soil suction
Soil swelling
ULTRAT (Computer program)

20. ABSTRACT (Continue on reverse side if necessary and identify by block number):
This study evaluates procedures for predicting one-dimensional potential heave of foundation soils and the rate at which heave may occur. A computer program ULTRAT (Ultimate and rate of heave) was developed for predictions of potential heave and heave with time based on two models for characterization of swell behavior: the soil suction and mechanical swell models. The soil suction model relates volume change with change in matrix soil suction and water content.

(Continued)

DD FORM 1 JAN 73 1473 EDITION OF 1 NOV 65 IS OBSOLETE

Unclassified

SECURITY CLASSIFICATION OF THIS PAGE (When Data Entered)

20. ABSTRACT (Continued).

Time rate of heave may be predicted from numerical solutions of a simplified advanced diffusion flow equation. The mechanical swell model uses results from swell tests performed in the consolidometer.

Laboratory tests were performed to provide data for characterization of swell behavior using the models in the program ULTRAT. Testing procedures for the soil suction model are simple, economical, and expedient. The data are also useful for soils with any degree of saturation and the effect of lateral pressures may be accounted for in analyses. Testing procedures for the mechanical swell model using consolidometers are time consuming. Therefore, relatively few tests are usually performed which may not provide adequate representation of field soil conditions. The data are useful only for soils with a final degree of saturation equal to 100 percent and lateral pressures are not accounted for in analyses. Swell tests must be performed for each initial water content encountered in the field, whereas suction tests need be performed only to evaluate the suction-water content relationship for the required range of water contents.

A parametric study led to the development of simple, empirical equations for predicting potential heave and heave with time of slab foundations on homogeneous swelling soils above a stable water table or above nonswelling soil. Field measurements taken from test sites were compared with predictions of potential heave using eight published empirical methods, the empirical equations developed as part of this study, and the program ULTRAT. Preliminary analyses of heave with time using the empirical equations were also compared with field observations.

The results indicate that several methods provided useful predictions of potential heave of the field test sections. These methods include the empirical equations developed as part of this study and use of ULTRAT. The soil suction model provided upper and lower limits of heave at the field test sections if all or 1/3 of the volumetric swell, respectively, is assumed to occur as heave in the vertical direction. Heave with time predictions are burdened with the problem of determining effective field coefficients of permeability or swell. Effective coefficients of permeability or swell are a function of the availability of water as well as a measure of the field permeability. Maximum upper limits of 0.001 ft/day and 0.02 ft^2/day for the effective coefficients of permeability and swell, respectively, were determined for the soils beneath the field test sections.

PREFACE

This study is one phase of the RDT&E Work Unit AT40 A3 007 "Foundations on Swelling Soils" sponsored by the Office, Chief of Engineers. Earlier reports completed in 1977 as part of this Work Unit were MP S-77-13 entitled "Swell Behavior of NAF-II Sigonella Foundation Soil" and TR S-77-7 entitled "Evaluation of Laboratory Suction Tests for Prediction of Heave in Foundation Soils." The work reported herein was performed by Dr. Lawrence D. Johnson, Research Group, Soil Mechanics Division (SMD), Geotechnical Laboratory (GL), U. S. Army Engineer Waterways Experiment Station (WES). The report was reviewed by Mr. W. C. Sherman, Jr., and Dr. D. R. Snethen, Research Group, SMD, and MR. C. L. McAnear, Chief, SMD. Mr. J. P. Sale was Chief, GL.

COL John L. Cannon, CE, BG E. D. Peixotto, CE, COL G. H. Hilt, CE, and COL Levi A. Brown, CE, were Directors of WES during the conduct of this study. Mr. F. R. Brown was Technical Director.

CONTENTS

CONTENTS

CONVERSION FACTORS, U. S. CUSTOMARY TO METRIC (SI)
UNITS OF MEASUREMENT

U. S. customary units of measurement used in this report can be converted to metric (SI) units as follows:

Multiply	By	To Obtain
inches	2.54	centimetres
feet	0.3048	metres
square feet	0.09290304	square metres
pounds (force) per square inch	6894.757	pascals
tons (force) per square foot	95.76052	kilopascals
Fahrenheit degrees	0.555	Celsius degrees or Kelvins*

* To obtain Celsius (C) temperature readings from Fahrenheit (F) readings, use the following formula: $C = (5/9)(F-32)$. To obtain Kelvin (K) readings, use: $K = (5/9)(F-32) + 273.15$.

PREDICTING POTENTIAL HEAVE AND HEAVE WITH TIME IN SWELLING FOUNDATION SOILS

PART I: INTRODUCTION

Background

Effects of heaving soil on structures

1. Changes in volume and strength of foundation and embankment soils with time are important variables that must be considered in the design of foundations of structures, pavements, slopes and embankments, and retaining walls. Volume changes and strength losses (in less than fully saturated soils) commonly occur from changes in soil moisture content with time as a result of construction causing changes in field conditions. The placement of a structure or an impervious cover on a level ground surface, for example, inhibits natural transpiration by vegetation and evaporation from the ground surface. Heave can subsequently occur from the reduction in effective stress of soil beneath the structure due to decreased capillary stresses (reduced negative pore water pressure) on imbibition of moisture from various sources. Sources of moisture include seepage of water from the ground surface following rainfall and ponding; leakage from underground drains, water lines and sewers; and capillary rise from a water table.

2. Heave often occurs in soil beneath excavations because the reduction in overburden pressure causes the pore water pressure to decrease (increase in negative pore water pressure). Moisture flows into the soil beneath such an excavation from regions of greater pore pressure (smaller negative pore pressure) until equilibrium again occurs with the pore pressures in the surrounding soils. Heave in fills is usually less troublesome than heave in soils beneath excavations, but heave may occur in fills (especially in heavy clays) that are compacted dry of optimum water content. Other possible causes of volume change

include frost action[1,2] and chemical reactions between various components of the soil.[3]

3. Differential heave of swelling soils beneath foundations of structures and pavements due to changes in moisture often causes cracking and noticeable displacements in the overlying structures.[4-6] These fractures and movements not only detract from the esthetic appearance, but often cause substantial damage that limit the usefulness of the affected structures, and often lead to unpleasant riding characteristics of highway pavements.[5-7] Many structures with designs to resist damage from differential heave based on potential swell data from laboratory tests, may be overdesigned because the potential for swell may never be fully realized in the field during the life of the structure.[8] Reliable predictions of time rate of heave beneath various areas of the foundation of structures and pavements would permit estimates of differential heave at various times during the life of the structure, and thus aid in more economical and efficient designs.[5,6]

4. The time to failure of slopes cut in heavily overconsolidated clays appears to be related to the rate of moisture accumulation which can lead to swell and a reduction in soil strength initially along fissure planes.[9-11] This mechanism is progressive and is associated with a first-time failure that is not due to any pre-existing slip plane.[11] Reliable heave with time predictions should aid analysis of long-term stability and expected life-span of overconsolidated clay slopes.

5. Retaining structures constructed to support swelling soil slopes and embankments should be designed to resist swelling pressure in the soil confined behind the wall caused by the accumulation of moisture and restricted volume expansion. Reliable predictions of moisture changes and heave would permit estimates of the lateral displacements needed to reduce swell pressures to tolerable amounts.

Progress in predicting
potential heave and heave with time

6. Considerable work has been done in many countries to develop procedures for determining the swelling behavior of expansive soils and

predicting maximum potential heave,[4-6,8,12,13] but very little information is available on predicting time rate of heave.[8,9,14] Progress in developing reliable procedures for predicting rate of heave has been slow because many complicating factors influence the magnitude and rate of volume change (see Table 1). In addition, actual field permeabilities and equilibrium moisture profiles are difficult to determine. Local experience, if available, is probably the best means of estimating heave with time. Using this as a determining factor most heave appears to occur within 5 to 8 years following construction.[15-18]

7. The soil properties listed in Table 1 are indicative of the potential for swell, while the environmental conditions mostly influence the actual amount and rate of swell beneath structures and pavements. Environmental conditions produce the equilibrium moisture profile, or the amount of moisture that will eventually accumulate in the foundation soil. This information is needed to predict heave and rates of heave. Inadequate knowledge of the factors listed in Table 1, and variations in environmental conditions with time, have contributed to the generally poor understanding of the types of moisture profiles that may be observed in certain soils in different areas.[2,19,20]

8. A correct three-dimensional (3D) theory for moisture flow and volume change should technically couple the equilibrium of total stresses with the total pore pressure potential. Biot[21] developed such a coupled formulation for 3D consolidation of an elastic soil skeleton. Analytical solutions of Biot's equations for consolidation have been obtained for simple geometries and boundary conditions.[22-25] Solutions for complicated geometries and boundary conditions of soils that behave as linear-elastic porous mediums have been found by the finite element method.[26-29] A 3D formulation and computer code for time rates of swell were developed by Richards[30] using Biot's equations, soil suction data, and the finite element method, but solutions with this code require sophisticated soil data, a high capacity computer, and excessive computer time.

9. The finite element method was recently applied by Chang[31] to a practical two-dimensional (2D) solution of the consolidation and pore

pressure dissipation of partly saturated soils of earth and rockfill dams. This solution uses an extended Cam Clay nonlinear model to simulate the stress-strain behavior of compacted clays and the concept of a homogenized pore fluid to treat the three-phase system of soil, water, and air as a two-phase soil-pore fluid system. Modification of Chang's formulation to account for the swell behavior of soils, and the effect of increasing moisture on the loss of soil strength and collapse of the soil structure,[32] may lead to a reasonable approach to solutions of time rates of heave.

10. Much work has recently been completed toward the understanding of moisture flow by diffusion through all types of saturated and unsaturated soils.[7,9,14,30,33] Numerical solutions of diffusion flow equations assuming an uncoupled relationship between total stress and moisture flow (the assumption of constant total stress) have provided many successful comparisons of moisture flow with laboratory and field observations.[7,34-36] A relatively simple, expedient, and economical 2D finite difference formulation and computer code was developed from published swell data and a diffusion flow equation for rough estimates of heave with time.[14] Solutions to time rates of heave have also been found by simply using an inverse (reverse) application of Terzaghi's consolidation equation, or some modification of the consolidation equation, to improve correlation of theoretical results with laboratory and field observations.[9,37-39] The Terzaghi one-dimensional (1D) consolidation equation is a special case of diffusion flow. All of the models discussed above ignore many factors described in Table 1, especially many of the environmental conditions that influence field heave and rates of heave.

Purpose and Scope

Objective

11. The objective of this study is to develop relatively simple, economical, and practical means to routinely and accurately predict (total) potential heave, and heave with time, in swelling foundation soils caused by changes in moisture. This objective is achieved if potential heave for certain defined field conditions (such as the final

loading and moisture conditions) expected to be the most significant is accurately predicted. In addition heave with time must then be predicted using diffusion flow theory and boundary conditions defined by the predicted potential heave and the defined field conditions. Two models soil suction and mechanical swell are described herein for predicting 1D potential heave and heave with time based on isothermal diffusion flow.

12. Soil suction model. Potential heave may be predicted from matrix suction-water content relationships evaluated by thermocouple psychrometers. The soil suction model, which relates volume change with change in soil suction, was developed from an earlier phase of this project.[12] The soil suction data for the model were obtained from the thermocouple psychrometric technique developed during a previous study.[40] Time rate of heave may be predicted from numerical solutions of a simplified advanced diffusion flow equation, which was developed and evaluated as part of this study.

13. Mechanical swell model. Potential heave may also be predicted from several types of mechanical swell tests performed in the 1D consolidometer. Three of the most appropriate, and most commonly used tests, denoted as swell overburden, constant volume swell, and improved simple oedometer tests are described and applied herein. Time rate of heave may then be predicted from analytical solutions of the Terzaghi consolidation theory applied to swelling, rather than to consolidating soils.

Computer program

14. A computer program entitled ULTRAT (Ultimate and rate of heave), an improved version of ULTHE1,[5] was developed to obtain solutions for potential heave and heave with time from results of soil suction and/or mechanical swell tests. ULTRAT permits practical, useful, and economical solutions for simulation of the following field conditions:

a. Heterogeneous or layered soils.

b. Variable (soil suction model only) or constant coefficient of permeability.

c. Variable surcharge pressure due to the weight of the superstructure on the foundation.

d. Heave beneath the center of circular, center or corner of rectangular, and center or edge of long continuous footings or foundations.

e. Heave in foundation soils beneath excavations.

f. Choice of two equilibrium moisture profiles depending on the probable environmental conditions.

g. Heave due to a change in the water table level.

h. Settlements from consolidation and dissipation of pore pressures when effective stresses exceed the swelling pressure of the soil.

Conditions a, b, c, d, f, and g above are evaluated as part of the subject study. However only heave beneath the center of square slabs are evaluated herein although the program ULTRAT contains the capability of computing heave of other conditions as described in d above. Condition e will be evaluated in a later study. Users with little or no computer experience may use ULTRAT because the computer code is programmed with an interactive mode to facilitate use.

Analyses and verification

15. Analyses were performed to verify the applicability of the procedures described herein. The program ULTRAT was developed as part of this study to produce practical and reliable predictions of potential heave of foundations on swelling soils. A parametric study was also performed to develop simple empirical equations for predicting potential heave, and heave with time, of slab foundations on homogeneous swelling soils above a water table, or above nonswelling soil. Classification data such as the plasticity index, and initial water content, may be used in these equations. More extensive laboratory test results are not needed. Predictions of potential heave, and heave with time, were made for slab foundations on swelling soils at test sites located in Clinton, Mississippi; Lackland Air Force Base, Texas; Fort Carson, Colorado; and Sigonella, Sicily. Field measurements taken from all test sites (except Sigonella) were compared with predictions computed using the following: published empirical methods for predicting potential heave, empirical equations developed as part of this study, and the program ULTRAT based on results of laboratory soil tests.

PART II: THE PREDICTION OF POTENTIAL HEAVE AND HEAVE WITH TIME

16. Foundation clay soils may swell under the following conditions: a source of moisture is available, a driving force exists to move the moisture, and mechanisms are available to cause the volume change.[41] The environmental factors in Table 1 illustrate ways that moisture can become available to the soil. The driving force to move moisture is characterized by the pore pressure potential. Three important volume change susceptibility mechanisms[41] in clay soils are:

a. Clay particle attraction. Clay particles possess a net negative charge on their surfaces which result in attractive forces, or the major "holding" force for various cations* including the dipolar molecular water. Such soil takes on water in an attempt to satisfy the charge imbalance thereby increasing the volume of the soil mass.

b. Cation hydration. Cations substituted into or attached to clay particles may hydrate. Hydration of these cations increases their ionic radii which also increases the volume of the soil mass.

c. Osmotic repulsion. Variations in concentration of ions in pore water cause pressure gradients. The greatest concentration of ions occurs near the clay particles decreasing away from the surfaces. The pressure gradients draw water into the soil mass (osmosis) in an attempt to reduce the ionic concentration, which also increases the volume of the soil mass. This mechanism is more significant in soils containing significant concentrations of dissolved salts.

An additional mechanism, capillary imbibition, arises from surface tension effects of water and air mixtures in the pores of clay or nonclay soil masses. Capillary imbibition contributes to the pore pressure potential, but it may not result in volume change. For example, partially saturated sands (which do not swell) can exhibit apparent cohesive strength due to high capillary forces. The procedures for predicting potential heave, and heave with time, are developed below based on

---

* A positively charged ion.

the pore pressure potential, and the diffusion flow of moisture by gradients in the pore pressure potential.

The Pore Pressure Potential

17. The pore pressure potential quantitatively describes the interaction between soil particles and water.[42] This interaction determines physical behavior such as the volume and strength properties of the soil.[41-45] The pore pressure potential for the flow of moisture in soils can be defined as the sum of the soil suction and gravity heads[2,46,47]

$$\Phi = \frac{\tau}{\gamma_w} + x \quad * \tag{1}$$

where

Φ = pore pressure potential, ft**

τ = total soil suction, tsf

γ_w = unit weight of water, 0.0312 tons/ft^3

x = vertical coordinate or elevation head above a reference datum, ft

Natural forces that contribute to the magnitude and gradients in the magnitude of the pore pressure potential include the following: mechanisms discussed above, applied external pressure, the force of gravity, and temperature gradients.

18. The total soil suction τ is essentially a measure of the energy available to the microscale mechanisms that cause soil heave. The total soil suction can be given by[48,49]

$$\tau = \tau^{\circ} - \alpha_{\sigma}\sigma \tag{2}$$

---

* For convenience, symbols and unusual abbreviations are listed and defined in the Notation (Appendix H).

** A table of factors for converting U. S. customary units of measurement to metric (SI) units is presented on page 4.

where

τ° = total soil suction without surcharge pressure, tsf

α_σ = compressibility factor for change in confining pressure σ

σ = total mean normal confining pressure, tsf

19. The total soil suction without surcharge pressure is defined from thermodynamics[44]

$$\tau^\circ = \frac{RT}{v} \ell n \ RH \tag{3}$$

where

R = ideal gas constant, 86.81 cc-tsf/mole-deg K

T = absolute temperature, deg K

v = volume of a mole of liquid water, 18.02 cc/mole

RH = relative humidity, fraction

τ° is often given as the sum of matrix τ_m° and osmotic τ_s components for convenience.[44] The osmotic suction τ_s is related primarily to the osmotic repulsion mechanism and chemical content of the pore water, while the matrix suction without surcharge pressure τ_m° is primarily related to clay particle attraction, cation hydration, and capillary imbibition.

20. The matrix suction under surcharge pressure τ_m is a measure of the negative pore water pressure for any degree of saturation[12,46,48,50]

$$\tau_m = \tau_m^\circ - \alpha_\sigma \sigma = - u_w \tag{4}$$

where u_w is the pore water pressure. Increases in water content or applied pressure reduce the matrix component of soil suction. The osmotic suction, which is not affected by applied pressure, will be zero if the pore water does not contain dissolved salts. The effect of the osmotic suction on swell is not well known. The osmotic suction is assumed herein (and justified elsewhere[41]) to cause negligible swell compared to the effect of matrix suction.

21. The compressibility factor α_σ, defined as the fraction of applied pressure that is effective in altering the pore water pressure (Equation 4), may be related to a volumetric compressibility factor α_s. α_s is derived by multiplying the unit weight of water γ_w by the slope of a curve relating the reciprocal of the dry density γ_d to water content[50] or

$$\alpha_s = 100 \frac{\Delta V_T}{\Delta w} \tag{5}$$

where

α_s = volumetric compressibility factor for change in volume

ΔV_T = change in specific total volume V_T ; $V_T = (1 + e)/G_s$

e = void ratio

G_s = specific gravity

Δw = change in water content w, percent dry weight

Although the α_σ and α_s factors are not necessarily identical,[46] they are assumed equivalent herein to simplify the following derivations for predicting heave with time. Research beyond the scope of this report is needed to more fully understand the relationship between these factors. The α_σ is analogous with the Skempton pore pressure parameter B.

Diffusion Flow

22. Moisture flows in vapor and liquid phases through soil pores and as films on soil particles.[46] Gradients in the total pore pressure potential of the pore fluid are responsible for the flow of moisture in these different forms of water. The following equation for diffusion flow in the vertical direction was derived in terms of volumetric water content from a combination of thermodynamic principles, the continuity condition, and Darcy's law for fluid flow:[2,46,47]

$$\frac{\partial \theta}{\partial t} = \frac{\partial}{\partial x}\left(D \frac{\partial \theta}{\partial x} + D_T \frac{\partial T}{\partial x} + k\right) \tag{6}$$

where

$\theta = wG_s/100(1 + e)$, fraction of volumetric water content

t = time, days

$D = -(k/\gamma_w)\alpha\tau/\partial\theta$, moisture diffusivity, ft^2/day

$D_T = (k/\gamma_w)\tau\gamma_T$, thermal diffusivity for liquid water, $ft^2/day \cdot deg\ C$

k = coefficient of permeability, ft/day

$\gamma_T = dT_s/T_s dT$, relationship between surface tension of water and temperature or $-2.09 \cdot 10^{-3}\ C^{-1}$ between 10 and 30 C

T_s = surface tension of liquid water, ton/ft

23. The vapor diffusivity of water can be ignored for most natural soils since liquid flow is dominant at the higher degrees of saturation usually encountered in foundation soils. The effect of the mechanisms that cause swell on flow is included in the term of the volumetric water content θ . The effect of applied pressure is included in the moisture diffusivity D . The effect of the temperature gradient is included in the $D_T\ \partial T/\partial x$ term, and the force of gravity is accounted for by the last term k .

24. The thermal diffusivity D_T is very small, and for some field cases the effect of normally encountered thermal gradients on swell beneath structures could not be detected.[13] Philip and DeVries[47] estimated the thermal diffusivity of Yolo clay to be about $2.5 \cdot 10^{-7}\ cm^2/sec \cdot deg\ C$. Moisture diffusivities of some natural clays in contrast were much larger than this being on the order of $10^{-5}\ cm^2/sec$.[51] Moisture flow due to thermal gradients are assumed insignificant herein compared to moisture flow by gradients in the total pore pressure potential Φ . The total stress exerted on the foundation soil is also assumed to be independent of moisture flow.

25. A detailed theoretical and laboratory study of the diffusion equation for isothermal flow by Wong[7] indicated that Equation 6 without the thermal term $D_T\ \partial T/\partial x$ can adequately describe isothermal flow in unsaturated nonswelling soils. The change in volume during moisture flow in swelling soils alters the continuity equation for flow and Equation 6 does not then apply. The isothermal diffusion flow equation modified for swelling soils becomes[7]

$$\frac{\partial \theta}{\partial t} = \frac{\partial}{\partial x}\left(D \frac{\partial \theta}{\partial x} + k\right) - \frac{\theta}{1 + e} \frac{\partial e}{\partial t} \tag{7}$$

26. The 1D vertical flow diffusion Equation 7 may be given in terms of matrix soil suction if the effect of osmotic suction is negligible

$$\frac{\partial \tau_m}{\partial t} = \frac{\partial \tau_m}{\partial \theta}\left[\frac{\partial}{\partial x}\left(-\frac{k}{\gamma_w}\right)\left(\frac{\partial \tau_m}{\partial x} + \gamma_w\right)\right] - \frac{\theta}{1 + e} \frac{\partial \tau_m}{\partial \theta} \frac{\partial e}{\partial t} \tag{8}$$

Solutions of diffusion flow by Equation 8 in terms of soil suction τ_m is preferable to solutions in terms of volumetric water content θ because:

a. Greater accuracy is possible due to the large changes in matrix soil suction with small changes in water content.

b. Diffusion in terms of soil suction is directly related to the microscale mechanisms for swell and the pressure gradient that leads to moisture flow.

c. Boundary conditions of the diffusion equation in terms of soil suction can be more easily adapted to field environmental conditions such as the type of climate, ground water table and observed piezometric pore water pressures.

d. Models described herein for characterizing swell behavior can be easily coupled with Equation 8.

The Solution of Potential Heave And Heave With Time

27. The diffusion flow of moisture from soil of lower in situ suction to soil of higher suction reduces the pore pressure potential in the latter soil. The decrease in pore pressure potential causes effective stress to decrease and leads to heave in compressible or swelling clay soils.[52] For an idealized case (Figure 1) placement of an instantaneous loading pressure q causes pore water pressure u_w to increase, or matrix soil suction τ_m to decrease, such that the initial mean normal effective stress $\bar{\sigma}_o$ does not change. In such a case pore water pressure readjusts by diffusion flow over a period of time until an

equilibrium distribution of pore water pressure u_{wf} and equilibrium mean normal effective stress $\bar{\sigma}_f$ are obtained. Consolidation or recompression occurs when pore water pressure decreases (soil suction increases) such as below point A in Figure 1. Swell occurs when pore water pressure increases (soil suction decreases) such as above point A.

28. The bottom of the soil profile should be set at depth X_a, which is defined as the depth below which no change in moisture occurs and volume changes are negligible. The depth X_a is often less than 10 ft from the ground surface, but can extend deeper. X_a is set equal to the depth of water table if less than 20, 10, or 5 ft from the ground surface in clays, sandy clays and silts, and sands, respectively.[50,53] The final or equilibrium water table is denoted by DGWT for depth to groundwater table.

29. The total potential vertical heave at the bottom of the foundation in Figure 1 is initially determined by

$$\Delta H = N \sum_{i=NBX}^{i=NEL} DELTA(i) = N \cdot DX \sum_{i=NBX}^{i=NEL} \frac{e_f(i) - e_o(i)}{1 + e_o(i)} \qquad (9)$$

where

ΔH = potential (vertical) heave at the bottom of the foundation, ft

N = fraction of volumetric swell that occurs as heave in the vertical direction

$DELTA(i)$ = potential volumetric swell of soil element i, fraction

NEL = total number of elements

NBX = number of nodal point at bottom of the foundation

DX = increment of depth, ft

$e_o(i)$ = initial void ratio of element i

$e_f(i)$ = final void ratio of element i

The fraction of volumetric swell N that occurs as heave in the vertical direction depends on the soil fabric. Vertical heave of intact soils with few fissures may equal all of the volumetric swell ($N = 1$),

while vertical heave of heavily fissured soils may be as low as N = 1/3 of the volumetric swell.[53,54] The initial void ratio may be measured on undisturbed specimens using standard laboratory test procedures[55] or during the coarse of laboratory swell tests. The final void ratio depends on initial field conditions and changes in field conditions (such as those shown in Table 1) caused by construction of a structure. Predictions of the final void ratio are made using physical models for characterizing swell behavior. Such predictions are limited by boundary conditions that attempt to simulate final or equilibrium conditions that actually occur in the field.

30. Solutions of heave beneath a foundation over a period of time are initially found from

$$\Delta HT = N \cdot \sum_{i+NBX}^{i=NEL} F(i, t + 1) \cdot DELTA(i) \qquad (10)$$

where

ΔHT = potential (vertical) heave at the bottom of the foundation at time $t + 1$, ft

$F(i, t + 1)$ = fraction of the potential volumetric swell of soil element i at time $t + 1$

Predictions of the fraction $F(i, t + 1)$ are made using the same physical models for predictions of the final void ratio. These predictions are limited by boundary conditions that attempt to simulate field conditions as a function of time.

31. Two physical models, soil suction and mechanical swell, were adopted for characterizing swell behavior. The soil suction model is useful for interpreting swell behavior from results of soil suction-water content-void ratio relationships and permeability data. The mechanical swell model applies the Terzaghi consolidation theory to swelling soils and permits useful interpretation of primary swell-time results of soils tested in the consolidometer. The boundary conditions, assumptions, and limitations applied in use of these two physical models for simulating actual field conditions are subsequently described.

Soil suction model

32. Potential heave. Matrix suction-water content relationships evaluated by thermocouple psychrometers may be used to determine potential heave[12] from

$$DELTA(i) = DX\left[\frac{C_\tau(i)}{1 + e_o(i)} \log_{10} \frac{\tau^o_{mo}(i)}{\tau^o_{mf}(i)}\right] \qquad (11)$$

where

$C_\tau(i) = \alpha(i)G_s(i)/100B(i)$, suction index of soil increment i

$\alpha(i)$ = volume compressibility factor of soil increment i

$\tau^o_{mo}(i)$ = initial matrix soil suction without surcharge pressure of soil increment i , tsf

$\tau^o_{mf}(i)$ = final matrix suction without surcharge pressure of soil increment i , tsf

The initial matrix suction without surcharge pressure is determined by

$$\log_{10} \tau^o_{mo}(i) = A(i) - B(i) \cdot w_o(i) \qquad (12)$$

where

A(i),B(i) = soil suction parameters of soil element i corresponding to the ordinate intercept and slope, respectively of the τ-w relationship

$w_o(i)$ = initial water content of soil element i , percent dry weight

The final matrix suction without surcharge pressure depends on field conditions which are described later. Settlements can be predicted from Equation 11 if final matrix suction without surcharge pressure is greater than initial matrix suction without surcharge pressure.

33. Equation 11 does not directly consider changes in compressibility factor α due to changes in confining pressure, i.e., high confining pressure may cause some soils to collapse on wetting due to weakening of particle-to-particle bonds. The effect of soil collapse on volume changes of each soil element i is approximated herein by setting[12]

$$\tau_{mo}^{o}(i) = p_s(i) \tag{13}$$

where p_s is the suction swell pressure. The p_s may be found from[12]

$$\log p_s(i) = A(i) - \frac{100B(i)e_o(i)}{G_s(i)} \tag{14}$$

Suction swell pressure, which is derived from energy relationships, is taken herein as a measure of confining pressure required to prevent swell, and is therefore considered equivalent to the swell pressure evaluated from mechanical swell tests.

34. Heave with time. Heave with time is evaluated from Equation 10 with computed known values of total potential heave as found in Equation 9, and the known matrix soil suction for given time $\tau_m^{t+1}(i)$. The parameter $F(i, t + 1)$ is

$$F(i, t + 1) = \frac{\log_{10}\left[\frac{\tau_{mo}(i)}{\tau_m^{t+1}(i)}\right]}{\log_{10}\left[\frac{\tau_{mo}(i)}{\tau_{mf}(i)}\right]} \tag{15}$$

where

$\tau_m^{t+1}(i)$ = in situ matrix soil suction of soil element i at time $t + 1$, tsf

$\tau_{mo}(i)$ = initial in situ matrix soil suction of soil element i, tsf

$\tau_{mf}(i)$ = final or equilibrium in situ matrix soil suction of soil element i, tsf

35. The in situ matrix soil suction τ_m is related to the matrix soil suction without surcharge pressure τ_m^o as in Equation 4

$$\tau_{mo}^{o}(i) = \alpha(i)\sigma_o(i) + \tau_{mo}(i) \tag{16a}$$

$$\tau_{mf}^{o}(i) = \alpha(i)\sigma_f(i) + \tau_{mf}(i) \tag{16b}$$

where

$\sigma_o(i)$ = initial total mean normal confining pressure in soil element i, tsf

$\sigma_f(i)$ = final total mean normal confining pressure in soil element i, tsf

Equation 16 is valid for any degree of saturation as discussed in paragraph 20.

36. The total mean normal pressure is related to the total vertical pressure

$$\sigma_o(i) = \frac{1 + 2K_T(i)}{3} p_o(i) \tag{17a}$$

$$\sigma_f(i) = \frac{1 + 2K_T(i)}{3} p_f(i) \tag{17b}$$

where

$p_o(i)$ = initial total vertical pressure in soil element i, tsf

$p_f(i)$ = final total vertical pressure including applied foundation loads in soil element i, tsf

$K_T(i)$ = ratio of total horizontal stress to total vertical stress in situ

The $K_T(i)$ may be calculated for soils within a water table or zone containing positive pore water pressures by[12]

$$K_T = \frac{3(\tau^o_{mo} + u_w) - p_o}{2p_o} \tag{18}$$

37. The matrix soil suction for an advance in time $t + 1$ can be evaluated from the alternating special explicit finite difference solution of Equation 8 by

$$\tau_m^{t+1}(i) = \frac{[1 - B\,k^t(i) + C]\tau_m^t(i) + B\,k^{t+1}(i-1)\tau_m^{t+1}(i-1) + B\,k^t(i)\tau_m^t(i+1) + [k^t(i) - k^t(i+1)]\gamma_w\,DX}{1 + B\,k^{t+1}(i-1) + C} \tag{19}$$

where

$\bar{D}$ = time parameter, days/ft

$k^t(i)$ = coefficient of vertical permeability at time t for soil increment i, ft/day

$\bar{C}$ = volume parameter

The change in matrix soil suction τ_m with vertical distance x and time t is illustrated schematically in the finite difference mesh shown in Figure 2. The parameters $\bar{D}$ and $\bar{C}$ depend on the physical model for characterizing the swell behavior.

38. The time parameter of Equation 19 is given by

$$\bar{D} = \frac{\Delta t}{\gamma_w (DX)^2} \frac{\partial \tau_m}{\partial \theta} \tag{20}$$

where Δt is the increment of time t The incremental change in soil suction with volumetric water content is derived from the soil suction model, Appendix A.

$$\frac{\partial \tau_m}{\partial \theta} = - \frac{23{,}000\ \bar{B}\ \tau_m^o (1 + e)^2}{G_s [100(1 + e_o) - \alpha w_o G_s]} \tag{21}$$

39. The volume parameter derived from the soil suction model, Appendix B, is

$$\bar{C} = \frac{\alpha G_{sw}}{[100(1 + e_o) - \alpha w_o G_s]} \tag{22}$$

The parameter $\bar{C}$ is zero for nonswelling soil as expected because the compressibility factor α is zero.

40. Equation 8 is simplified further by assuming a single vertical permeability within a stratum of homogeneous soil such that the $[k^t(i) - k^t(i + 1)]$ term is negligible

$$\tau_m^{t+1}(i) = \frac{(1 - D_t + \bar{C})\tau_m^t(i) + D_t\,\tau_m^{t+1}(i - 1) + D_t\,\tau_m^t(i + 1)}{1 + D_t + \bar{C}} \qquad (23)$$

where $D_t = k^t(i)\cdot\bar{D} = k^{t+1}(i - 1)\cdot\bar{D}$

41. Continuity of flow across interfaces of different permeability from horizontal layers of heterogeneous soil is provided by

$$k_n^t\left(\frac{\partial\tau_m}{\partial x}\right)_n = k_{n+1}^t\left(\frac{\partial\tau}{\partial x}\right)_{n+1} \qquad (24)$$

where n refers to the number of the soil layer.

42. A variable permeability is approximated as a function of void ratio and degree of saturation by the method of Chang[31]

$$k^t = k_s G_e S^3 \qquad (25)$$

where

k_s = initial coefficient of vertical permeability of the saturated soil at void ratio e_o, ft/day

$G_e = e^t/(1 + e^t) \Big/ e_o/(1 + e_o)$

e^t = void ratio at time t

S = degree of saturation, fraction

Other formulations for defining effects of soil properties on permeability are not considered herein because field permeabilities are usually only roughly known and often not well correlated with laboratory values due to sample disturbance, fissures, and effects of sample size.

Mechanical swell model

43. Potential heave. Total potential heave DELTA(i) may be determined from results of swell tests in the 1D consolidometer by[12]

$$\text{DELTA}(i) = \text{DX}\left[\frac{C_s(i)}{1 + e_o(i)}\log_{10}\frac{p_s(i)}{\bar{p}_f(i)}\right] \qquad (26)$$

where

$C_s(i)$ = swell index of soil element i

$p_s(i)$ = swell pressure of soil element i, tsf

$\bar{p}_f(i)$ = final vertical effective pressure of soil element i, tsf

Initial void ratio e_o is defined as the void ratio following compression to the original vertical overburden pressure p_o before distilled water is added to the specimen. The swell pressure p_s is defined as the final or equilibrium vertical applied pressure needed to prevent swell following inundation of the specimen in distilled water.

44. The final vertical effective pressure is found from the principle of effective stress for saturated soils[56]

$$\bar{p}_f(i) = p_f(i) - u_{wf}(i) \tag{27}$$

where $u_{wf}(i)$ is the final pore water pressure in soil element i. Equation 16b reduces to Equation 27 for the conditions of the swell tests, i.e., the degree of saturation is one such that the compressibility factor is one. Lateral pressures are not evaluated during swell tests in the consolidometer. Earth pressures are assumed ($K_T = 1$, Equation 17b) so that

$$\sigma_f(i) = p_f(i) \tag{28}$$

The final matrix suction without surcharge pressure τ^o_{mf} is therefore equivalent to the final effective pressure $\bar{p}_f$. The final matrix suction τ_{mf} is equivalent to the final negative pore water pressure $-u_{wf}$.

45. The time t needed to reach a given fraction of potential volumetric swell $F(i, t + 1)$, Equation 10, is approximated from results of laboratory swell tests by an inverse (reverse) application of the Terzaghi consolidation equation[56]

$$t = \frac{T X_a^2}{c_{vs}} \tag{29}$$

where

T = time factor for various fractions of the total potential heave $F(i, t + 1)$

X_a = depth of the active zone for sorption of moisture from one surface, ft

$\bar{c}_{vs}$ = average coefficient of swell for all soils in the active zone, sq ft/day

The relationship between the time factor T and the fraction $F(i, t + 1)$ is a complex function depending on the stress distribution and location of the source of water. The time factor applied herein is representative of consolidation for triangular stresses with single drainage beneath the foundation equivalent to Case 3, Reference 57.

46. The average coefficient of swell in a layered soil profile is computed from[5]

$$\bar{c}_{vs} = \frac{X_a^2}{\sum_{i=NBX}^{i=NEL} \frac{DX}{c_{vs}(i)m_v(i)} \sum_{i=NBX}^{i=NEL} m_v(i)DX} \tag{30}$$

where

$c_{vs}(i)$ = coefficient of swell of soil element i, sq ft/day

$m_v(i)$ = coefficient of volume change of soil element i, tsf^{-1}

The coefficient of volume change is determined from[56]

$$m_v(i) = \frac{0.435\, C_s(i)}{[1 + e_o(i)]\bar{p}_f} \tag{31}$$

If the final effective pressure $\bar{p}_f$ is greater than the swell pressure of the soil element i, the compression index $C_c(i)$ rather than the swell index $C_s(i)$ is used in Equations 26 and 31.

Simulation of field
boundary conditions

47. The problems of simulating the factors that influence potential heave and heave with time in foundation soils (Table 1) greatly

complicates originating means to predict heaves. The reliability of heave predictions are often questionable because environmental conditions that occur following construction are often uncertain. The exact location and time that water may become available, perhaps by infiltration from the ground surface or by upward capillary rise from a water table, is very difficult, if not impossible, to predict. Predictions of potential heave and heave with time are therefore determined for certain defined conditions which attempt to simulate actual field conditions. Potential heave and heave with time are computed by the program ULTRAT using the equations of the two previously described models for the following soil properties and environmental conditions.

48. Soil properties. Soil property input parameters used in Tables 2 and 3 characterize swell behavior of a heterogeneous soil profile by defining the composition, dry density, and structure of each horizontally layered stratum in the foundation soil. These properties also quantify the effect of the climate prior to construction and the original vegetative cover on swell. Laboratory tests performed on undisturbed specimens of boring samples from each stratum determine the properties described in Tables 2 and 3 of each soil layer in the profile. Assumptions and limitations of the soil property input parameters are described in Table 4.

49. The soil input parameters needed to compute heave using the soil suction model are given in Table 2. The specific gravity G_s, initial water content w_o, and initial void ratio e_o are found by standard testing procedures[55] on undisturbed specimens of soil. These properties define the initial dry density. The compressibility factor α and the A and B parameters (Equations 11 and 12) characterize the effect of the composition and structure of soil on its swell behavior. The ratio of total horizontal to vertical stresses in situ K_T may be estimated, or calculated, from Equation 18 if the initial pore water pressure u_{wo} is measured in the field. The coefficient of permeability k_s is needed if rates of heave are to be calculated.

50. The soil input parameters needed to compute heaves using the mechanical swell model are given in Table 3. The G_s, w_o, and e_o

define the initial dry density. The points on the void ratio-log pressure chart, Figure 3a, determined by the given input parameters, characterize the effect of the type of soil and initial field conditions on swell behavior. The overburden pressure p_o is applied and e_o determined, water is then added, and the pressure increased to avoid swelling. The applied pressure is reduced incrementally to measure void ratios e_{po} and e_s. The void ratios e_o, e_{po}, and e_s permit a bilinear line between the swell pressure p_s and 0.1 tsf, which may be more representative of the swell index C_s than a single linear line.

51. If the swell pressure p_s is less than p_o, which is possible for collapsible soils or soils taken from borings within a water table of positive pore water pressure, a better test may be that illustrated in Figure 3b. The overburden pressure p_o is applied for about 5 minutes to determine e_o, the pressure is removed to the seating pressure (0.02 tsf), water is added until primary swell is complete, and pressure is then applied incrementally to determine e_s, p_s, and e_{po}. Procedures for performing these swell tests and determining void ratios are presented later.

52. Environmental conditions. The environmental conditions following construction of a structure are described by such variables as confinement, water table depth, drainage pattern, and field permeabilities and affect both the potential heave and heave with time, e.g., these conditions affect the changes in void ratio that develop in the soil beneath a foundation of a structure. Confinement is computed by ULTRAT from the soil density and foundation loading pressure q. The water table depth input parameter is defined as DGWT (Figure 1), the depth from ground surface to the water table. The drainage pattern is defined by the choice of the equilibrium moisture profile or final pore water pressure u_{wf}. Field permeabilities determine the rate at which heave will develop for the two physical models of soil behavior adopted in this study. Water is assumed to be immediately available on one drainage surface following construction of the structure. Coefficients of permeability and swell are therefore assumed to be effective coefficients that include effects of droughts, or an intermittent supply of water,

as well as the effect of fissures and soil density. Other assumptions and limitations of input parameters describing environmental conditions are given in Table 5.

53. Confinement. The final total vertical confining pressure p_f used in Equations 17b and 27 by ULTRAT is determined by[5]

$$p_f(i) = p_{fo}(i) + \Delta p_{st}(i) \tag{32}$$

where

$p_{fo}(i)$ = final total soil vertical overburden pressure of soil element i, tsf

$\Delta p_{st}(i)$ = increase in vertical pressure of soil element i due to the foundation and superstructure, tsf

54. The $p_{fo}(i)$ of element i at depth DXX, Figure 1, is computed from

$$p_{fo}(i) = p_{fo}(i - 1) + DX \cdot \gamma(i) \tag{33}$$

where each $p_{fo}(i - 1)$ is known from the prior computation of $p_{fo}(i)$ at the smaller depth of DXX-DX. The unit weight $\gamma(i)$ of each soil element i is computed from the following input properties of the soil

$$\gamma(i) = \frac{\gamma_w G_s(i)}{1 + e_o(i)} \left[1 + \frac{w_o(i)}{100}\right] \tag{34}$$

55. The increase in vertical pressure $\Delta p_{st}(i)$ caused by a foundation and the superstructure and exerted on each element i is approximated for a variety of foundation types and locations by the equations tabulated in Table 6 formulated after the Boussinesq method.[60,61] The increase in pressure at the bottom of a foundation placed below the ground surface or for a deep foundation, Table 6, is

$$\Delta p_b = q - p_{fo}(NBX) \tag{35}$$

where

Δp_b = increase in pressure at base of foundation, tsf

q = total foundation and superstructure pressure, tsf

$p_{fo}(NBX)$ = vertical overburden pressure of surrounding soils at bottom of the foundation, tsf

The pressure q at the base of the foundation, Figure 1, is estimated from foundation and superstructure loads.

56. Swelling of soils surrounding deep foundations such as piers may cause uplift forces $\bar{T}$ on the shaft and reduce the structure pressure q at the base of the footing. The amount of reduction in q is complicated by the relationship of the foundation stiffness to the soil stiffness, slippage between soil and pier foundation, and lengthening of the pier from tension forces. If a void occurs beneath the footing because of sufficiently high uplift forces due to swelling soil along the shaft, q will be reduced to zero. Heave at the top of the pier will be greater than heave of soils beneath the foundation, and such pier heave will be a function of heave in the surrounding soils.[5]

57. The total foundation and superstructure pressure q after subtraction of uplift force $\bar{T}$ may be estimated from[62]

$$q = \frac{L - \bar{T}}{AREA} \tag{36}$$

$$\bar{T} = 2\pi RAD \int_0^{DXX} (C + K_o \gamma \, DXX \tan\phi) DX \tag{37}$$

where

L = vertical load applied at top of pier at ground surface, tons

$AREA$ = area of base of pier, ft^2

RAD = radius of shaft, ft

C = soil cohesion, tsf

K_o = ratio of intergranular pressure on horizontal and vertical planes, coefficient of earth pressure

ϕ = angle of internal friction, deg

The most appropriate laboratory tests to evaluate the C, ϕ, and K_o parameters are uncertain at this time. The results of drained ($\bar{S}$) direct shear tests and assuming K_o equal to one may provide practical interim values until further information is available.[62]

58. Water table depth. The program ULTRAT subtracts γ_w from the moist unit weight γ (Equation 34) when the final or equilibrium depth to the water table DGWT is less than the depth of soil increment i. This provision permits predictions of heave due to variations in DGWT (Figure 4), e.g., heave from a rise in water table level may be estimated by the difference in potential heave between the levels.

59. Equilibrium moisture profile. The final pore water pressure u_{wf} depends on drainage and a variety of other field conditions. ULTRAT permits input of two final moisture profiles: a saturated (SAT) profile ($u_{wf} = 0$) down to the depth of the shallow water table DGWT, Figure 4, or the depth of the active zone X_a if a shallow water table does not exist, Figure 5. A negative hydrostatic head (HYD) profile, $u_{wf} = \gamma_w$(DXX-DGWT) down to the depth of a shallow water table, Figure 4. A HYD profile down to the depth of the active zone X_a may also be used if a shallow water table does not exist, Figure 5, with the suction model. The DGWT should be set greater or equal to X_a, or the bottom of the soil profile.

60. The saturated profile may be preferred if localized saturation of the foundation soil appears probable. Localized saturation can result from leaking water pipes, drains, sewers, lawn watering, and/or ponding of surface water. The standard procedure used in military construction for estimating foundation soil swell assumes a saturated equilibrium profile.[63] The negative hydrostatic head profile may be preferred for field conditions beneath structures with good drainage and not subject to local saturation. Water is assumed to diffuse vertically downward from the ground surface beneath the foundation for the SAT profile, and diffuse vertically upward from the bottom of the active zone for the HYD profile, Table 5.

PART III: FIELD OBSERVATIONS

Description of Field Test Sites

Location and climate

61. The location and climate of the four test sites chosen for study are briefly described as follows:

Test Site	Location	Climate	Elevation ft, msl	Annual Rainfall in.
Clinton	Clinton, Miss.	Warm, humid	328	50
Lackland	San Antonio, Tex.	Semiarid	770	28
Fort Carson	Colorado Springs, Colo.	Semiarid	6000	17
Sigonella	Sigonella, Sicily	Temperate	75	22

The semiarid climates of the Lackland and Fort Carson test sites are generally more conducive to severe swelling soil problems than at Clinton or Sigonella.[5]

Field test sections

62. Test sections were constructed at the Clinton, Lackland, and Fort Carson test sites in October 1969, July 1974, and October 1973, respectively. These test sections were each constructed of two 100-ft square impermeable membranes separated by a 0.8-ft thick layer of sand as shown in Figures 6 to 8. The covers were placed on graded level surfaces which had been stripped of up to 6 in. of top soil and vegetation. The Lackland test section includes a pier, Figure 7, as part of an earlier investigation.[64]

63. Instrumentation includes permanent bench marks, open tube Casagrande piezometers, surface and deep heave plugs, soil suction thermocouple psychrometers and temperature thermocouples at the Clinton and Lackland test sections, and aluminum access tubes for measurement of water contents by nuclear probes. Thermocouple psychrometers were not included at the Fort Carson test section, Figure 8, because past experience indicated that these psychrometers could not be depended on for long-term service.[65] A description of instruments is provided in References 3, 65, and 66. Three piezometers were installed at

Sigonella 8, 16, and 25 ft below ground surface.[67] A test section was not constructed at Sigonella.

Soils

64. Clinton. The predominant soil at the Clinton test site is Yazoo clay, a plastic, stiff marine clay of the Jackson group.[68] The Yazoo clay was deposited in glacial times with a thickness of about 400 ft. In later periods, a lean, loessial material ranging in thicknesses of up to 12 ft, covered the Yazoo clay.[69,70]

65. The upper 10 to 15 ft of the Yazoo clay was weathered to a yellowish or greenish-yellow color, frequently stained by limonite and manganese along joints while it was exposed to the environment during its early history. At depths below 10 to 27 ft, the Yazoo clay is unweathered, unjointed, fairly homogeneous and consists of blue-green to blue-gray calcareous, fossiliferous clay with some pyrite. Further details may be found in References 68 to 71.

66. Classification data of soil from boring samples in or adjacent to the instrumented quadrant, Figure 6, are shown in Figures 9 and 10. The transition between the lean loess and plastic Yazoo clay is clearly indicated by the abrupt difference in water content at about 6 to 8 ft below the ground surface. The natural water content/plastic limit ratio exceeds 1.2 below 8 ft of depth. Gradation data, Appendix C, indicate a relatively coarse soil of 20 percent less than 2 microns at depths less than 6 ft and a relatively fine soil, 65 percent less than 2 microns, at depths greater than 8 ft.

67. Lackland. The test site lies directly on an overburden material that varies from 12.5 to 13.5 ft in thickness. About 9 ft of the overburden consists of silty black to gray CH clays containing lime derived from the clay shales of the underlying formation.

68. The primary material underlying the overburden is the Upper Midway group of the Tertiary system. The Upper Midway is a CH montmorillonite clayey shale with the tan, weathered form extending to a depth of about 55 ft; the unweathered bluish form is encountered below this depth. The Upper Midway is highly jointed and slickensided to a depth of about 31 ft below the ground surface. Further details

may be found in References 64 and 72.

69. Classification data from boring samples located in the instrumented quadrant of the test section, Figure 7, are shown in Figure 11. Boring PU-7 was obtained in December 1970 following a drought, while boring No. 1 was obtained in April 1973 following a period of rainfall. Natural water contents in the overburden less than 7 ft from the ground surface, Figure 11, reflect the climatic conditions; e.g., 18 to 24 percent in PU-7 compared to 22 to 34 percent water content in No. 1. These natural water contents are approximately equal to respective plastic limits. Gradation data, Appendix D, indicate that the overburden above 7 ft is coarser than the Upper Midway below 12 ft, e.g., 40 percent compared to 60 percent less than 2 microns. The clayey gravel between 7 and 12 ft contains about 60 percent coarse gravel and 27 percent silt or clay with smaller amounts of fine gravel and sand.

70. Fort Carson. The primary material underlying about 4 ft of brown CH overburden clay is Pierre Shale, a sedimentary swelling rock derived from clays and silts.[73,74] The shale was compressed by weight of the overlying sediments and glacial ice causing it to be overconsolidated with considerable strength. The shale contains bentonite beds from 1/4 to 6 in. thickness.

71. The shale, which is badly faulted with frequent slickensided zones, cracks rapidly when exposed to dry air and decomposes to a sticky, gumbo-like mud from repeated wetting and drying. The shale is not chemically cemented. Further details may be found in References 73 and 74.

72. Classification data from boring samples located in the southeast corner, BOQ3 of June 1973, and in the instrumented quadrant, P2 and P8 of October 1973 are shown in Figure 12. Natural water contents are 1.3 times the plastic limit above 8 ft and falls to less than 0.8 times the plastic limit below 15 ft. Gradation data, Appendix E, indicate that 40 to 50 percent of the soil particles are less than 2 microns throughout the entire profile.

73. Sigonella. The soils are characterized by stiff CH marine clays that have eroded and desiccated near the surface following uplift

during recent geologic time. Sands and gravels eroded from terraces of the Simeto and Dittanino rivers were subsequently deposited on the old marine erosion surface. An additional mantle of clay was probably deposited during the most recent intrusion by the sea. Tertiary bedrock underlies the marine clays from a minimum of 300 ft near the mouth of the Simeto-Dittanino river to more than 1500 ft in other areas.

74. Marine CH clays of varying colors of light brown, brown, gray-brown, bluish gray, and blue are observed in the area of the test site down to 100 ft. Sandy CL clay from 5.5 to 6.5 and 16 to 22 ft are interspersed in the CH clay, Figure 13. Slickensides and shrinkage cracks have been observed in the desiccated soil down to about 5 ft below ground surface. Further details may be found in Reference 67.

75. Natural water contents in all boring samples obtained in November 1976 are greater than the plastic limits, Figure 13. The water content/plastic limit ratio of the CH clay was 1.2 or greater, while that of the sandy CL clay was 1.5 or greater. Gradation data, Appendix F, show that more than 50 percent of the soil particles in the CH clay are less than 2 microns in size. Sample U-5 in the sandy CL clay at about 20 ft of depth contains about 27 percent less than 2 microns and about 40 percent of fine sand particles.

Observation of Instruments

General

76. Following construction of test sections field observations of water levels in piezometers and elevations of surface and deep heave plates at the Clinton, Lackland, and Fort Carson test sites up to 31 May 1977 are provided below. Observations of water levels in piezometers on the Sigonella test site are provided from 15 January 1977 to 4 June 1977. Data scatter of readings from nuclear probes in aluminum access tubes prevented useful measurements of changes in field water content with time. Soil suctions from the field thermocouple psychrometers are given in Reference 65.

Clinton test site

77. Piezometers. Piezometric readings indicate a perched

water table with a water level about 5 ft below ground surface in August 1971, Figure 14. The pore pressures are consistent with a hydrostatic head in the loess and Yazoo clay down to at least 20 ft below ground surface. The pore pressure head has increased 2 to 3 ft since August 1971 indicating wetter soil conditions within 20 ft of the ground surface. Deep piezometers with tips at 45 and 70 ft below ground surface have remained dry since installation in November 1968. A deep water level is encountered 124 ft below ground surface.

78. Vertical heave plates. Field observations with time of the vertical movement of surface heave plates at the center (point A), 20 ft inside the edge (point B), 5 ft inside the edge (point C), and 15 ft outside of the test section (point D) are shown in Figure 15. A slight settlement was observed initially up to 500 days following construction of the test section. Heave of about 0.1 ft has subsequently accumulated slowly at a decreasing rate up to the most recent observations 2793 days following construction. Heave is greatest at the center and decreases to 0.04 ft toward the edge 2793 days following construction of the test section. Differential heave between points A and C beneath the test section at 2973 days is 0.36 of the maximum heave at point A.

79. Observations of deep heave plates show the distribution of heave with depth, Figure 16. More than 50 percent of the heave originates at depths below 25 ft from the ground surface in the desiccated zone indicated by the piezometric observations. Nearly all heave noted at location D outside of the test section is caused by deep seated heave below 30 ft of depth. Very little heave occurs within 10 ft of the ground surface, which is consistent with the low swelling capability of the loess overburden. Although the effect of deeply located heave plugs and piezometers on the observed heave has not been determined, it should be noted that moisture from the perched water table could be seeping down the perimeters of instruments extending beneath the perched table to contribute to the deep seated heave.

Lackland test site

80. Piezometers. Piezometric readings indicate a perched water table with a water level 8 ft below ground surface in September 1972,

Figure 17. The pressure is consistent with a hydrostatic head in the overburden and Upper Midway soils down to 33 ft below ground surface. The pore pressure head decreases between 33 ft to 45 ft below ground surface. A deep water table is encountered below 55 ft of depth. The pore pressure head in the perched water table is 5 ft larger in May 1977 compared to September 1972 down to 33 ft of depth, but the head has decreased below 33 ft to zero at 55 ft of depth.

81. The zone of soil between 33 and 55 ft is desiccated or deficient in pore pressure with respect to pressure heads in the perched and deep water tables above 33 ft and below 55 ft, respectively. This pore pressure deficiency may be a potential source of heave.

82. Vertical heave plates. Field observations with time of the vertical movement of surface heave plates 100 ft west (points A and B), 15 ft west (point C), edge (point D), and center (point E) of the test section are shown in Figure 18. Heave of nearly 0.1 ft appeared within 100 days of construction of the test section. Much of this heave dissipated 500 days following construction at the edge and outside of the test section due to environmental conditions, but heave continued to accumulate beneath the covered area to 0.18 ft 1029 days following construction. Heave beneath the test section has generally increased uniformly across the test section and the movements are about the same as that of the uncovered natural surrounding area 1029 days following construction. Differential heave beneath the test section at 1029 days was negligible. However, differential heave at 500 days was 0.73 of the maximum observed heave at point E.

83. The distribution of heave with depth, Figure 19, shows that nearly all of the 0.16 ft of heave 1029 days following construction 100 ft from the edge of the test section originated in the top 5 ft of the plastic soil overburden. Very little heave (about 0.03 ft) occurred between 5 and 40 ft of depth, and negligible heave occurred below 40 ft. Most of the 0.18 ft of heave beneath the test section also occurred within the top 5 ft of overburden soil, and about 0.04 ft of the heave occurred between 5 and 40 ft of depth. Some deep seated heave of about 0.04 ft originated below 40 ft of depth beneath the test section in

contrast to the negligible heave observed below 40 ft of depth 100 ft from the edge of the test section. Again it should be noted that moisture from the perched water table could be seeping down the perimeters of the deep heave plates into the desiccated zone below 40 ft of depth.

Fort Carson test site

84. Piezometers. Piezometric readings, Figure 20, indicate a perched water table with a water level about 3 ft below ground surface in October 1974. The pressure is consistent with a hydrostatic head in the Pierre shale down to 30 ft of depth. The pressure head decreased from about 25 to 10 ft between 30 and 50 ft of depth. The pressure head in the shale is about 2 ft greater in May 1977 as compared with October 1974.

85. The deep piezometer P-7 with tip at 80 ft indicated that the pore pressure increased below 50 ft of depth. The zone of soil between 30 and 70 ft appears desiccated or deficient with respect to the hydrostatic head indicated by the pressure heads above 30 ft and below 80 ft. This pore pressure deficiency may also be a potential source of heave.

86. Vertical heave plates. Field observations with time of the vertical movement of surface heave plates at the center (point A), 30 ft from the center (point B), edge (point C), and 15 ft outside the edge (point D) of the test section are shown in Figure 21. Small heave of about 0.08 ft and less, similar to that of the Clinton test site, have occurred 1291 days following construction. Most heave has occurred at points B, 20 ft inside the edge, and D outside of the test section, while only about 0.02 ft has occurred at the center, point A, 1291 days following construction. Heave at point D outside of the covered test section is cyclic and strongly influenced by the climatic environment, while heave beneath the covered area is less affected by cyclic changes in the climate. Differential heave between points A and B at 1291 days was 0.75 with maximum heave at point B.

87. Observations of the vertical movement of the deep heave plates, Figure 22, show that nearly all heave has occurred within 5 ft of the ground surface. Deep seated heave below 30 ft is negligible 1291 days following construction. The deepest heave plates located 30 ft below

ground surface is still within the perched water table and does not provide an opportunity for moisture to seep into the desiccated zone beneath the perched water table. Some slight settlement between 5 and 30 ft of depth was observed at the edge and outside of the test section about 500 days following construction.

Sigonella test site

88. Water levels in piezometers on the Sigonella test site decreased from 30 January to 4 June 1977, Figure 23. Piezometer P-2, with tip 8.2 ft below ground surface, indicated the deepest water level. The pressure head in the piezometers is hydrostatic, Figure 24. The ground water level appears to increase in depth from about 2.3 to 4.5 ft below ground surface from 30 January to 4 June 1977.

PART IV: CHARACTERIZATION OF SWELL BEHAVIOR FROM LABORATORY TESTS

Testing Procedures

Soil suction model

89. Swell behavior can be characterized by evaluation of the suction index C_τ, Equation 11, and the suction swell pressure p_s, Equation 14 (see paragraphs 32 and 33). These parameters are determined from matrix soil suction coupled with respective water contents and void ratios. The procedure for evaluation of matrix suctions by thermocouple psychrometers is described below. Water contents and void ratios were determined by standard procedures.[55]

90. Thermocouple psychrometers measure the relative humidity in soil by a technique called Peltier cooling.[75] By causing a current to flow through a single thermocouple junction in the proper direction, the junction will cool, causing water to condense on the junction when the dewpoint temperature is reached. Condensation of this water inhibits further cooling, and the voltage developed between the thermocouple and reference junctions is measured by the proper equipment. Less than 1 day of technician time is required for setup, testing, and evaluation of data to obtain a 12-point soil suction-water content curve, void ratios, and the compressibility factor.

91. Calibration. The outputs of the thermocouple psychrometers (in microvolts) were calibrated by tests with potassium chloride salt solutions that produce a given relative humidity for known concentration[76] as shown in the following tabulation,

Gram-Formula Weight per 1000 Grams Water, M	Grams of KCl per 1000 ml Water	Relative Humidity percent	Suction at 25 C, atm
0.05	3.728	99.83	2.3
0.20	14.91	99.36	8.8
0.50	37.27	98.42	21.6
1.00	74.55	96.84	43.4
2.00	149.10	93.68	88.5

Relative humidities are converted to total soil suctions by Equation 3, paragraph 19. These are also the osmotic suctions of the potassium chloride salt solutions. The resultant calibration curve was

$$\tau^{\circ} = 2.8E_{25} - 1.675 \tag{38}$$

where

τ° = total soil suction, tsf

E_{25} = microvolt output at 25 C

The E_{25} is computed from the voltage E developed from the thermocouple psychrometers at the measurement temperature by

$$E_{25} = \frac{E}{0.325 + 0.027t} \tag{39}$$

where t is the temperature in degrees C.

92. Preparation. Laboratory measurements to evaluate total suction were made with the apparatus illustrated in Figure 25. Thermocouple psychrometers were inserted into pint-capacity metal containers with the specimens and the assembly sealed with No. 13 1/2 rubber stoppers. The assembly was inserted into a 1- by 1- by 1.25-ft chest capable of holding six pint-sized containers and insulated with 1.5 in. of foamed polystyrene. Cables from the psychrometers were passed through a 0.5-in.-diam hole centered in the chest cover. Temperature equilibrium was attained within a few hours after placing the lid. Equilibrium of the relative humidity in the air measured by the psychrometer and the relative humidity in the specimen was usually obtained within 48 hours.

93. Soil test. The soil suction test was performed on 12 undisturbed specimens (of about 1-in. dimension) of each clay soil. The water content of each specimen was varied by permitting the pore water to evaporate at room temperature for various periods of time up to 48 hours from about half of the specimens. Various amounts of distilled water were added to the remaining specimens.

94. Matrix soil suction. The logarithm of the soil suctions was subsequently plotted as a function of water content to determine the

A and B parameters, Equation 12, paragraph 32. The matrix suction was determined as the difference between osmotic and total soil suctions. The osmotic suction was estimated by noting the total soil suction at high water contents, i.e., this is the osmotic suction. Further details of evaluating soil suction by this procedure are available in References 5, 12, and 40.

Mechanical swell model

95. Swell behavior can be characterized by evaluation of swell index C_s and swell pressure p_s, Equation 26 (see paragraph 43). These parameters were determined from results of the three swell tests described in Table 7: swell overburden (SO), constant volume swell (CVS), and improved simple oedometer (ISO) tests. These three tests are representative of the types of swell tests commonly performed in the consolidometer.[5,6,12,13,77] A single test usually required 2 to 4 weeks. Five identical tests may be needed within each soil stratum in order to estimate the compressibility to within 10 percent.[78] In many cases, the large number of tests required may be prohibitive.

96. Preparation. Undisturbed specimens for swell tests were identically trimmed, e.g., 4.25 in. in diameter by 1.15 in. high. They were seated in a fixed ring consolidometer between air-dry porous stones with a small seating load (approximately 0.02 tsf). Filter paper was not used in order to eliminate error resulting from compression of the paper. The inside of the reservoir was moistened and the specimen and consolidometer assembly were covered with impervious plastic to maintain constant moisture conditions. All applied pressures prior to adding free water were held not more than 30 min to minimize loss of moisture. Swell tests were performed with distilled water added to both the top and bottom porous ceramic stones. Further details describing these tests can be found in Reference 12.

97. Void ratios. The void ratios needed for input into the program ULTRAT are evaluated from results of the swell tests, Figure 26, as follows:

a. All swell tests, e_o. The initial in situ void ratio at natural water content and at the original vertical applied soil overburden pressure p_o.

b. SO test, e_{po}. The void ratio at p_o following inundation in distilled water and completion of primary swell. CVS test: the void ratio at p_o following rebound and completion of primary swell from p_s. ISO test: the void ratio following saturation and recompression from the seating load (0.02 tsf) to p_o.

c. SO and CVS tests, e_s. The void ratio at 0.1 tsf following rebound and completion of primary swell from p_o. ISO test: the void ratio following saturation and recompression from 0.02 tsf to 0.1 tsf.

98. Swell index. The selection of the three points (e_s, 0.1), (e_{po}, p_o), and (e_o, p_s) of Figure 26 permits evaluation of a bilinear line which represents the swell index of the foundation soil by:

$$C_s = \frac{\Delta e}{\Delta \log p} \tag{40}$$

where

Δe = change in void ratio e

$\Delta \log p$ = change in logarithm of the vertical applied pressure p

The program ULTRAT evaluates C_s depending on the pressure in the soil, i.e., slope of line from 0.1 to p_o or p_o to p_s. The compression index C_c is evaluated from Equation 40 when the pressure exceeds p_s. C_c may be a measure of recompression rather than virgin consolidation.

99. The swell index may be evaluated from results of the SO test performed at several different overburden pressures p by

$$C_s = \frac{(1 + e_o)\ \Delta S_p}{100\ \Delta \log p} \tag{41}$$

where ΔS_p is the change in the percent swell S_p, Figure 27. The percent swell is determined by

$$S_p = \frac{100\ (e_{po} - e_o)}{1 + e_o} \tag{42}$$

where

e_{po} = void ratio at the vertical applied pressure p_o following inundation in distilled water and completion of primary swell

e_o = initial void ratio at natural water content w_o and pressure p_o

Void ratios e_{po} and e_s may be evaluated by

$$e_{po} = e_o + C_s \log \frac{p_s}{p_o} \tag{43a}$$

$$e_s = e_o + C_s \log \frac{p_s}{0.1} \tag{43b}$$

100. Swell pressure. Swell pressure p_s, which is a measure of the confining pressure needed to prevent swell, is defined with respect to the type of swell test performed:

a. SO test. The vertical applied pressure required to recompress the specimen from e_{po} to e_o, Figure 26a; or, the vertical applied pressure at which S_p is zero, Figure 27.

b. CVS test. The vertical applied pressure needed to prevent swell following inundation of the specimen in distilled water, Figure 26b.

c. ISO test. The vertical applied pressure required to recompress the specimen to the initial in situ void ratio e_o from the void ratio following primary swell at the seating load (0.015 tsf), Figure 26c.

101. Coefficients of permeability and swell. Falling head permeability tests were performed on some specimens at approximately the initial in situ void ratio e_o during swell tests using standard procedures.[55] Coefficients of permeability were also evaluated from results of pressure plate tests using methods for analysis of flow data described by Kunze and Kirkham[79] and Klute.[80] A description of the equipment and procedures used to perform the tests is given by Johnson.[12,81] Permeabilities were evaluated from flow data of specimens at a matrix suction of 0.07 tsf and an overburden pressure equivalent to that in the in situ soil.

102. Curves of time rates of swell from some of the mechanical swell test results following saturation, and at surcharge pressures less than the overburden pressures, were evaluated to determine the

coefficients of swell by

$$c_{vs} = \frac{T_{90}\bar{H}^2}{t_{90}} \times 10 \qquad (44)$$

where

c_{vs} = coefficient of swell, ft^2/day

T_{90} = time factor needed to complete 90 percent of primary swell, 0.848

$\bar{H}$ = one-half of the thickness of the specimen for sorption from both top and bottom of the specimen, in.

t_{90} = time to complete 90 percent of primary swell, min

Soil Suction Test Results

103. The soil suction tests provided data on natural water content, initial void ratio, soil suction parameters A and B, initial matrix soil suction, suction swell pressure (Equation 14), compressibility factor (Equation 5), and the suction index (Equation 11) for use in the soil suction model for characterizing swell. Initial void ratio e_o is assumed equal to the initial in situ void ratio under the original overburden pressure. Suction swell pressure p_s, which is the matrix soil suction at e_o with all voids filled with water, is considered equivalent to the swell pressure evaluated from mechanical swell tests. Results of the suction tests for all test sites are presented in Table 8.

Clinton test site

104. Matrix suction, water content, and void ratio relationships were evaluated for specimens from boring No. 1, March 1973. Osmotic suctions were not observed in these specimens.

105. Initial void ratio. Initial void ratios varied from 0.72 to 0.85 for the loess, and 1.14 to 1.39 for the Yazoo clay.

106. Initial matrix suction. Initial matrix suctions τ^o_{mo} varied from 0.23 to 0.76 tsf from ground surface to 16.1 ft in depth. The τ^o_{mo} at 30 ft of depth was 3.09 tsf.

107. Suction swell pressure. Suction swell pressures p_s were

about 0.4 tsf in the loess overburden and varied from 0.10 to 1.93 tsf in the Yazoo clay. Smaller p_s of 0.10 to 0.77 tsf were observed from 3.5 to 11.1 ft of depth.

108. Compressibility factor. The compressibility factors α of the loess overburden at 7 ft of depth or less varied from 0.41 to 0.73. The α of the Yazoo clay at depths greater than 7 ft were close to one (0.87 to 1.00).

109. Suction index. The suction index C_τ of the loess overburden was 0.069 at 4 ft of depth. The C_τ varied from 0.151 to 0.251 below 6.5 ft from the ground surface.

110. Ratio of horizontal to vertical stress. The ratio of total horizontal to vertical stress in situ (K_T) may be calculated by Equation 18 from the initial soil suction τ^o_{mo} (Table 8) pore water pressure u_w in the perched water table (Figure 14) and the overburden pressure p_o. Results of these calculations (Table 9) indicate a K_T of about 1 for the soil at Clinton. This value of K_T is smaller than the estimate obtained in Reference 12 from earlier data.

Lackland test site

111. Matrix suction, water content, and void ratio relationships were evaluated on specimens from boring No. 1, April 1973. Osmotic suctions of about 2 tsf were observed in the Upper Midway formation at depths greater than 13.1 ft. The overburden clay from 0.5 to 6.7 ft in depth contained negligible osmotic suctions. Undisturbed samples were not available at depths between 7 and 12 ft.

112. Initial void ratio. The initial void ratios at natural water content varied from 0.89 to 1.04 in the overburden at depths from 0.5 to 7.6 ft. The e_o varied from 0.77 to 0.95 in the Upper Midway formation below 13.1 ft of depth.

113. Initial matrix suction. The initial matrix suction τ^o_{mo} was relatively high at 4.3 tsf in the overburden near the ground surface (less than 1.0 ft), essentially zero at 3.2 to 4.2 ft, and 1.0 to 1.7 from 4.3 to 7.6 ft. The τ^o_{mo} varied from 2.0 to 5.2 tsf in the Upper Midway below 14.3 ft of depth.

114. Suction swell pressure. Suction swell pressures were

essentially zero for the near surface overburden at 4.2 ft or less in depth, 0.2 to 0.4 tsf in the overburden from 4.3 to 7.6 ft, and 0.8 to 5.0 in the Upper Midway below 13.1 ft in depth.

115. Compressibility factor. Compressibility factors varied from 0.91 to 1.00 in all of the test specimens.

116. Suction index. Suction indices C_τ were smallest in the near surface overburden clay varying from 0.087 to 0.105 between 0.5 to 4.2 ft in depth. The indices of deeper overburden material from 4.3 to 7.6 ft of depth varied from 0.151 to 0.206. The indices of the Upper Midway below 13.1 ft of depth varied from 0.123 to 0.228.

117. Ratio of horizontal to vertical stress. The ratio of total horizontal to vertical stress in situ (K_T) calculated by Equation 18 from the initial soil suction τ^o_{mo} (Table 8) pore water pressure u_w in the perched water table (Figure 17) and overburden pressure p_o are shown in Table 10. The K_T of the overburden soil is about 1. The K_T of the Upper Midway is about 3 between 20 and 40 ft of depth and about 2 at 45 ft of depth. These calculated values of K_T are consistent with those estimated from preliminary data in Reference 12. These high calculated values of K_T may be attributed to the high degree of consolidation of the Upper Midway.

Fort Carson test site

118. Matrix suction, water content, and void ratio relationships were evaluated for specimens from boring BOQ3, June 1973. Large osmotic suctions of 21 and 14 tsf were observed in samples 1 and 2, respectively. These samples were taken at depths less than 4 ft from the ground surface. The osmotic suctions in the remaining samples of the soil profile varied from 2 to 7 tsf.

119. Initial void ratio. Initial void ratios at natural water content varied from a maximum of 0.83 at about 2 ft below the ground surface, and decreased uniformly and rapidly with increasing depth to 0.53 at about 10 ft below ground surface. Void ratios varied from 0.53 to a minimum of 0.38 at about 23 ft with the smaller void ratios generally observed at the deeper depths.

120. Initial matrix suction. Initial matrix suction was about

1.4 tsf from the ground surface down to 3.6 ft, 0.5 to 1.1 tsf from 3.7 to 8.9 ft, and varied from 1.6 to 5.2 below 9.0 ft from the ground surface.

121. Suction swell pressure. Suction swell pressures varied from 0.2 to 0.7 tsf from the surface down to 14.6 ft and 0.8 to 3.9 tsf below 14.7 ft from the ground surface.

122. Compressibility factor. Compressibility factors varied from 0.67 to 0.84 from the ground surface to 13.3 ft, 0.90 to 0.91 from 13.5 to 18.6 ft, and 0.74 to 0.80 below 18.7 ft from the ground surface.

123. Suction index. Suction indices vary from 0.120 to 0.155 from the ground surface to 7.0 ft, and 0.067 to 0.103 below 7.0 ft from the ground surface.

124. Ratio of horizontal to vertical stress. The ratios of total horizontal to vertical stress in situ (K_T) calculated by Equation 18 from the initial soil suction τ^{o}_{mo} (Table 8) pore water pressure of the perched water table u_w (Figure 20) and the overburden pressure p_o are shown in Table 11. The K_T of the Pierre Shale varied between 1.8 to 3.8 for an average of about 3. These calculated values of K_T were consistent with K_T estimated from earlier data in Reference 12. These high calculated values of K_T may be attributed to the high degree of consolidation of Pierre Shale.

Sigonella test site

125. Matrix suction, water content, and void ratio relationships were evaluated for specimens from boring No. 1, November 1976. Osmotic suctions in the top 5.5 ft of soil were substantial, ranging between 6 to 12 tsf. Osmotic suctions below 6.5 ft varied from 2 to 6 tsf.

126. Initial void ratio. Initial void ratios down to 8 ft below ground surface varied from 0.90 to 0.94, while e_o below 11.5 ft varied between 0.66 to 0.82 ft.

127. Initial matrix suction. Initial matrix suctions varied from 0.50 to 0.78 tsf down to 12.5 ft of depth, while τ^{o}_{mo} between 16.5 to 24.5 ft vary between 1.0 to 1.3 tsf.

128. Suction swell pressure. Suction swell pressures varied from 0.21 to 0.33 tsf down to 8.0 ft from the ground surface, and varied

from 0.64 to 1.06 from 11.5 to 24.5 ft below ground surface.

129. Compressibility factor. Compressibility factors were close to one (0.83 to 0.93) in the entire soil profile except for the sandy clay layer at 16.5 to 17.5 ft in which α was 0.34.

130. Suction index. Suction indices varied from 0.134 to 0.289 in the soil profile except in the sandy clay soil layer in which C_τ was 0.085.

131. Ratio of horizontal to vertical stress. The ratio of total horizontal to vertical stress in situ (K_T) calculated by Equation 18 from the initial soil suction τ^o_{mo} (Table 8) pore pressure u_w (Figure 24) and the overburden pressure p_o shows that the K_T of the Sigonella soil was about 1.7. However, the Sigonella soil was not significantly overconsolidated at the test site, and the K_T is probably high. A K_T of 1 is used in the analysis of Sigonella soil. Some water contents were adjusted upward slightly to reflect the water content distribution shown on Figure 13.

Data correlations

132. Correlations of compressibility factor and suction swell pressure were checked as follows to determine consistency with the presentation given in PART II:

a. Compressibility factor versus plasticity index. The measured volumetric compressibility factor α versus the plasticity index PI, Figure 28, correlates reasonably well with the empirical equations in Table 4. However, these equations may frequently overestimate α for PI greater than about 30.

b. Initial matrix suction versus suction swell pressure. Most initial matrix soil suctions τ^o_{mo} are greater than the suction swell pressures p_s, Figure 29, as expected from theory. Some (about 25 percent) p_s exceed τ^o_{mo}, presumably from experimental error.

Mechanical Swell Test Results

133. Results of swell overburden, constant volume swell, and improved simple oedometer tests provided data on natural water content w_o, initial in situ void ratio e_o, void ratios e_{po} and e_s, swell

pressure p_s, swell index C_s, compression index C_c, coefficient of swell c_{vs} and coefficient of permeability k (see paragraphs 95-102). Individual swell tests usually required two to four weeks to complete, considerably longer than suction tests.

Clinton test site

134. The results of swell tests of soil from the Clinton test site are given in Table 13. The SO tests on the March 1973 boring samples were performed at several different vertical applied pressures p to permit evaluation of the percent swell S_p as a function of p, Figure 30. Results of CVS and ISO tests were previously reported in Reference 66. The ISO test results are those of consolidation tests on specimens soaked under the seating load of boring samples PU-2 of December 1968.

135. Void ratio. The results show that initial in situ void ratios of the loess overburden at depths less than 7 ft were on the order of 0.6 to 0.85, while void ratios of the Yazoo clay were on the order of 1.0 and greater. These void ratios are generally consistent with those observed from results of suction tests, Table 8.

136. The loess generally showed very little difference in void ratio between e_o, e_{po}, and e_s, which is indicative of very low swelling capability. In contrast, the Yazoo clay generally showed substantial differences between e_o, e_{po}, and e_s. Void ratios e_{po} and e_s of the SO test results were computed by Equation 43 using the data in Figure 30.

137. Swell index. Swell indices were approximated from results of the SO tests by Equation 41 using the data in Figure 30. Swell indices from results of the CVS and ISO tests were evaluated from Equation 40. Swell indices were the smallest (0.03 or less) for the loess soil at the shallow depths less than 7 ft. They were maximum at 0.05 to 0.14 for depths from 10 to 20 ft below ground surface, and 0.03 to 0.07 for depths below 20 ft.

138. Compression index. Compression indices were evaluated from results of the ISO tests. C_c is about 0.2 for soils at depths less than 7 ft, about 0.5 between 8 and 30 ft, and about 0.25 for 35 ft of

depth. Suction indices, Table 8, performed on similar specimens were usually less than compression indices, but greater than swell indices as determined in Reference 12.

139. Swell pressure. Swell pressures from the SO tests were evaluated from Figure 30. Swell pressures from results of the CVS and ISO tests were evaluated by the methods illustrated in Figures 26b and 26c. Swell pressures varied from 0.26 to 2.6 tsf for samples down to about 20 ft of depth. They were 2.7 or greater at depths of 30 to 35 ft below ground surface. The high swell pressures of 2.7, 5, and 13 tsf at about 30 ft are indicative of a highly desiccated soil. The suction p_s, Table 8, of similar specimens were generally not as large as the p_s from these swell tests.

140. Coefficient of swell. Coefficients of swell c_{vs} were evaluated by Equation 44 from the time-swell curves of the SO test results, and the time-consolidation curves of the ISO test results. The values of c_{vs} were small and on the order of 0.005 ft^2/day for soil deeper than 5 ft. Values varied from 0.01 to 0.05 ft^2/day for soil less than 5 ft in depth from the ground surface.

141. Coefficient of permeability. Falling head permeability tests were performed during ISO tests. Permeabilities obtained were on the order of 0.0001 ft/day below 10 ft of depth and varied from 0.001 to 0.004 ft/day at depths less than 5 ft below ground surface at the initial in situ void ratio. Permeabilities evaluated from flow data of the pressure plate tests were about 0.0001 ft/day in specimens taken from borings at depths greater than 10 ft below ground surface.

Lackland test site

142. Results of the laboratory swell tests on undisturbed specimens are given in Table 14. SO tests on specimens from samples of boring PU-7, December 1970, and boring No. 1, April 1973, were performed at several different vertical applied pressures to evaluate the percent swell S_p as a function of the pressure, Figure 31. Specimens from samples 11 and 17 of boring No. 1 were tested by the SO method, Table 7 (to evaluate the swell index using the procedure illustrated in Figure 26a), but recompressed to pressure exceeding the swell pressure to

evaluate the compression index. CVS and ISO tests were performed by the previously described procedures, Table 7. Undisturbed samples of the gravel overburden between depths of 7 and 12 ft below ground surface were not available for swell tests.

143. Void ratio. Initial in situ void ratios of the overburden soils varied over a wide range from 0.66 to 1.05. The wide range of void ratios was a result of the variable composition of the soil which contained CH and CL clays as well as considerable gravel and some sand. Void ratios of the Upper Midway ranged from 0.75 to 0.95. Void ratios encountered were generally consistent with those observed from results of suction tests, Table 8. Void ratios e_{po} and e_s were often significantly more than e_o, indicating some potential for swell.

144. Swell index. Swell indices of the overburden varied over a wide range from 0.02 to 0.09, reflecting the variable composition of the overburden. Swell indices of the Upper Midway varied from about 0.03 to 0.05.

145. Compression index. Compression indices varied from 0.13 to 0.27. These relatively low compression (recompression) indices reflect high maximum past pressures observed for these clay shales. Such pressures may be on the order of 14 tsf in the Upper Midway.[12,64] Compression indices obtained were about the same or greater than suction indices, Table 8.

146. Swell pressure. Swell pressures from SO test results were evaluated from Figure 31, except for specimens from samples 11 and 17 of boring No. 1, April 1973. The latter values of p_s were evaluated using the method illustrated in Figure 26a. Swell pressures evaluated from Figure 31 were very rough estimates due to scatter in the results. Swell pressures from results of the CVS and ISO tests were evaluated using the methods illustrated in Figures 26b and 26c.

147. Swell pressures in specimens from samples of boring PU-7 taken from near the ground surface were about 2.3 tsf, which reflect the drought of 1970. Swell pressures of 0.4 to 1.2 tsf in specimens of boring No. 1, also taken near the ground surface, were significantly smaller than those in PU-7 reflecting the wetter field conditions in

April 1973. Swell pressures near the gravel material at depths from 5 to 7 ft varied from 0.4 to 1 tsf. The p_s in the Upper Midway below the gravel at about 12 ft of depth were about 2.4 tsf and increasing to 6.7 tsf or possibly higher at about 30 ft of depth. Swell pressures were obtained generally consistent with suction p_s, Table 8, except for the extremely high pressures of 33 tsf for specimens from samples 15, 23, and 28 of boring No. 1, April 1973, extrapolated from the SO results.

148. Coefficient of swell. Coefficients of swell c_{vs}, were variable, ranging from 0.004 to 0.116 ft^2/day in the Upper Midway and 0.01 to 0.25 ft^2/day in the overburden. The overburden was generally more pervious than the Upper Midway.

149. Coefficient of permeability. Permeabilities k were on the order of 0.0003 to 0.05 ft/day depending on the specimen. There appeared to be no clear correlation of permeability with any of the soils. Permeabilities obtained from the pressure plate data were all less than 0.0001 ft/day and substantially less than the permeabilities determined from the swell tests.

Fort Carson test site

150. Results of laboratory swell tests on undisturbed specimens are given in Table 15. SO tests were performed by the procedure illustrated in Figure 26a and extended to determine p_s and rebounded to determine C_s. Some specimens were also recompressed to evaluate C_c. The coefficients of swell c_{vs} were evaluated by Equation 44 during inundation at pressure p_o. The CVS tests, performed by the procedure illustrated in Figure 26b, were extended to recompress the specimen to evaluate C_c. The ISO test was performed by the procedure illustrated in Figure 26c.

151. Void ratio. Initial in situ void ratios of the soil vary from a maximum of 0.6 at about 5 ft below the ground surface to 0.25 about 35 ft below ground surface. Initial void ratios of the soil suction data, Table 6, are consistent with these results.

152. Swell index. Swell indices from results of the ISO tests varied from a maximum of 0.042 at about 5 ft below ground surface to a

minimum of 0.007 at 30 ft of depth. Indices obtained are generally larger than those from results of the SO and CVS tests at similar depths.

153. Compression index. Compression indices C_c varied from a minimum of 0.045 at about 30 ft of depth to a maximum of 0.124 at about 5 ft of depth. These relatively low values were determined for pressures less than the maximum past pressure of about 39 tsf in the Pierre shale.[12] The C_c obtained were about the same, or slightly lower, than the suction indices, Table 8.

154. Swell pressure. Swell pressures p_s varied from 0.41 to 1.47 tsf for soil down to 15.7 ft below ground surface. The p_s at about 30 ft of depth varied from 2.37 to 4.60 tsf between the different swell tests. Suction swell pressures were generally slightly less than the swell pressures from these tests.

155. Coefficient of swell. Coefficient of swell c_{vs} evaluated from the SO results varied from a minimum of 0.005 ft^2/day at about 30 ft of depth to a maximum of 0.057 ft^2/day at about 15 ft of depth.

156. Coefficient of permeability. Coefficient of permeability k varied from 0.007 to 0.011 ft/day based on results of the CVS tests. The k evaluated from pressure plate flow data were significantly smaller and varied from a minimum of 0.0001 ft/day at 35 ft of depth to a maximum of 0.0005 ft/day at about 6 ft below ground surface.

Sigonella test site

157. Results of laboratory swell tests are given in Table 16. CVS and ISO tests were performed on specimens from undisturbed samples taken from the Sigonella test site in November 1976 using the procedures in Table 7. SO tests were not performed.

158. Void ratio. Initial in situ void ratios of the CH soils (all samples except No. 5 from 16.5 to 17.5 ft of depth) varied from 0.756 to 0.979. The e_o of the CL soil of sample No. 5 vary from 0.685 to 0.701 and are smallest of the void ratios.

159. Void ratios e_{po} from the CVS results of specimens from samples 2 to 5 below 4 ft of depth were less than e_o, indicating consolidation following application of the overburden pressure p_o. The e_{po} of specimens from the ISO test results of sample 2 (4.0 to 5.5 ft) and

samples 4, 5, and 6 (11.5 to 24.5 ft) were about the same, or also less than e_o .

160. Swell index. Swell indices C_s of the CVS results varied from 0.017 to 0.025 except for specimens from samples 4 and 5 from 11.5 to 17.5 ft of depth. Indices for these were small at 0.006, indicating little potential for swell. The C_s of the ISO results were substantially larger varying from 0.03 to 0.062, except for a specimen from sample No. 5 at 16.5-17.5 ft of depth. The C_s of this specimen was 0.018, and smallest of the swell indices.

161. Compression index. Compression indices evaluated from results of the ISO tests were about 0.2. Suction indices, Table 8, were about the same or less than these C_c and substantially larger than C_s .

162. Swell pressure. Swell pressure p_s could not be evaluated from the CVS test results of specimens from samples 2 to 6 (below 4 ft of depth) because these specimens consolidated following inundation with water. The p_s were all less than the respective p_o . The p_s of sample 1 (1.5 to 3.5 ft of depth) was 0.43 tsf.

163. Results of the ISO tests indicated the largest swell pressure (1.4 tsf) in a specimen of sample 1. The p_s in specimens from deeper samples varied between 0.22 to 1.10 tsf. The p_s of specimens from samples 2, 5, and 6 were less than p_o . Swell pressures determined from the soil suction data, Table 8, were similar to swell pressures evaluated from these swell tests.

164. Coefficient of swell. Coefficient of swell c_{vs} computed from ISO results for inundation at 0.08 tsf varied from 0.0034 to 0.0006 ft^2/day for specimens from all the samples except No. 5. The c_{vs} of a specimen from No. 5 was 0.037, the largest of the coefficients.

165. Coefficient of permeability. Coefficient of permeability k measured from falling head permeability tests and void ratios near the in situ void ratio during the CVS tests varied from 0.0002 to 0.003 ft/day, except for a specimen of sample No. 5. The k of the specimen from No. 5 was substantially larger at 0.48 ft/day.

PART V: ANALYSES OF POTENTIAL HEAVE AND HEAVE WITH TIME

166. Analyses of potential heave and heave with time include a study to determine parameters that are most significant in causing heave, and a study of heave at field test sites. The parametric study was performed to develop empirical equations for predicting heave and heave with time in swelling foundation soils for use in designs of foundations where minimal soil data are available. The study of heave at field test sites was performed to provide verification of the reliability of the procedures and the computer program ULTRAT developed as part of this study. A users guide and listing of ULTRAT are given in Appendix G.

Parameters Affecting Heave

167. A parametric analysis was performed using the soil suction model with input parameters given in Table 17. The A and B parameters were estimated from matrix suction-water content-plasticity index relationships developed by Black[82] based on the properties of remolded British soils. The compressibility factor α was estimated by the equations in Table 2. A specific gravity G_s of 2.70 and a ratio of total horizontal to vertical stress K_T of 1.0 were assumed for the analysis. Initial water contents w_o taken for each plasticity index are consistent with the assumed matrix suction-water content relationships. Initial void ratios e_o were also chosen consistent with the above data.

168. A coefficient of saturated permeability k_s of 0.0001 ft/day was frequently used during the analysis of heave with time. The time increment DT for all analyses was set at 1 day. The mechanical swell model was also used with input parameters, Table 17, equivalent to those of the suction model, to investigate the relationship between the coefficient of swell c_{vs} and the coefficient of saturated permeability k_s for the chosen soil properties. A comparison of the model in Table 17 shows an advantage of the soil suction model, i.e.,

for the soil suction model only the soil suction-water content relationship needs to be determined for the range of water contents expected in the field, whereas for the mechanical swell model, a swell test must be performed at each water content.

169. The parametric analysis, performed for homogeneous soils of thicknesses from 5 to 20 ft below the ground surface, is sufficient for evaluation of potential heave and heave with time in swelling soil beneath a slab foundation above a stationary water table or above a stable, nonswelling stratum. Other parameters investigated to determine effects on heave include surcharge pressure q and the area of the slab foundation placed on the ground surface. The pressures q used in the parameter analyses were 0.072, 0.15, and 0.3 tsf. The areas were square with sides of 10, 25, 50, 100, and 200 ft.

Potential heave

170. Preliminary analysis. The preliminary analysis indicated that increasing the thickness of the soil element DX, Figure 1, from 0.125 to 0.5 ft reduced the predicted potential heave by only 3 percent. All remaining analyses were therefore performed using an element thickness of 0.5 ft to minimize computer costs. Increasing the covered area from 10- by 10-ft square to 200- by 200-ft square, or a 400 fold increase, reduced predicted potential heave by less than 5 percent for soil thicknesses less than 20 ft. Therefore, all remaining analyses were performed using a standard 100- by 100-ft square area similar to the dimensions of the field test sections.

171. Empirical formulations. Typical results, Figure 32, show that the predicted percent potential heave of a soil with a SAT moisture profile (paragraph 59) is reduced by increasing surcharge pressure q, increasing initial water content w_o of a given soil type, and increasing depth of soil H. Analysis of results for all five soil types indicated that the percent of potential heave may be predicted by the following equations:

$$PI \geq 40 \quad S_p = 24 + 0.76PI - 2.5q(1 + 0.1412PI) - 1.7w_o + 0.0025PI(w_o - 4H) - 0.14H - 0.08qH(1 - 0.2PI) \qquad (45a)$$

$$PI \leq 40\ S_p = -9 + 1.58PI - 2.5q(1 + 0.1412PI) + 0.1w_o$$

$$-0.0133PI(3.25w_o + H) + 0.09H - 0.08qH(1 - 0.2PI) \quad (45b)$$

where

S_p = percent potential heave, $\Delta H/H \times 100$

ΔH = potential heave, ft

H = depth of soil, ft

PI = plasticity index, percent

q = surcharge pressure, tsf

w_o = initial water content, percent

Assuming q is 0.072 tsf (1 psi) simulating a lightly loaded slab foundation, percent potential heave may be predicted by

$$PI \geq 40\ S_p = 23.82 + 0.7346PI - 0.1458H - 1.7w_o + 0.0025PIw_o$$

$$- 0.00884PIH \quad (46a)$$

$$PI \leq 40\ S_p = -9.18 + 1.5546PI + 0.08424H + 0.1w_o - 0.0432PIw_o$$

$$- 0.01215PIH \quad (46b)$$

The effect of pressure q on heave beneath a slab foundation is small for small surcharge pressures as compared with the effect of PI, w_o, and H.

172. Analysis of results of a HYD moisture profile (paragraph 59) for all five soil types indicated that percent potential heave S_p is less than that of a SAT profile, and the difference increases with decreasing PI, increasing w_o for a given soil type, and increasing H. Percent potential heave of a HYD profile may be empirically predicted by

$$PI \geq 40\ S_p = 23 + 0.675PI - 0.6H - 1.5w_o \quad (47a)$$

$$PI \leq 40\ S_p = -13 + 1.6PI + 0.2H - 0.02PIH - 0.0375PIw_o \quad (47b)$$

where q is 0.072 tsf.

Heave with time

173. Adjustments of the diffusion equation. Adjustment of the diffusion equation to include the volume parameter $\bar{C}$, Equation 23, substantially increases the time (about double) required to reach a certain fraction heave F for highly swelling soils of PI 80, as compared with the time required using the uncorrected diffusion equation where $\bar{C}$ is zero, Figure 33. The difference in time will be less for soils of smaller PI. Fraction heave is defined as

$$F = \frac{\Delta HT}{\Delta H} \tag{48}$$

where ΔHT is the heave observed at some given time, Equation 10.

174. Adjustment of the diffusion equation by using both the volume parameter $\bar{C}$ and permeability computed by Equation 25 resulted in nearly identical fraction heaves with time for the same soil using different initial water contents, Figures 33 and 34. The difference was less than 10 percent. All subsequent computations of heave with time were performed with the diffusion Equation 23 using the volume parameter $\bar{C}$ and permeability as defined by Equation 25.

175. Effect of parameters. A preliminary analysis indicated that reducing the thickness of elements increases the time required to achieve a certain fraction F, Figure 35. All subsequent analyses were performed with an element thickness of 0.5 ft because both computation time and accuracy appeared reasonable.

176. Results of the analysis indicated that fraction heave with time is relatively insensitive to PI, w_o of a given soil, amount of potential heave ΔH, and equilibrium moisture profile of either SAT or HYD (Figures 34, 36-38). Time was influenced primarily by fraction heave, depth of soil, and coefficient of permeability, empirically derived as

$$t = \frac{0.0086 F^3 H^{1.73}}{k_s} \tag{49}$$

where t is the time in days. Equation 49 is reasonable considering

past experience that field heave with time is consistent with a parabolic shape similar to that for consolidation with time.[15-18]

177. Predictions of heave with time using Equation 49 are compared with results from the program ULTRAT for a highly swelling soil in Figure 35. Decreasing element thickness, thereby increasing accuracy of the solution, causes results of ULTRAT to converge toward the results of the empirical Equation 49 up to a fraction heave F of 0.9. Differences in results of the empirical Equation 49 from results of program ULTRAT are not practically significant, especially since most heave already occurred for F exceeding 0.9.

178. Application of the mechanical swell model shows some differences in the shape of the fraction heave with time curve, Figure 39:

$$t = \frac{0.9F^{3.33}H^{2.25}}{c_{vs}} \tag{50}$$

The analytical solution of time for heave assuming a homogeneous, saturated soil with constant c_{vs} is[57]

$$t = \frac{(H/N)^2}{c_{vs}} T_3 \cong \frac{0.9F^3H^2}{c_{vs}} \tag{51}$$

where

N = 1 for single drainage (fraction of volumetric swell that occurs as heave in the vertical direction)

T_3 = time factor for Case 3, triangular stresses with single drainage at the base of the foundation

For reasonable agreement with the suction model, coefficient of swell c_{vs} using Equation 51 was slightly less than that for Equation 50 (Figure 39). For this example c_{vs} is about 200 times k_s.

179. Comparison of Equations 49 and 50 indicates that c_{vs} is empirically related to permeability by

$$c_{vs} \cong 100F^{1/3}H^{1/2}k_s \tag{52}$$

Equation 50, rather than Equation 51, was used in this comparison because errors from the finite difference approximations that led to both Equations 49 and 50 are similar. Since[56]

$$c_{vs} = \frac{k_s}{\gamma_w m_v} \tag{53}$$

where m_v is the coefficient of volume change in tsf.$^{-1}$ Combining Equations 52 and 53 results in

$$m_v = \frac{1}{3F^{1/3}H^{1/2}} \tag{54}$$

Consistent with other observations,[56] m_v decreases with increasing depth H (or increasing stress) and fraction F.

Heave of Field Test Sites

180. Heave at the field test sites described herein were far from complete as indicated by the generally increasing observed heave with time curves of the Clinton, Figure 15, Lackland, Figure 18, and Fort Carson, Figure 21 test sections. Significant additional heave is expected at each site over the next several years. Maximum observed heave is extrapolated in Figure 40 to arrive at estimates of the total in situ or ultimate heave and heave with time at each site. These observed trends and extrapolations are sufficient to permit useful comparisons with various methods for predicting potential heave and heave with time. Because the field observations indicate relatively substantial heave below the depth of perched groundwater levels at some test sites as illustrated in Figure 40, analyses were performed for potential heave above the groundwater level, that due to a rise in the groundwater level, and heave caused by wetting of desiccated zones below existing perched water tables. Analyses of heave with time were made for depths extending to the bottom of perched water tables. Predictions of potential heave at Sigonella are also included for general interest, although observations of field heaves are not available.

Potential heave

181. Above the water table using empirical methods. Potential heave above the water table was computed for the study field test sites using the empirical methods described in Table 18 in addition to potential heaves predicted by Equations 46 and 47. Input data required for these methods are given in Table 19. These methods, except Equations 46 and 47, were developed from results of mechanical swell tests. All of these methods, except Equation 47, assume a saturated equilibrium moisture profile. Volumetric swell is assumed to occur in the vertical direction. All of these methods are relatively simple to use. However, McDowell[83] and McKeen[84] methods require graphs. In using the McDowell method a judgment of how initial water content compared with maximum and minimum water contents is needed. Initial and final soil suctions are required to use the McKeen method. The plasticity index was assumed equal to the shrinkage limit herein to permit use of the McKeen method.

182. Empirical predictions of potential heave are compared with actual heave observed at field test sites in Table 20. These comparisons show that methods developed by McDowell,[83] McKeen,[84] Schneider and Poor,[87] Vijayvergiya and Ghazzaly,[88] Van Der Merwe,[90] and Equation 46 show the best overall correlations with observed and extrapolated field heave to date. Heave predicted by Equation 47 for a hydrostatic equilibrium moisture profile was somewhat less than heave predicted by Equation 46. A potential vertical rise (PVR), which is defined as 1/3 of the volumetric swell using McDowell's method,[83] is definitely too low.

183. Future field observations may show that some extrapolated heaves based on results of some of these methods may be low for at least one of the three field cases. Results predicted by Equation 46 appear to present good agreement and consistent upper limits of potential heave at these test sites. The good agreement using Van Der Merwe's method is interesting since only the plasticity index, percent clay content, and location of swelling soil in the profile is needed. However, initial water content or soil suction should also have a significant effect on the actual heave.

184. Potential heave using suction and mechanical swell models. Input data for the suction and mechanical swell models using results of laboratory tests are given in Table 21. Predictions of potential heave for soil profiles extending to a depth of 25 ft at Clinton, 34 ft at Lackland, 30 ft at Fort Carson, and 25 ft at Sigonella are shown in Table 22. These depths are near the bottom of perched water tables, except at Sigonella where the water table appears continuous. Predictions using results of the ISO tests appear to be excessive at the Clinton and Lackland test sites. Predictions using results of the CVS tests may be inadequate at the Fort Carson test site. The soil suction model appears to provide the best overall predictions of potential heave. Deficiencies in these heave predictions may be due to inadequate simulation of field conditions and sample disturbance. Predictions of potential heave may be corrected to some extent by computing potential heave above the original water table only at the time of construction, and adding potential heave due to a rise in the water table following construction. Heave from a rising water table will probably not contribute to differential heave provided soils and loading beneath the foundation are uniform.

185. Predictions above the water table. Results of predictions of potential heave above the water table, Table 23, show that the suction model provides an upper limit consistent with field observations. Results of the mechanical swell model using laboratory swell test results usually provide lower predictions of potential heave which are fairly consistent with results from empirical methods. This was expected since these empirical methods were usually developed from results of mechanical swell tests.

186. Some predictions of potential heave using the mechanical swell model may turn out to be too low after several more years of field observations. Predictions of heave at the Lackland test site using SO test results have already proved too low. These predictions were computed from data of specimens taken from the April 1973 boring samples several months prior to construction of the test section. Predictions of potential heave at the Fort Carson test site using CVS results also

proved too low, as may predictions using SO and ISO results after further field observations. Predictions of potential heave at the Clinton test site may be low using SO and ISO results. Predictions of potential heave using the suction model and suction data appear adequate for all three test sites. Predictions of potential heave at Sigonella are consistent with those reported earlier.[67]

187. Predictions from a rising water table. Results of predictions of potential heave for a rising water table, Table 24, show that both ISO results of the mechanical swell model, and results of the suction model are about the same or exceed the heave actually observed or extrapolated within the water table for the Clinton and Lackland sites. Heave predicted for the hydrostatic profile for a rising water table are usually slightly more than those for a saturated profile. Such heaves would probably not be fully realized because droughts and low rainfalls should allow the water table to fall periodically.

188. Total potential heave due to swell (a) above the water table, and (b) rise of the water table are shown in Table 25, and compared favorably with total observed and extrapolated heaves. Little difference exists between results of the SAT and HYD moisture profiles. Results of SO tests predict inadequate heave for the Clinton and Fort Carson test sites. Predictions using SO test results will also probably prove to be inadequate for the Lackland test site when compared with future field observations. Predicted potential heave using CVS and ISO test results are inadequate for the Fort Carson test site. Predictions of potential heave using the suction model appear to be adequate for all of the test sites, and may provide a reasonable upper limit of heave.

189. Potential heave in desiccated zones. Predictions of potential heave below the perched water table at the Clinton, Lackland, and Fort Carson test sites were made for desiccated zones using the suction model and data in Table 21. Depth of desiccated zones are assumed to extend only to 50 ft below ground surface although such zones actually extend to deeper depths. However, calculations predicting heave can provide trends expected if desiccated zones are wetted to hydrostatic

water pressures from the original groundwater level to 50 ft below ground surface.

190. Additional heave predicted for test sites are

	Test Site		
	Clinton	Lackland	Fort Carson
Predicted heave for saturated moisture profile, ft	1.07	0.16	0.91
Depth of desiccated zone, ft	25 to 50	34 to 50	30 to 50
Original groundwater level, ft	5	8	3

As indicated above predicted potential heave at the Clinton and Fort Carson test sites could be close to 1 ft, while that at Lackland much less. These rough predictions emphasize the importance of avoiding placement of foundations and footings into desiccated zones beneath perched water tables thereby disturbing the desiccated zones.

Heave with time

191. Predictions of heave with time can only be roughly computed in this study because field permeabilities are uncertain, and some heave originates below the perched water tables at the Clinton and Lackland test sites. Furthermore, the program ULTRAT is limited to computing heaves with time for uncorrected potential heaves as illustrated by Table 22. Some of the values shown therein are not considered reasonable. Deficiencies in the state-of-the-art and need for additional long-term field observations at test sites preclude extensive analyses of heave with time. Detailed analyses will be made following completion of future field observations.

192. The parametric study described herein led to development of empirical equations which illustrate that time needed for heave to develop is essentially independent of the potential heave. Therefore, Equations 49, 50, and 51 may be used to roughly predict heave with time based on corrected potential heave, Table 25, assuming homogeneous saturated soil profiles. These preliminary analyses of heave with time were performed for the three field test sites where field observations were available for comparison using Equations 49 to 51 and respective corrected potential heave.

193. The effective coefficients of permeability k_s and swell c_{vs} used in Equations 49 to 51 were functions of the availability of water and fissures in the soil mass as well as functions of other properties of the soil. Droughts, for example, reduce the availability of water and prolong the time needed for heave. Effective coefficients of permeability k_s and swell c_{vs} were estimated by matching extrapolated heave from Figure 40 for soil down to depths of 25, 34, and 30 ft at the Clinton, Lackland, and Fort Carson test sections, respectively. Results of this matching indicated a maximum effective k_s of about 0.0001 ft/day and a maximum effective c_{vs} of about 0.02 ft^2/day, Figure 41. Among the lowest of the laboratory observed permeabilities was a k_s of 0.0001 ft/day, which was representative of permeabilities obtained from pressure plate tests. A value of 0.02 ft^2/day was representative of the relatively large coefficients calculated from swell tests.

194. Predicted heave with time using the above values of k_s and c_{vs} in Equations 49 to 51 are compared below with heave observed at field test sections. Predicted heave with time results from the entire volumetric swell occurring in the vertical direction. Fissures can reduce heave in the vertical direction to as little as 1/3 of volumetric swell. These analyses do not include heave in desiccated zones below perched water tables at field test sections.

195. Clinton test site. Results of the suction tests over-predict observed heave with time, whereas results of the CVS and ISO tests were in reasonable agreement except for extrapolated long-term heaves, Figure 42. Results of the SO tests were too low.

196. Lackland test site. Results of the suction and ISO tests appeared to agree reasonably well with observed heave with time, whereas results of CVS and SO tests were too low, Figure 43. Predictions of Equation 51 fell between the predictions of Equations 49 and 50.

197. Fort Carson test site. Results of the suction tests appeared to agree reasonably well with observed heave with time, whereas results of the SO, CVS, and ISO tests appear too low, Figure 44. Predictions by Equation 51 fell between the predictions of Equations 49 and 50.

198. Although these predictions of heave with time may be speculative because of the complex nature of field swelling and simplifying assumptions made for these analyses, a comparison of the predictions of heave with time using corrected potential heaves, Table 25, the suction model, and Equations 49 to 51 indicate that these predictions provide reasonable upper limits. Results of the mechanical swell tests do not apparently provide adequate levels of predicted heave with time for all three test sites, especially since heave predicted from the rising water tables, Table 24, would probably not be fully realized. Equation 50 leads to slower rates of heave than Equation 49, although c_{vs} is relatively large and k_s is relatively small as compared with laboratory results. Relatively small k_s are needed in Equation 49 to match field rates of heave because Equation 49 was derived from the suction model which predicts much larger swelling ability in soils than the mechanical swell model. Heave predicted using Equation 51 occurs slightly faster than that predicted from Equation 50. Using the suction model and assuming an N of 1/3, rather than N of 1, provides estimates of heave in the range of the lower observed limits.

PART VI: CONCLUSIONS

199. The nature of field heave is complex as illustrated by the need to consider numerous variables as described herein for proper analysis and prediction of potential heave and heave with time in swelling foundation soils. The computer program ULTRAT is capable of simulating numerous field conditions for predictions of 1D potential heave and heave with time beneath foundations in swelling soils using the suction and mechanical swell models; this program is practical, economical, and easy to use.

200. Analysis of the diffusion theory shows that a parameter must be included in the diffusion equation to properly account for the effect of volume change on the time to achieve heave. Inclusion of the volume parameter in the diffusion equation significantly increases the time predicted to achieve heave in highly swelling soils, while little difference occurs for low swelling soils. The diffusion equation was also modified to include a variable coefficient of permeability which is dependent on the degree of saturation and void ratio. These were found to affect the time predicted to achieve heave.

201. Comparison of laboratory procedures between the suction and mechanical swell models for characterization of swell behavior shows that suction tests are simple, economical, and expedient. The suction model was also found capable of simulating field conditions, such as the degree of saturation and lateral pressures, better than the mechanical swell model. Also swell tests are required to be performed for each initial water content, whereas suction tests need be performed only to evaluate the suction-water content relationship for the range of water contents encountered in the field.

202. A parametric analysis using the program ULTRAT and published soil suction data led to the development of empirical equations for predictions of potential heave and heave with time in swelling homogeneous soils beneath slab foundations above a water table, or above nonswelling soils for saturated and hydrostatic equilibrium moisture profiles. The saturated moisture profile was found to provide the most conservative

predictions of potential heave. Relatively easy to obtain data was needed to use these equations. Potential heave was found to be primarily a function of the plasticity index, initial water content, and depth of the soil subject to swelling for lightly loaded slab foundations. Time required to achieve predicted heave was found to be primarily a function of the fraction of potential heave, depth of the soil, and the coefficients of permeability or swell.

203. Field observations of vertical movement at field test sites indicate that heave has increased with time beneath test sections and potential exists for significant additional future heave over many years. Differential heave beneath test sections varied from negligible to 75 percent of the maximum observed heave depending on time of observation. The largest fraction difference was observed at the Fort Carson test section, which has a deep, low permeable swelling soil with a high water table near the ground surface. Several empirical methods provided useful predictions of potential heave. Of those, the empirical equation for prediction of potential heave of a saturated equilibrium moisture profile, Equation 46, compared favorably with observed field heave and appears to provide reasonable upper limits for all test sites.

204. Predictions of potential heave using the soil suction model of the program ULTRAT and soil suction data measured with undisturbed samples from the test sites provide adequate and reasonable upper limits for all test sites when compared with field observations. Lower limits can be estimated by assuming an N of 1/3 instead of 1. Predictions of potential heave using the mechanical swell model and swell test results often proved too low and were actually representative of minimum heave when compared with field observations. The conclusion that swell tests may not provide adequate predictions of potential heave is consistent with previous observations.[78,92]

205. Preliminary analysis of heave with time using the empirical Equations 49 to 51 (with corrected predicted potential heaves of the suction model) provide practical and reasonable upper limits, whereas results of mechanical swell tests often provide predictions that are too low and are more representative of minimum heave with time at the

field test sites. The empirical equations developed herein for predicting heave with time are consistent with the analytical Terzaghi model, Equation 51, except that the effective coefficient of permeability is needed in the equation using the suction model, Equation 49. The maximum probable effective coefficients of permeability and swell were found to be 0.0001 ft/day and 0.02 ft^2/day, respectively.

PART VII: RECOMMENDATIONS

206. Observations of heave at the field test sites should be continued as long as practical to confirm predictions of potential heave and heave with time made as part of this study.

207. Results of both laboratory soil suction and mechanical swell tests on undisturbed specimens would be helpful to develop reasonable upper and lower limits of the potential heave. Soil suction-water content relationships should be determined at frequent intervals; e.g., 1 or 2 ft increments with at least five tests for each soil stratum. At least five identical CVS and/or ISO tests should be performed within each stratum to the groundwater table or the bottom of the active zone.

208. Analyses should be performed using both the soil suction and mechanical swell models in an attempt to provide reasonable upper and lower limits of the potential heave. Several of the better empirical methods should be used simultaneously as cross-checks to roughly predict potential heave; e.g., Equation 46, McKeen, McDowell, Schneider & Poor, Vijayvergiya & Ghazzaly, and Van der Merwe methods. As many field conditions as possible should be accounted for to improve predictions; therefore, the program ULTRAT or better techniques as they become available are recommended.

209. Research is needed to determine reliable procedures for evaluating effective coefficients of permeability and swell (or their equivalent) to permit practical predictions of heave with time. These effective coefficients should consider availability of water and the environmental conditions as well as actual field coefficients of permeability and swell.

REFERENCES

1. Kaplar, C. W., "Phenomenon and Mechanism of Frost Heaving," Highway Research Record 304, Highway Research Board, National Research Council, Washington, D. C., 1970, pp 1-13.

2. Dempsey, B. J., "Climatic Effects on Airport Pavement Systems; State of the Art," Contract Report S-76-12, Jun 1976, U. S. Army Engineer Waterways Experiment Station, CE, Vicksburg, Miss; prepared by B. J. Dempsey under Contract No. DACW39-75-M-1651.

3. Johnson, L. D., Sherman, W. C., Jr., and McAnear, C. L., "Field Test Sections on Expansive Clays," Proceedings, Third International Conference on Expansive Soils, Jul 30-Aug 1, 1973, Haifa, Israel, Vol 1, 1973, pp 239-248.

4. Jones, D. E., Jr., and Holtz, W. G., "Expansive Soils--The Hidden Disaster," Civil Engineering, Vol 43, No. 8, Aug 1973, pp 49-51.

5. Johnson, L. D. and Stroman, W. R., "Analysis of Behavior of Expansive Soil Foundations," Technical Report S-76-8, Jun 1976, U. S. Army Engineer Waterways Experiment Station, CE, Vicksburg, Miss.

6. Snethen, D. R. et al., "A Review of Engineering Experiences with Soils in Highway Subgrades," Report No. FHWA-RD-75-48, Jun 1975; prepared for the Federal Highway Administration, Washington, D. C., U. S. Army Engineer Waterways Experiment Station, CE, Vicksburg, Miss.

7. Wong, H. Y., Unsaturated Flow in Clay Soils, Ph. D. Thesis, Department of Civil Engineering and Applied Mechanics, McGill University, Montreal, Quebec, 1974.

8. Johnson, L. D. and Snethen, D. R., "Review of Expansive Soils," Journal, Geotechnical Engineering Division, American Society of Civil Engineers, Vol 101, No. GT2, Feb 1975, pp 213-214.

9. Ullrich, C. R., An Experimental Study of the Time-Rate of Swelling, Ph. D. Thesis, Department of Civil Engineering, University of Illinois, Urbana, 1975.

10. Skempton, A. W., "Long-Term Stability of Clay Slopes," Geotechnique, Vol 14, No. 2, 1964, pp 77-102.

11. James. P. M., "The Role of Progressive Failure in Clay Slopes," Proceedings, First Australia-New Zealand Conference on Geomechanics, Aug 9-13, 1971, Melbourne, Vol 1, 1971, pp 344-348.

12. Johnson, L. D., "Evaluation of Laboratory Suction Tests for the Prediction of Heave in Foundation Soils," Technical Report S-77-7, Aug 1977, U. S. Army Engineer Waterways Experiment Station, CE, Vicksburg, Miss.

13. Johnson, L. D., "Review of Literature on Expansive Clay Soils," Miscellaneous Paper S-69-24, Jun 1969, U. S. Army Engineer Waterways Experiment Station, CE, Vicksburg, Miss.

14. Johnson, L. D. and Desai, C. S., "A Numerical Procedure for Predicting Heave," Proceedings, Second Australia-New Zealand Conference on Geomechanics, Jul 21-25, 1975, Brisbane, Australia, 1975, pp 269-273.

15. Jennings, J. E. and Kerrich, J. E., "The Heaving of Buildings and the Associated Economic Consequences, with Particular Reference to the Orange Free State Goldfields," Civil Engineer in South Africa, Vol 4, No. 11, Nov 1962, pp 221-248.

16. Abelev, Y. M., Sazhin, V. S., and Burov, E. S., "Deformational Properties of Expansive Soils," Proceedings, Third Asian Regional Conference on Soil Mechanics and Foundation Engineering, Sep 25-28, 1967, Haifa, Israel, Vol 1, 1967, pp 57-59.

17. Donaldson, G. W., "A Study of Level Observations on Buildings as Indications of Moisture Movements in the Underlying Soil," Moisture Equilibria and Moisture Changes in Soils Beneath Covered Areas, A Symposium in Print, G. D. Aitchison, ed., Butterworth, Australia, 1965, pp 156-163.

18. Sokolov, M. and Amir, J. M., "Moisture Distribution in Covered Clays," Proceedings, Third International Research and Engineering Conference on Expansive Soils, Jul 30-Aug 1, 1973, Haifa, Israel, Vol 1, 1973, pp 129-136.

19. Redus, J. F., "Field Moisture Content Investigation: Oct 1945-Nov 1952 Phase," Technical Memorandum No. 3-401, Report 2, Apr 1955, U. S. Army Engineer Waterways Experiment Station, CE, Vicksburg, Miss.

20. Womack, L. M., Mathews, M. J., and Fry, Z. B., "Field Moisture Content Investigation: Nov 1952-May 1956 Phase," Technical Memorandum No. 3-401, Report 3, May 1961, U. S. Army Engineer Waterways Experiment Station, CE, Vicksburg, Miss.

21. Biot, M. A., "General Theory of Three-Dimensional Consolidation," Journal of Applied Physics, Vol 12, No. 2, Feb 1941, pp 155-164.

22. _____, "Theory of Elasticity and Consolidation for a Porous Anisotropic Solid," Journal of Applied Physics, Vol 26, No. 2, Feb 1955, pp 182-185.

23. Josselin De Jong, G., "Application of Stress Functions to Consolidation Problems," Proceedings, Fourth International Conference on Soil Mechanics and Foundation Engineering, Aug 12-24, London, Vol 1, 1957, pp 320-323.

24. McNamee, J. and Gibson, R. E., "Displacement Functions and Linear Transforms Applied to Diffusion Through Porous Elastic Media," Quarterly Journal of Mechanics and Applied Mathematics, Vol 13, Feb 1960, pp 98-111.

25. Gibson, R. E., Schiffman, R. L., and Pu, S. L., "Plane Strain and Axially Symmetric Consolidation of a Clay Layer on a Smooth Impervious Base," Quarterly Journal of Mechanics and Applied Mathematics, Vol 16, No. 4, Nov 1970, pp 505-520.

26. Sandhu, R. S. and Wilson, E. L., "Finite Element Analysis of Seepage in Elastic Media," Journal, Engineering Mechanics Division, American Society of Civil Engineers, Vol 95, No. EM3, Jun 1969, pp 641-652.

27. Yokoo, Y., Yamagata, K., and Nagaoka, H., "Finite Element Method Applied to Biot's Consolidation Theory," Soils and Foundations, Vol 11, No. 1, Mar 1971, pp 29-46.

28. Christian, J. T. and Boehmer, J. W., "Plane Strain Consolidation by Finite Elements," Journal, Soil Mechanics and Foundation Division, American Society of Civil Engineers, Vol 96, No. SM4, Jul 1970, pp 1435-1457.

29. Hwang, C. T., Morgenstern, N. R., and Murray, D. W., "On Solutions of Plane Strain Consolidation Problems by Finite Element Methods," Canadian Geotechnical Journal, Vol 8, No. 1, Feb 1971, pp 109-118.

30. Richards, B. G., "The Use of the Finite Element Method in the Solution of the Flow Equations in Soils," Proceedings, First International Conference on Finite Element Methods in Engineering, University of New South Wales, Australia, 1974, pp 533-537.

31. Chang, C. S., Analysis of Consolidation of Earth and Rockfill Dams, Ph. D. Thesis, Department of Civil Engineering, University of California, Berkeley, 1976.

32. Jennings, J. E. B. and Burland, J. B., "Limitations to the Use of Effective Stresses in Partly Saturated Soils," Geothechnique, Vol 12, No. 2, 1962, pp 125-144.

33. Lytton, R. L. and Watt, W. G., "Prediction of Swelling in Expansive Clays," Research Report 118-4, Sep 1970, Center for Highway Research, University of Texas, Austin.

34. Lytton, R. L. and Kher, R. K., "Prediction of Moisture Movement in Expansive Clays," Research Report 118-3, May 1970, Center for Highway Research, University of Texas, Austin.

35. Selim, H. M. E., Transient and Steady Two-Dimensional Flow of Water in Unsaturated Soils, Ph. D. Thesis, Iowa State University, published by University Microfilms International, Ann Arbor, Mich., 1974.

36. Elzeftawy, A. A., Water and Solute Transport in Lakeland Fine Sand, Ph. D. Thesis, Department of Civil Engineering, University of Florida, Gainesville, 1974.

37. Dewet, J. A., "The Time-Heave Relationship for Expansive Clays," Transactions, South African Institution of Civil Engineers, 1957, Vol 7, No. 9, pp 282-298.

38. Blight, G. E., "The Time-Rate of Heave of Structures on Expansive Clays," Moisture Equilibria and Moisture Changes in Soils Beneath Covered Areas, Symposium in Print, G. D. Aitchison, ed., Butterworth, Australia, 1965, pp 78-88.

39. Knight, K. and Greenberg, J. A., "The Analysis of Subsoil Moisture Movements During Heave and Possible Methods of Predicting Field Rates of Heave," Civil Engineer in South Africa, Feb 1970, Vol 12, No. 2, pp 27-31.

40. Johnson, L. D., "An evaluation of the Thermocouple Psychrometric Technique for the Evaluation of Suction in Clay Soils," Technical Report S-74-1, Jan 1974, U. S. Army Engineer Waterways Experiment Station, CE, Vicksburg, Miss.

41. Snethen, D. R., Johnson, L. D., and Patrick, D. M., "An Investigation of the Natural Microscale Mechanisms that Cause Volume Change in Expansive Clays," Report No. FHWA-RD-77-75, Jan 1977, U. S. Army Engineer Waterways Experiment Station, CE, Vicksburg, Miss.; prepared for the Federal Highway Administration, Washington, D. C.

42. Snethen, D. R. and Johnson, L. D., "Characterization of Expansive Soil Subgrades Using Soil Suction Data," Moisture Influence on Pavement Materials Characterization and Performance, presented at the 56th Annual Meeting, Transportation Research Board, National Research Council, Jan 24-28, 1977, Washington, D. C.

43. Olson, R. E. and Langfelder, L. J., "Pore Water Pressure in Unsaturated Soils," Journal, Soil Mechanics and Foundation Division, American Society of Civil Engineers, Vol 91, No. SM4, Jul 1965, pp 127-150.

44. Statement of the Review Panel, "Engineering Concepts," Moisture Equilibria and Moisture Changes in Soils Beneath Covered Areas, Symposium in Print, G. D. Aitchison, ed., Butterworth, Australia, 1965, pp 7-21.

45. Mitchell, J. K., Fundamentals of Soil Behavior, Wiley, New York, 1976.

46. Lytton, R. L., "Theory of Moisture Movement in Expansive Clays," Research Report 118-1, Sep 1969, Center for Highway Research, University of Texas, Austin.

47. Philip, J. R. and DeVries, D. A., "Moisture Movement in Porous Materials Under Temperature Gradients," American Geophysical Union Transactions, Vol 38, No. 2, Apr 1957, pp 222-232.

48. Croney, D., Coleman, J. D., and Black, W. P. M., "Movement and Distribution of Water in Soil in Relation to Highway Design and Performance," Water and Its Conduction in Soils, Highway Research Board Special Report No. 40, 1958, National Academy of Science - National Research Council, Washington, D. C., pp 226-252.

49. Kassiff, G., Livneh, M., and Wiseman, G., Pavements on Expansive Clays, Jerusalem Academic Press, Jerusalem, Israel, 1969

50. Russam, K., "Distribution of Moisture in Soils at Overseas Air-Fields," Road Research Technical Paper No. 58, 1962, Road Research Laboratory, Department of Scientific and Industrial Research, London, England.

51. Richards, B. G., "Determination of the Unsaturated Permeability and Diffusivity Functions from Pressure Plate Outflow Data with Non-Negligible Membrane Impedance," Moisture Equilibria and Moisture Changes in Soils Beneath Covered Areas, Symposium in Print, G. D. Aitchison, Ed., Butterworth, Australia, 1965, pp 47-54.

52. Skempton, A. W., "Effective Stress in Soils, Concrete, and Rocks," Proceedings, Pore Pressure and Suction in Soils, London, 1961, pp 4-16.

53. Richards, B. G., "Moisture Flow and Equilibria in Unsaturated Soils for Shallow Foundations," Permeability and Capillarity of Soils, Technical Publication 417, pp 4-34, Aug 1967, American Society for Testing and Materials, Philadelphia, Pa.

54. Lytton, R. L. and Meyer, K. T., "Stiffened Mats on Expansive Clay," Journal, Soil Mechanics and Foundations Division, American Society of Civil Engineers, Vol 97, No. SM7, Jul 1971, pp 999-1019.

55. Department of the Army, "Engineering Design: Laboratory Soils Testing," Engineer Manual EM 1110-2-1906, Nov 1970, Washington, D. C.

56. Lambe, T. W. and Whitman, R. V., Soil Mechanics, Wiley, New York, 1969.

57. Leonards, G. A., Foundation Engineering, McGraw-Hill, New York, 1962, p 576.

58. Russam, K., "Estimation of Subgrade Moisture Distribution," Transportation Community Monthly Review, Vol 176, 1961, pp 151-159.

59. Skempton, A. W., "Notes on the Compressibility of Clays," Quarterly Journal, Geological Society of London, Vol C, Parts I and II, Nos. 397-398, 1944, pp 119-134.

60. Newmark, N. M., "Simplified Computations of Vertical Pressures in Elastic Foundations," Circular No. 24, 1935, Engineering Experiment Station, University of Illinois, Urbana.

61. Bowles, J. E., Foundation Analysis and Design, McGraw-Hill, New York, 1968.

62. Collins, L. E., "A Preliminary Theory for the Design of Underreamed Piles," Transactions, South African Institution of Civil Engineers, Vol 3, No. 11, Nov 1953, pp 305-313.

63. Department of the Army, "Engineering and Design: Procedures for Foundation Design of Buildings and Other Structures (Except Hydraulic Structures)," Technical Manual TM 5-818-1, Aug 1965, Washington, D. C.

64. U. S. Army Engineer District, Fort Worth, "Investigations for Building Foundations in Expansive Clays," Vol 1, Apr 1968, Fort Worth, Tex.

65. Johnson, L. D. and McAnear, C. L., "Controlled Field Tests of Expansive Soils," Bulletin, Association of Engineering Geologists, Vol XI, No. 4, 1974, pp 353-369.

66. Johnson, L. D., "Properties of Expansive Clay Soils: Report 1, Jackson Field Test Section Study," Miscellaneous Paper S-73-28, May 1973, U. S. Army Engineer Waterways Experiment Station, CE, Vicksburg, Miss.

67. _____, "Swell Behavior of NAF-II Sigonella Foundation Soil," Miscellaneous Paper S-77-13, Sep 1977, U. S. Army Engineer Waterways Experiment Station, CE, Vicksburg, Miss.

68. Moore, W. H. et al., "Hinds County Geology and Mineral Resources," Bulletin 105, 1965, Mississippi Geological, Economic and Topographical Survey, Jackson, Miss.

69. Redus, J. F., "Experiences with Expansive Clay in Jackson (Miss.) Area," Moisture, Density, Swelling and Swell Pressure Relationships, Highway Research Board Bulletin No. 313, pp 40-46, 1962, National Academy of Sciences - National Research Council, Washington, D. C.

70. Krinitzsky, E. L. and Turnbull, W. J., "Loess Deposits of Mississippi," Special Paper No. 94, 1967, Geological Society of America, Boulder, Colo., p 4.

71. Buck, A. K., "Mineral Composition of the Yazoo Clay by X-Ray Diffraction Methods," Journal of Sedimentary Petrology, Vol 26, No. 1, 1956, p 67.

72. U. S. Army Engineer District, Fort Worth, "Geological and Foundation Investigation, Lackland Air Force Base, San Antonio, Texas," Apr 1967, Fort Worth, Tex.

73. Knight, D. K., "Foundation Design on Soft Shale," Eleventh Annual Conference on Soil Mechanics and Foundation Engineering, April 11, 1963, Center for Continuation Study, General Extension Division, University of Minnesota, pp 29-39.

74. Hart, S. S., "Potentially Swelling Soil and Rock in the Front Range Urban Corridor, Colorado," Environmental Geology No. 7, 1974, Colorado Geological Survey, Department of Natural Resources, Denver, Colo.

75. Spanner, D. C., "The Peltier Effect and Its Use in the Measurement of Suction Pressure," Journal of Experimental Botany, Vol 2, No. 5, 1951, pp 145-168.

76. Frazer, J. C. W., Taylor, R. K., and Grollman, A., "Two-Phase Liquid-Vapor Isothermal Systems, Vapor Pressure Lowering," International Critical Tables, Vol 3, p 298.

77. Jennings, J. E. et al., "An Improved Method for Predicting Heave Using the Oedometer Test," Proceedings, Third International Conference on Expansive Clay Soils, Jul 30-Aug 1, 1973, Haifa, Israel, Vol 2, 1973, pp 149-154.

78. Jennings, J. E. B. and Kerrich, J. E., "The Heaving of Buildings and the Associated Economic Consequences, with Particular Reference to the Orange Free State Goldfields," Transactions, South African Institution of Civil Engineers, Vol 5, No. 5, May 1963, pp 129-130.

79. Kunze, R. J. and Kirkham, D., "Simplified Accounting for Membrane Impedance in Capillary Conductivity Determinations," Soil Science Society of America Proceedings, Vol 26, No. 5, Sep-Oct 1962, pp 421-426.

80. Klute, A., "Water Diffusivity," Physical and Mineralogical Properties, Including Statistics of Measurement and Sampling, Methods of Soil Analysis, Part 1, American Society of Agronomy, Madison, Wis., 1965, pp 262-272.

81. Johnson, L. D., "Influence of Suction on Heave of Expansive Soils," Miscellaneous Paper S-73-17, Apr 1973, U. S. Army Engineer Waterways Experiment Station, CE, Vicksburg, Miss.

82. Black, W. P. M., "A Method of Estimating the California Bearing Ratio of Cohesive Soils from Plasticity Data," Geotechnique, Vol 12, No. 4, 1961, pp 271-282.

83. McDowell, C., "The Relation of Laboratory Testing to Design for Pavements and Structures on Expansive Soils," Quarterly, Colorado School of Mines, Vol 54, No. 4, Oct 1959, pp 127-153.

84. McKeen, R. G., "Characterizing Expansive Soils for Design," presented at the Joint Meeting of the Texas, New Mexico, and Mexico Sections of the American Society of Civil Engineers, Oct 6-8, 1977, Albuquerque, N. Mex.

85. Nayak, N. V. and Christensen, R. W., "Swelling Characteristics of Compacted Expansive Soils," Clays and Clay Minerals, Vol 19, No. 4, 1974, pp 251-261.

86. Seed, H. B., Woodward, R. J., Jr., and Lundgren, R., "Prediction of Swelling Potential for Compacted Clays," Journal, Soil Mechanics and Foundations Division, American Society of Civil Engineers, Vol 88, No. SM3, Jun 1962, pp 53-87.

87. Schneider, G. L. and Poor, A. R., "The Prediction of Soil Heave and Swell Pressures Developed by an Expansive Clay," Research Report TR-9-74, Nov 1974, Construction Research Center, University of Texas, Arlington.

88. Vijayvergiya, V. N. and Ghazzaly, O. I., "Prediction of Swelling Potential for Natural Clays," Proceedings, Third International Conference on Expansive Clay Soils, Vol 1, Jul 30-Aug 1, 1973, Haifa, Israel, pp 227-234.

89. Vijayvergiya, V. N. and Sullivan, R. A., "Simple Technique for Identifying Heave Potential," Proceedings, Workshop on Expansive Clays and Shales in Highway Design and Construction, Federal Highway Administration, Washington, D. C., Vol 1, May 1973, pp 275-294.

90. Van der Merwe, D. H., "The Prediction of Heave from the Plasticity Index and Percentage Fraction of Soils," Civil Engineer in South Africa, Vol 6, No. 6, Jun 1964, pp 103-105.

91. Prendergast, J. D. et al., "Concept Development for Structures on Expansive Soils by the Pattern Language Design Methodology," Technical Report M-151, Oct 1975, Construction Engineering Research Laboratory, Champaign, Ill.

Table 1

Factors Influencing Magnitude and Rate of Volume Change

Factor	Description
	Soil Properties
Composition of solids	The type and amount of clay minerals determine the ability of the soil to expand. Montmorillonites are usually highly expansive. Clay minerals of smaller particle sizes promote expansive characteristics
Composition of pore fluid	Pore fluids containing high concentrations of cations tend to reduce the magnitude of volume change from suppression of the double layer; however, swell from osmosis (diffusion of relatively pure water external to the soil into the soil mass to dilute the pore fluid) can become significant over long periods of time
Dry density	Larger dry densities result in closer particle spacings and larger swells caused by greater forces from the microscale mechanisms
Soil fabric and structure	Flocculated particles tend to swell more than dispersed particles. Highly cemented particles tend to reduce swell. Fabrics that slake readily may promote swell from reorientation and separation of the particles
	Environmental Conditions
Climate	The climate greatly influences the initial water content and soil suction, especially in well drained areas with deep water tables. Arid climates promote desiccation, while humid climates promote wet soil profiles.
Water table depth	Shallow water tables provide a source of moisture for heave of soils above the water table. Placement of impervious covers reduces surface evaporation and transpiration from vegetation; soil moisture will increase from capillary rise
Drainage	The drainage pattern greatly influences the water content; poor surface drainage leads to moisture accumulation or ponding which can provide moisture for

(Continued)

Table 1 (Concluded)

Factor	Description
Drainage (Continued)	swell by infiltration from the surface or through verge slopes. Cracks in pavements and seepage from higher ground can increase soil moisture
Vegetative cover	Vegetation such as trees, shrubs, and grasses are conducive to moisture movement or depletion by transpiration. Moisture tends to accumulate beneath areas denuded of vegetation
Confinement	Larger confining pressures reduce swell. Cut areas are more likely to swell due to decreases in confining pressure, while fills tend to reduce swell in underlying soils. Lateral pressures may not equal vertical overburden pressures
Field permeability	Larger permeabilities promote faster rates of swell. Fissures in the soil mass can significantly increase permeability. Permeability is also a function of the water content, density, and soil structure

Table 2

Suction Model Soil Input Parameters

Parameter*	Description
G	Specific gravity, G_s
WC	Initial water content w_o, percent
EO	Initial void ratio without confining pressure, e_o
PI	Plasticity index
ALPHA	Compressibility factor, α
A, B	Soil suction A and B parameters, Equation 12
AKO	Ratio of total horizontal to vertical stress in situ, K_T
PERM	Coefficient of permeability of saturated soil at void ratio e_o, k_s, ft/day

* Symbols used in ULTRAT.

Table 3

Mechanical Swell Model Soil Input Parameters

Parameter*	Description
G	Specific gravity, G_s
WC	Initial water content w_o, percent
EO	Initial in situ void ratio e_o; void ratio under the overburden pressure p_o prior to construction
EPO	Void ratio under the overburden pressure p_o when the pore water pressure is zero, e_{po}
ES	Void ratio under the pressure 0.1 tsf when the pore water pressure is zero, e_s
PO	Initial soil overburden pressure p_o, tsf
PS	Swell pressure p_s, tsf
CC	Compression index, C_c
CVS	Coefficient of swell c_{vs}, ft^2/day

* Symbols used in ULTRAT.

Table 4

Assumptions and Limitations of Input Parameters Describing Soil Properties

Parameter	Remarks
	Soil Suction Model
Initial void ratio, e_o	Initial void ratio determined without surcharge pressure
Compressibility factor	The slope of the specific volume, $(1 + e)/G_s$, with water content w is identical with the slope of the matrix suction τ_m with applied pressure. If α is input ≤ 0, ULTRAT will set[58] $\alpha = 0$ for $PI \leq 5$ $\alpha = 0.0275PI - 0.125$ for $5 \leq PI \leq 40$ $\alpha = 1$ for $PI \leq 5$ PI = plasticity index $\alpha = 1$ in the suction index C_τ, Equation 11, when settlement occurs and the initial pore water pressure u_w is positive or the depth DXX > DGWT, depth to the water table, Figure 1. $\alpha = 1$, Equation 16, when u_w is positive or DXX > DGWT
Degree of saturation	Heave is computed for any degree of saturation
Lateral pressure	Heave is computed for lateral pressures determined by using the ratio of total horizontal to vertical pressures in situ, K_T
Osmotic suction	Swell from osmosis of external water diluting soluble salts in the pore water is not considered
	Mechanical Swell Model
Initial void ratio, e_o	Initial void ratio determined after the vertical surcharge pressure prior to construction is placed on the specimen
Swell pressure, p_s	The swell pressure may be less than the overburden pressure p_o to evaluate settlements, but p_s must be greater than 0.1 tsf
Compression index, C_c	The slope of the line between p_s and p_o, Figure 3b, is equivalent to the compression index if $p_s \geq$ the maximum past pressure p_{max} or equivalent to the recompression index if $p_{max} > p_s$. If C_c is input ≤ 0, ULTRAT sets $C_c = 0.007(LL-10)$[59] where LL = liquid limit
Degree of saturation	The final degree of saturation is unity
Lateral pressure	Lateral pressures are ignored
Secondary swell	Swell in excess of primary swell is not considered

Table 5

Assumptions and Limitations of Input Parameters Describing Environmental Conditions

Parameter	Remarks
Elastic strains	Instantaneous compression and rebound caused by loading or excavating are not considered
Lateral creep	Horizontal dimensional changes in soil beneath foundations on slopes caused by lateral creep of soft clays are not considered
Horizontal layers	Each stratum of soil is horizontal
Fraction of volumetric heave, N	Heave computed in the vertical direction is 100 percent of the volumetric heave; i.e., N = 1
Δp_{st}	The increase of vertical pressure in the soil caused by foundation loads is simulated by the Boussinesq method. Equations for the long, continuous footing were approximated from graphical plots. Computations of vertical pressure by the Boussinesq method assume a uniform pressure distributed at the base of the footing Δp_b exerted on a weightless, elastic, homogeneous, semi-infinite isotropic soil with no change in volume
Foundation loading, q	The net applied foundation pressure after estimated tension forces T have been subtracted from the load L , Equation 36. The minimum value of q that may be input is zero
Number of problems, NPROB	A series of heaves for different values of q , dimensions of the foundation, location of heave (center or corner/edge, Table 6), depth to the water table DGWT, and type of equilibrium moisture profile may be predicted for the soil properties input into the code
Water table depth, DGWT	The equilibrium or final water table depth should be input to predict the potential heave
Equilibrium moisture profile (drainage)	Two profiles are available: saturated (SAT) for poor drainage at the surface and diffusion vertically downward from the surface beneath the foundation; hydrostatic (HYD) for good surface drainage and diffusion of groundwater from the bottom of the active zone vertically upward. These cases are equivalent to Case 3 for triangular stresses with a single drainage surface.[57]
X_a	Moisture changes and/or volume changes do not occur below the depth X_a . The bottom of the soil profile should be set at X_a

Table 6

Equations for the Increase in Soil Pressure From the Foundation and Superstructure

Type of Footing	Location	Reference	$\Delta\rho_{st}$
Rectangular	Center	60	$\frac{\Delta\rho_b}{\pi}\left[\frac{2A_nV_e}{V_e^2+A_n^2}\cdot\frac{V_e^2+1}{V_e^2}+\text{Arctan}\left(\frac{2A_nV_e}{V_e^2-A_n^2}\right)\right]$ $A_n=\frac{BLEN\cdot BWID}{4(DXX)^2}\quad V_e^2=\frac{\left(\frac{BLEN}{2}\right)^2+\left(\frac{BWID}{2}\right)^2+(DXX)^2}{(DXX)^2}$
Rectangular	Corner	60	$\frac{\Delta\rho_b}{4\pi}\left[\frac{2A_nV_e}{V_e^2+A_n^2}\cdot\frac{V_e^2+1}{V_e^2}+\text{Arctan}\left(\frac{2A_nV_e}{V_e^2-A_n^2}\right)\right]$ $A_n=\frac{BLEN\cdot BWID}{(DXX)^2}\quad V_e^2=\frac{(BLEN)^2+(BWID)^2+(DXX)^2}{(DXX)^2}$
Circular	Center	61	$\Delta\rho_b\left\{1-\frac{1}{\left[1+\frac{(RAD)^2}{DXX}\right]^{1.5}}\right\}$
Long-continuous	Center	61	$\frac{DXX}{BWID}<2.5$ $\quad \Delta\rho_b\left[{}_{10}^{\quad -0.28\left(\frac{DXX}{BWID}\right)}\right]$ $\frac{DXX}{BWID}>2.5$ $\quad \Delta\rho_b\left[{}_{10}^{\quad -0.157-0.22\left(\frac{DXX}{BWID}\right)}\right]$
Long-continuous	Edge	61	$\Delta\rho_b\left[{}_{10}^{\quad -0.157-0.22\left(\frac{DXX}{BWID}\right)}\right]$

Note: $\Delta\rho_b$ = increase of pressure at base of foundation, tsf
DXX = depth below bottom of foundation, ft
BLEN = Length of foundation, ft
BWID = width of foundation, ft
RAD = radius of circular foundation, ft

Table 7

Description of Mechanical Swell Tests

Test	Description
Swell overburden (Figure 26a)	After the seating load has been applied for 1/2 hour (0.015 tsf, step 1), the specimen is loaded to the overburden pressure p_o in one increment (step 2) and held for 1/2 hour. Distilled water is then added to the reservoir and the swell of the specimen measured (step 3) until primary swell is complete. The test may be extended to evaluate the swell pressure and swell index, for example, by compressing the specimen to e_o (step 4) and rebounding to p_o (step 5) and 0.1 tsf (step 6)
Constant volume swell (Figure 26b)	After 1/2 hour under the seating load (about 0.015 tsf, step 1), the specimen is loaded to the overburden pressure p_o in one increment and held for 1/2 hour (step 2). Distilled water is added to the reservoir and sufficient load applied in small increments to prevent swelling until the swelling pressure p_s is fully developed (step 3) as verified by examination of time versus pressure plot. The submerged specimen is unloaded to p_o (step 4) and 0.1 tsf (step 5) in decrements. Each load decrement is held until primary swell is complete. The test may be extended to evaluate recompression and the compression index by applying additional load increments
Improved simple oedometer (Figure 26c)	After the specimen is loaded for 1/2 hour under the seating load (0.015 tsf, step 1), the specimen is loaded to the overburden pressure p_o in one increment and held for 1/2 hour (step 2). After determining the void ratio e_o, the pressure is reduced to the seating load in one increment and held for 1/2 hour (step 3). Distilled water is added and the swell under the seating load observed until primary swell is complete (step 4). Increments of load are applied to achieve consolidation to e_s (step 5), e_{po} (step 6), and e_o (step 7). Additional loads may be applied to evaluate the compression index

Table 8

Results of Soil Suction Tests

Sample	Depth, ft	Natural Water Content, w_o	Initial Void Ratio, e_o	Suction Parameters A	Suction Parameters B	Pressure, tsf τ^s_{mo}	Pressure, tsf p_o	Pressure, tsf p_s	Compressibility Factor α	Suction Index C_r
				Clinton Test Site, March 1973, Boring No. 1						
3	3.5-4.0	24.0	0.724	3.764	0.161	0.76	0.27	0.43	0.41	0.069
4	6.5-7.0	32.0	0.850	3.694	0.130	0.34	0.41	0.40	0.73	0.151
5	7.0-8.0	42.0	1.140	4.504	0.114	0.51	0.46	0.48	1.00	0.237
6	9.0-10.0	40.8	1.185	5.544	0.154	0.23	0.57	0.10	0.89	0.160
7	10.1-11.1	44.5	1.180	4.124	0.100	0.47	0.63	0.77	0.89(est)	0.246
11	15.0-16.1	48.9	1.390	5.504	0.116	0.67	0.91	1.48	0.95	0.227
25	30.1-30.6	45.0	1.290	4.764	0.095	3.09	1.74	1.93	0.87	0.251
				Lackland Test Site, April 1973, Boring No. 1						
2	0.5-1.0	23.0	0.890	7.604	0.303	4.30	0.05	0.01	1.00	0.087
3	3.2-4.2	33.0	0.970	6.774	0.250	0.01	0.22	0.01	0.94	0.105
4	4.3-5.2	32.0	1.040	4.544	0.135	1.70	0.27	0.30	0.94	0.194
5	6.2-6.7	30.0	0.910	5.044	0.167	1.00	0.36	0.40	0.91	0.151
6	6.7-7.6	30.0	0.950	5.044	0.167	1.00	0.42	0.20	1.00	0.157
10	13.1-14.2	33.0	0.870	6.565	0.208	0.50	0.78	1.10	1.00	0.134
11	14.3-15.3	32.0	0.870	4.704	0.130	3.50	0.87	4.00	1.00	0.212
12	16.0-17.1	30.1	0.890	6.565	0.208	2.00	0.96	0.80	1.00	0.134
13	17.2-18.3	29.8	0.880	6.565	0.208	2.30	1.02	1.00	1.00	0.134
14	22.6-22.9	32.7	0.950	6.704	0.196	2.00	1.34	1.00	1.00	0.142
15	27.3-28.3	30.7	0.870	5.690	0.167	3.60	1.65	2.50	0.96	0.158
17	29.0-30.0	29.8	0.870	5.859	0.179	3.30	1.77	1.60	0.96	0.148
18	30.1-31.1	29.8	0.830	5.690	0.167	5.20	1.82	4.60	0.96	0.159
21	35.0-36.1	29.8	0.830	5.690	0.167	5.20	2.07	4.60	0.96	0.159
23	37.4-38.7	29.8	0.830	7.304	0.222	5.00	2.25	3.60	1.00	0.123
27	45.4-46.4	29.8	0.830	6.135	0.185	4.10	2.74	3.20	1.00	0.148
28	46.5-47.4	29.8	0.810	4.264	0.120	4.90	2.80	5.00	1.00	0.228
29	47.8-48.5	29.8	0.770	4.806	0.145	2.90	2.86	4.90	1.00	0.188
				Fort Carson Test Site, June 1973, Boring BOQ-3						
1	1.1-2.3	26.0	0.830	4.540	0.170	1.40	0.12	0.30	0.73	0.120
2	2.6-3.6	26.0	0.800	4.540	0.170	1.40	0.18	0.50	0.73	0.120
3	3.7-4.7	25.5	0.75	3.500	0.150	0.50	0.25	0.30	0.84	0.155
4	5.7-7.0	23.2	0.670	3.500	0.150	1.10	0.37	0.70	0.78	0.143
5	7.5-8.9	18.3	0.585	3.913	0.217	0.90	0.50	0.20	0.75	0.096
6	9.0-9.9	17.0	0.530	3.913	0.217	1.70	0.60	0.60	0.76	0.096
7	11.2-12.1	16.3	0.494	4.359	0.256	1.60	0.74	0.60	0.67	0.072
8	12.4-13.3	16.1	0.490	4.359	0.256	1.80	0.84	0.70	0.75	0.080
9	13.5-14.6	16.1	0.510	4.538	0.256	2.70	0.90	0.70	0.91	0.098
10	14.7-15.7	16.1	0.430	4.538	0.256	2.70	0.97	3.60	0.91	0.098
12	16.9-17.4	15.5	0.510	4.341	0.244	3.80	1.10	0.80	0.90	0.103
13	17.6-18.6	15.4	0.437	4.341	0.244	4.00	1.17	3.10	0.91	0.103
14	18.7-19.7	15.0	0.400	4.514	0.270	3.10	1.24	3.90	0.74	0.075
15	19.8-20.8	15.0	0.420	4.514	0.270	3.10	1.32	2.70	0.74	0.075
16	20.9-21.9	15.0	0.440	4.341	0.244	5.00	1.43	3.00	0.75	0.085
18	22.9-23.7	14.7	0.380	4.636	0.303	1.60	1.55	2.80	0.80	0.072
20	24.7-26.0	13.0	0.410	4.636	0.303	5.20	1.67	1.40	0.74	0.067
				Sigonella Test Site, November 1976, Boring No. 1						
1	1.5-3.5	30.5	0.900	5.069	0.172	0.67	0.20	0.33	0.93	0.151
2	4.0-5.5	30.2	0.930	5.069	0.172	0.75	0.30	0.21	0.83	0.134
3	6.5-8.0	32.1	0.940	5.545	0.182	0.50	0.42	0.27	0.87	0.134
4	11.5-12.5	29.6	0.810	4.394	0.152	0.78	0.72	0.70	0.88	0.158
5	16.5-17.5	22.5	0.660	2.448	0.109	1.00	1.03	0.64	0.34	0.085
6	23.0-24.5	28.6	0.820	3.524	0.119	1.30	1.46	1.06	0.89	0.209

Table 9

Ratio of Total Horizontal to Vertical Stresses

In Situ, Clinton Test Site

Sample	Depth, ft	Pressure, tsf			Ratio of Total Horizontal to Vertical Stresses, K_T
		τ^{o}_{mo}	u_w*	p_o	
4	6.5-7.00	0.34	0.07	0.41	1.0
5	7.0-7.95	0.51	0.10	0.46	1.5
6	9.0-10.00	0.23	0.16	0.57	0.5
7	10.1-11.10	0.47	0.19	0.63	1.1
11	15.0-16.10	0.67	0.34	0.91	1.2

* Pore pressure profile of August 1971.

Table 10

Ratio of Total Horizontal to Vertical Stresses

In Situ, Lackland Test Site

Sample	Depth, ft	Pressure, tsf			Ratio of Total Horizontal to Vertical Stresses, K_T
		τ^{o}_{mo}	u_w*	p_o	
10	13.1-14.2	1.0	0.22	0.78	0.9
12	16.0-17.1	2.0	0.30	0.96	2.5
13	17.2-18.3	2.3	0.34	1.02	3.4
14	22.6-22.9	2.0	0.50	1.34	2.3
15	27.3-28.3	3.6	0.66	1.65	3.3
17	29.0-30.0	3.3	0.72	1.77	2.9
21	35.0-36.1	5.2	0.87	2.07	3.9
23	37.4-38.7	5.0	0.60	2.25	3.2
27	45.4-46.4	4.1	0.31	2.74	1.9
28	46.5-47.4	4.9	0.38	2.80	2.3
29	47.8-48.5	2.9	0.40	2.86	1.3

* Profile of September 1972.

Table 11

Ratio of Total Horizontal to Vertical Stresses

In Situ, Fort Carson Test Site

Sample	Depth, ft	Pressure, tsf			Ratio of Total Horizontal to Vertical Stresses, K_T
		σ^o_{mo}	u_w*	p_o	
3	3.7-4.7	0.5	0.00	0.3	2.0
4	5.7-7.0	1.1	0.06	0.4	3.8
5	7.5-8.9	0.9	0.12	0.5	2.6
7	11.2-12.1	1.6	0.22	0.74	3.2
14	18.7-19.7	3.1	0.47	1.24	3.8
15	19.8-20.8	3.1	0.50	1.32	3.6
18	22.9-23.7	1.6	0.59	1.55	1.8

* Profile of October 1974.

Table 12

Ratio of Total Horizontal to Vertical Stresses

In Situ, Sigonella Test Site

Sample	Depth, ft	Pressure, tsf			Ratio of Total Horizontal to Vertical Stresses, K_T
		σ^o_{mo}	u_w	p_o	
3	6.5-8.0	0.50	0.15	0.42	1.8
4	11.5-12.5	0.78	0.31	0.72	1.7
5	16.5-17.5	1.00	0.46	1.03	1.6
6	23.0-24.5	1.30	0.70	1.46	1.5

* Profile of 30 January 1977.

Table 13

Swell Data on Clinton Test Site Samples

Sample	Depth, ft	G_s	w_o, %	Void Ratio			Pressure, tsf		C_s	C_c	c_{vs} ft^2/day	k ft/day
				e_o	e_{po}	e_s	p_o	p_s				
Swell Overburden, No. 1, Mar 1973												
3	3.5-4.9	2.70	26.0	0.730	0.734	0.737	0.23	1.10	0.006		0.050	
4	6.0-7.0	2.70	32.0	0.850	0.849	0.851	0.38	0.26	0.004		0.003	
7	10.1-11.1	2.78	44.5	1.180	1.225	1.248	0.61	1.50	0.051		0.003	
12	16.1-17.1	2.73	49.7	1.300	1.327	1.364	1.00	1.50	0.053		0.003	
25	30.1-31.2	2.73	45.5	1.150	1.199	1.240	1.77	13.00	0.051		0.003	
Constant Volume Swell, PU-3, Oct 1969												
2	5.1-6.1	2.70*	22.1	0.600	0.615	0.624	0.31	1.15	0.020			
3	9.0-10.4	2.72*	37.1	0.985	0.991	1.016	0.55	1.20	0.030			
5	15.0-15.9	2.75*	47.4	1.264	1.285	1.382	0.90	1.60	0.100			
7	20.2-21.1	2.73*	43.9	1.215	1.230	1.298	1.20	1.80	0.075			
8	29.3-30.2	2.71*	44.6	1.200	1.213	1.295	1.70	2.70	0.067			
Improved Simple Oedometer, PU-2, Dec 1968												
3	2.3-3.4	2.68	22.4	0.740	0.745	0.747	0.15	0.26	0.015	0.20	0.010	0.0040
5	4.4-5.4	2.68	25.1	0.701	0.710	0.720	0.31	0.40	0.030	0.20		0.0010
9	9.4-10.2	2.74	43.8	1.190	1.310	1.390	0.55	1.70	0.140	0.44	0.007	0.0001
17	19.7-20.8	2.73	47.9	1.275	1.340	1.440	1.15	2.60	0.090	0.52	0.005	0.0001
29	34.8-35.9	2.71	38.2	1.030	1.070	1.110	2.03	5.00	0.030	0.25	0.007	0.0001
Pressure Plate, PU-2												
4	3.5-4.3	2.68	23.0	0.693								
10	11.0-12.1	2.74	50.0	1.368								0.0006
18	21.0-22.1	2.73	46.7	1.288								0.0001
26	31.0-32.1	2.71	43.8	1.188								0.0001
												0.0001

* Estimated.

Table 14

Swell Data on Lackland Test Site Samples

Sample	Depth, ft	G_s	w_o, %	Void Ratio e_o	Void Ratio e_{po}	Void Ratio e_s	Pressure, tsf p_o	Pressure, tsf p_s	C_s	C_c	c_{vs} ft²/day	k ft/day
Swell Overburden, PU-7, Dec 1970												
2	1.2-2.3	2.68	18.4	0.708	0.810	0.834	0.18	2.30	0.092		0.203	
5	5.0-6.0	2.71	24.0	0.756	0.773	0.798	0.40	1.00	0.042		0.250	
9	12.9-13.7	2.75	30.9	0.852	0.878	0.933	0.90	2.50	0.057		0.005	
Swell Overburden, No. 1, Apr 1973												
3	3.2-4.2	2.69	31.6	0.930	0.943	0.951	0.24	1.20	0.020		0.010	0.0034
4	4.3-5.2	2.78	34.5	1.044	1.045	1.051	0.29	0.40	0.080	0.27		
11	14.3-15.3	2.76	31.9	0.902	0.923	0.948	1.00	6.70	0.026		0.012	0.0155
15	27.3-28.3	2.75	31.2	0.823	0.867	0.887	1.80	33.10	0.034		0.116	0.0035
17	29.0-30.0	2.75	28.5	0.832	0.861	0.920	1.84	6.40	0.049	0.20		
23	37.4-38.7	2.73	30.4	0.793	0.832	0.856	2.50	33.10	0.034		0.004	0.0057
28	46.5-47.4	2.73	30.0	0.743	0.778	0.804	3.00	33.10	0.034		0.006	0.0013
Constant Volume Swell, PU-7, Dec 1970												
2	1.2-2.3	2.68	17.9	0.800	0.847	0.860	0.18	2.20	0.050			
5	5.0-6.0	2.71	23.8	0.745	0.752	0.770	0.40	0.70	0.030			
9	12.9-13.7	2.75	31.0	0.838	0.860	0.910	0.90	2.40	0.052			
Constant Volume Swell, No. 1, Apr 1973												
4	4.3-5.2	2.78	33.5	1.006	1.007	1.011	0.29	0.30	0.090	0.26		0.0540
17	29.0-30.0	2.76	29.0	0.884	0.892	0.954	1.84	2.85	0.052	0.20		0.0084
Improved Simple Oedometer, PU-7, Dec 1970												
3	2.5-3.6	2.73	20.8	0.790	0.960	0.978	0.23	2.40		0.22		0.0003
6	6.1-7.1	2.73	15.9	0.660	0.680	0.711	0.50	0.80		0.18		0.0009
Improved Simple Oedometer, No. 1, Apr 1973												
4	4.3-5.2	2.78	32.9	1.014	1.021	1.039	0.29	0.39	0.070	0.27		
17	29.0-30.0	2.76	28.9	0.802	0.881	0.968	1.84	8.00	0.050	0.13		
Pressure Plate, PU-7												
3	2.5-3.6	2.69	20.8	0.800								0.0001
6	6.1-7.1	2.70	24.8	0.756								0.0001
12	17.0-17.6	2.75	31.1	0.872								0.0001
36	46.9-48.4	2.78	29.1	0.802								0.0001

Table 15

Swell Data on Fort Carson Test Site Samples

Sample	Depth, ft	G_s	w_o, %	Void Ratio e_o	Void Ratio e_{po}	Void Ratio e_s	Pressure, tsf p_o	Pressure, tsf p_s	C_s	C_c	c_{vs} ft^2/day	k ft/day
Swell Overburden												
P1-5	4.0-5.2	2.75	15.8	0.582	0.604	0.611	0.29	1.00	0.029	0.124	0.024	
P4-7	7.0-8.1	2.76	18.1	0.499	0.503	0.509	0.45	1.06	0.011		0.012	
P4-9	14.6-15.7	2.78	15.8	0.510	0.512	0.526	0.85	0.94	0.018		0.057	
BOQ3-23	29.5-30.5	2.74	10.0	0.305	0.308	0.316	1.88	3.11	0.007	0.045	0.005	
Constant Volume Swell												
P1-5	4.0-5.2	2.75	17.2	0.525	0.527	0.534	0.29	0.41	0.015	0.100		0.011
P4-7	7.0-8.1	2.76	18.1	0.520	0.520	0.529	0.45	0.45	0.014			
P4-9	14.6-15.7	2.78	14.7	0.424	0.427	0.439	0.85	1.47	0.014			
BOQ3-23	29.5-30.5	2.74	10.3	0.304	0.306	0.318	1.88	2.37	0.010	0.046		0.007
Improved Simple Oedometer												
P1-5	4.0-5.2	2.75	16.3	0.485	0.507	0.516	0.29	1.06	0.042	0.088		
BOQ3-23	29.5-30.5	2.74	11.1	0.305	0.315	0.330	1.88	4.60	0.020	0.048		
Pressure Plate												
BOQ3-4	5.7-7.0	2.75	22.0	0.60								0.0005
BOQ3-10	14.7-15.7	2.75	17.3	0.42								0.0003
BOQ3-20	24.7-26.0	2.76	13.0	0.37								0.0002
BOQ3-27	34.2-35.2	2.71	9.6	0.25								0.0001

Table 16

Swell Data of Sigonella Test Site Samples

Sample	Depth, ft	G_s	w_o, %	Void Ratio e_o	Void Ratio e_{po}	Void Ratio e_s	Pressure, tsf p_o	Pressure, tsf p_s	C_s	C_c	c_{vs} ft^2/day	k ft/day
				Constant Volume Swell, Nov 1976								
1	1.5-3.5	2.79	29.6	0.906	0.914	0.922	0.21	0.43	0.025			0.0002
2	4.0-5.5	2.78	27.3	0.850	0.835	0.843	0.33		0.017			0.0013
3	6.5-8.0	2.80	33.3	0.949	0.943	0.957	0.46		0.021			0.0003
4	11.5-12.5	2.74	28.1	0.800	0.777	0.782	0.73		0.006			0.003
5	16.5-17.5	2.72	23.6	0.701	0.671	0.675	1.00		0.006			0.48
6	23.0-24.5	2.79	27.0	0.782	0.723	0.748	1.40		0.022			0.0003
				Improved Simple Oedometer								
1	1.5-3.5	2.79	29.6	0.875	0.926	0.946	0.21	1.40	0.062	0.20	0.0006	
2	4.0-5.5	2.78	25.2	0.846	0.832	0.857	0.33	0.22	0.030	0.20	0.0034	
3	6.5-8.0	2.80	33.3	0.979	0.991	1.022	0.46	0.80	0.047	0.19	0.0016	
4	11.5-12.5	2.74	28.2	0.766	0.768	0.800	0.73	0.84	0.037	0.20	0.0011	
5	16.5-17.5	2.72	22.2	0.685	0.669	0.700	1.00	0.50	0.018	0.19	0.0370	
6	23.0-24.5	2.79	26.3	0.756	0.748	0.795	1.40	1.10	0.037	0.18	0.0022	

Table 17

Input Data For Parametric Analysis

Parameter	Plasticity Index (Soil Type) 10	20	40	60	80
	Suction Model				
A	2.609	2.567	2.586	2.592	2.582
B	0.217	0.149	0.101	0.077	0.061
Plastic limit	18	20	24	28	32
Initial void ratio, e_o	0.4	0.5	0.7	0.8	0.9
Compressibility factor, α	0.15	0.43	1.00	1.00	1.00
Initial water contents w_o, percent	7 8 9 10	10 12 14 16	16 18 20 22	21 24 27 30	26 30 34 38

PI	w_o, %	τ^o_{mo}, tsf	p_o, tsf	e_o	e_{po}	e_s	LL
			Mechanical Swell Model				
80	26	9.91	1.0	0.900	1.341	1.783	112
	30	5.65	1.0	0.900	1.233	1.675	
	34	3.22	1.0	0.900	1.125	1.567	
	38	1.84	1.0	0.900	1.017	1.459	
60	21	9.44	1.0	0.800	1.142	1.492	88
	24	5.55	1.0	0.800	1.061	1.411	
	27	3.26	1.0	0.800	0.980	1.330	
	30	1.91	1.0	0.800	0.899	1.250	
40	16	9.33	1.0	0.700	0.959	1.227	64
	18	5.86	1.0	0.700	0.905	1.173	
	20	3.68	1.0	0.700	0.851	1.115	
	22	2.31	1.0	0.700	0.797	1.065	
20	10	11.94	1.0	0.500	0.578	0.651	40
	12	6.01	1.0	0.500	0.557	0.629	
	14	3.03	1.0	0.500	0.535	0.607	
	16	1.52	1.0	0.500	0.513	0.586	
10	7	12.30	1.0	0.400	0.420	0.439	28
	8	7.46	1.0	0.400	0.416	0.435	
	9	4.53	1.0	0.400	0.412	0.431	
	10	2.75	1.0	0.400	0.408	0.427	

Table 18

Empirical Methods For Predicting Heave

Method	Reference	Description
McDowell	83	A procedure based on swell test results of many specimens of compacted Texas soils, usually applied in design of highway subgrades. Field heave is estimated from a family of curves using Atterberg limits, initial water content, and surcharge pressures of each soil stratum. The potential vertical rise (PVR) is 1/3 the volume change. The initial water content is compared with maximum (0.47LL + 2) and minimum (0.2LL + 9) water contents
McKeen	84	A procedure of relating soil suction with percent swell including effect of surcharge pressure. Requires use of graphs, shrinkage limit, PI, LL, percent clay fraction, and estimates of initial and final soil suctions
Nayak and Christensen	85	$S_p = 0.0229PI^{1.45}C/w_o + 6.38$, C = percent clay fraction for compacted soil and 1 psi surcharge pressure, w_o = percent initial water content, S_p = percent swell
Seed, Woodward and Lundgren	86	$S_p = 0.00216PI^{2.44}$, PI = percent plasticity index, for soil compacted at optimum water content at maximum density to saturation for 1 psi surcharge pressure
Schneider and Poor	87	Logarithm of percent swell given for soil below various depths of fill: Surcharge, ft / $\text{Log}_{10} S_p$: 0 / $0.90(PI/w_o)-1.19$; 3 / $0.65(PI/w_o)-0.93$; 5 / $0.51(PI/w_o)-0.76$; 10 / $0.41(PI/w_o)-0.69$; 20 / $0.33(PI/w_o)-0.62$
Vijayvergiya and Ghazzaly	88	$\text{Log}_{10} S_p = 1/12\ (0.44LL - w_o + 5.5)$ from initial water content to saturation for 0.1 tsf surcharge pressure, LL = percent liquid limit

(Continued)

Table 18 (Concluded)

Method	Reference	Description
Vijayvergiya and Sullivan	89	$\text{Log}_{10} S_p = 0.0526\gamma_d + 0.033LL - 6.8$ from initial water content to saturation for 1 psi surcharge pressure, γ_d = dry density, lb/ft^3
Van Der Merwe	90	$S_p = \frac{100}{n} \sum_{D=1}^{D=n} F_D(PE)_D$ F_D = reduction factor to account for pressure with depth; PE = 1, 1/2, 1/4, 0 in. per foot of depth for very high, high, medium, and low degrees of expansion, respectively; D = 20log F, D = depth, ft. The degree of expansion PE is found from a chart of PI and percent clay fraction

Table 19

Input Parameters For Prediction of Potential Heave by Empirical Methods

	Test Site			
	Clinton	Lackland	Fort Carson	Sigonella
Depth of soil H (depth to water table), ft	5	8	3	5
Plasticity Index, percent	20	40	30	40
Liquid Limit, percent	45	60	50	65
Surcharge Pressure q , tsf	0.072	0.072	0.072	0.072
Average pressure in soil, tsf	0.22	0.31	0.17	0.22
Initial water content w_o , percent	27	27	26	30
Clay content, percent < 2 microns	22	50	30	60
Dry density, lb/ft^3	100	88	112	91
Change in soil suction, $\Delta\tau_m$, tsf	0.5	1.0	1.4	0.7

Table 20

Predictions of Potential Heave by Empirical Methods

Method	Test Site Heave, ft			
	Clinton	Lackland	Fort Carson	Sigonella
McDowell (volumetric swell)	0.01	0.28	0.02	0.10
McKeen	0.06	0.45	0.07	0.33
Nayak & Christensen	0.39	1.22	0.30	0.80
Seed, Woodward & Lundgren	0.16	1.40	0.26	0.88
Schneider & Poor	0.01	0.11	0.02	0.05
Vijayvergiya & Ghazzaly	0.04	0.20	0.04	0.07
Vijayvergiya & Sullivan	0.04	0.05	0.17	0.07
Van Der Merwe	0.08	0.44	0.11	0.32
Equation 46 (saturated case)	0.02	0.48	0.17	0.11
Equation 47 (hydrostatic case)	-0.11	0.46	0.14	0.11
Observed in field to date:				
Above water table	-0.01 to 0.02	0.11	0.01 to 0.05	
Total heave	0.11	0.19	0.02 to 0.08	
Extrapolated above water table	0.04	0.30	0.13	

Table 21

Input Parameters For Prediction of Heave

Test Site	Depth, ft	Specific Gravity, G_s	Initial Water Content, w_o %	Initial Void Ratio, e_o	Plasticity Index PI, Percent	Compressibility Factor, a	Suction Parameters A	Suction Parameters B	Ratio of Total Horizontal to Vertical Stress In Situ, K_T
Suction Model									
Clinton	0.0-5.0	2.70	27.0	0.724	20	0.41	3.764	0.161	1.0
	5.0-7.0	2.70	32.0	0.850	35	0.73	3.694	0.130	1.0
	7.0-8.0	2.75	42.0	1.140	56	1.00	4.504	0.114	1.0
	8.0-10.0	2.76	40.8	1.185	70	0.90	5.544	0.154	0.5
	10.0-15.0	2.76	44.5	1.180	70	0.90	4.124	0.100	1.0
	15.0-25.0	2.75	48.9	1.390	70	0.95	5.504	0.116	1.0
	25.0-50.0	2.74	45.0	1.290	70	0.87	4.764	0.095	1.0
Lackland	0.0-5.0	2.70	25.0	0.970	40	0.94	6.774	0.250	1.0
	5.0-8.0	2.75	30.0	0.950	40	1.00	5.044	0.167	1.0
	8.0-13.0	2.75	30.0	0.870	14	0.26	5.044	0.167	1.0
	13.0-20.0	2.76	30.0	0.890	55	1.00	6.565	0.208	3.0
	20.0-30.0	2.76	30.0	0.870	55	1.00	5.859	0.179	3.0
	30.0-50.0	2.76	30.0	0.830	55	1.00	6.135	0.185	2.0
Fort Carson	0.0-5.0	2.80	26.0	0.830	30	0.73	4.540	0.170	2.0
	5.0-7.0	2.77	23.5	0.670	30	0.78	3.500	0.150	3.0
	7.0-10.0	2.77	18.0	0.585	30	0.75	3.913	0.217	3.0
	10.0-16.0	2.76	16.1	0.494	30	0.67	4.359	0.256	3.0
	16.0-20.0	2.76	15.0	0.420	30	0.74	4.514	0.270	3.0
	20.0-30.0	2.74	13.0	0.410	30	0.74	4.636	0.303	3.0
	30.0-50.0	2.71	10.0	0.410	30	0.74	4.636	0.303	3.0
Sigonella	0.0-5.5	2.79	32.0	0.900	40	0.88	5.069	0.172	1.0
	5.5-6.5	2.72	27.5	0.750	25	0.34	2.448	0.109	1.0
	6.5-11.0	2.80	32.1	0.940	40	0.87	5.545	0.182	1.0
	11.0-15.5	2.74	31.0	0.810	40	0.88	4.394	0.152	1.0
	15.5-21.5	2.72	22.5	0.660	20	0.34	2.448	0.109	1.0
	21.5-25.0	2.79	29.0	0.820	40	0.89	3.524	0.119	1.0

				Void Ratio			Pressure, tsf		Compression Index C_c
				e_o	e_{po}	e_s	p_o	p_s	
Mechanical Swell Model									
Clinton									
SO	0.0-7.0	2.70	26.0	0.730	0.734	0.737	0.23	1.10	0.20
	7.0-15.0	2.78	44.5	1.180	1.225	1.248	0.61	1.50	0.20
	15.0-28.0	2.73	49.7	1.300	1.327	1.364	1.00	1.50	0.50
	28.0-50.0	2.73	45.0	1.150	1.199	1.240	1.77	13.00	0.25
CVS	0.0-7.0	2.70	22.1	0.600	0.615	0.624	0.31	1.15	0.20
	7.0-12.0	2.72	37.1	0.985	0.991	1.016	0.55	1.20	0.20
	12.0-18.0	2.75	47.4	1.264	1.285	1.382	0.90	1.60	0.40
	18.0-28.0	2.73	43.9	1.215	1.230	1.298	1.20	1.80	0.50
	28.0-50.0	2.71	44.6	1.200	1.213	1.295	1.70	2.70	0.25
ISO	0.0-3.5	2.68	22.4	0.740	0.745	0.747	0.15	0.26	0.20
	3.5-7.0	2.68	25.1	0.701	0.710	0.720	0.31	0.40	0.20
	7.0-15.0	2.74	43.8	1.190	1.310	1.390	0.55	1.70	0.20
	15.0-28.0	2.73	47.9	1.275	1.340	1.440	1.15	2.60	0.50
	28.0-50.0	2.71	38.2	1.030	1.070	1.110	2.03	5.00	0.25
Lackland									
SO	0.0-5.0	2.69	31.6	0.930	0.943	0.951	0.24	1.20	0.27
	5.0-13.0	2.78	34.5	1.044	1.045	1.051	0.29	0.40	0.27
	13.0-25.0	2.76	31.9	0.902	0.923	0.948	1.00	6.70	0.20
	25.0-50.0	2.76	28.5	0.832	0.861	0.920	1.84	6.40	0.13
CVS	0.0-5.0	2.68	17.9	0.800	0.847	0.860	0.18	2.20	0.27
	5.0-13.0	2.71	23.8	0.745	0.752	0.770	0.40	0.70	0.27
	13.0-25.0	2.75	31.0	0.838	0.860	0.910	0.90	2.40	0.20
	25.0-50.0	2.76	29.0	0.884	0.892	0.954	1.84	2.85	0.13
ISO	0.0-5.0	2.73	20.8	0.790	0.960	0.978	0.23	2.40	0.22
	5.0-13.0	2.73	15.9	0.660	0.680	0.711	0.50	0.80	0.18
	13.0-50.0	2.76	28.9	0.802	0.881	0.968	1.84	8.00	0.13
Fort Carson									
SO	0.0-5.0	2.75	15.8	0.582	0.604	0.611	0.29	1.00	0.12
	5.0-10.0	2.76	18.1	0.499	0.503	0.509	0.45	1.06	0.12
	10.0-25.0	2.78	15.8	0.510	0.512	0.526	0.85	0.94	0.12
	25.0-50.0	2.74	10.0	0.305	0.308	0.316	1.88	3.11	0.05
CVS	0.0-5.0	2.75	17.2	0.525	0.527	0.534	0.29	0.41	0.12
	5.0-10.0	2.76	18.1	0.520	0.520	0.529	0.45	0.45	0.12
	10.0-25.0	2.78	14.7	0.424	0.427	0.439	0.85	1.47	0.12
	25.0-50.0	2.74	10.3	0.304	0.306	0.318	1.88	2.37	0.05
ISO	0.0-25.0	2.75	16.3	0.485	0.507	0.516	0.29	1.06	0.12
	25.0-50.0	2.74	11.1	0.305	0.315	0.330	1.88	4.60	0.05
Sigonella									
CVS	0.0-5.0	2.79	29.6	0.906	0.914	0.922	0.21	0.43	0.20
ISO	0.0-4.0	2.79	29.6	0.875	0.926	0.946	0.21	1.40	0.20
	4.0-5.5	2.78	25.2	0.846	0.832	0.857	0.33	0.22	0.20
	5.5-6.5	2.72	27.5	0.740	0.736	0.748	0.37	0.27	0.19
	6.5-11.0	2.80	33.3	0.979	0.991	1.022	0.46	0.80	0.19
	11.0-15.5	2.74	28.2	0.766	0.768	0.800	0.73	0.84	0.20
	15.5-21.5	2.72	22.2	0.685	0.669	0.700	1.00	0.50	0.19
	21.5-25.0	2.79	26.3	0.756	0.748	0.795	1.40	1.10	0.18

Table 22

Predictions of Potential Heave (Uncorrected)

		Test Site			
		Clinton	Lackland	Fort Carson	Sigonella
		Observed Data			
Depth of soil H, ft		25	34	30	25
Initial groundwater level, ft		5	8	3	5
Heave observed to H, ft		0.05	0.15	0.08	
Total heave observed at ground surface, ft		0.11	0.19	0.08	
Extrapolated heave above H, ft		0.10	0.50	0.20	
Model	Equilibrium Moisture	Predicted Heave to Depth H			
Suction	Sat	0.08	0.62	0.38	0.21
	Hyd	0.01	0.52	0.36	0.14
Mechanical Swell					
SO	Sat	0.34	0.31	0.15	
	Hyd	0.33	0.29	0.14	
CVS	Sat	0.29	0.42	0.08	
	Hyd	0.28	0.38	0.07	
ISO	Sat	0.88	1.75	0.27	0.06
	Hyd	0.86	1.65	0.26	0.03

Table 23

Predictions of Potential Heave Above the Water Table

		Test Site			
		Clinton	Lackland	Fort Carson	Sigonella
		Observed Data			
Depth of soil H (water table depth), ft		5	8	3	5
Heave observed above the water table, ft		-0.01 to 0.02	0.11	0.05	
Extrapolated heave above water table, ft		0.04	0.30	0.13	
Total heave observed at ground surface, ft		0.11	0.19	0.08	
Model	Equilibrium Moisture	Predicted Heave to Depth H, ft			
Suction	Sat	0.10	0.46	0.17	0.14
	Hyd	0.04	0.36	0.15	0.07
Mechanical Swell					
SO	Sat	0.01	0.04	0.05	
	Hyd	0.01	0.02	0.05	
CVS	Sat	0.06	0.15	0.01	0.03
	Hyd	0.05	0.11	0.01	0.01
ISO	Sat	0.02	0.53	0.05	0.11
	Hyd	0.00	0.43	0.05	0.08

Table 24

Predictions of Potential Heave from Rising Water Table

		Test Site			
		Clinton	Lackland	Fort Carson	Sigonella
		Observed Data			
Initial groundwater level, ft		5	8	3	5
Rise in water table, ft		2	5	1.5	3
Depth containing initial groundwater level, ft		5 to 25	8 to 34	5 to 30	5 to 25
Heave observed for rise in water table, ft		0.03	0.04	0.03	
Extrapolated heave for rise in water table, ft		0.04	0.08	0.06	
Model	Equilibrium Moisture	Predicted Data, ft			
Suction	Sat	0.10	0.11	0.02	0.16
	Hyd	0.13	0.19	0.03	0.21
Mechanical swell					
SO	Sat	0.01	0.11	0.01	
	Hyd	0.02	0.13	0.01	
CVS	Sat	0.03	0.07	0.01	
	Hyd	0.03	0.10	0.01	
ISO	Sat	0.05	0.11	0.02	0.10
	Hyd	0.06	0.21	0.03	0.14

Table 25

Predictions of Potential Heave (Corrected), ft

		Test Site			
		Clinton	Lackland	Fort Carson	Sigonella
Depth of soil H, ft		25	34	30	25
Initial groundwater level, ft		5	8	3	5
Rise in groundwater level, ft		2	5	1.5	3
Total heave observed in soil to depth H, ft		0.05	0.15	0.08	
Extrapolated heave observed in soil to depth H, ft		0.10	0.50	0.20	
Total heave observed at ground surface, ft		0.11	0.19	0.08	
Model	Equilibrium Moisture				
Suction	Sat	0.20	0.57	0.19	0.30
	Hyd	0.17	0.55	0.18	0.28
Mechanical swell					
SO	Sat	0.02	0.15	0.06	
	Hyd	0.03	0.15	0.06	
CVS	Sat	0.09	0.22	0.02	
	Hyd	0.08	0.21	0.02	
ISO	Sat	0.07	0.64	0.07	0.21
	Hyd	0.06	0.64	0.07	0.22

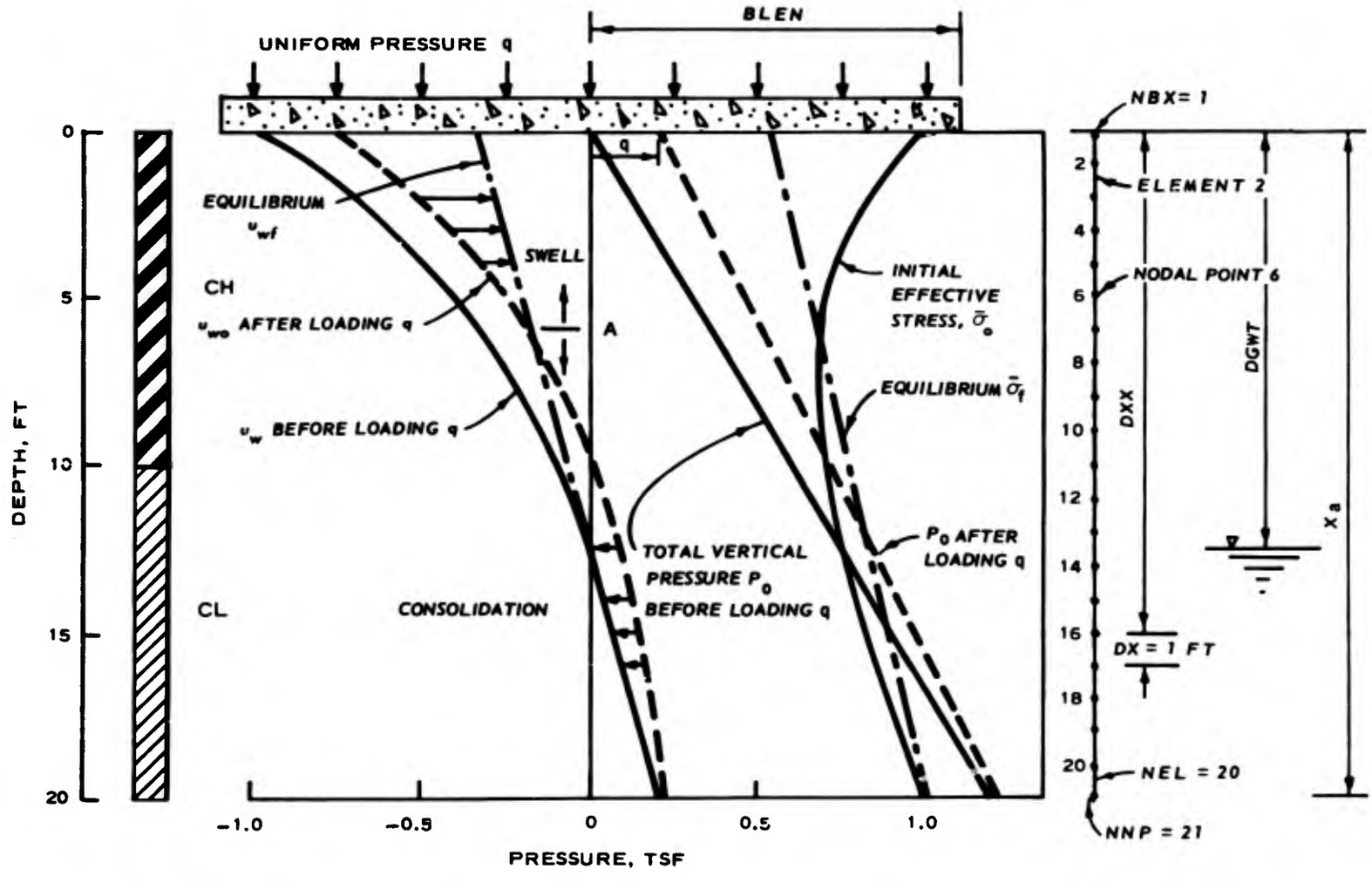

Figure 1. Simulation of stress conditions beneath a slab foundation

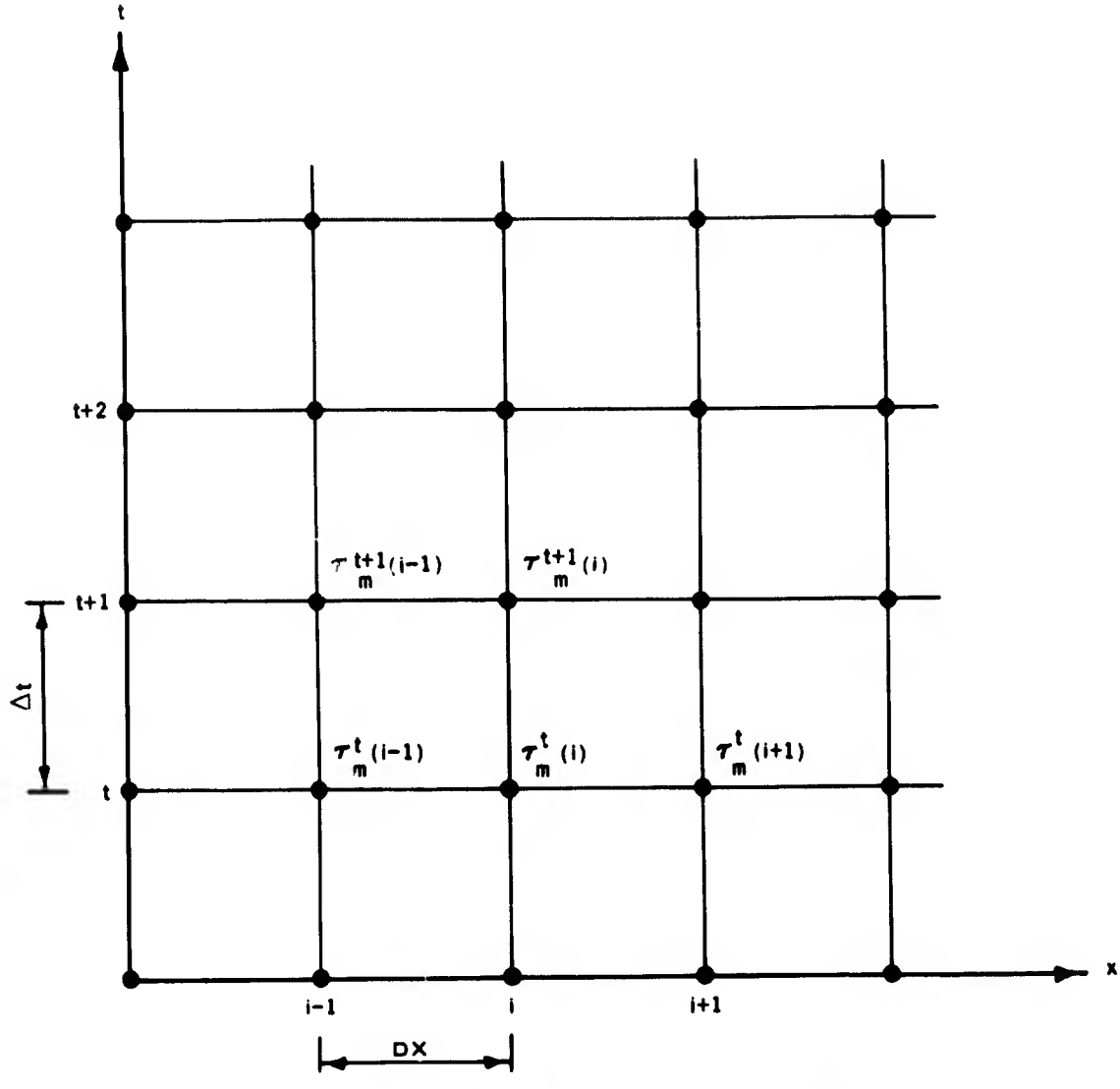

Figure 2. Finite difference mesh

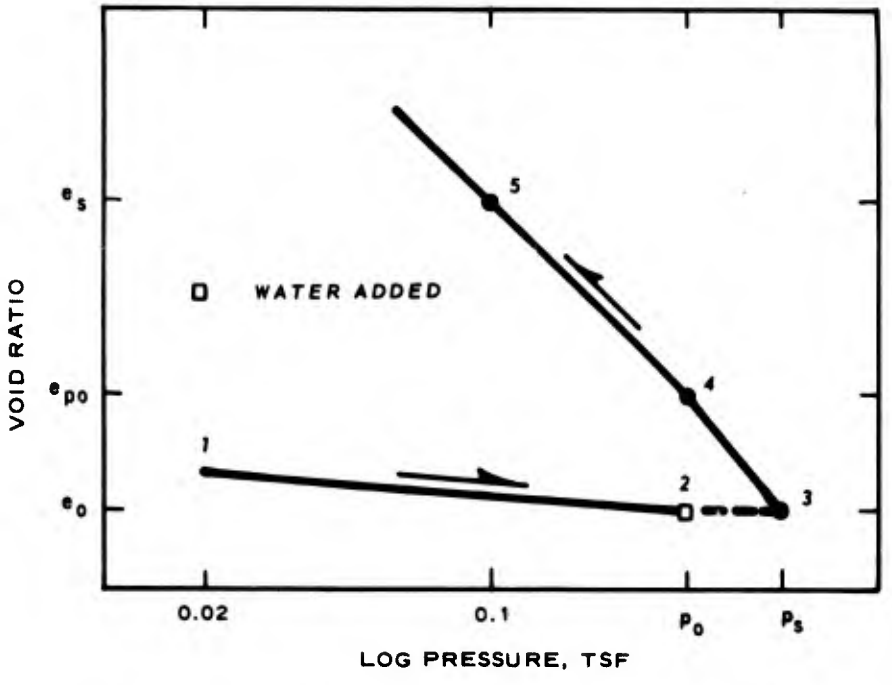

a. SWELL PRESSURE EXCEEDING OVERBURDEN PRESSURE

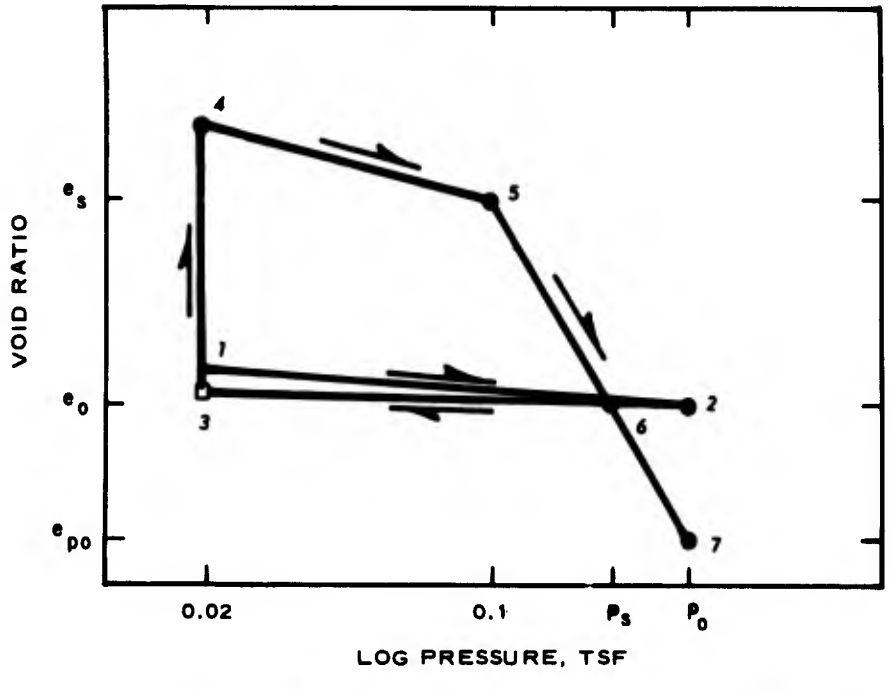

b. OVERBURDEN PRESSURE EXCEEDING SWELL PRESSURE

Figure 3. Characterization of swell behavior from swell tests

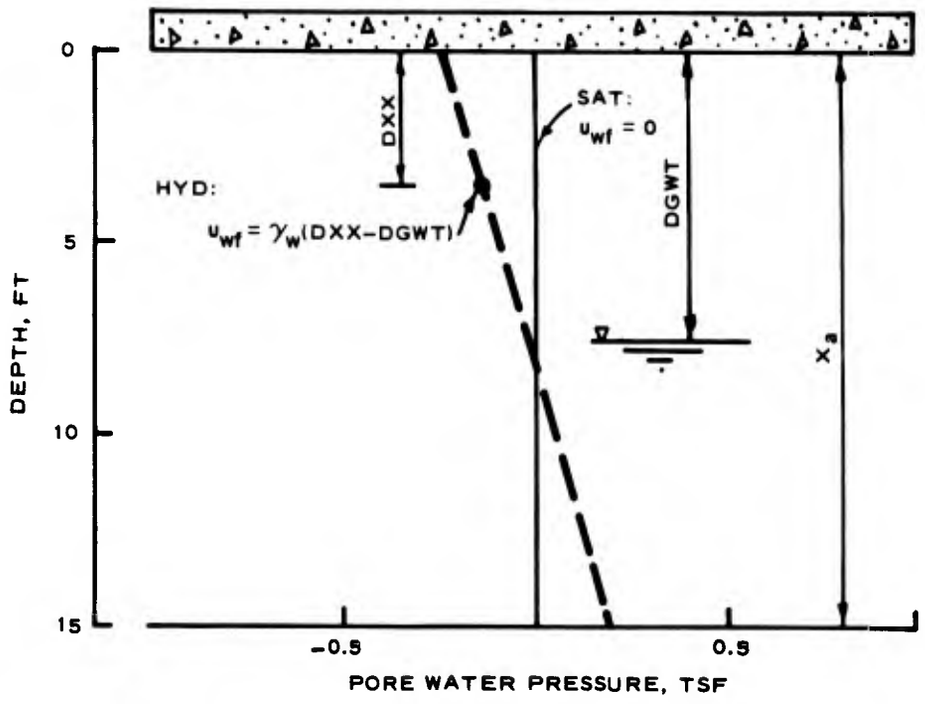

Figure 4. Equilibrium pore water pressure with a shallow water table

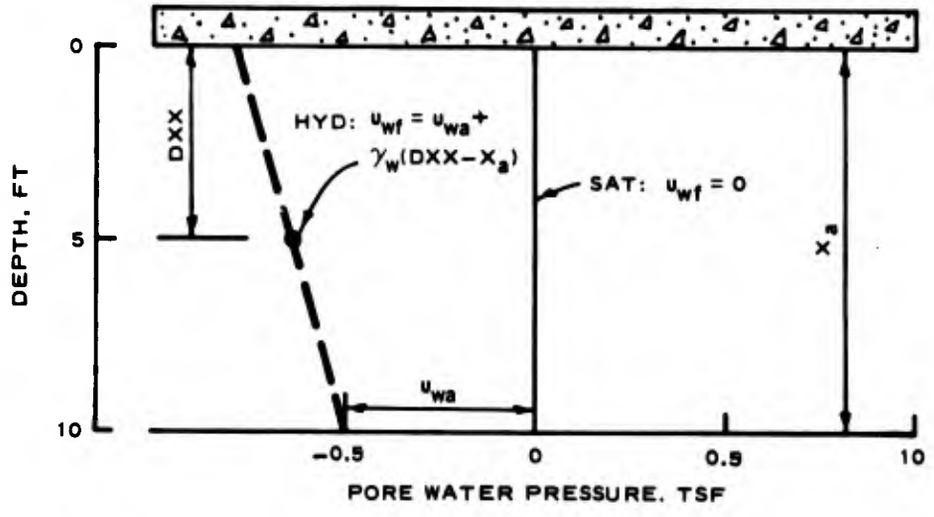

Figure 5. Equilibrium pore water pressure without a shallow water table

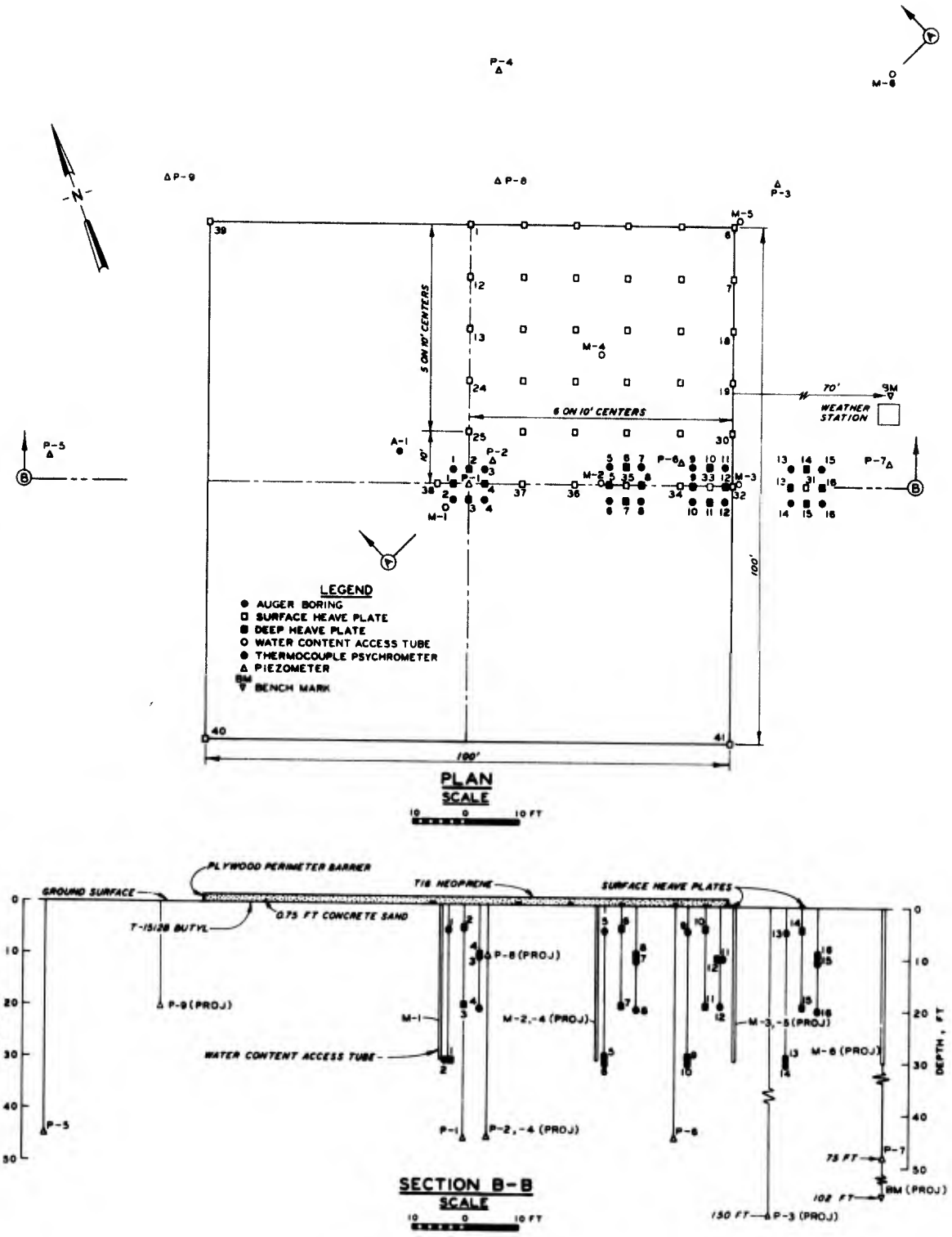

Figure 6. Layout of the Clinton test section

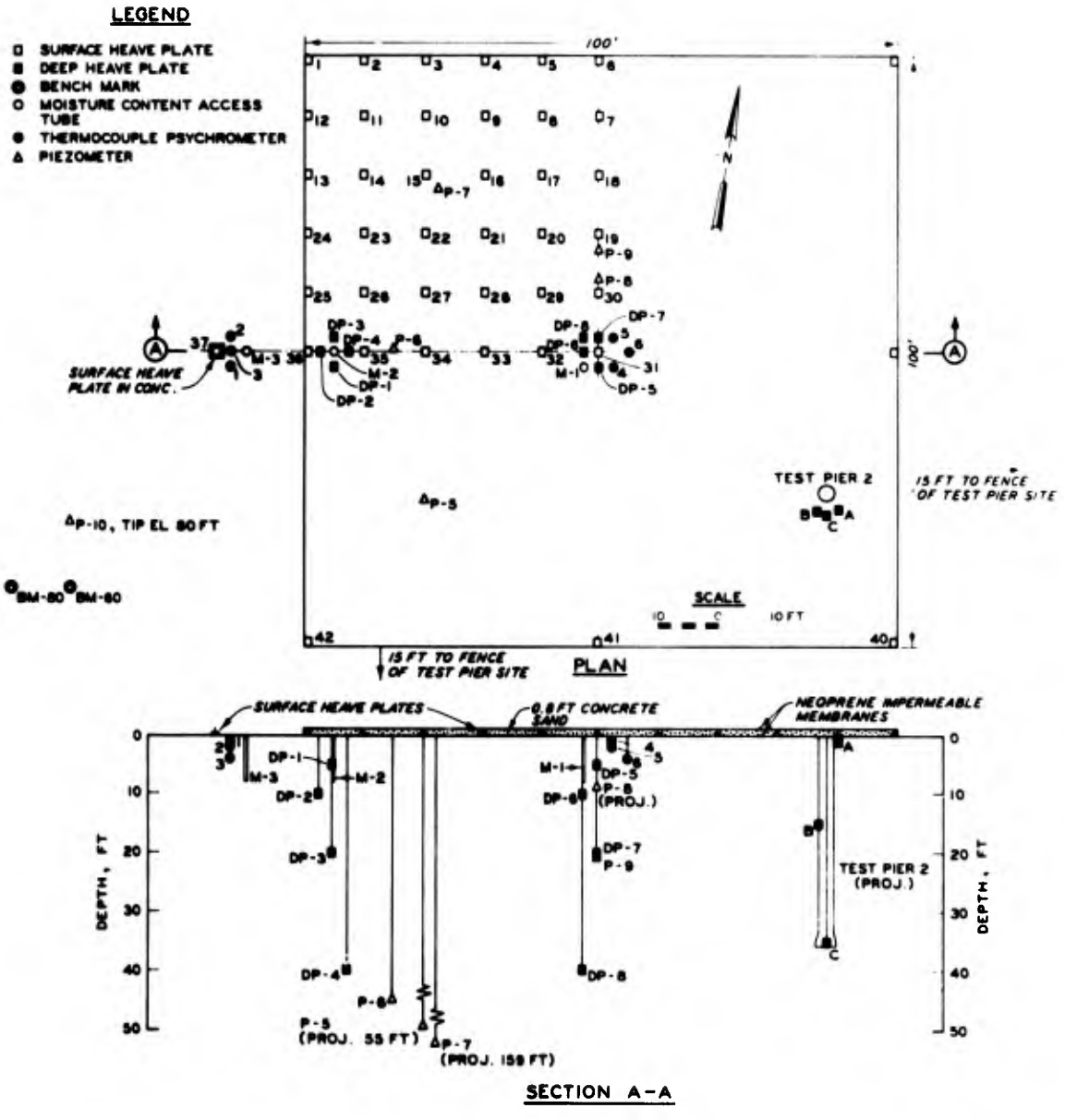

Figure 7. Layout of the Lackland test section

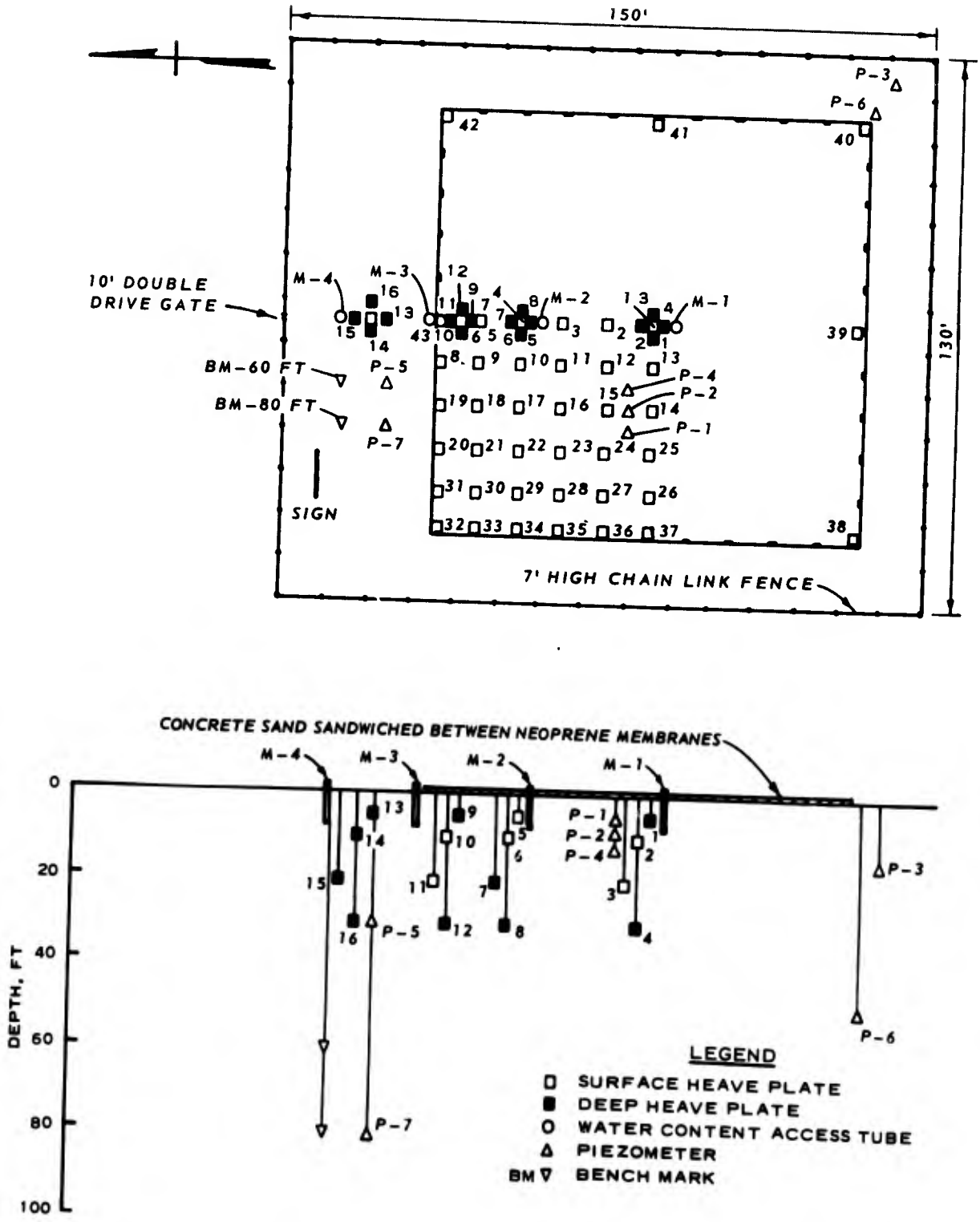

Figure 8. Fort Carson test section

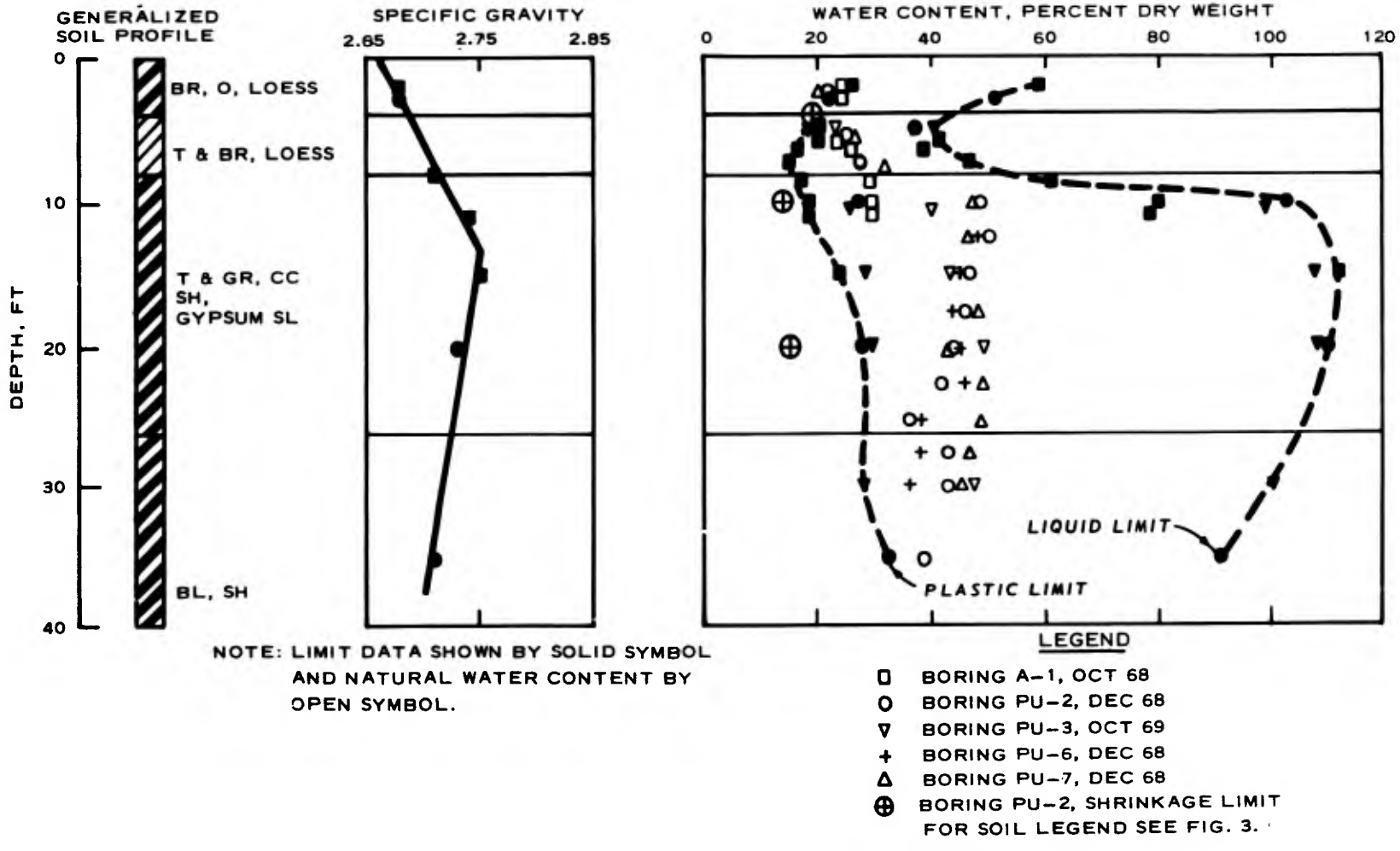

Figure 9. Generalized soil profile, specific gravity, Atterberg limits, and natural water content of Jackson test section soil

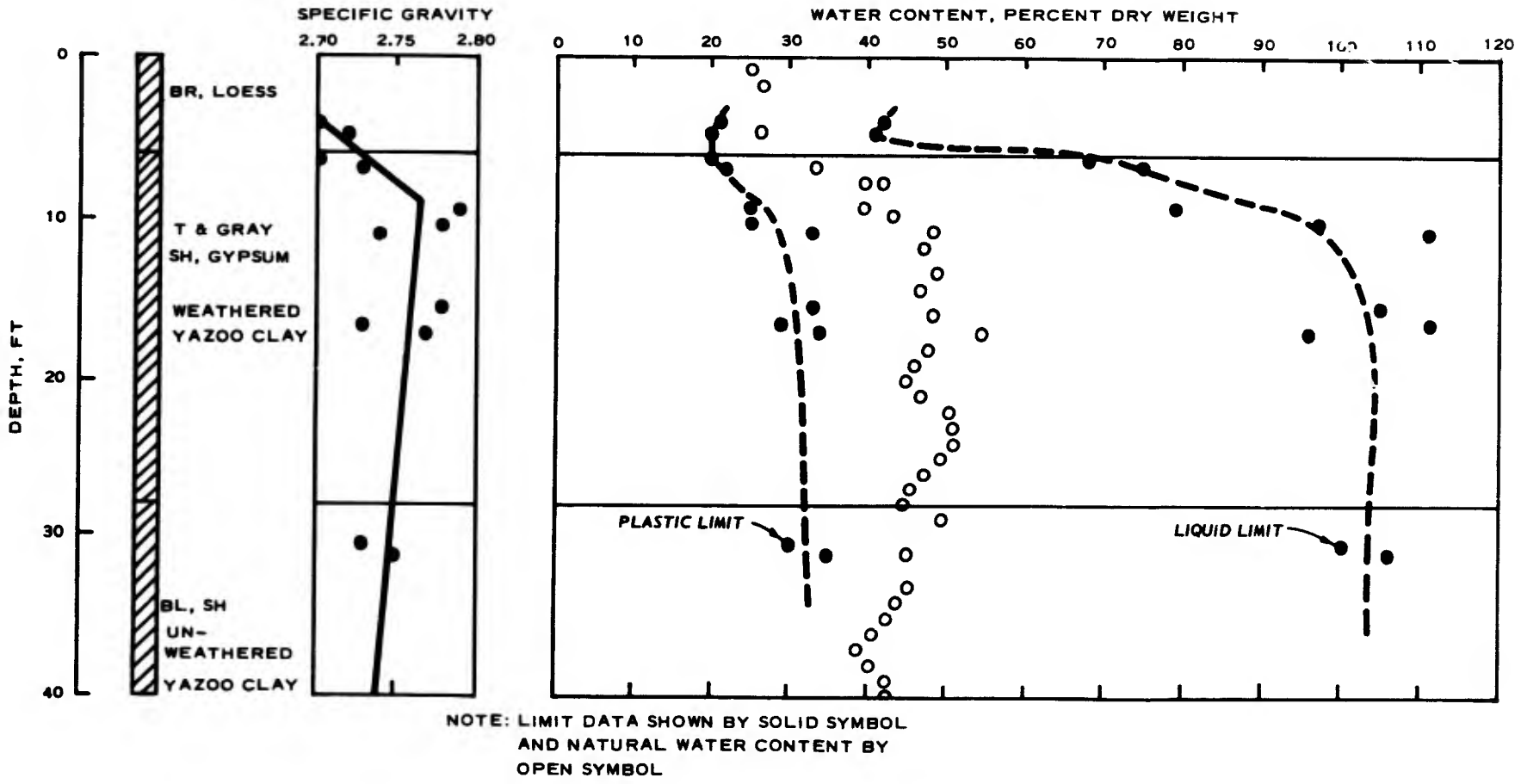

Figure 10. Classification of boring samples taken March 1973, Clinton test site

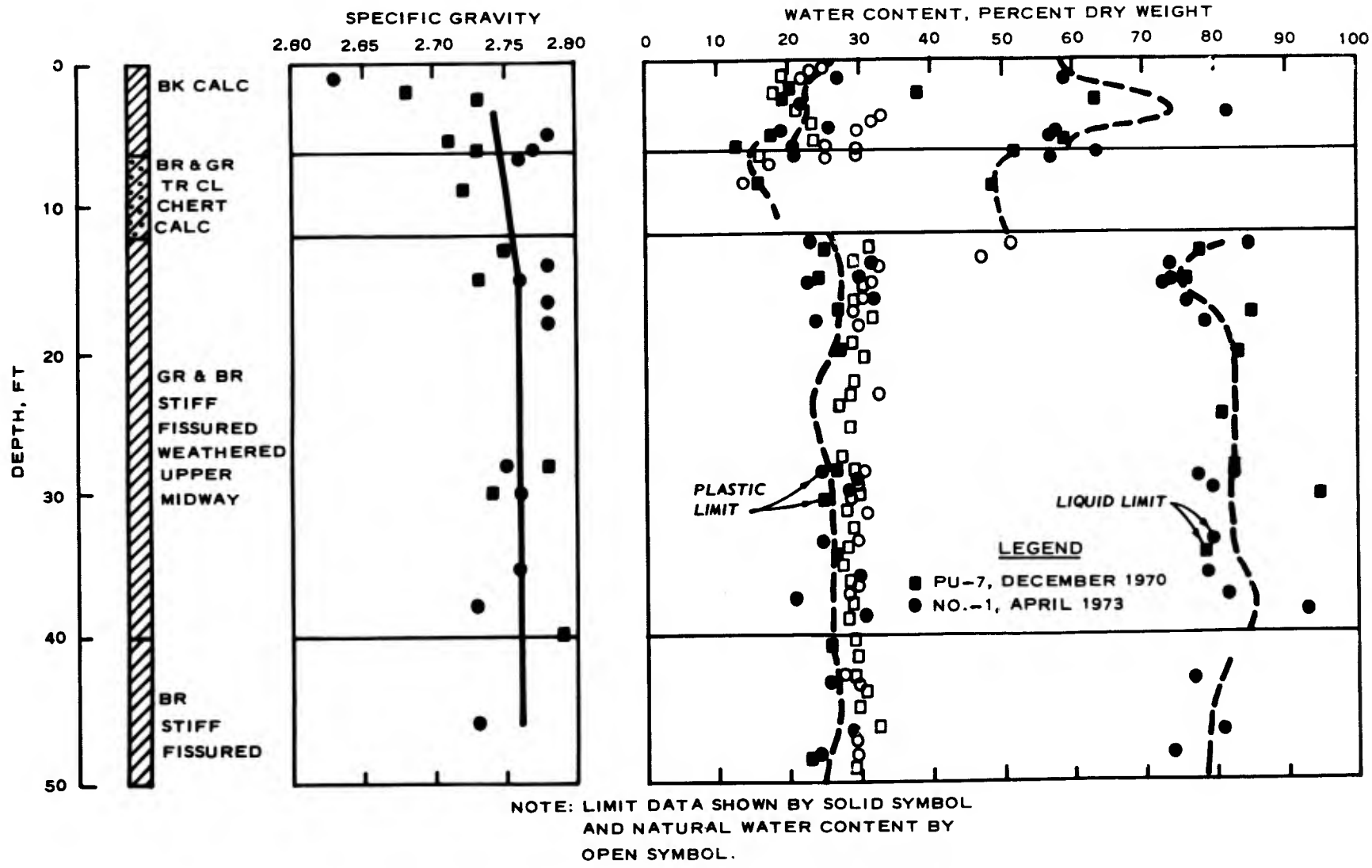

Figure 11. Classification of boring samples, Lackland test site

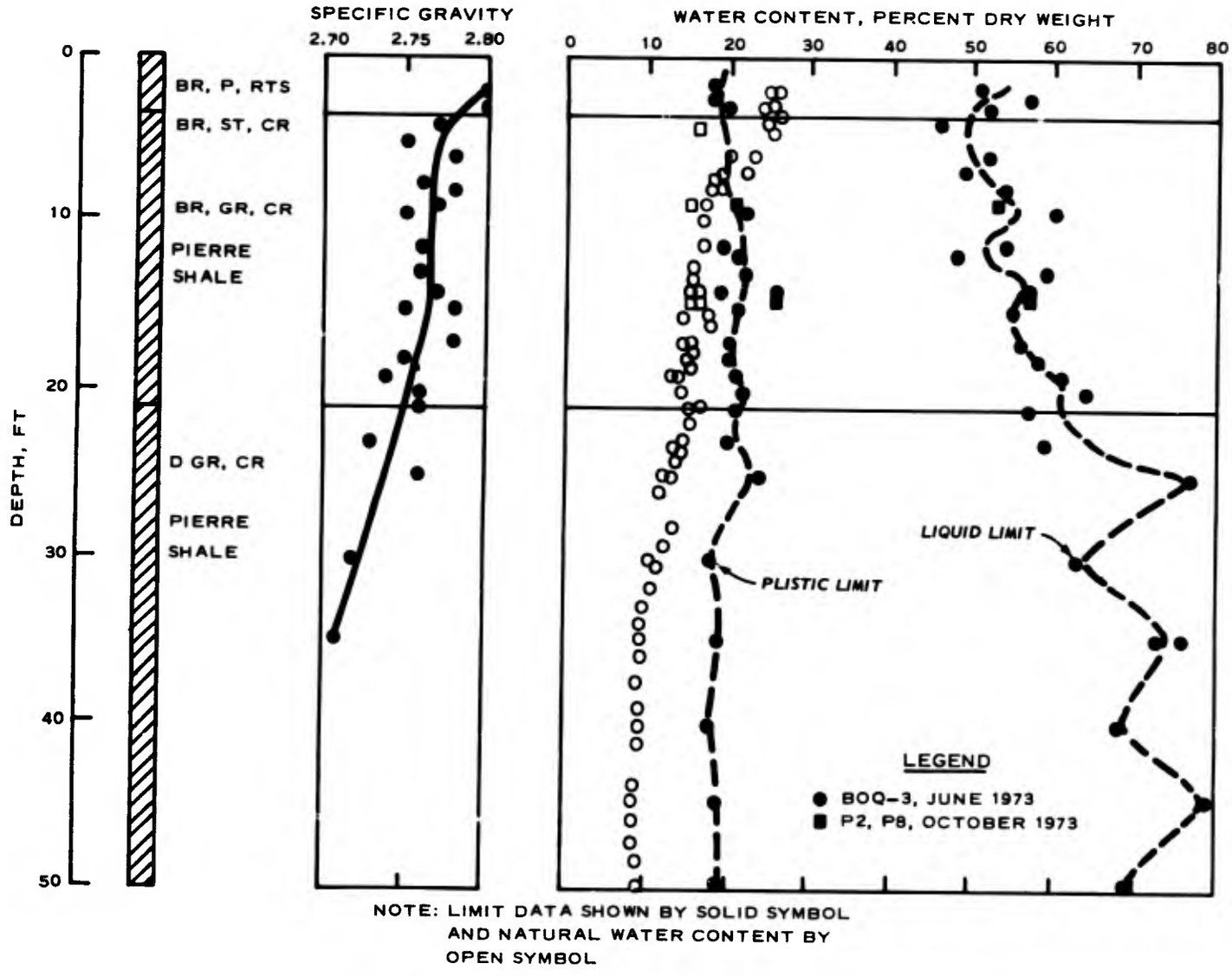

Figure 12. Classification of boring samples, Fort Carson test site

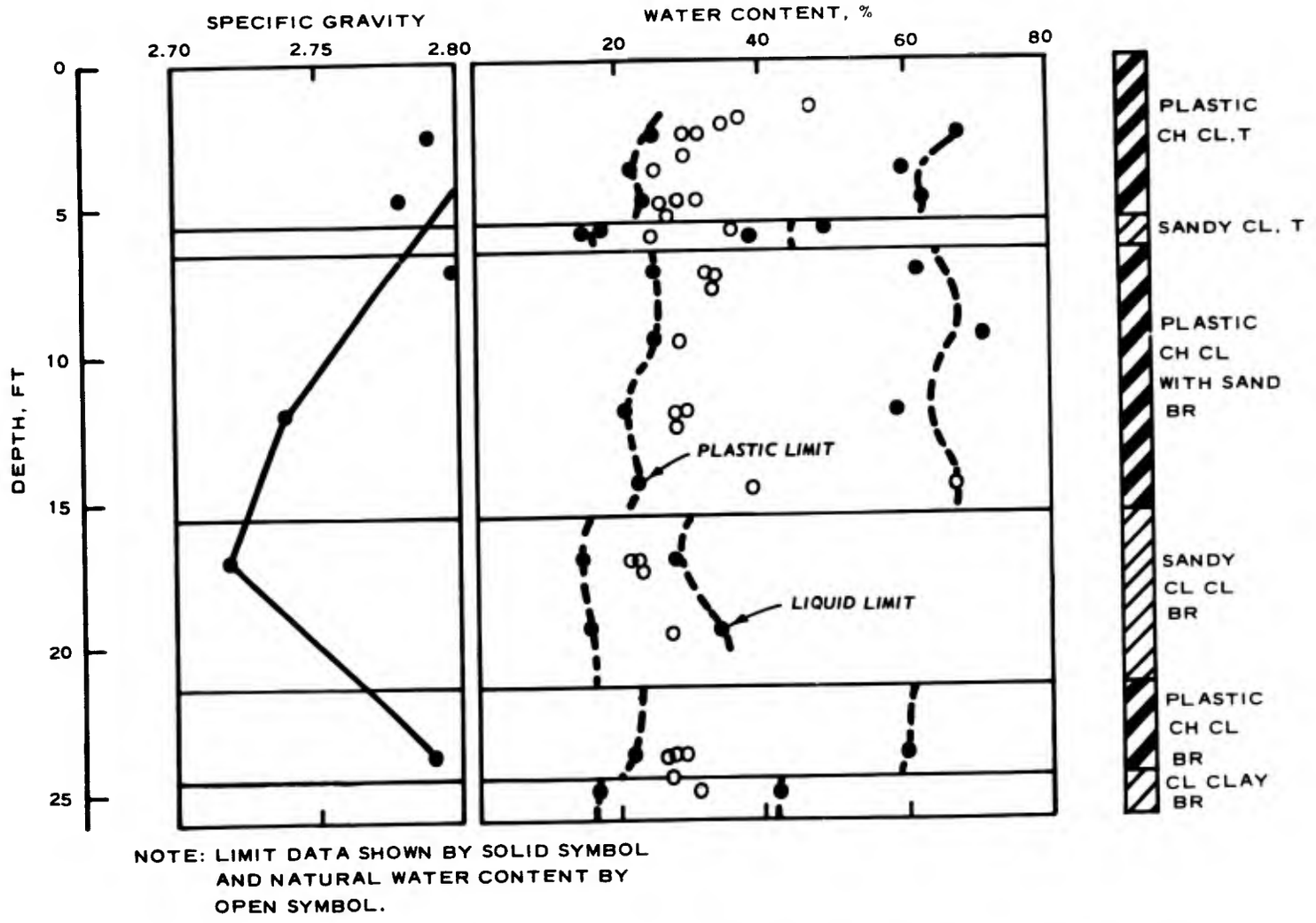

Figure 13. Classification of boring samples taken November 1976, Sigonella test site

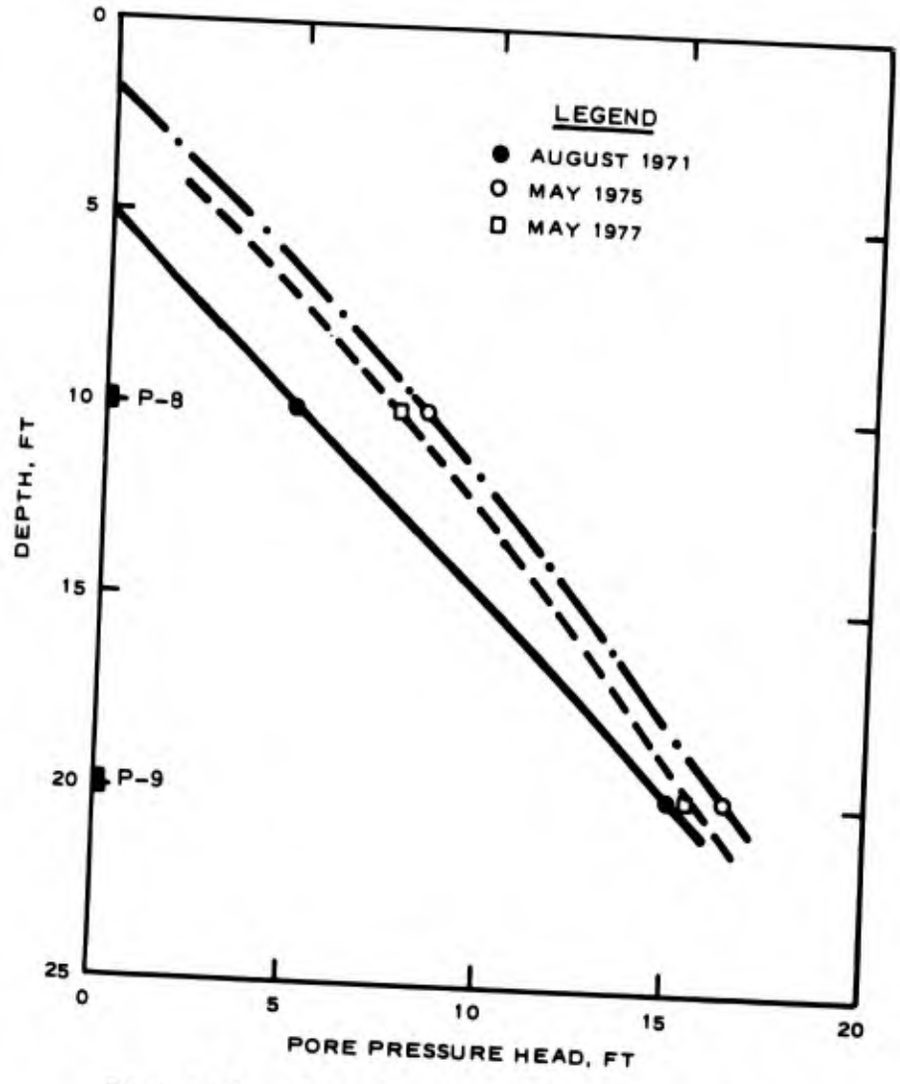

Figure 14. Profile of the pore pressure head at the Clinton test site

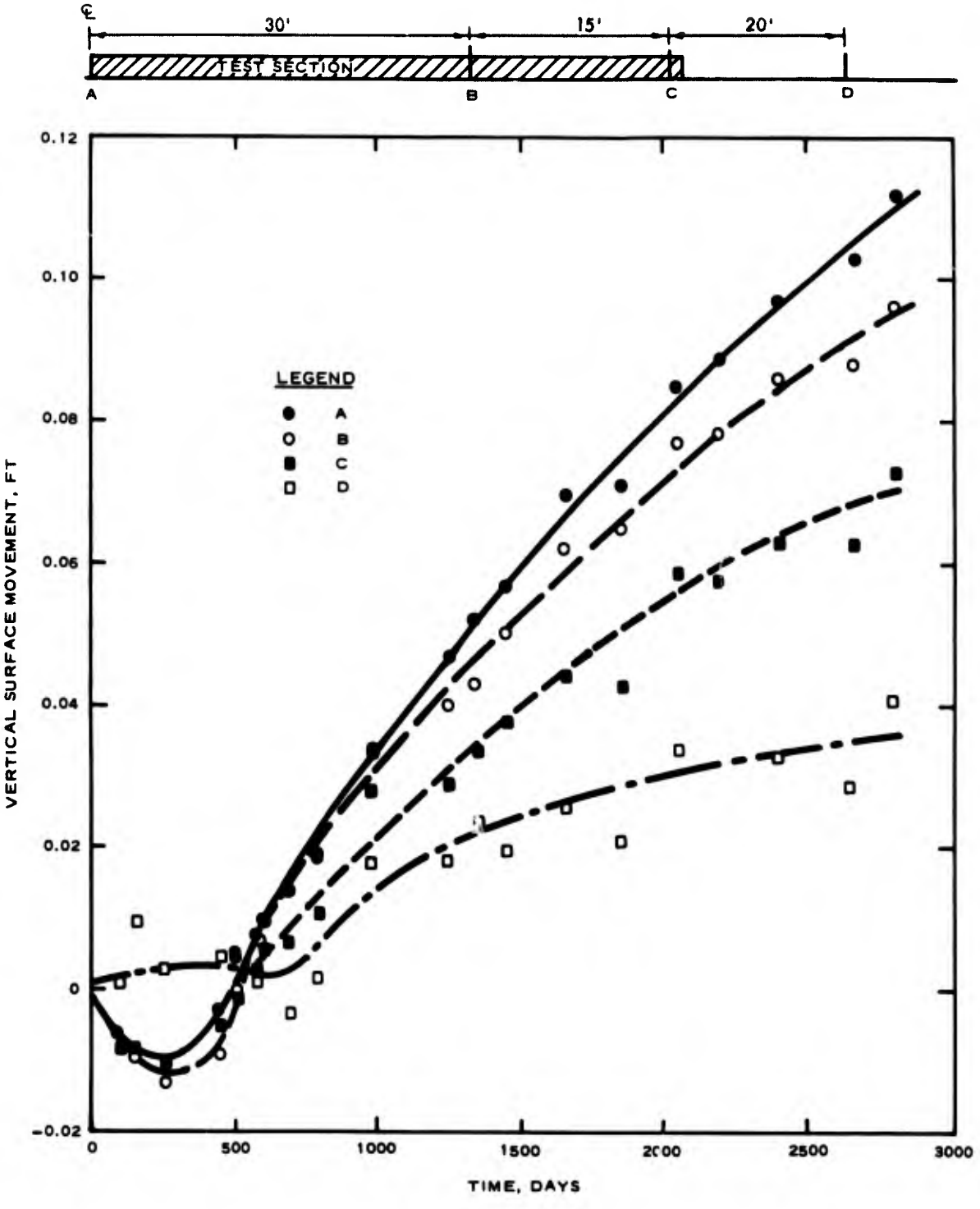

Figure 15. Vertical surface movement with time at the Clinton test site

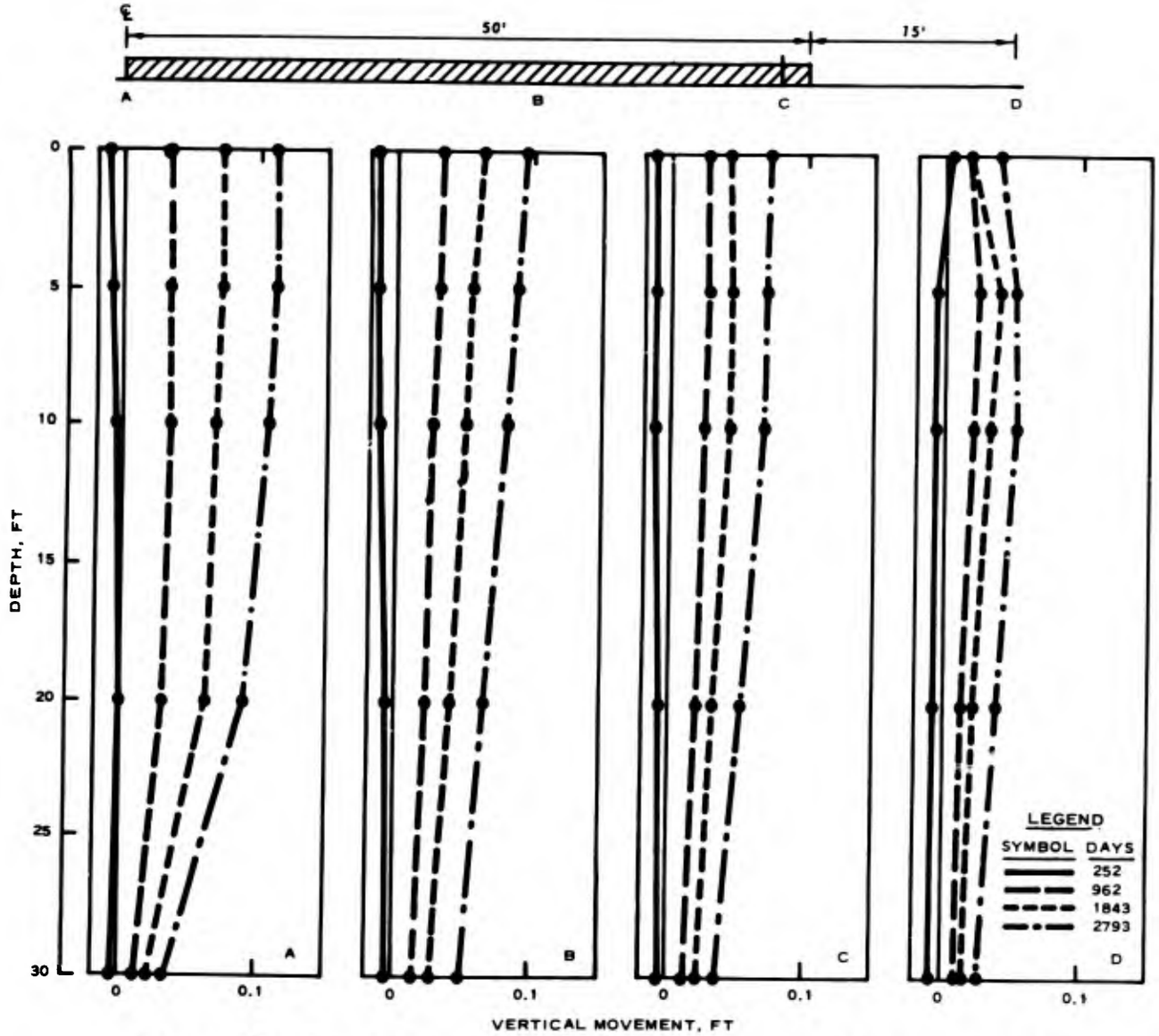

Figure 16. Vertical movement with depth at the Clinton test site

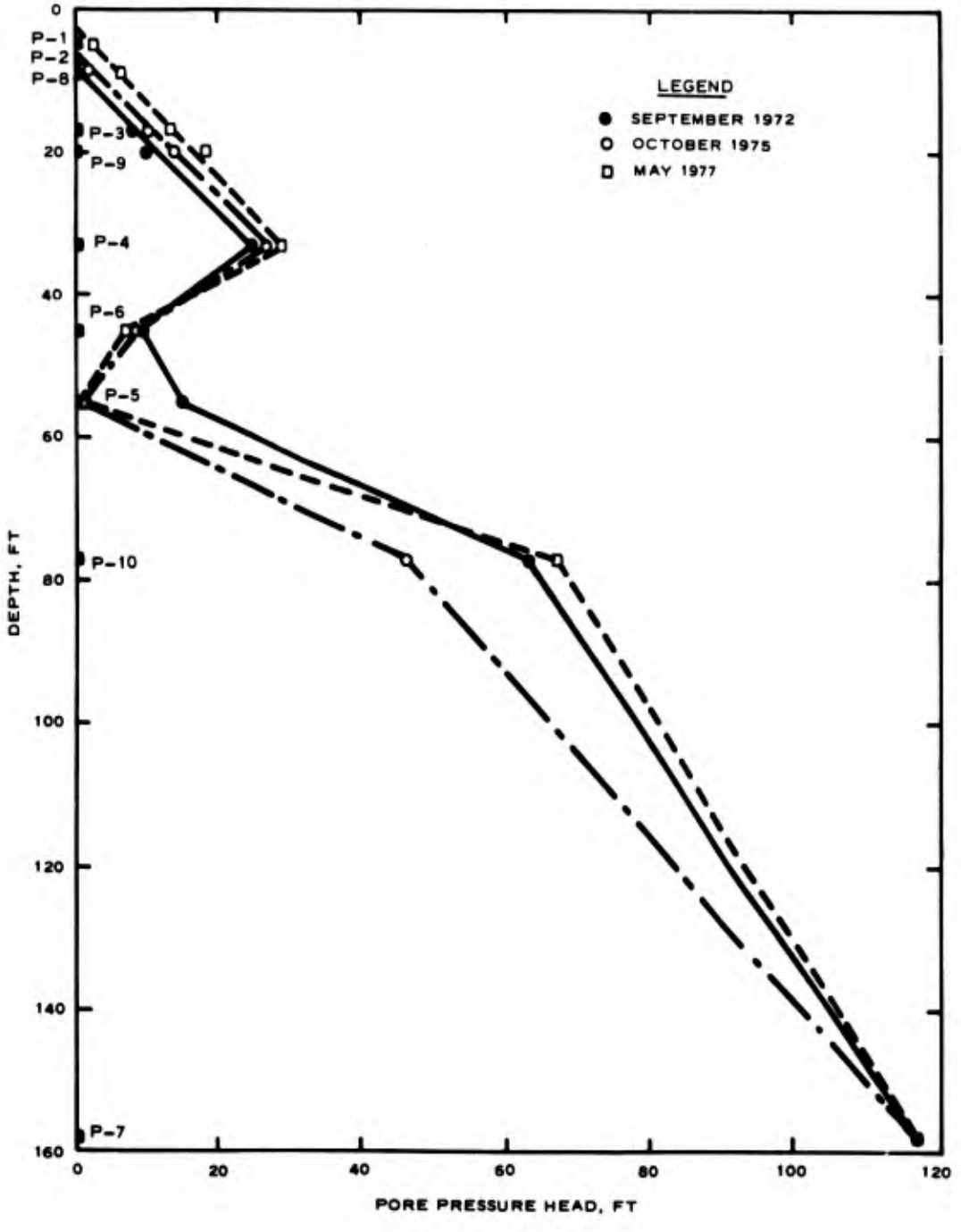

Figure 17. Profile of pressure head at the Lackland test site

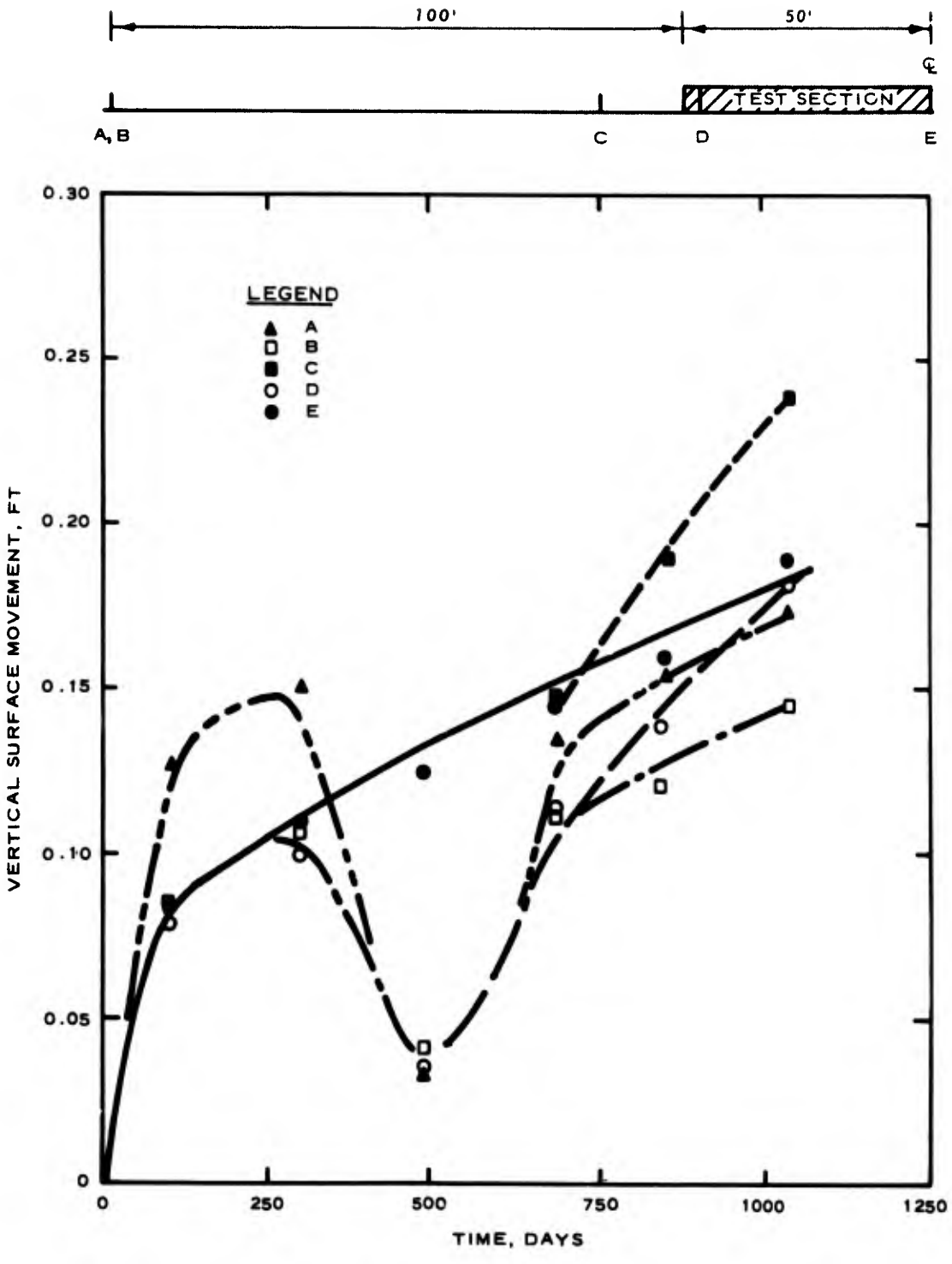

Figure 18. Vertical surface movement with time at the Lackland test site

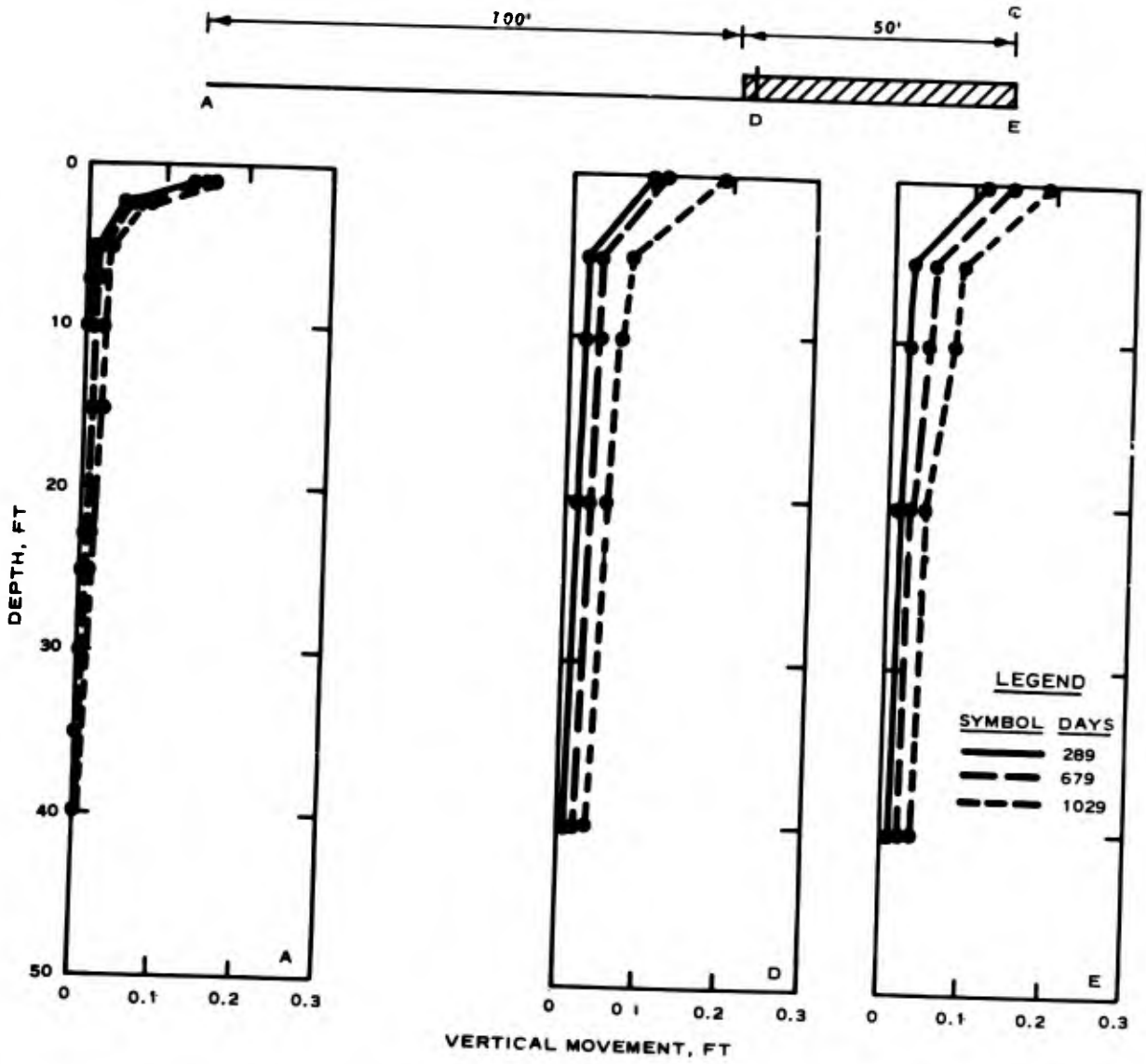

Figure 19. Vertical movement with depth at the Lackland test site

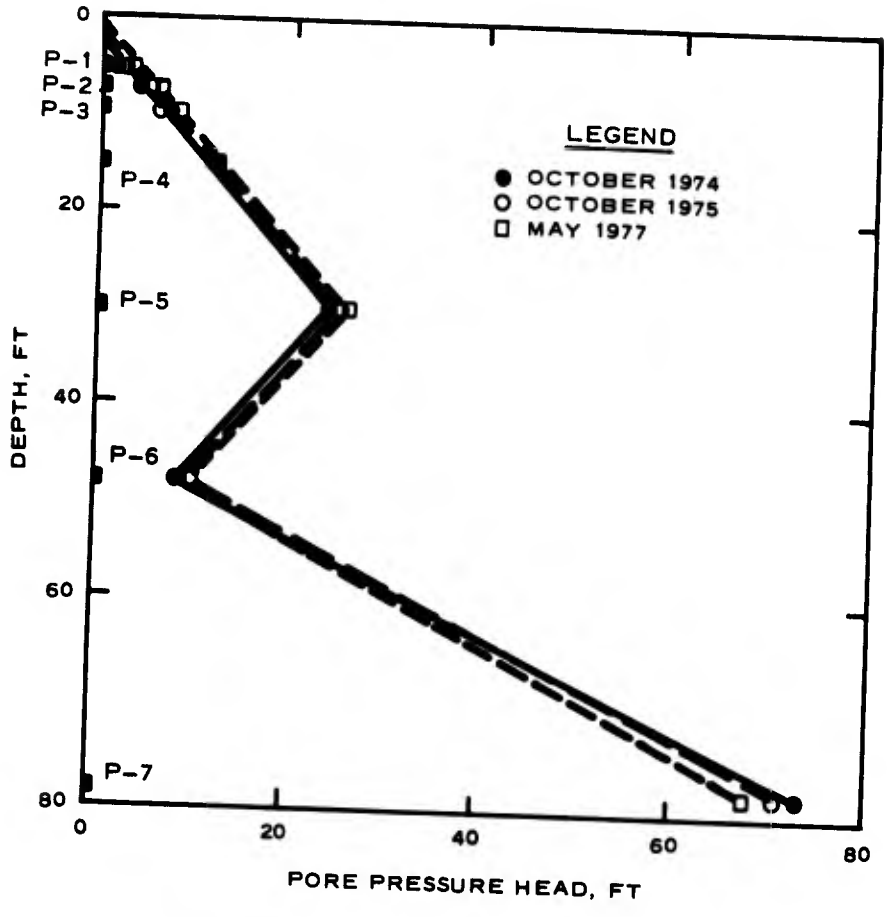

Figure 20. Profile of pore pressure head at the Fort Carson test site

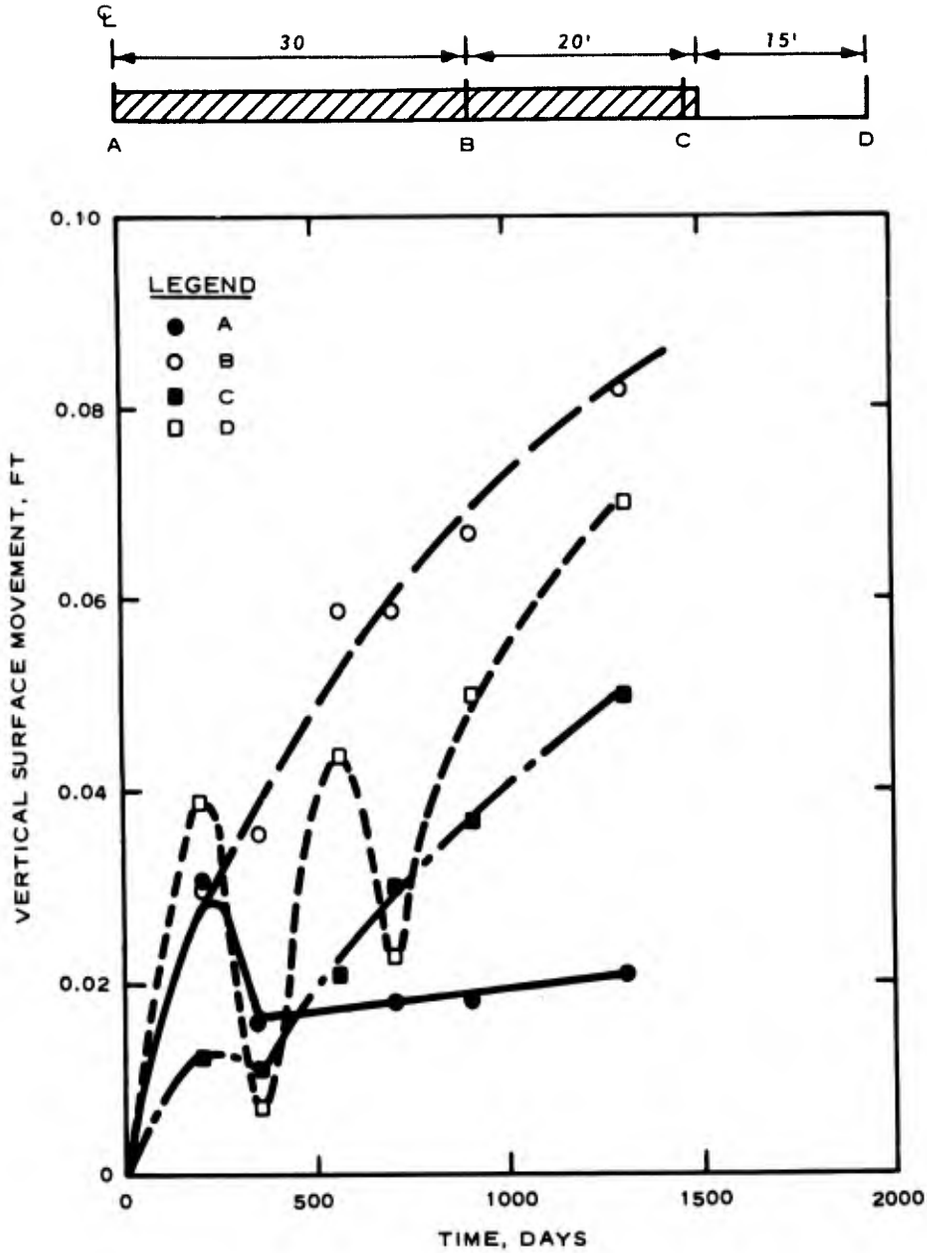

Figure 21. Vertical surface movement with time at the Fort Carson test site

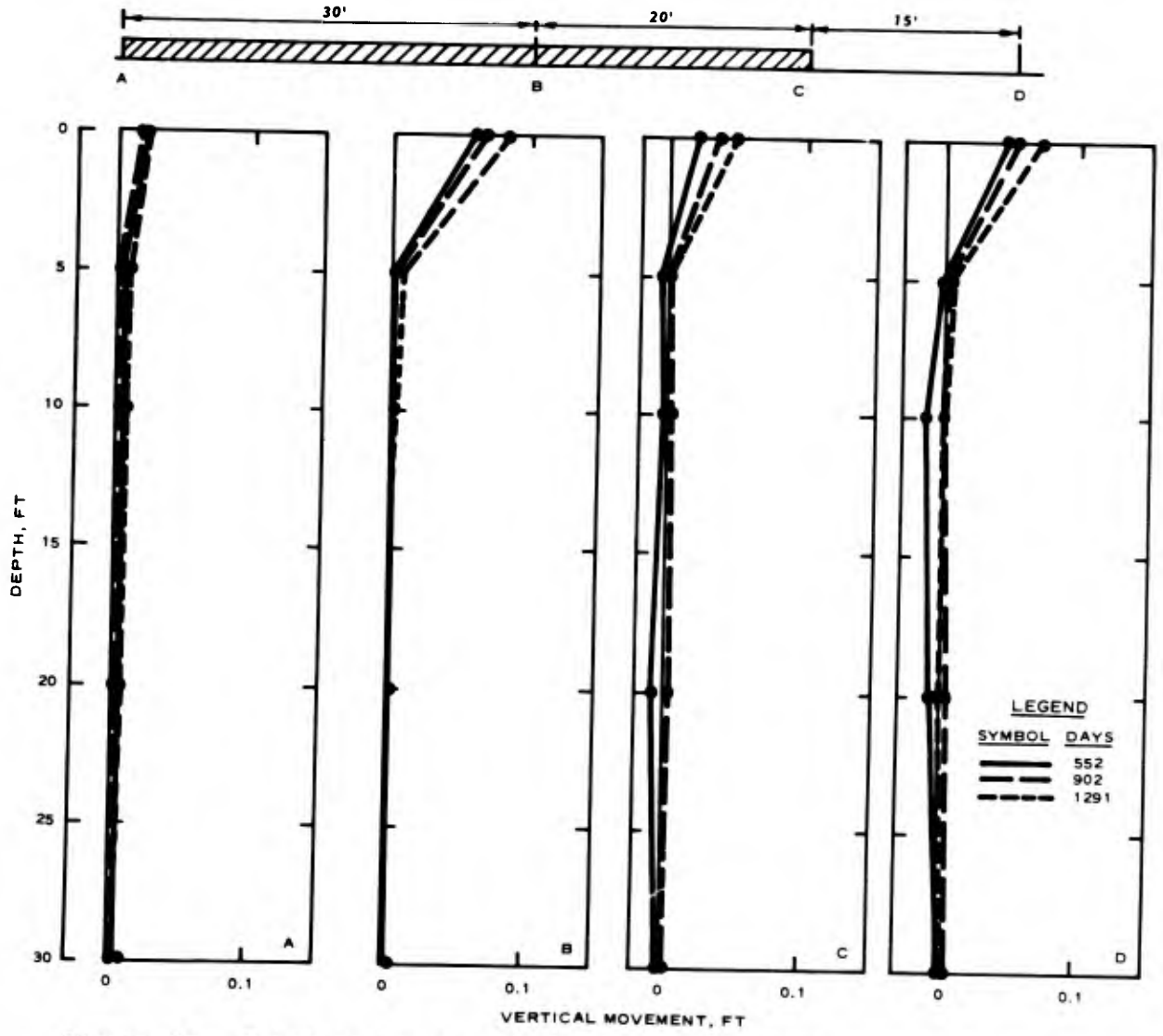

Figure 22. Vertical heave with depth at the Fort Carson test site

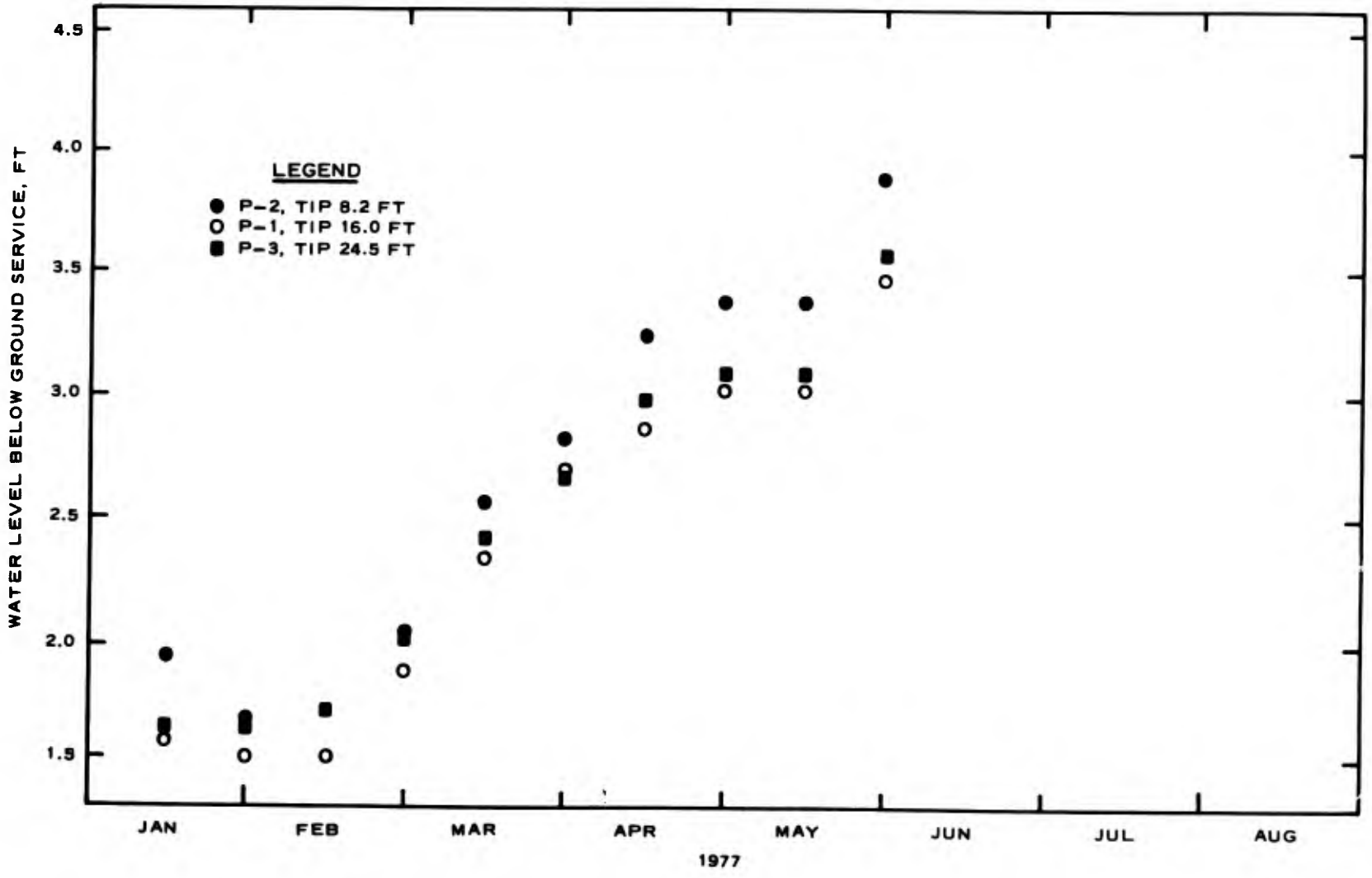

Figure 23. Water levels below ground surface at the Sigonella test site

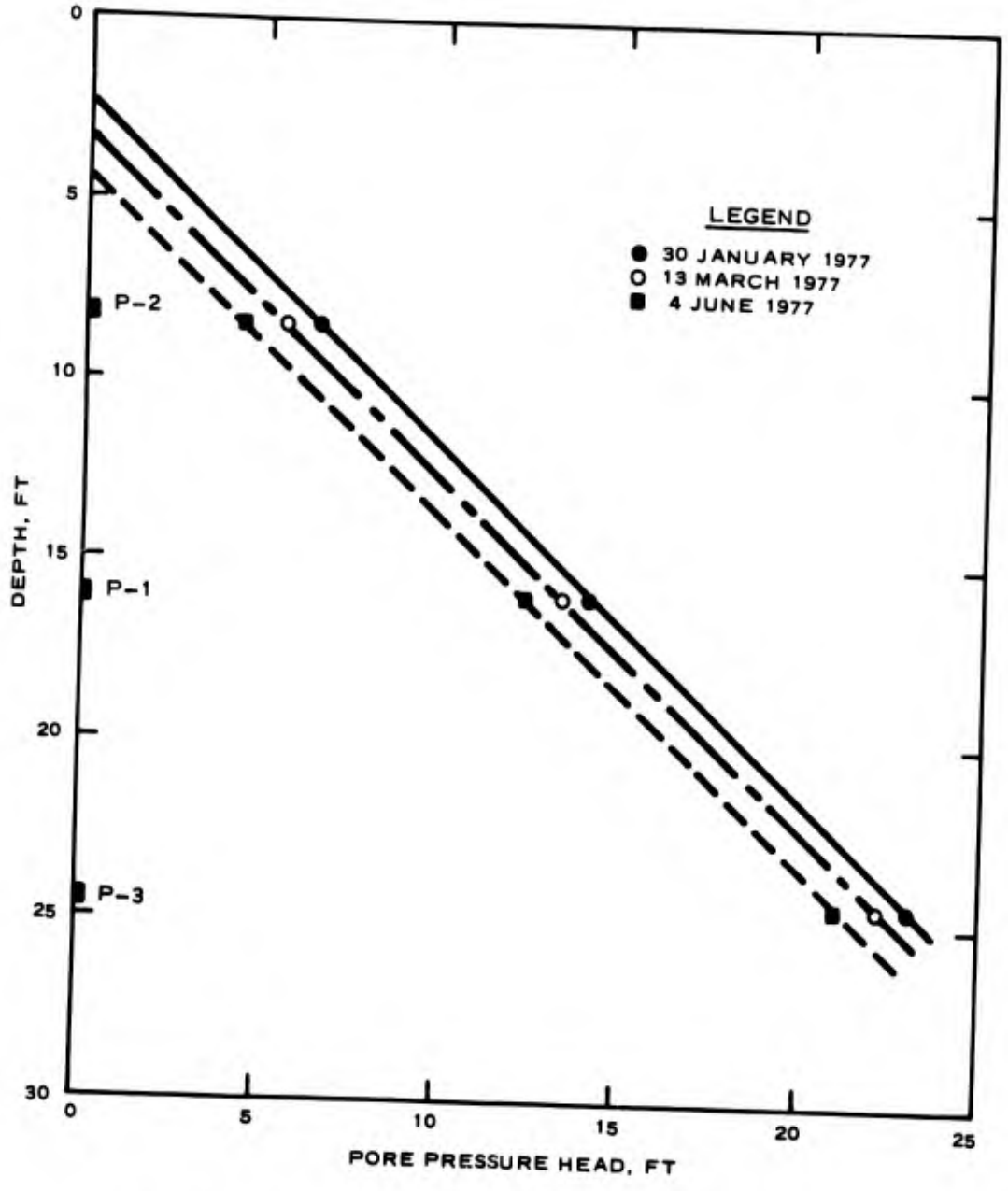

Figure 24. Profile of the pore pressure head at the Sigonella test site

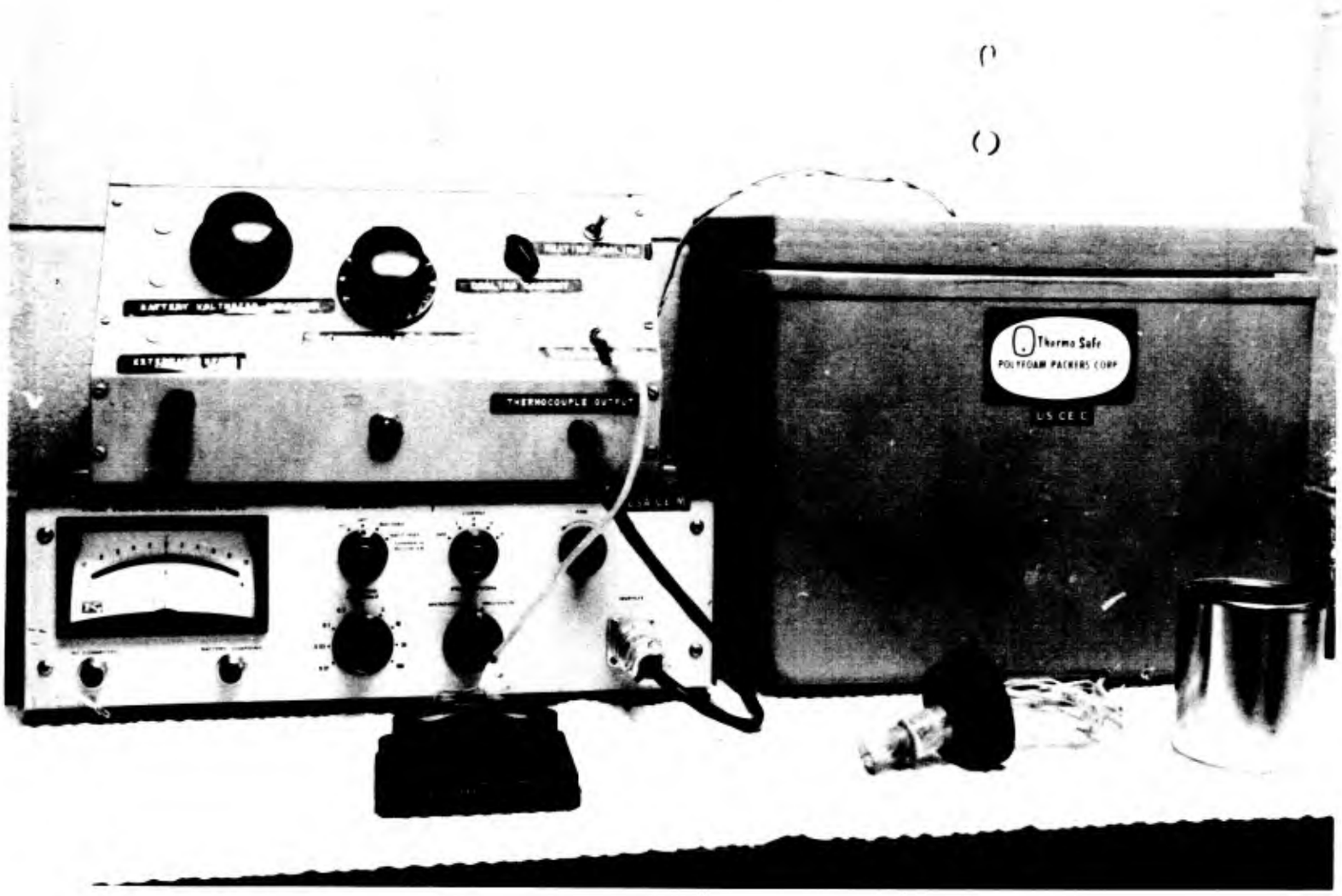

Figure 25. Monitoring system

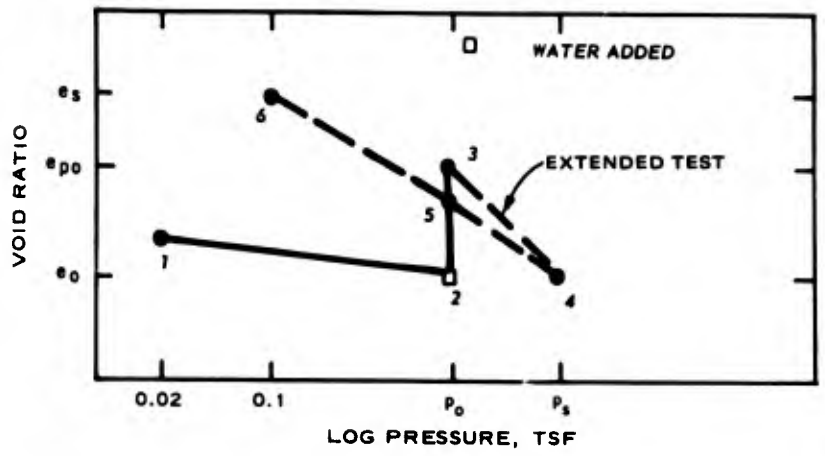

a. SWELL OVERBURDEN

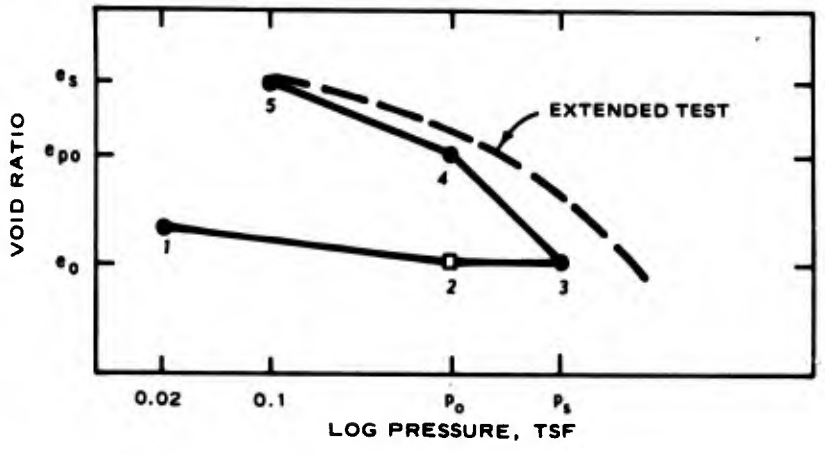

b. CONSTANT VOLUME SWELL

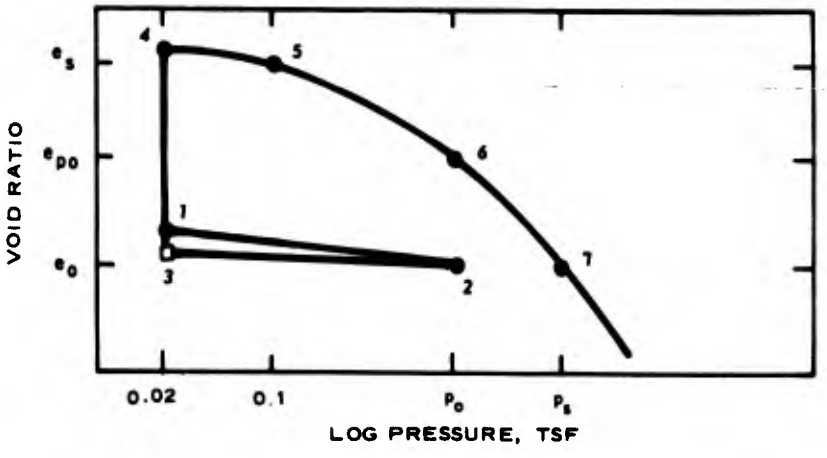

c. IMPROVE SIMPLE OFDOMETER

Figure 26. Schematic diagrams of void ratio - log pressure relationships of three types of swell tests

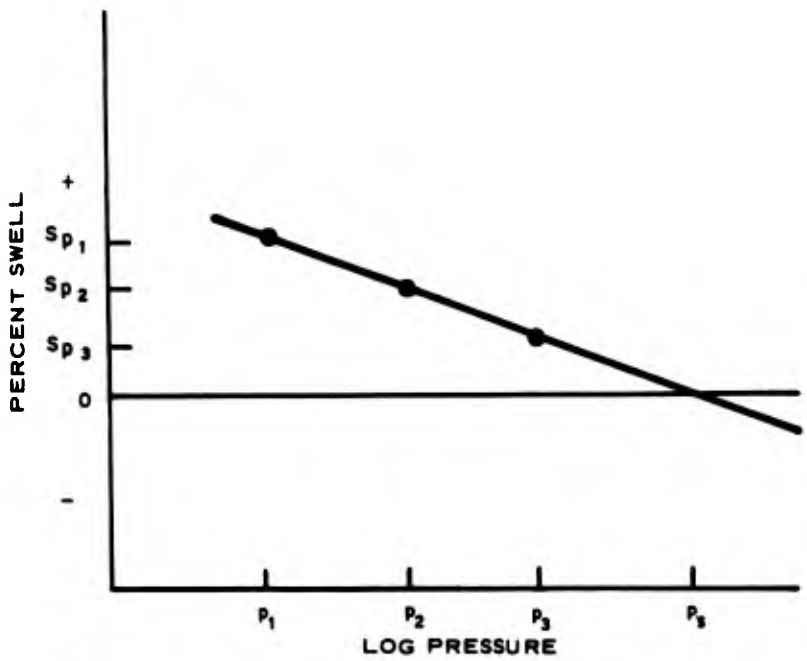

Figure 27. Schematic diagram of percent swell-log pressure relationships of SO test results

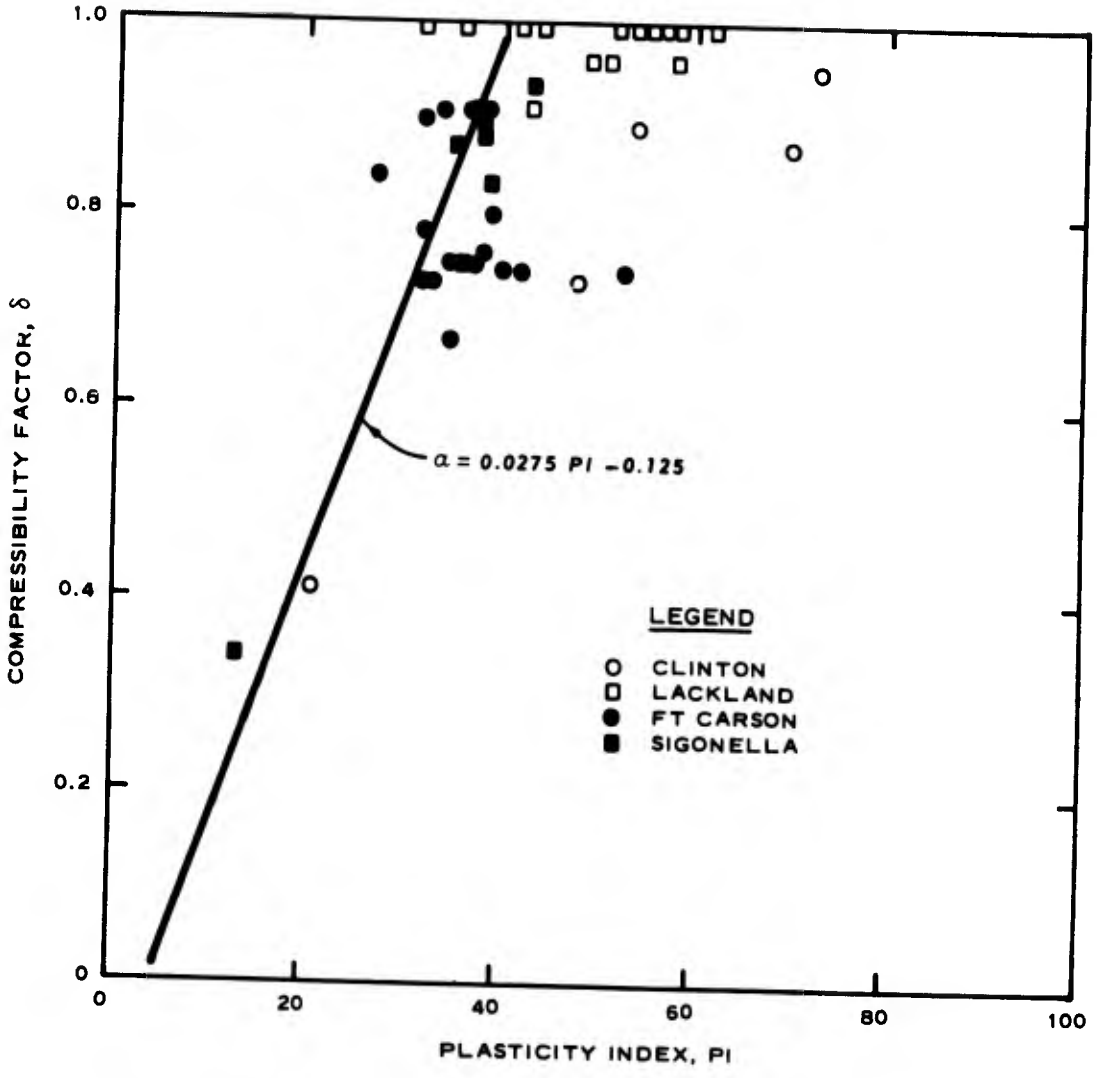

Figure 28. Volumetric compressibility factor as a function of the plasticity index

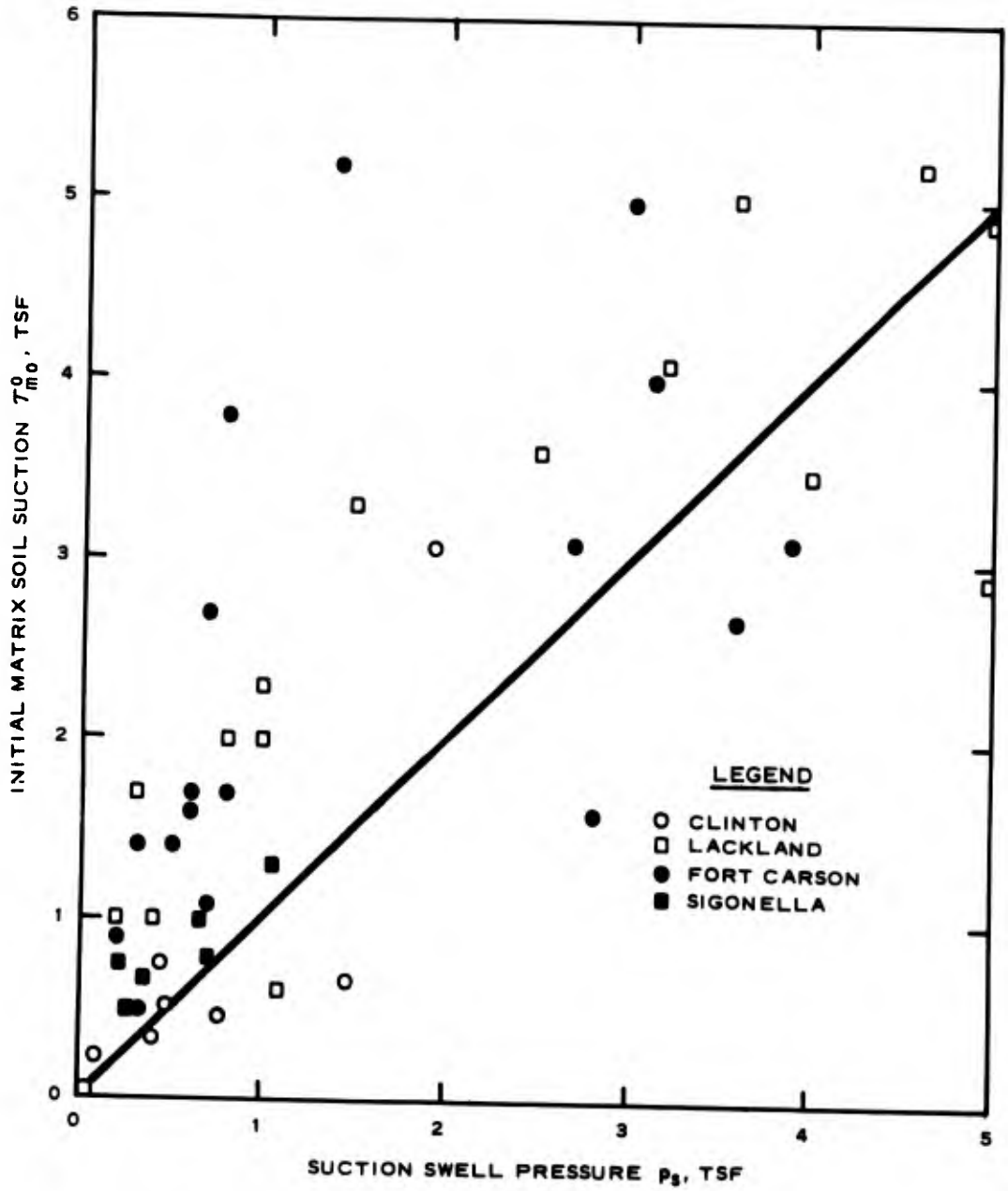

Figure 29. Comparison of the initial matrix soil suction with the suction swell pressure

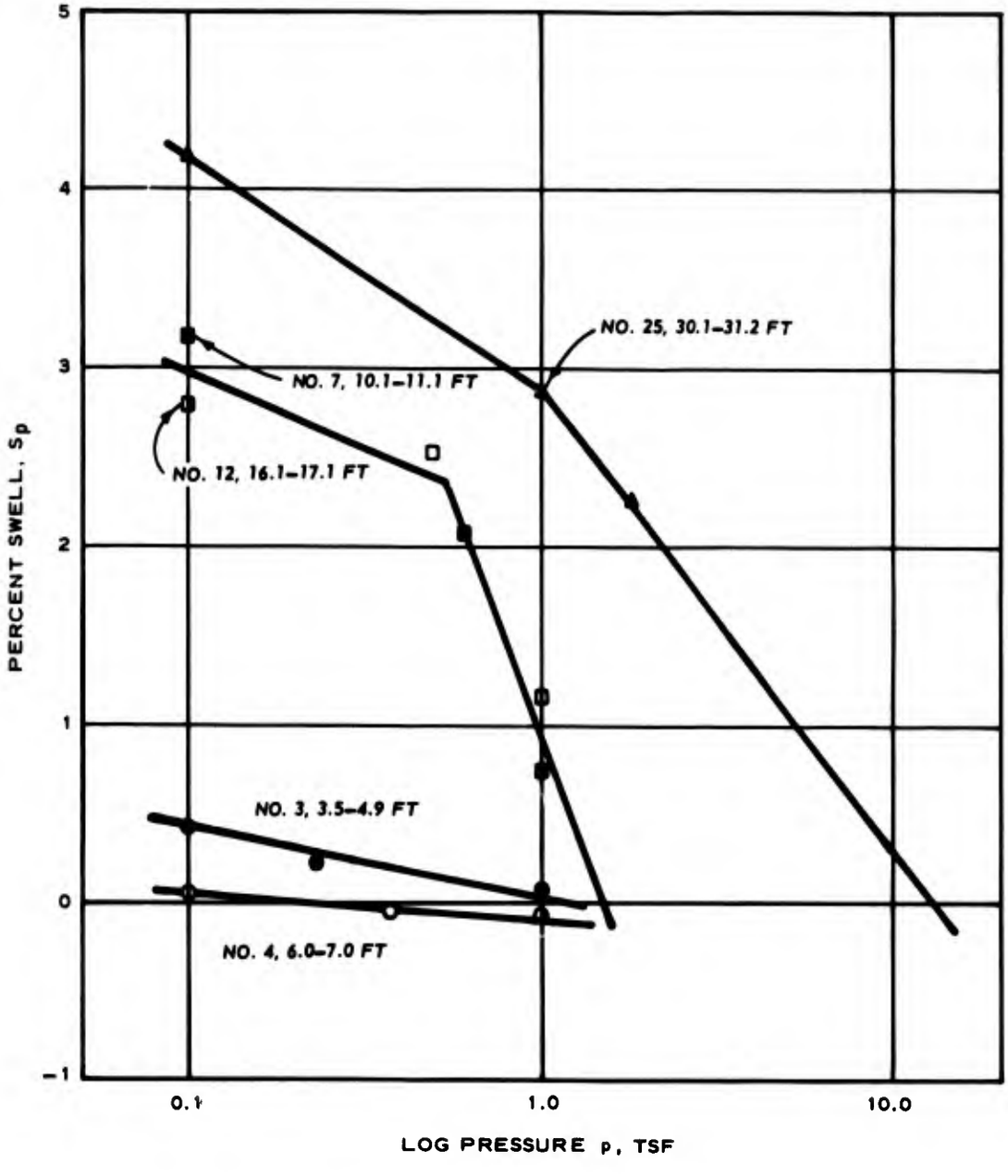

Figure 30. Swell overburden test results, Clinton test section, March, 1973

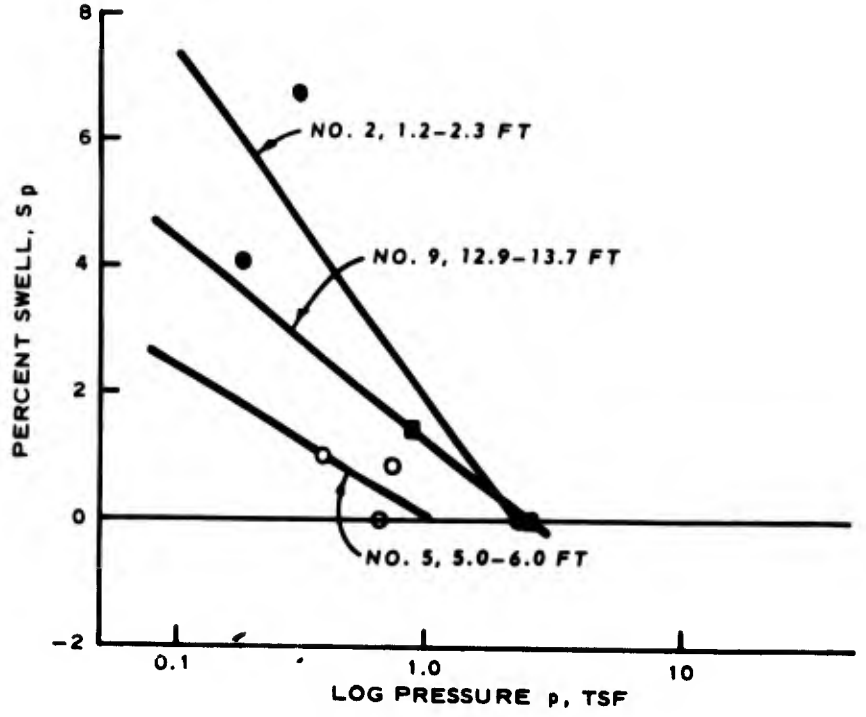

a. BORING PU-7. DEC 1970

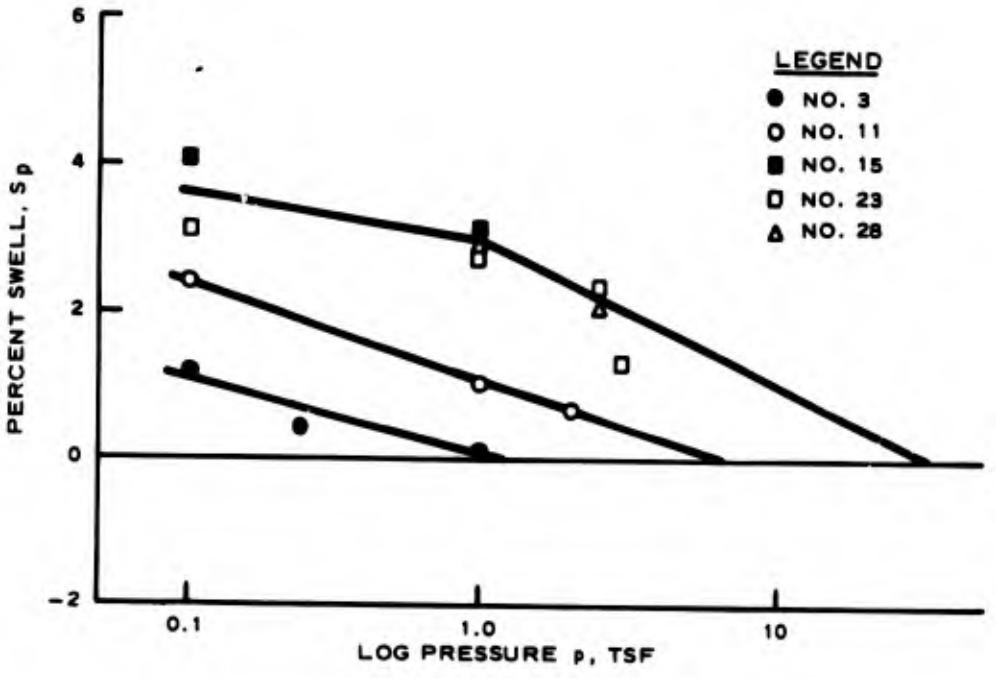

b. BORING NO. 1, APR 1973

Figure 31. Percent swell-log pressure relationships from results of swell overburden tests of boring samples from the Lackland test site

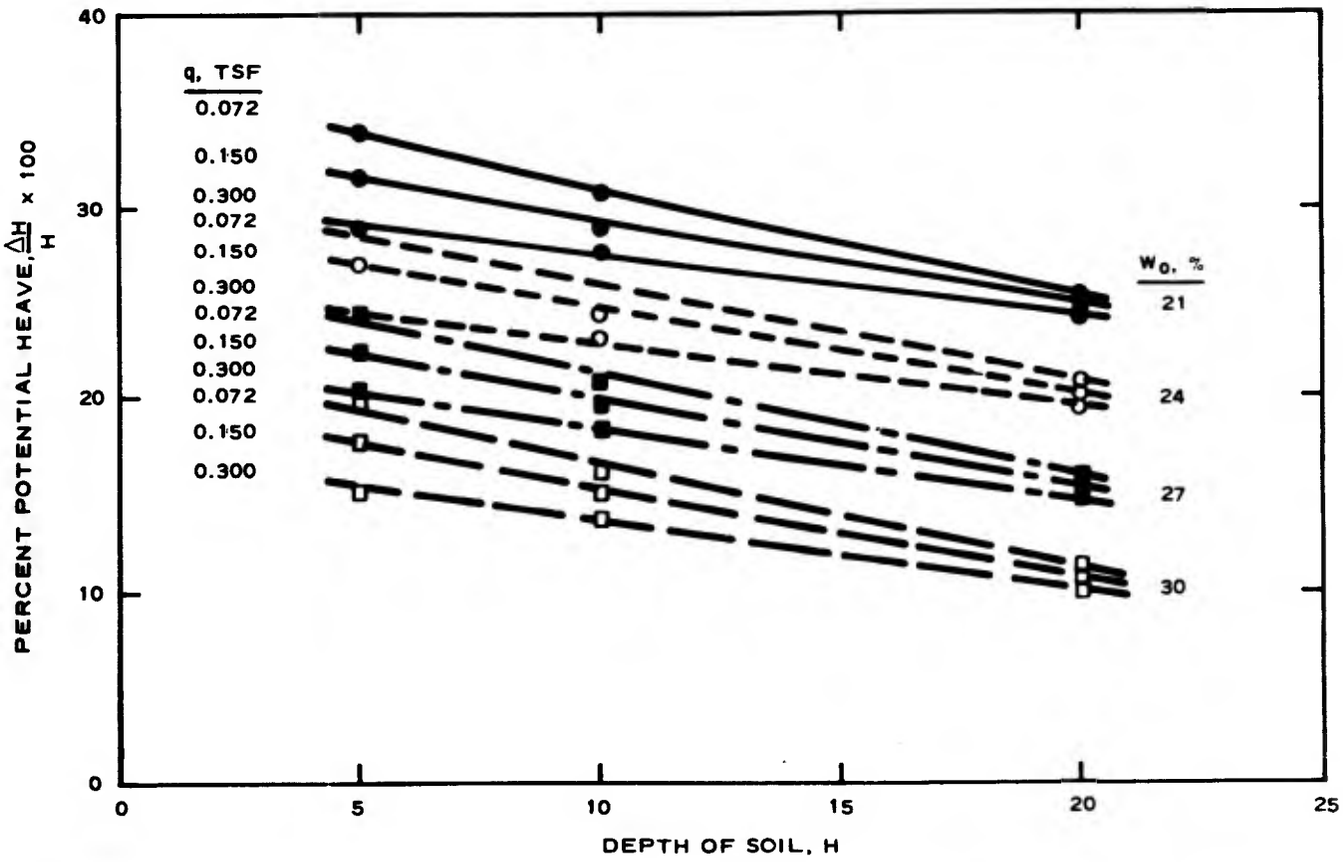

Figure 32. Fraction of potential heave for a soil with plasticity index of 60

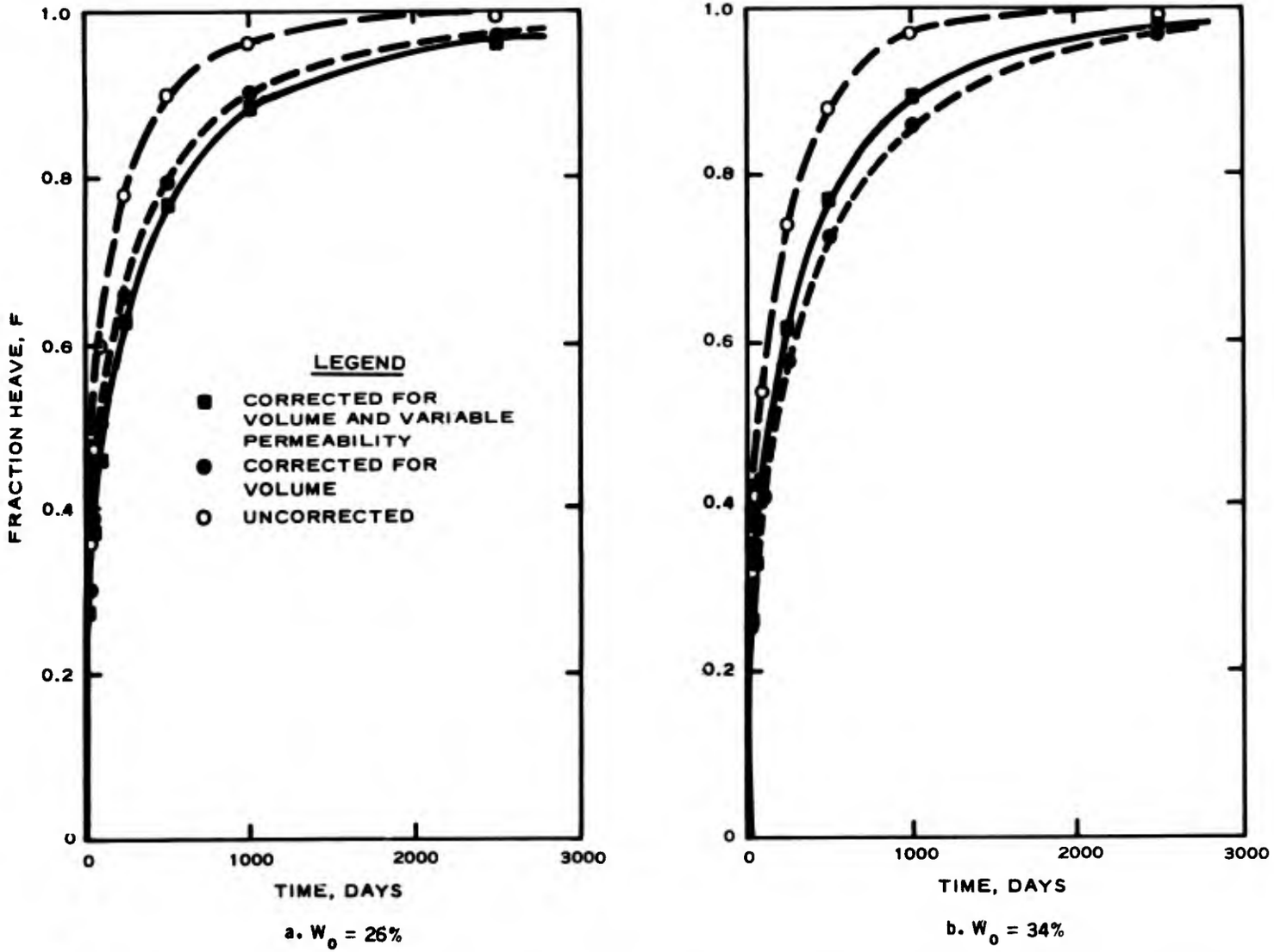

Figure 33. Comparison of heave with time between corrected and uncorrected curves for saturated soil of 5 ft depth, plasticity index 80, and surcharge pressure 0.072 tsf

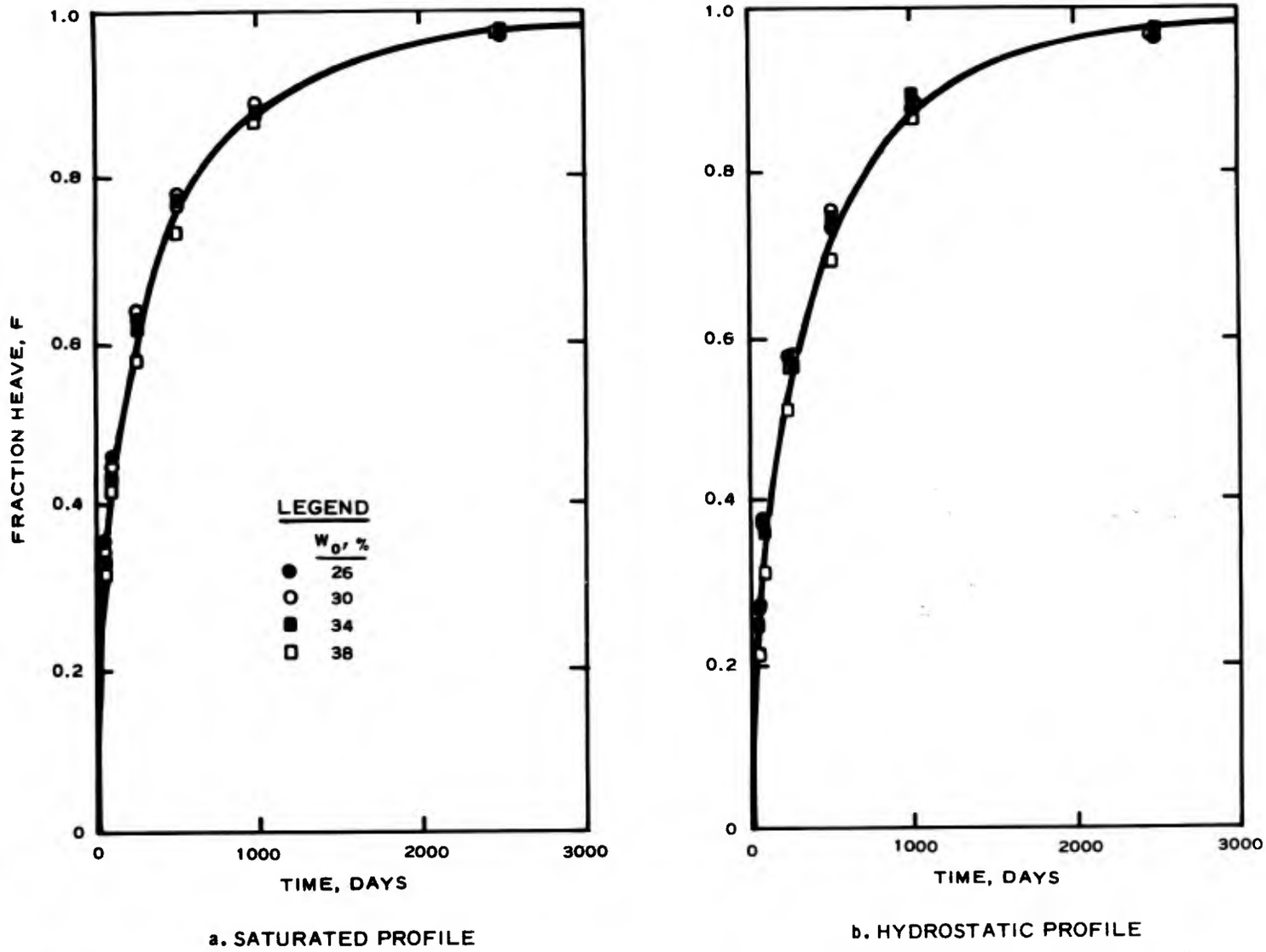

Figure 34. Comparison of heave with time for soil of 5 ft depth, plasticity index 80, surcharge pressure 0.072 tsf with different initial water contents

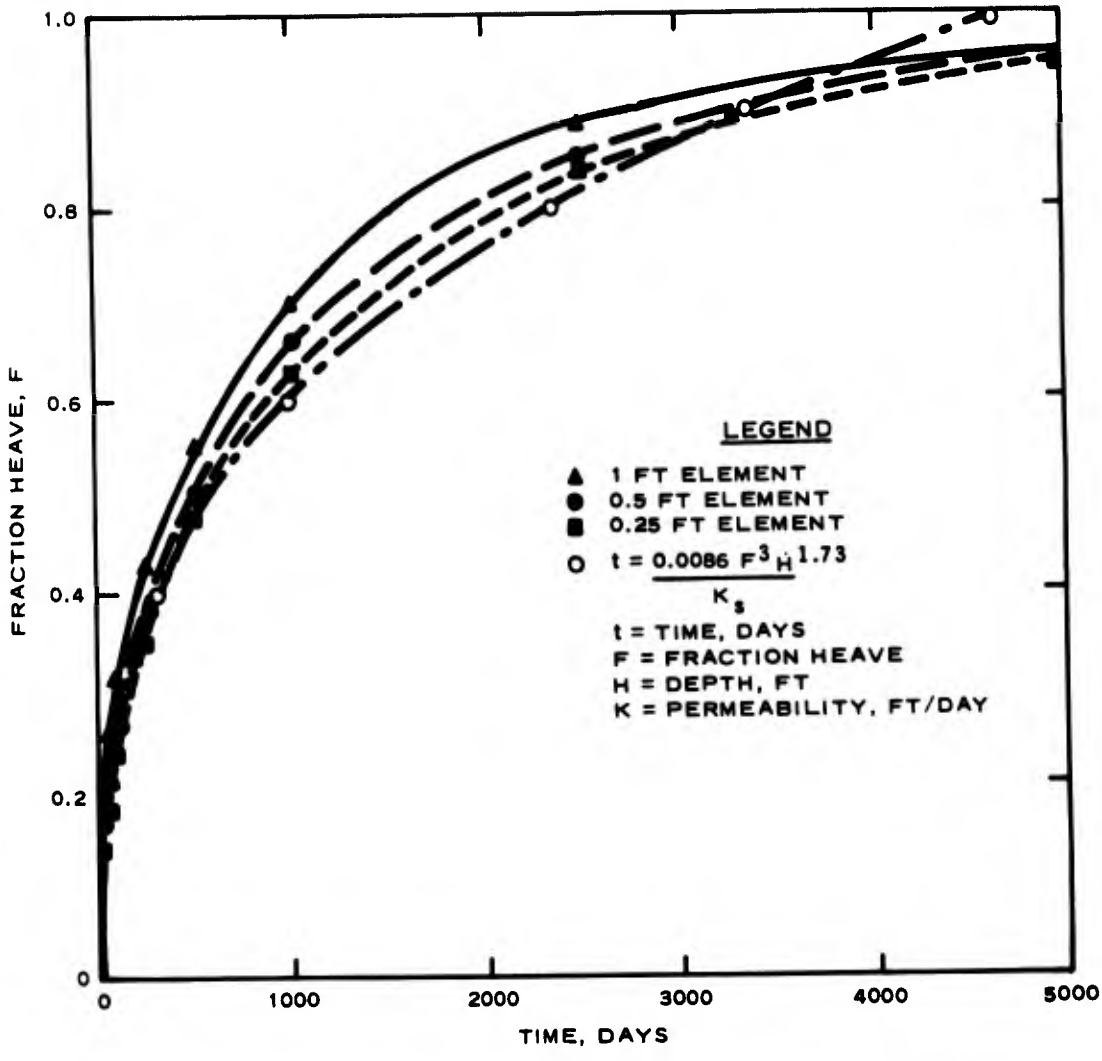

Figure 35. Comparison of heave with time between different element thicknesses for saturated profile of 10 ft depth, plasticity index 80, initial water content 30 percent, and permeability 0.0001 ft/day

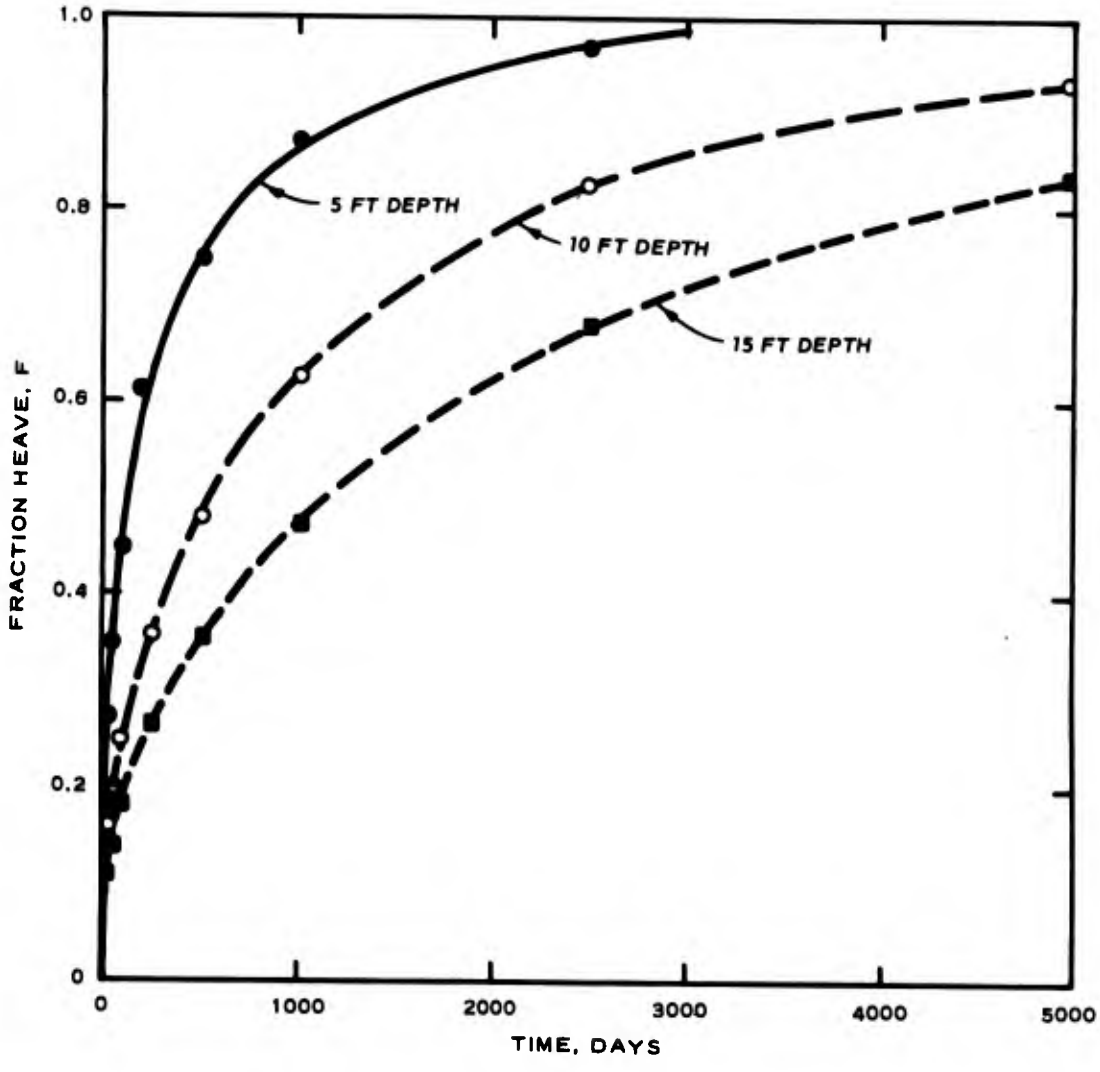

Figure 36. Comparison of heave with time between depths for saturated profile of plasticity index 80, initial water content 30 percent and permeability 0.0001 ft/day

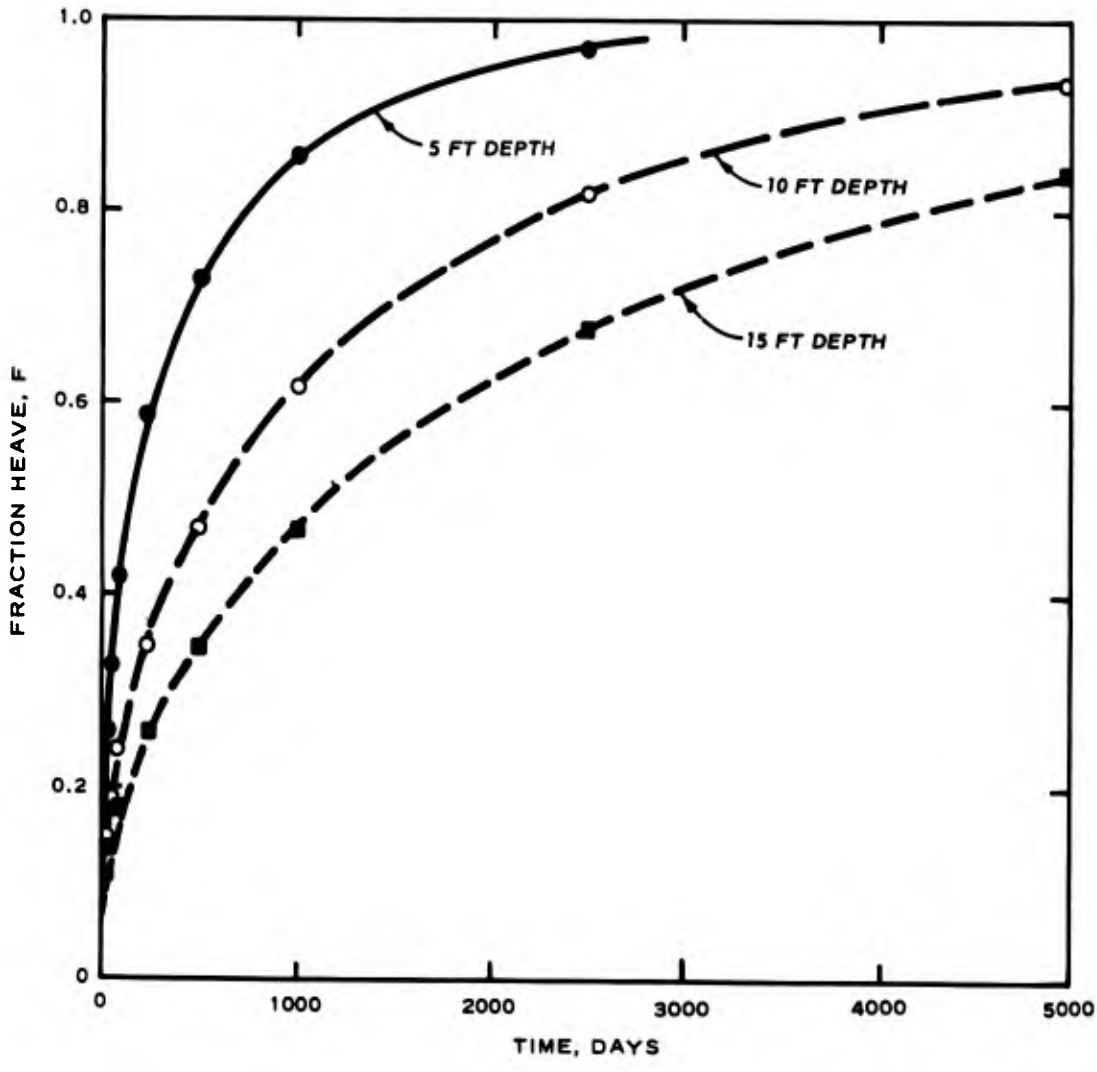

Figure 37. Comparison of heave with time between depths for saturated profile of plasticity index 40, initial water content 16 percent, and permeability 0.0001 ft/day

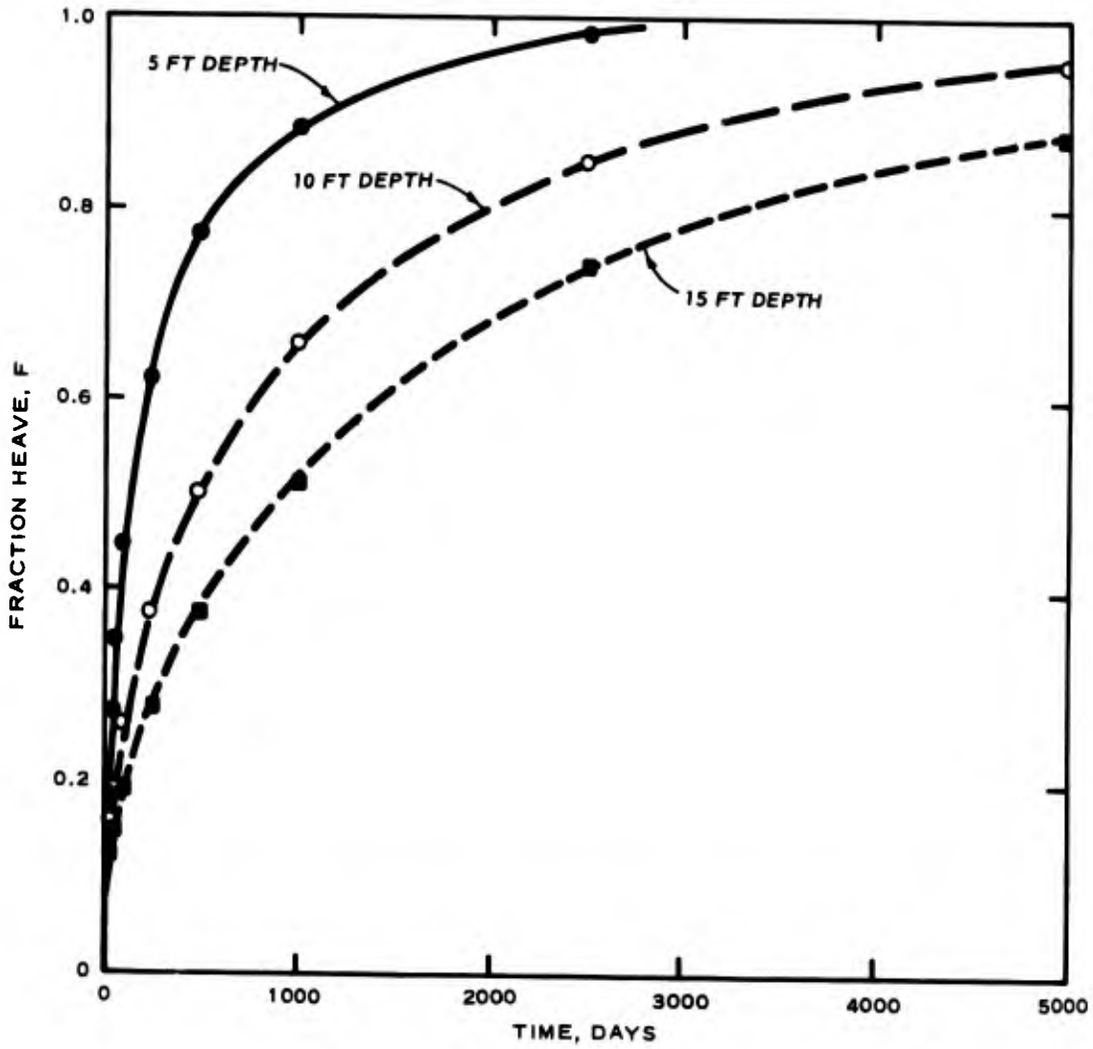

Figure 38. Comparison of heave with time between depths for saturated profile of plasticity index 20, initial water content 14 percent, and permeability 0.0001 ft/day

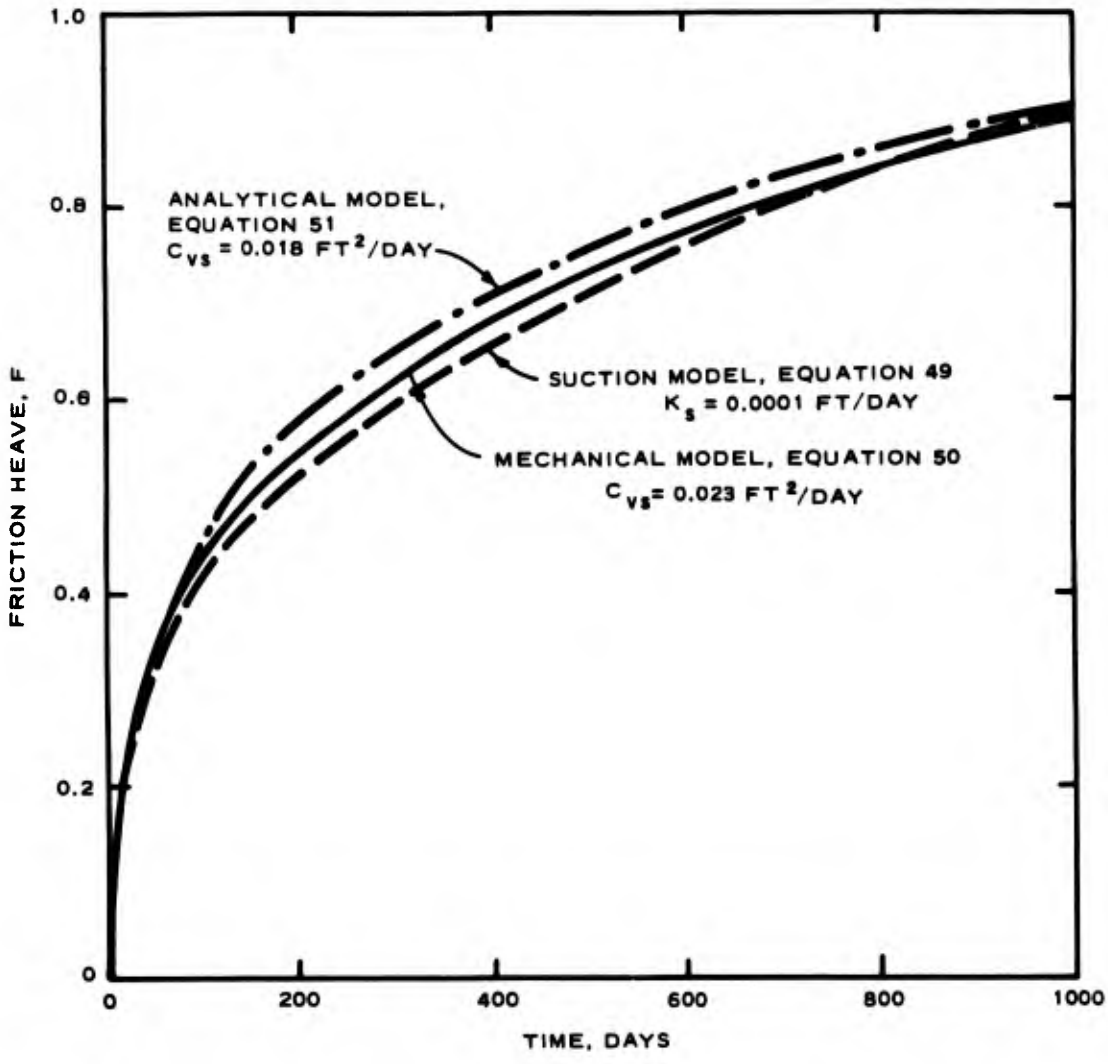

Figure 39. Comparison of heave with time between the suction and mechanical swell models for the saturated profile of 5 ft depth

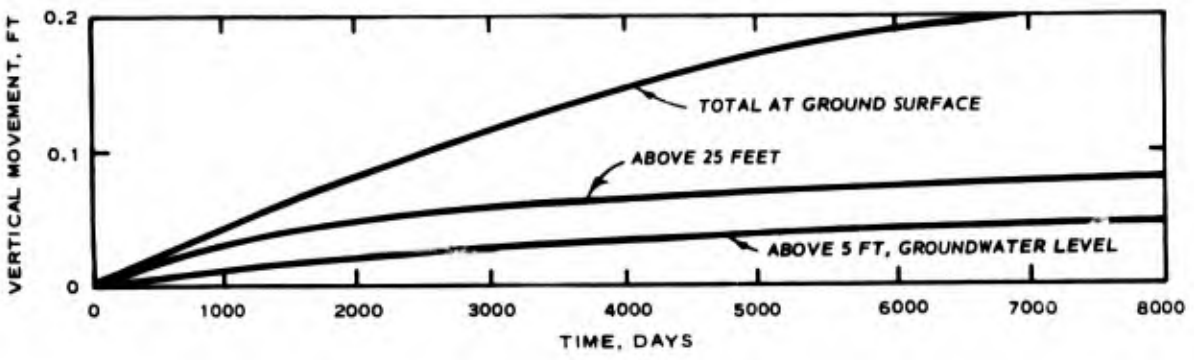

a. CLINTON TEST SECTION

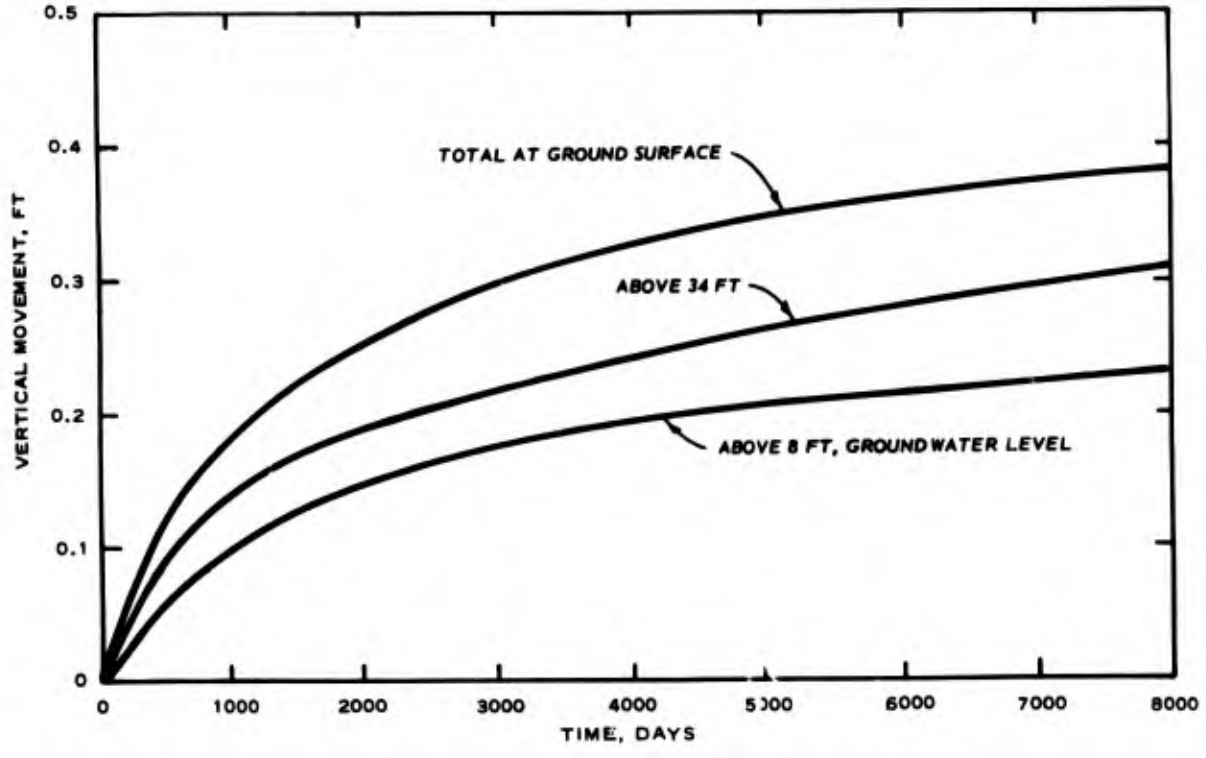

b. LACKLAND TEST SECTION

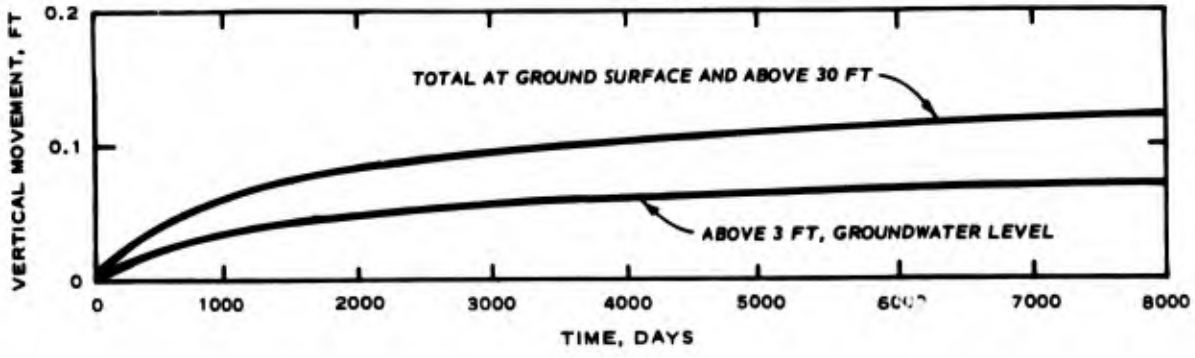

c. FORT CARSON TEST SECTION

Figure 40. Extrapolated heave at the field test sections

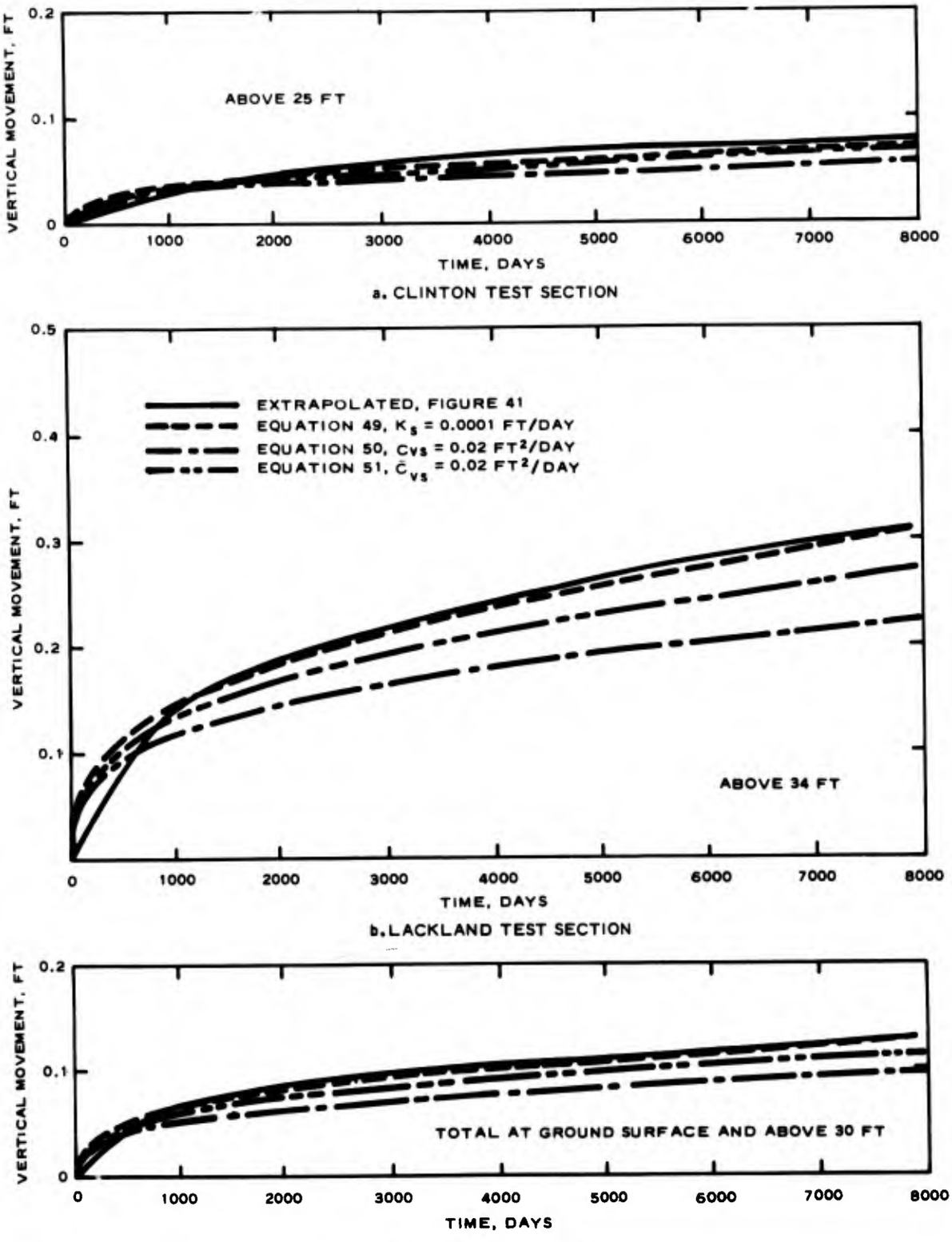

Figure 41. Comparison of extrapolated and computed heaves at the field test sections

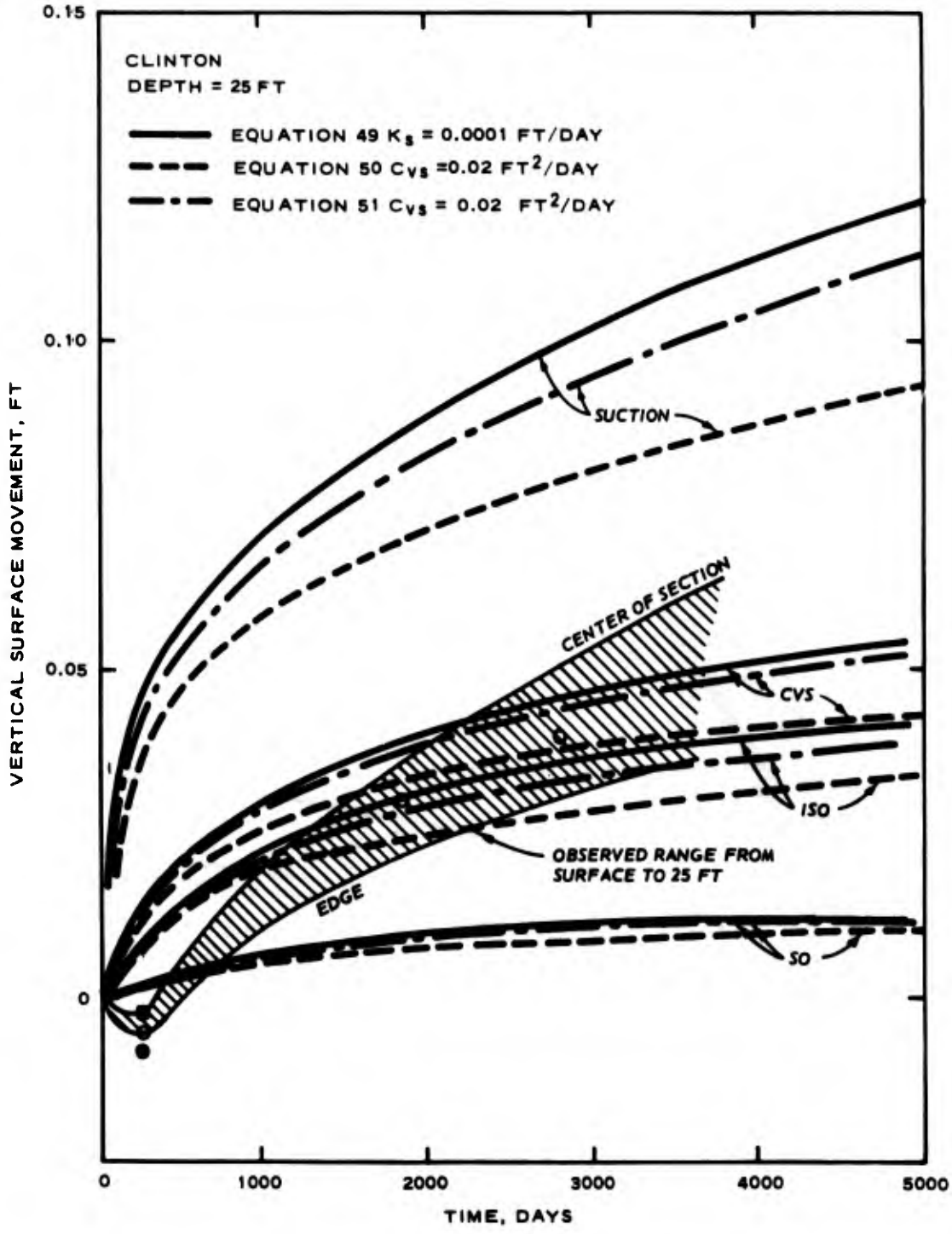

Figure 42. Comparison of observed and predicted heave with time beneath the Clinton test section

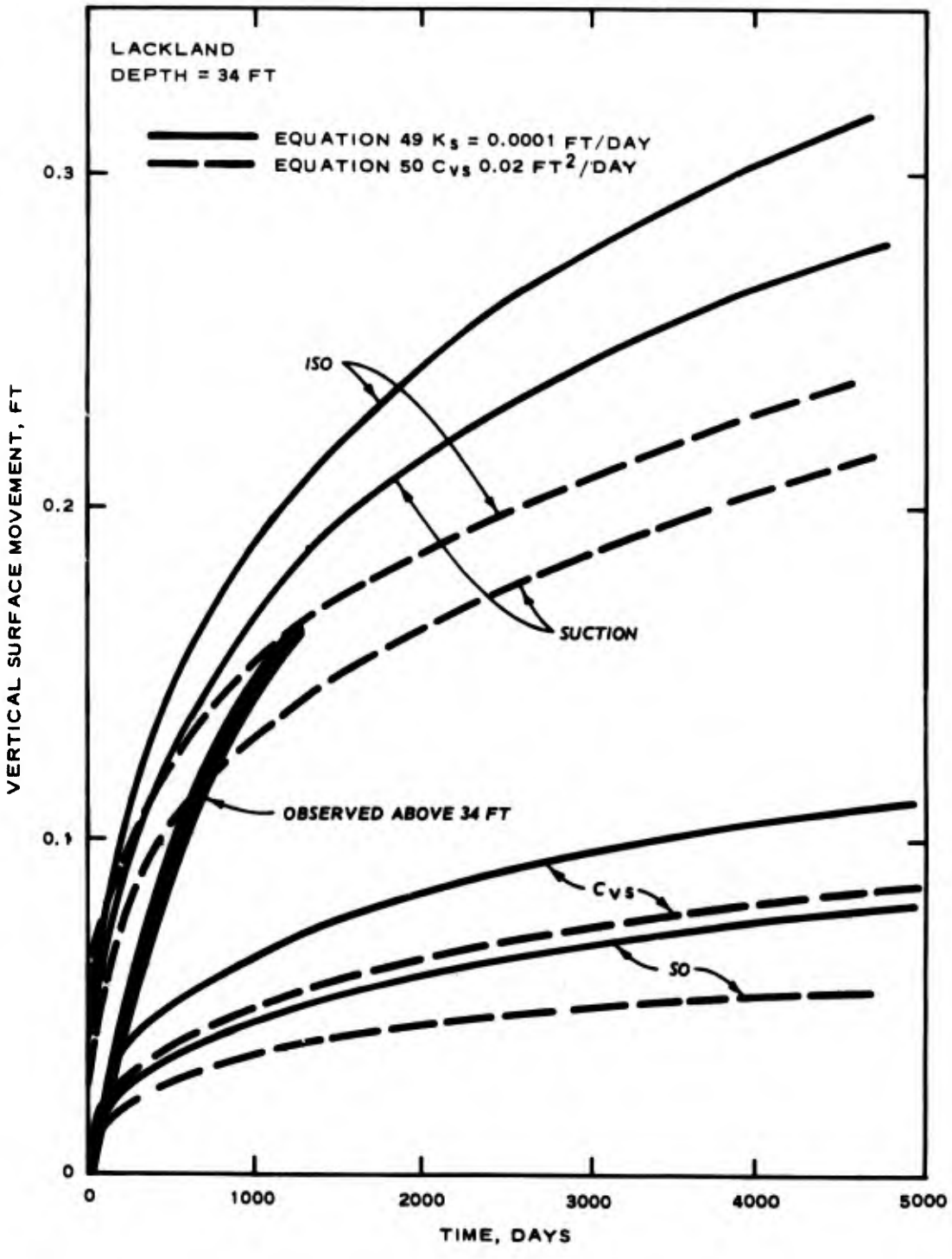

Figure 43. Comparison of observed and predicted heave with time beneath the Lackland test section

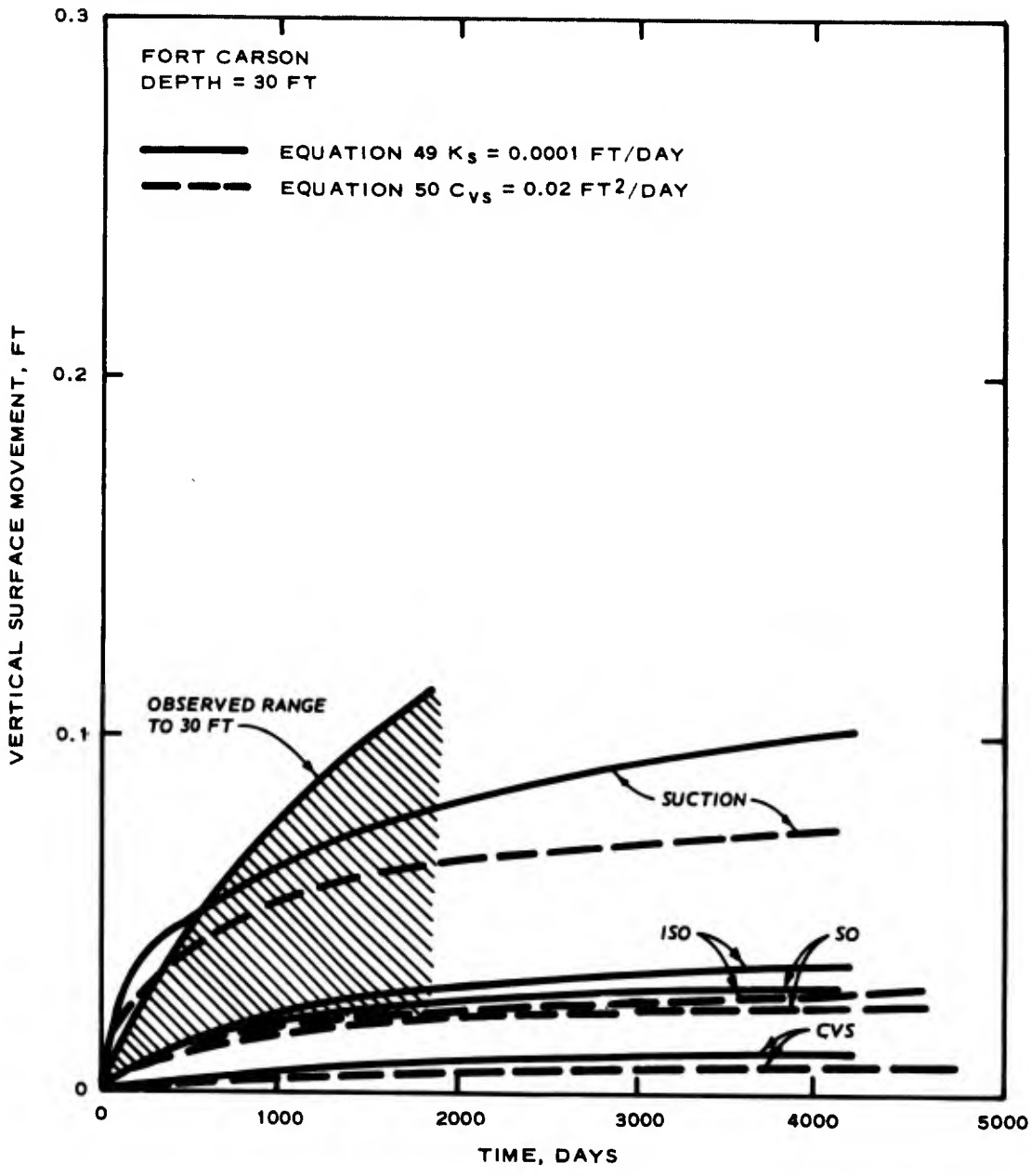

Figure 44. Comparison of observed and predicted heave with time beneath the Fort Carson test section

APPENDIX A: SOIL SUCTION AND VOLUMETRIC WATER CONTENT

1. The partial of soil suction with respect to volumetric water content is assumed herein as

$$\frac{\partial \tau_m}{\partial \theta} = \frac{\partial \tau_m}{\partial w} \cdot \frac{\partial w}{\partial \theta} \tag{A1}$$

where

τ_m = matrix soil suction, tsf

θ = volumetric water content, V_w/V

V_w = volume of water, ft^3

V = total volume, ft^3

w = water content, percent dry weight

2. The derivative of Equation 12 is

$$\frac{\partial \tau_m^o}{\partial w} = - 2.3B\tau_m^o \tag{A2}$$

3. The derivative of Equation 4 at constant confining pressure is

$$\partial \tau_m^o = \partial \tau_m \tag{A3}$$

4. The volumetric water content may be given as

$$\theta = \frac{w}{100\ V_{TO} - \alpha w_o + \alpha w} \tag{A4}$$

where

$V_{TO} = (1 + e_o)/G_s$

α = constant compressibility factor

5. The derivative of Equation A4 with respect to θ is

$$\frac{\partial w}{\partial \theta} = \frac{(100\ V_{TO} - \alpha w_o + \alpha w)^2}{100\ V_{TO} - \alpha w_o} = \frac{10{,}000\ V_T^2}{100\ V_{TO} - \alpha w_o} \tag{A5}$$

6. Combining Equations A1, A2, A3, and A5 leads to

$$\frac{\partial \tau_m}{\partial \Theta} = - \frac{23{,}000\ B\ \tau_m^{\circ}\ V_T^{\ 2}}{100\ V_{TO} - \alpha w_o} \qquad (A6)$$

which is identical with Equation 21, but in terms of void ratio rather than specific total volume.

APPENDIX B: VOLUME PARAMETER $\bar{C}$

1. The volumetric water content[7] in terms of water content in percent of dry weight is

$$\theta = \frac{V_w}{V} = \frac{wG_s}{100(1 + e)} \tag{B1}$$

2. The derivative of Equation 11 is

$$\partial e = \frac{\alpha G_s}{230\ B} \frac{\partial \tau_m^o}{\tau_m^o} \tag{B2}$$

3. Substitution of Equations 21, A3, B1, and B2 into the last term of Equation 8 leads to

$$\frac{\theta}{1 + e} \frac{\partial \tau_m}{\partial \theta} \frac{\partial e}{\partial t} = - \frac{\alpha G_s\ w}{100(1 + e_o) - \alpha w_o G_s} \frac{\partial \tau_m}{\partial t} = - \overline{C} \frac{\partial \tau_m}{\partial t} \tag{B3}$$

APPENDIX C: CLASSIFICATION DATA OF THE CLINTON TEST SITE

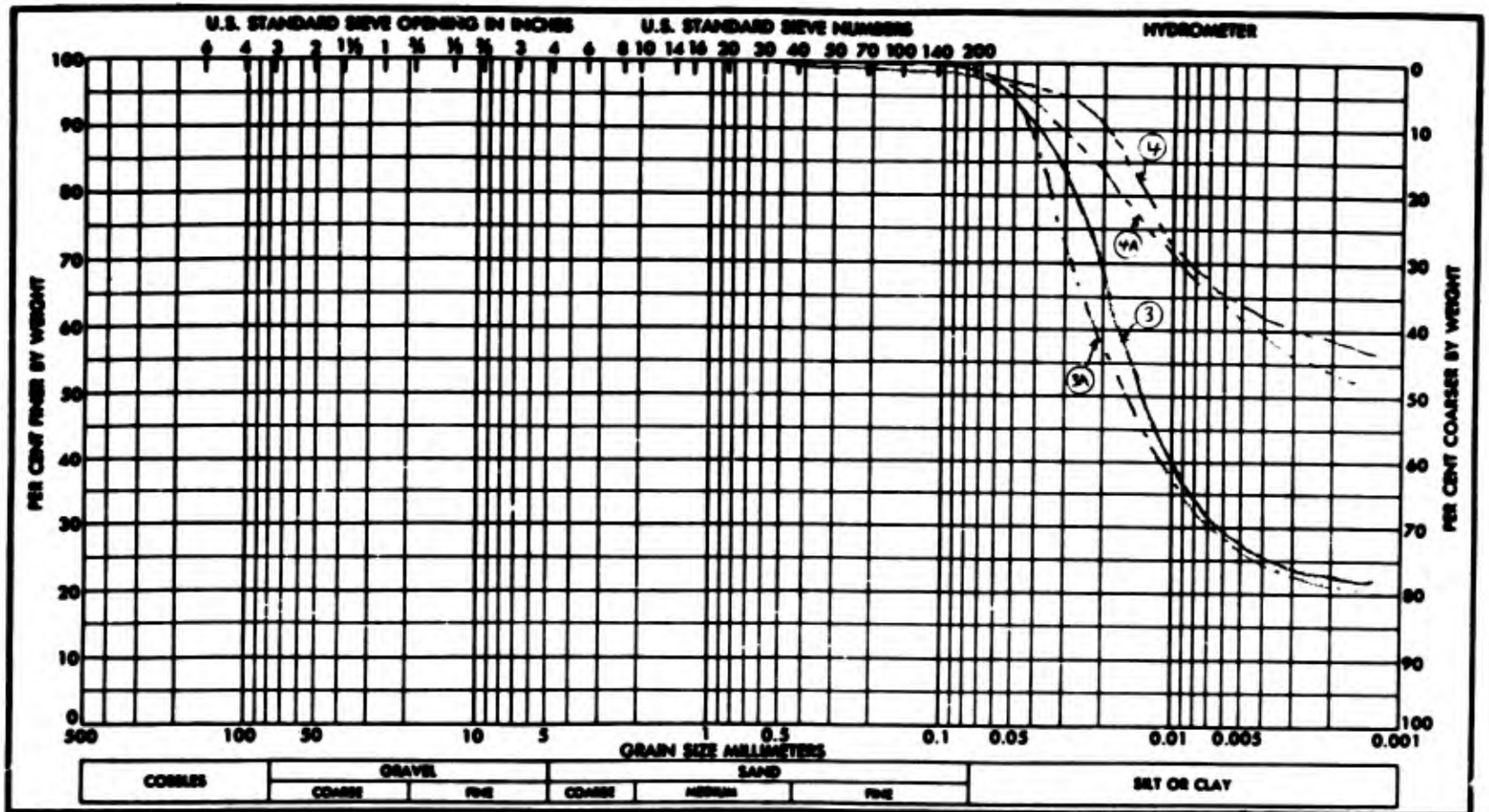

SAMPLE NO.	ELEV OR DEPTH	CLASSIFICATION	NAT WC	LL	PL	PI
3	3.5-4.9 ft	CL, brown, G_s=2.70		42	21	21
3A	4.9-5.0 ft	CL, lt brown, G_s=2.72		41	20	21
4	6.0-6.95 ft	CH, brown, G_s=2.70		68	20	48
4A	6.95-7.0 ft	CH, lt brown, G_s=2.73		75	22	53

GRADATION CURVES

PROJECT Foundations on Swelling Soils

AREA Clinton

BORING NO. 1

DATE April, 1973

ENG FORM 2087
1 MAY 63

REPLACES WES FORM NO. 1241, SEP 1962, WHICH IS OBSOLETE.

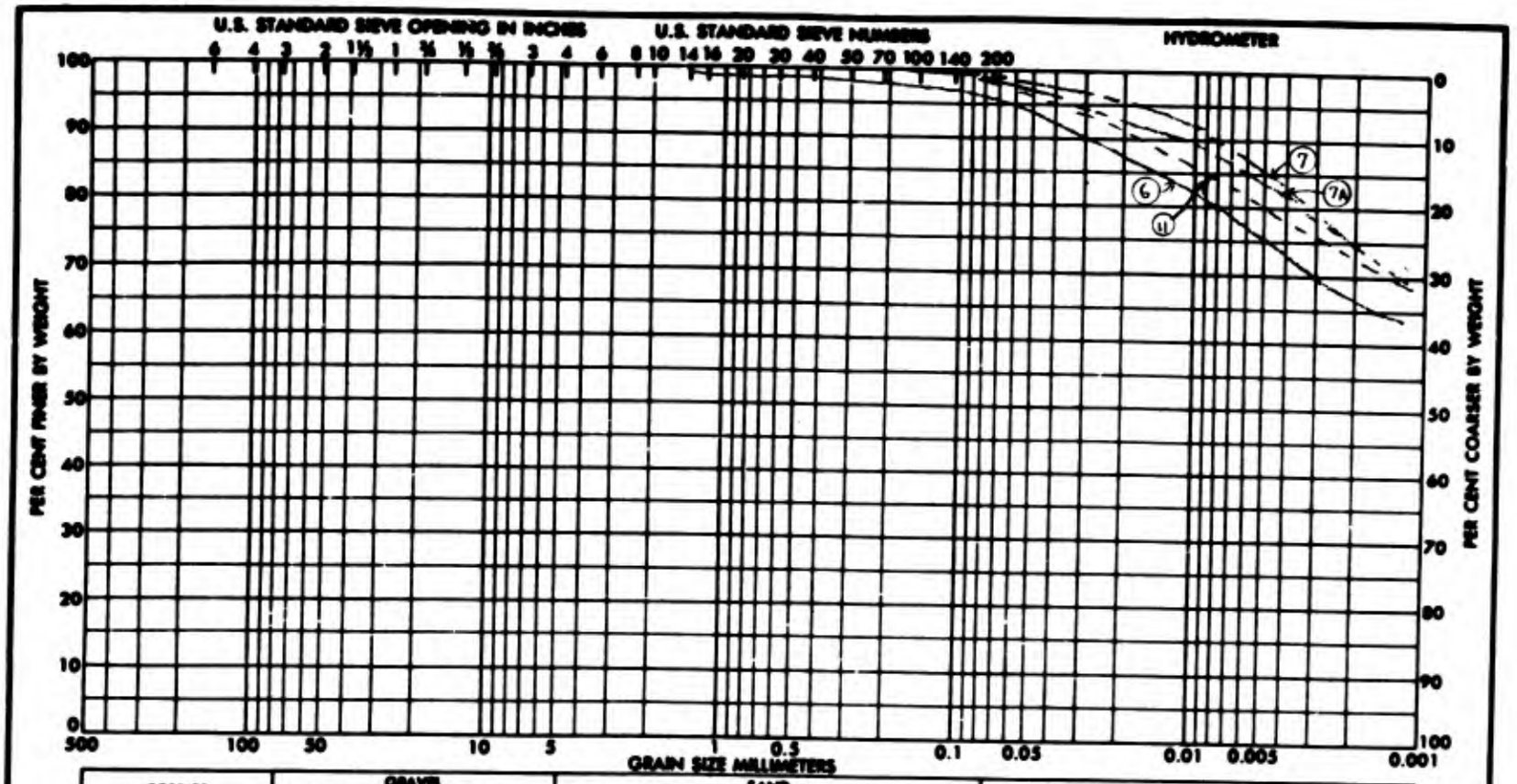

SAMPLE NO.	DEV OF DEPTH	CLASSIFICATION	NAT W%	LL	PL	PI
6	9.0-10.0 ft	CH, lt brown, G_s=2.79	39.6	79	25	54
7	10.1-11.05 ft	CH, brown, G_s=2.78		97	25	72
7A	11.05-11.01ft	CH, lt brown, G_s=2.74		111	33	78
11	15.0-16.1 ft	CH, lt brown, G_s=2.78	48.4	106	33	73

GRADATION CURVES

PROJECT Foundations on Swelling Soils

AREA Clinton

BORING NO. 1

DATE April, 1973

ENG FORM 2087
1 MAY 63

REPLACES WES FORM NO. 1341, SEP 1962, WHICH IS OBSOLETE.

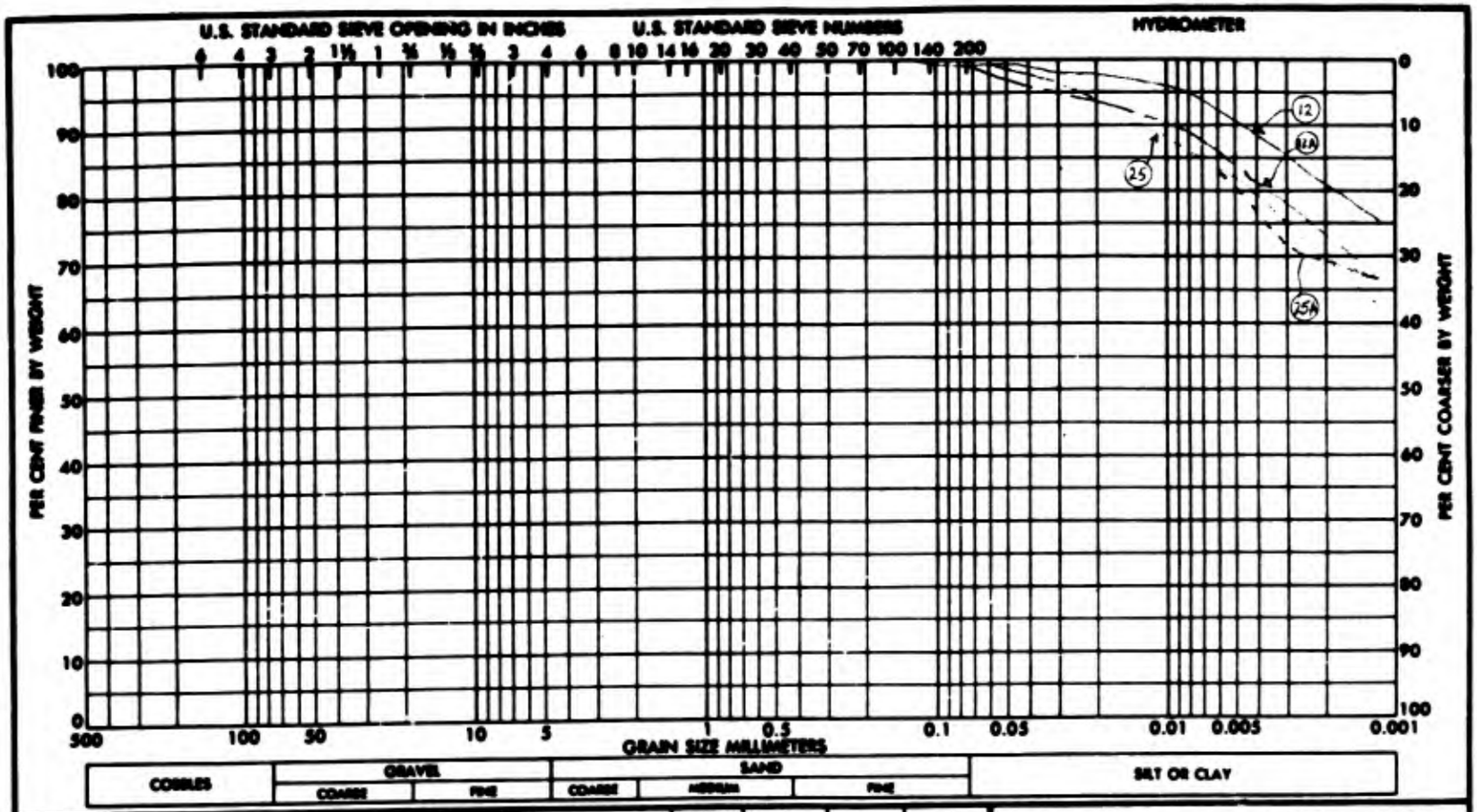

SAMPLE NO.	ELEV OR DEPTH	CLASSIFICATION	NAT W%	LL	PL	PI
12	16.1-17.1 ft	CH, brown, G_s=2.73		111	29	82
12A	17.1-17.2 ft	CH, lt brown, G_s=2.77		96	34	62
25	30.1-31.2 ft	CH, gray, G_s=2.73		100	30	70
25A	31.2-31.3 ft	CH, dark gray, G_s=2.75		106	35	71

GRADATION CURVES

PROJECT Foundations on Swelling Soils

AREA Clinton

BORING NO. 1

DATE April, 1973

ENG FORM 2087
1 MAY 63

REPLACES WES FORM NO. 1241, SEP 1962, WHICH IS OBSOLETE.

APPENDIX D: CLASSIFICATION DATA OF THE LACKLAND TEST SITE

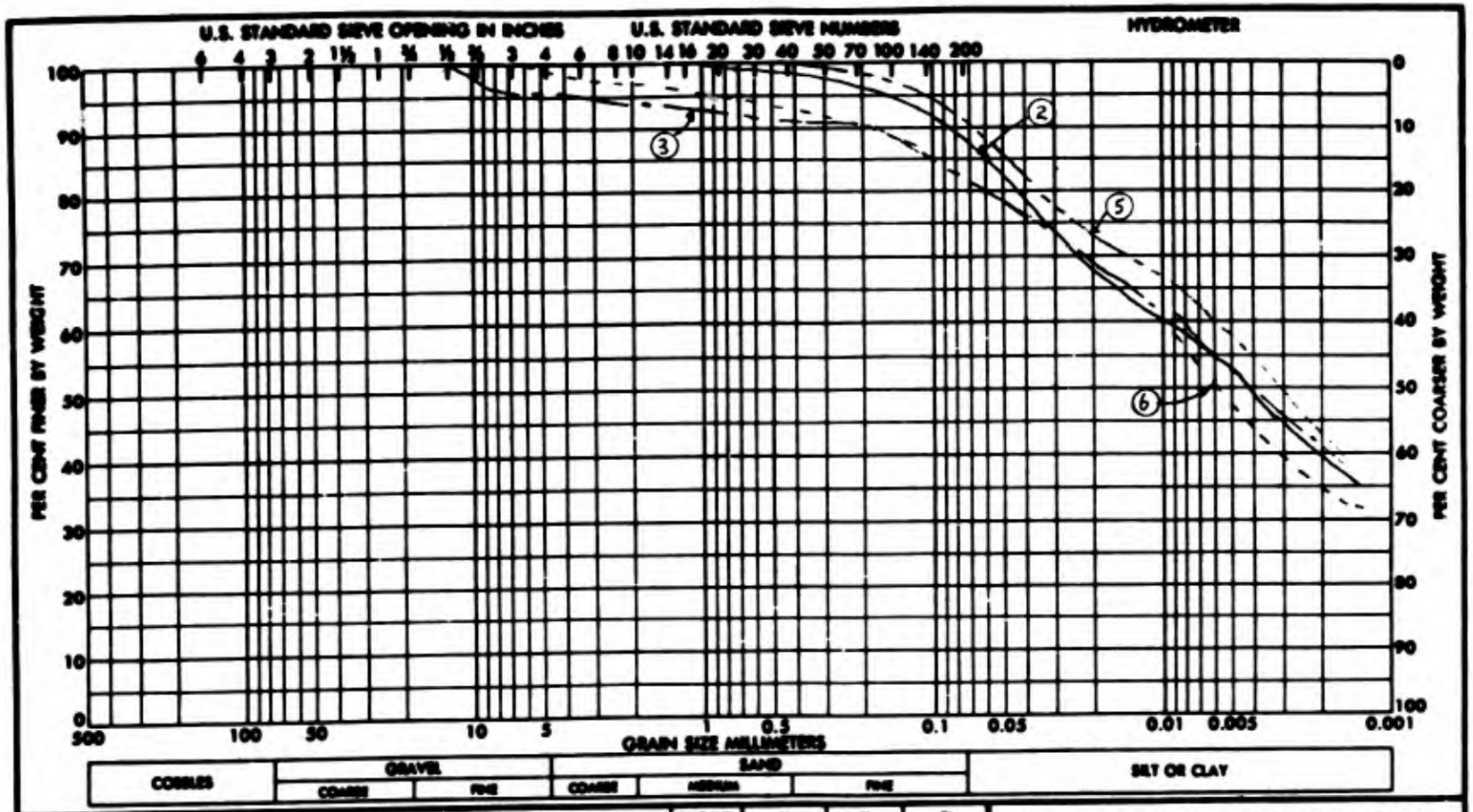

SAMPLE NO.	DEV OR DEPTH	CLASSIFICATION	NAT W%	LL	PL	PI
2	1.2-2.3 ft	CL,silty,dk gray, G_s=2.68		38	20	18
3	2.5-2.6 ft	CH,sand & gravel, G_s=2.73		63	19	44
5	5.0-6.0 ft	CH,sand, lt brown, G_s=2.71		59	18	41
6	6.1-7.1 ft	CH,sand, lt brown, G_s=2.73		52	13	39

GRADATION CURVES

PROJECT Foundations on Swelling Soils

AREA Lackland

BORING NO. PU-7

DATE April, 1971

USGS FORM 2087
1 MAY 60
REPLACES WES FORM NO. 1241, SEP 1962, WHICH IS OBSOLETE.

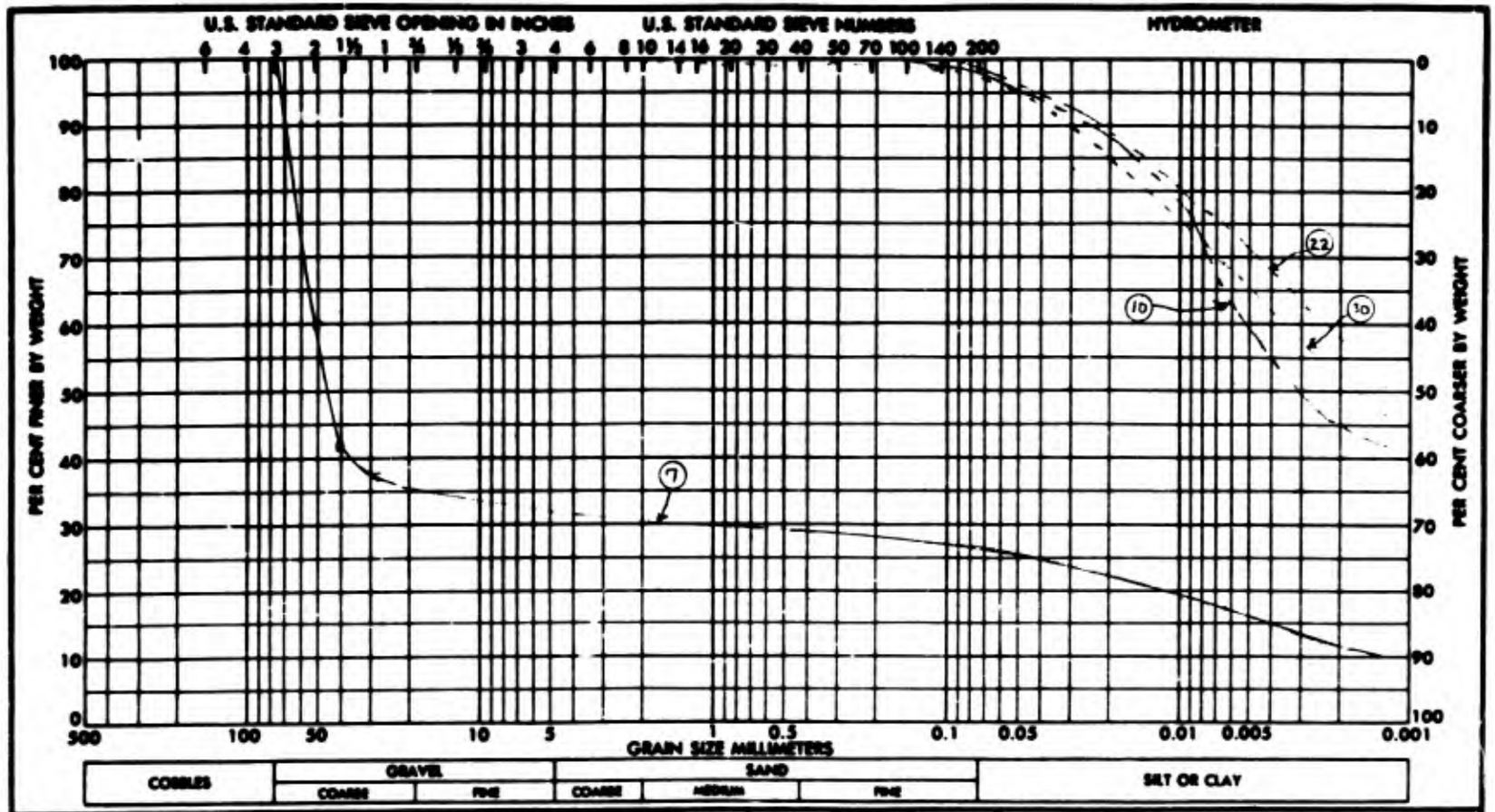

SAMPLE NO.	DEV OR DEPTH	CLASSIFICATION	NAT W%	LL	PL	PI
7	7.4-11.0 ft	CL, sand & gravel		49	16	33
10	14.5-15.5 ft	CH, lt brown, G_s=2.73		76	24	52
22	24.7-30.8 ft	CH, lt brown, G_s=2.74		95	25	70
30	39.7-40.8 ft	CH, brown, G_s=2.79		91	26	65

GRADATION CURVES

PROJECT Foundations on Swelling Soils

AREA Lackland

BORING NO PU-7

DATE December, 1971

ENG FORM 2087 1 MAY 63

REPLACES WES FORM NO. 1241, SEP 1962, WHICH IS OBSOLETE.

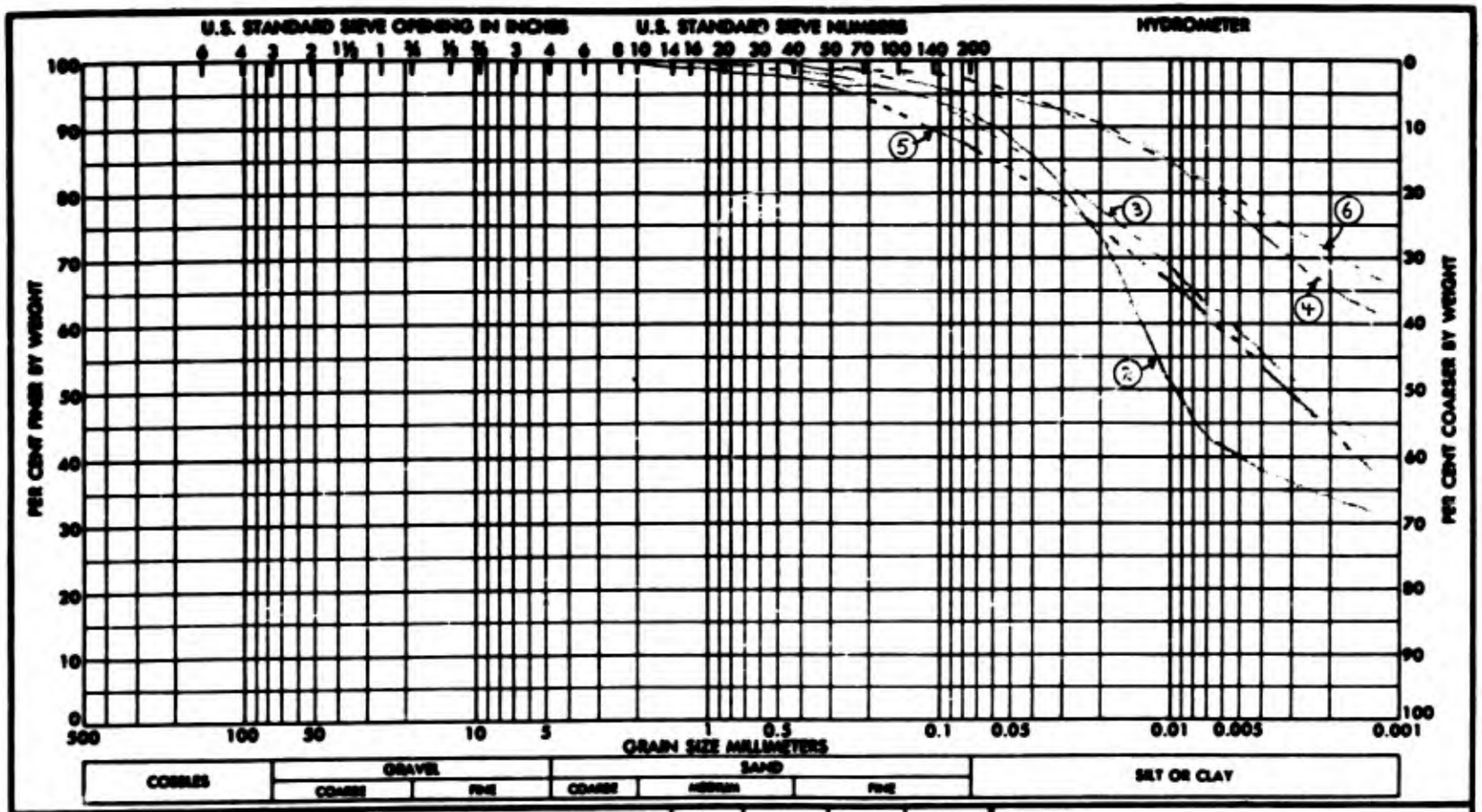

SAMPLE NO.	DEV OR DEPTH	CLASSIFICATION	NAT WC	LL	PL	PI
2	0.2-1.0 ft	CH, sand,black, G_s=2.63	22.3	59	27	32
3	3.2-4.2 ft	CH, sand, G_s=		82	22	60
4	4.3-5.2 ft	CH, sand, gray, G_s=2.78		58	26	32
5	6.2-6.7 ft	CH, sand,lt brown, G_s=2.77	25.8	64	21	43
6	6.7-7.6 ft	CH, lt brown, G_s=2.76	25.7	57	21	36

GRADATION CURVES

PROJECT Foundations on Swelling Soils

AREA Lackland

BORING NO. 1

DATE June, 1976

DD FORM 2087

REPLACES WES FORM NO. 1241, SEP 1942, WHICH IS OBSOLETE.

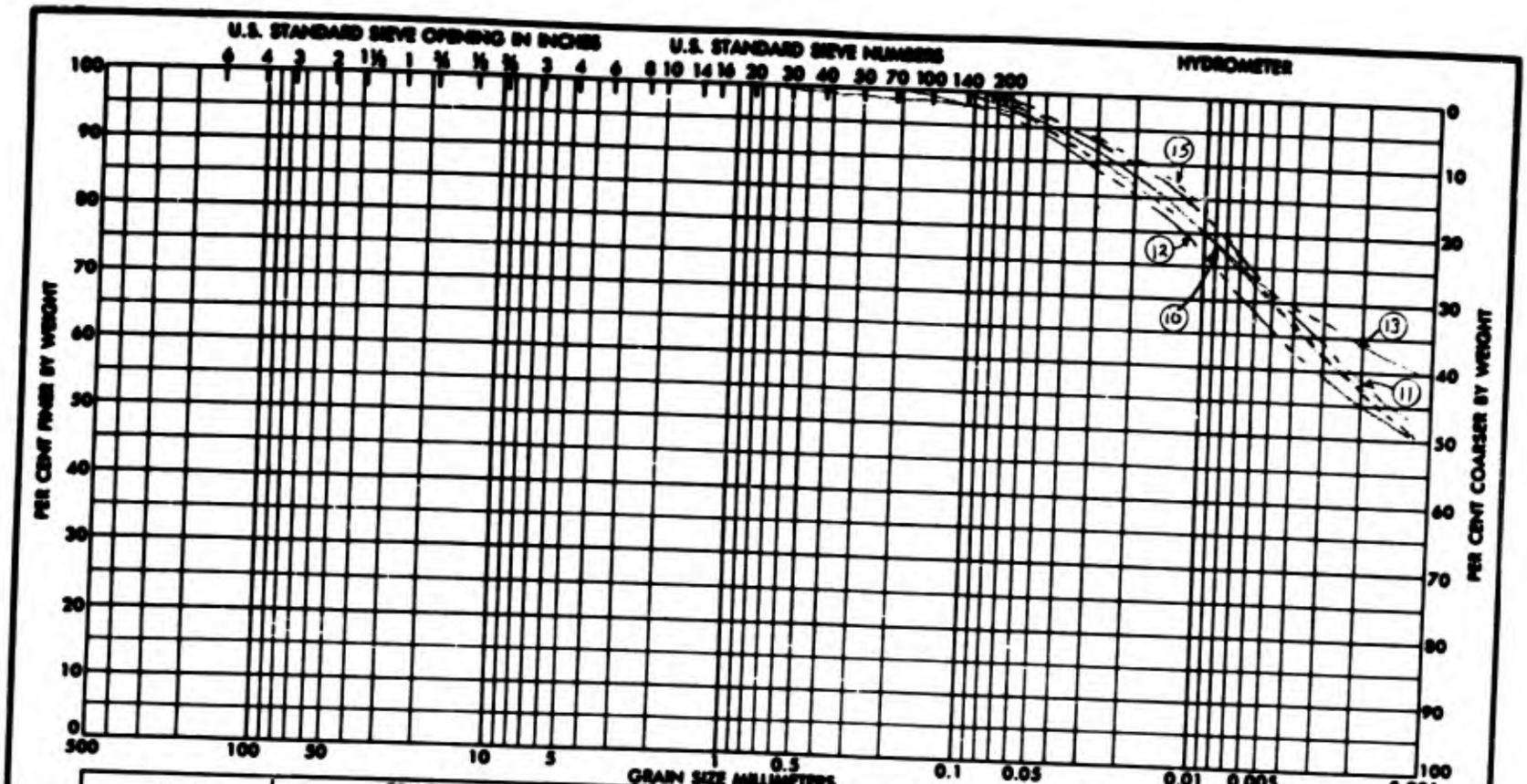

SAMPLE NO.	ELEV OR DEPTH	CLASSIFICATION	NAT WC%	LL	PL	PI
10	13.1-14.2 ft	CH,lt brown, G_s=2.78	30.0	74	32	42
11	14.3-15.3 ft	CH,lt brown, G_s=2.76		74	30	44
12	16.0-17.1 ft	CH, tan, G_s=2.78	28.4	76	32	44
13	17.2-18.3 ft	CH, lt tan, G_s=2.78	28.5	79	24	55
15	27.3-28.3 ft	CH, lt brown, G_s=2.75		83	25	58

GRADATION CURVES

PROJECT Foundations on Swelling Soil

AREA Lackland

BORING NO. 1

DATE June, 1976

ENG FORM 2087

REPLACES WES FORM NO. 1341, SEP 1962, WHICH IS OBSOLETE.

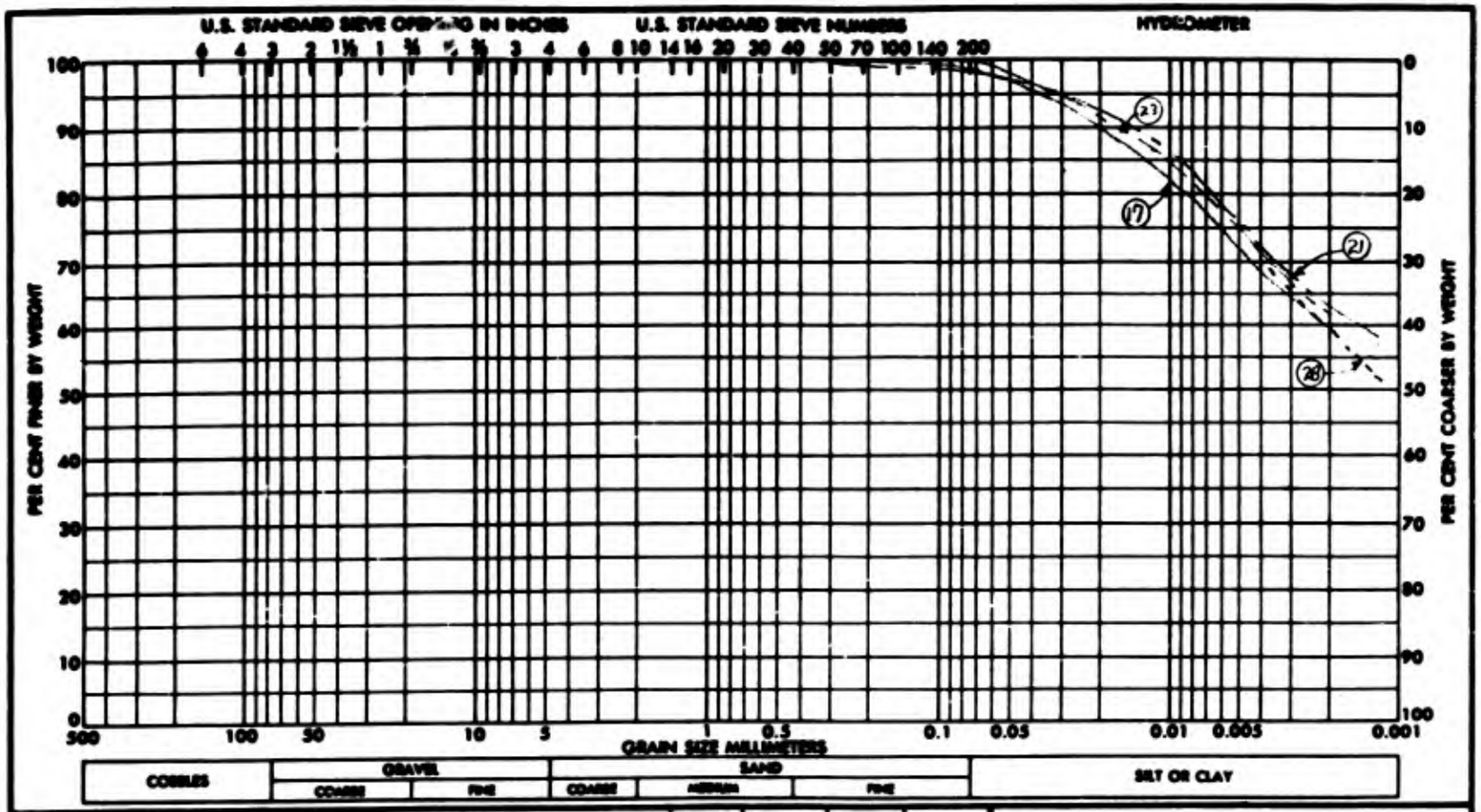

SAMPLE NO.	ELEV OR DEPTH	CLASSIFICATION	NAT WC	LL	PL	PI
17	29.0-30.0 ft	CH, gray,		80	29	51
21	35.0-36.1 ft	CH, lt gray, G_s=2.76	31.0	79	30	49
23	37.4-38.7 ft	CH, brown, G_s=2.73		93	31	62
28	46.5-47.4 ft	CH, tan, G_s=2.73		81	29	52

GRADATION CURVES

PROJECT Foundations on Swelling Soils

AREA Lackland

BORING NO. 1

DATE June, 1976

ENG FORM 2087

REPLACES WES FORM NO. 1341, SEP 1962, WHICH IS OBSOLETE.

APPENDIX E: CLASSIFICATION DATA OF THE FORT CARSON TEST SITE

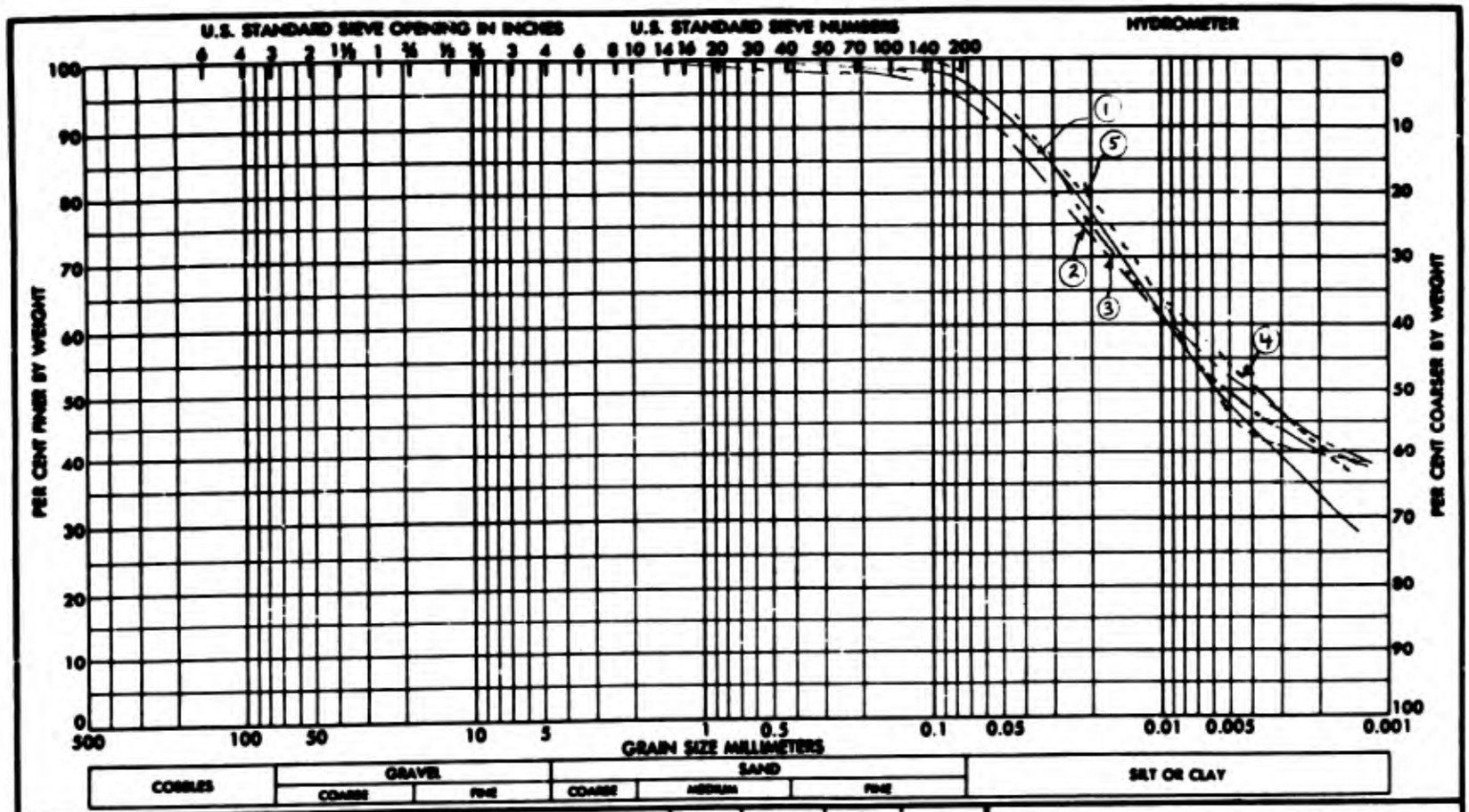

SAMPLE NO.	DEV OR DEPTH	CLASSIFICATION	NAT W%	LL	PL	PI
1	1.1-2.3 ft	CH,dark gray, G_s=2.80	26.0	51	18	33
2	2.6-3.6 ft	CH,dark gray, G_s=2.80	24.7	52	20	32
3	3.7-4.7 ft	CH w tr sand, G_s=2.77	24.5	46	19	27
4	5.7-7.0 ft	CH,dark brown,G_s=2.78		52	20	32
5 B*	7.5-8.9 ft	CH,lt gray, G_s=2.78	18.2	54	19	35

*Blenderized

GRADATION CURVES

PROJECT Foundations on Swelling Soils

AREA Fort Carson

BORING NO. BOQ-3

DATE June, 1976

ENG FORM 2087
1 MAY 63

REPLACES WES FORM NO. 1241, SEP 1962, WHICH IS OBSOLETE.

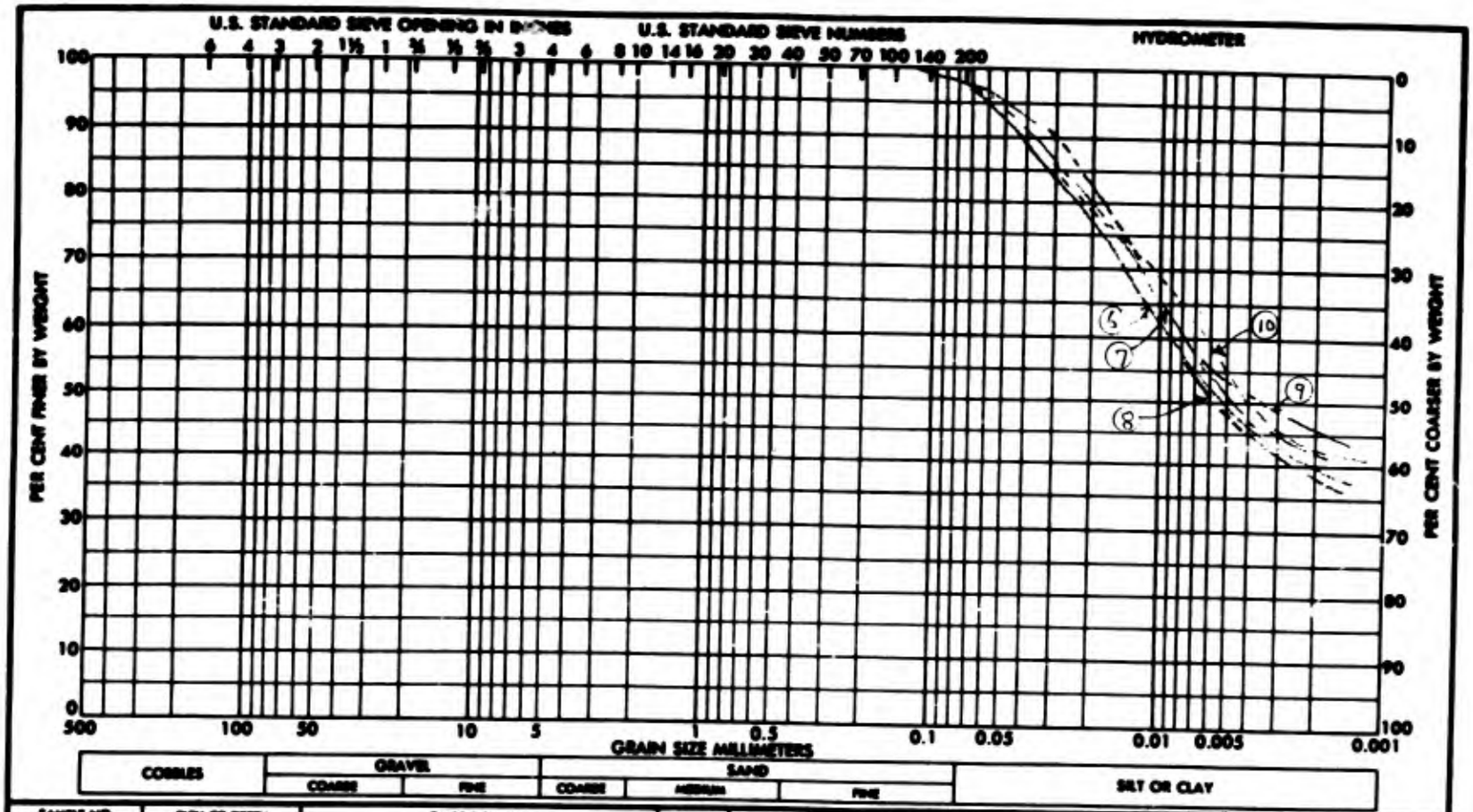

SAMPLE NO.	ELEV OR DEPTH	CLASSIFICATION	NAT WC	LL	PL	PI
6 B*	9.0-9.9 ft	CH,dark gray, G_s=2.80	16.6	60	22	38
7 B	11.2-12.1 ft	CH,lt gray, G_s=2.76	16.6	54	19	35
8 B	12.4-13.3 ft	CH,lt gray, G_s=2.76	15.7	59	22	37
9 B	13.5-14.6 ft	CH,lt gray, G_s=2.77	15.3	56	19	37
10 B	14.7-15.7 ft	CH, gray, G_s=2.75		55	21	34

*Blenderized

GRADATION CURVES

PROJECT Foundations on Swelling Soils

AREA Fort Carson

BORING NO. BOQ-3

DATE June, 1976

ENG FORM 2087
1 MAY 63

REPLACES WES FORM NO. 1241, SEP 1962, WHICH IS OBSOLETE.

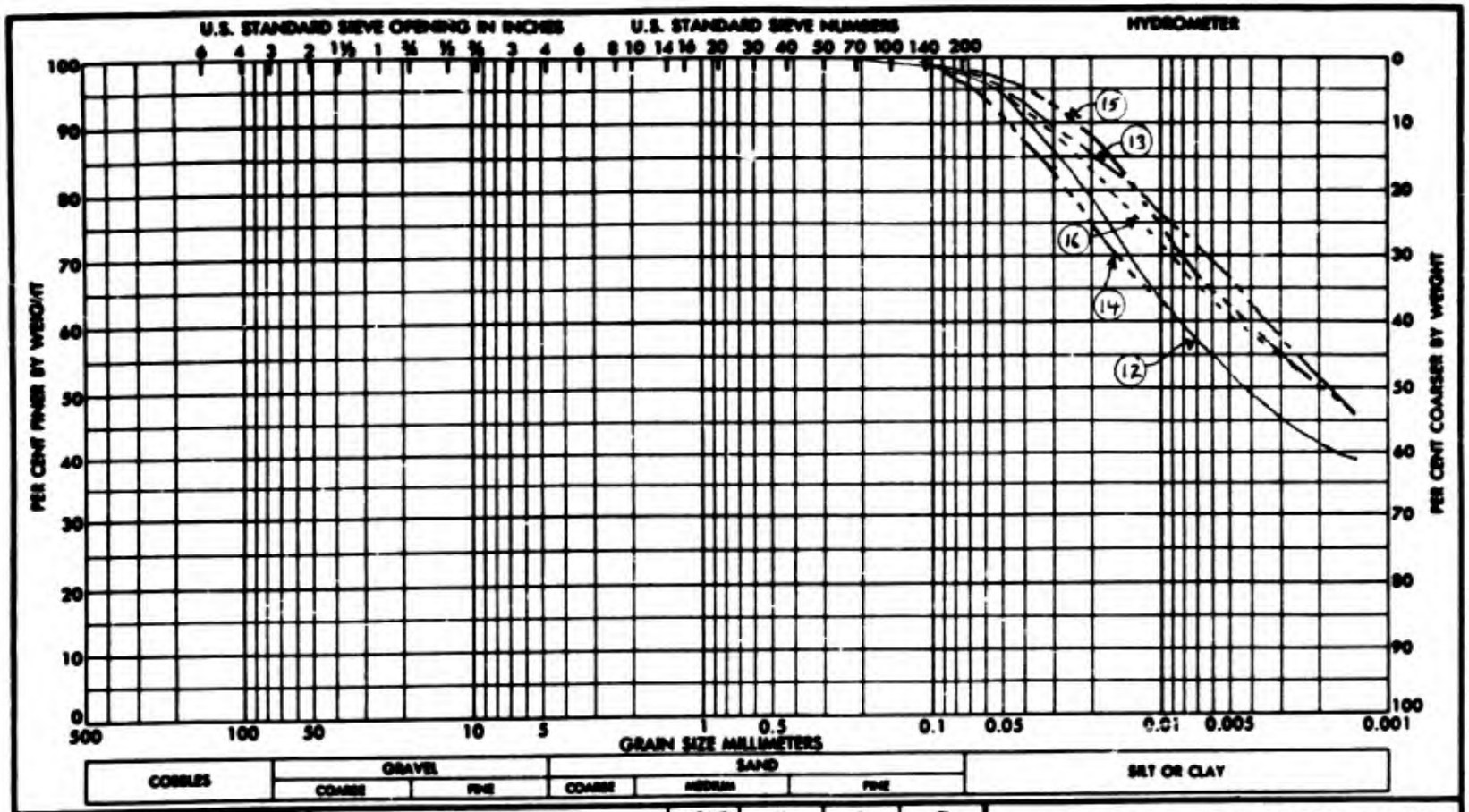

SAMPLE NO.	ELEV OR DEPTH	CLASSIFICATION	NAT W%	LL	PL	PI
12 B*	16.9-17.4 ft	CH, dark gray, G_s=2.78	14.3	56	20	36
13 B	17.6-18.6 ft	CH, lt gray, G_s=2.75	15.2	58	20	38
14 B	18.7-19.7 ft	CH, dark gray, G_s=2.74	14.3	61	21	40
15 B	19.8-20.8 ft	CH, dark gray, G_s=2.76	15.0	64	22	42
16 B	20.9-21.9 ft	CH, dark gray, G_s=2.76	15.6	57	21	36

*Blenderized

GRADATION CURVES

PROJECT Foundations on Swelling Soils

AREA Fort Carson

BORING NO. BOQ-3

DATE June, 1976

ENG FORM 2087 1 MAY REPLACES WES FORM NO. 1241, SEP 1962, WHICH IS OBSOLETE.

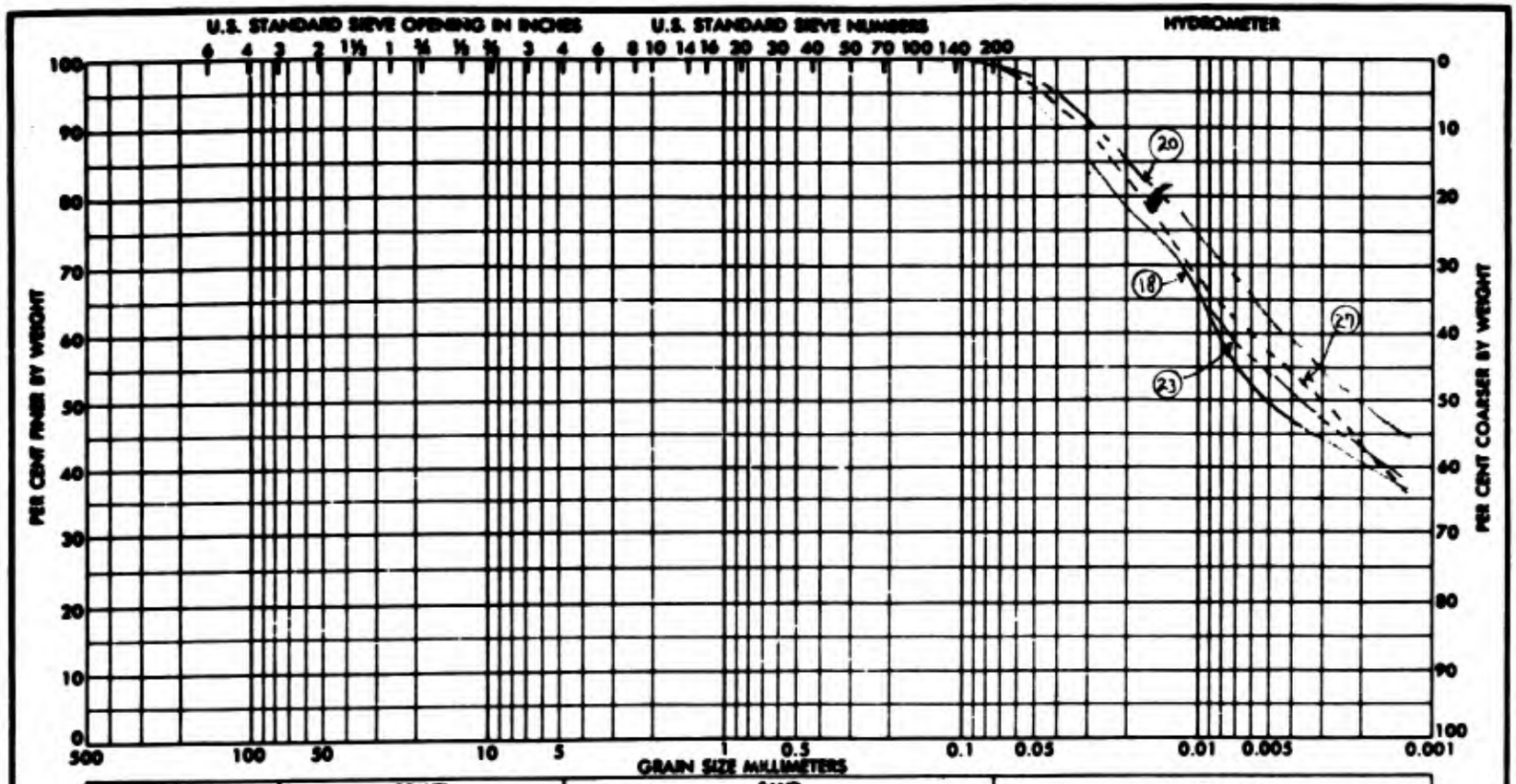

SAMPLE NO.	ELEV OR DEPTH	CLASSIFICATION	NAT W%	LL	PL	PI
18 B*	22.9-23.7 ft	CH, dark gray, G_s=2.73	13.6	59	20	39
20 B	24.7-26.0 ft	CH, gray, G_s=2.76		77	24	53
23 B	29.5-30.5 ft	CH, gray, G_s=2.72		63	18	45
27 B	34.2-35.2 ft	CH, gray, G_s=2.72		76	19	57

*Blenderized

GRADATION CURVES

PROJECT Foundations on Swelling Soils

AREA Fort Carson

BORING NO. BOQ-3

DATE June, 1976

ENG FORM 2087

REPLACES WES FORM NO. 1241, SEP 1963, WHICH IS OBSOLETE.

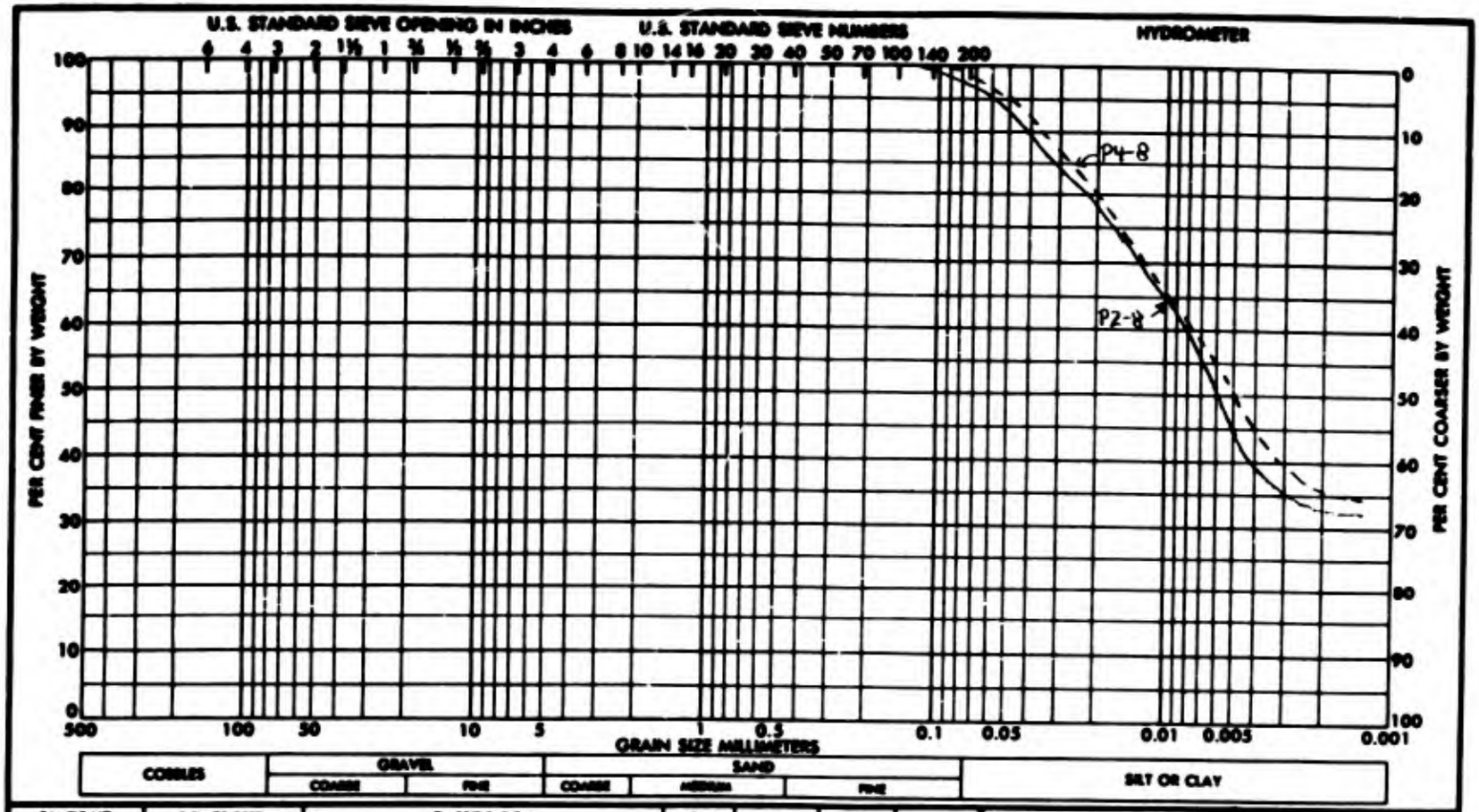

SAMPLE NO.	ELEV OR DEPTH	CLASSIFICATION	NAT W%	LL	PL	PI
P2-8 B*	8.2-9.2 ft	CH, lt gray, G_s=2.77	15.0	53	21	32
P4-8 B	13.5-14.5 ft	CH, dark gray, G_s=2.77	16.3	57	26	31

*Blenderized

GRADATION CURVES

PROJECT Foundations on Swelling Soils

AREA Fort Carson

BORING NO. BOQ-3

DATE June, 1976

ENG FORM 2087 1 MAY 63

REPLACES WES FORM NO. 1241, SEP 1963, WHICH IS OBSOLETE.

APPENDIX F: CLASSIFICATION DATA OF THE SIGONELLA TEST SITE

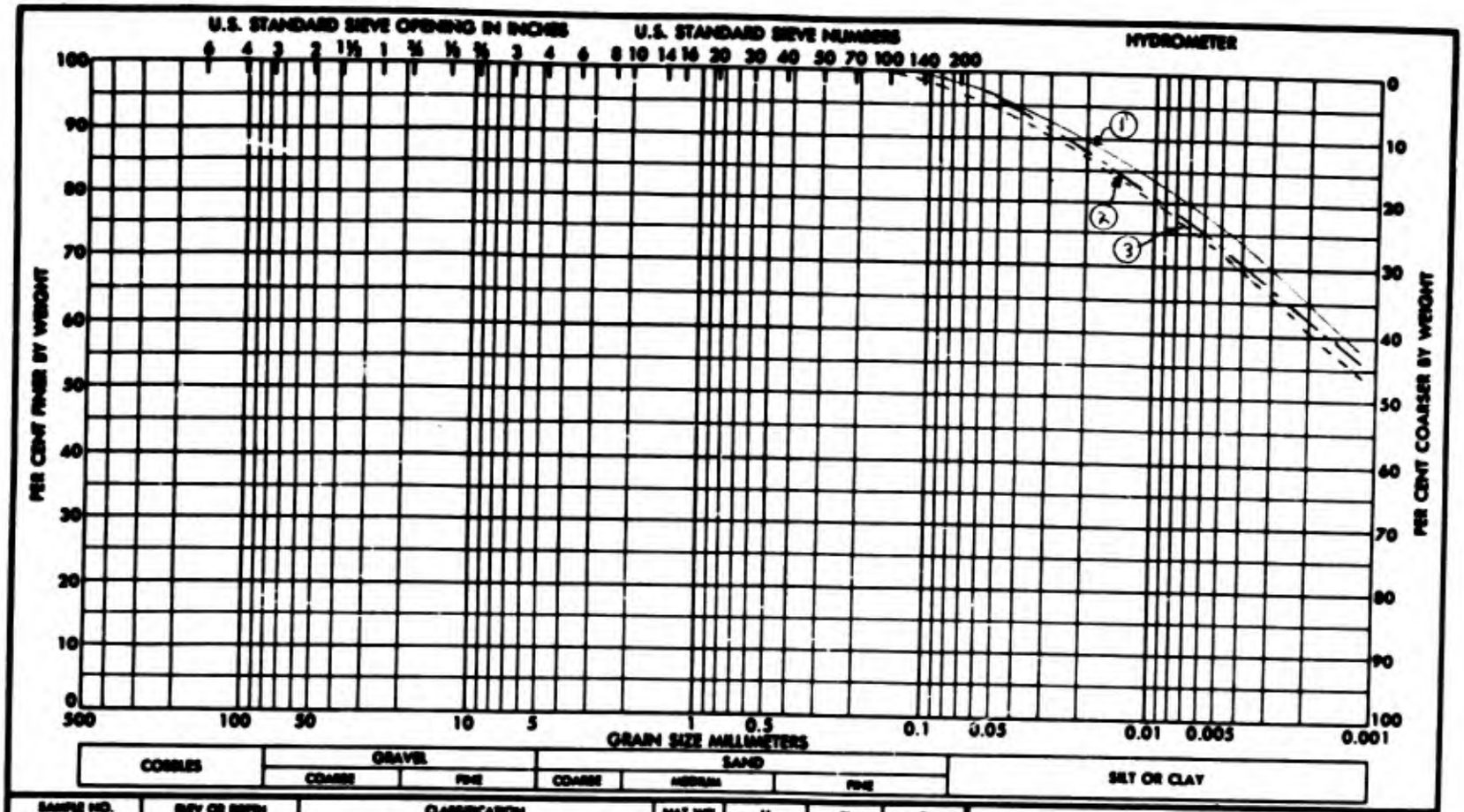

SAMPLE NO.	DEV OR DEPTH	CLASSIFICATION	NAT W%	LL	PL	PI
1	0.5-1.0 M	CH,brown, G_s=2.79		68	25	43
2	1.2-1.7 M	CH,brown, G_s=2.78		63	24	39
3	2.0-2.4 M	CH,brown, G_s=2.80		62	25	37

GRADATION CURVES

PROJECT Foundations on Swelling Soils

AREA Sigonella, Sicily

BORING NO. U-1 to U-3

DATE 19 January, 1977

ENG FORM 2087 REPLACES WES FORM NO. 1241, SEP 1962, WHICH IS OBSOLETE.

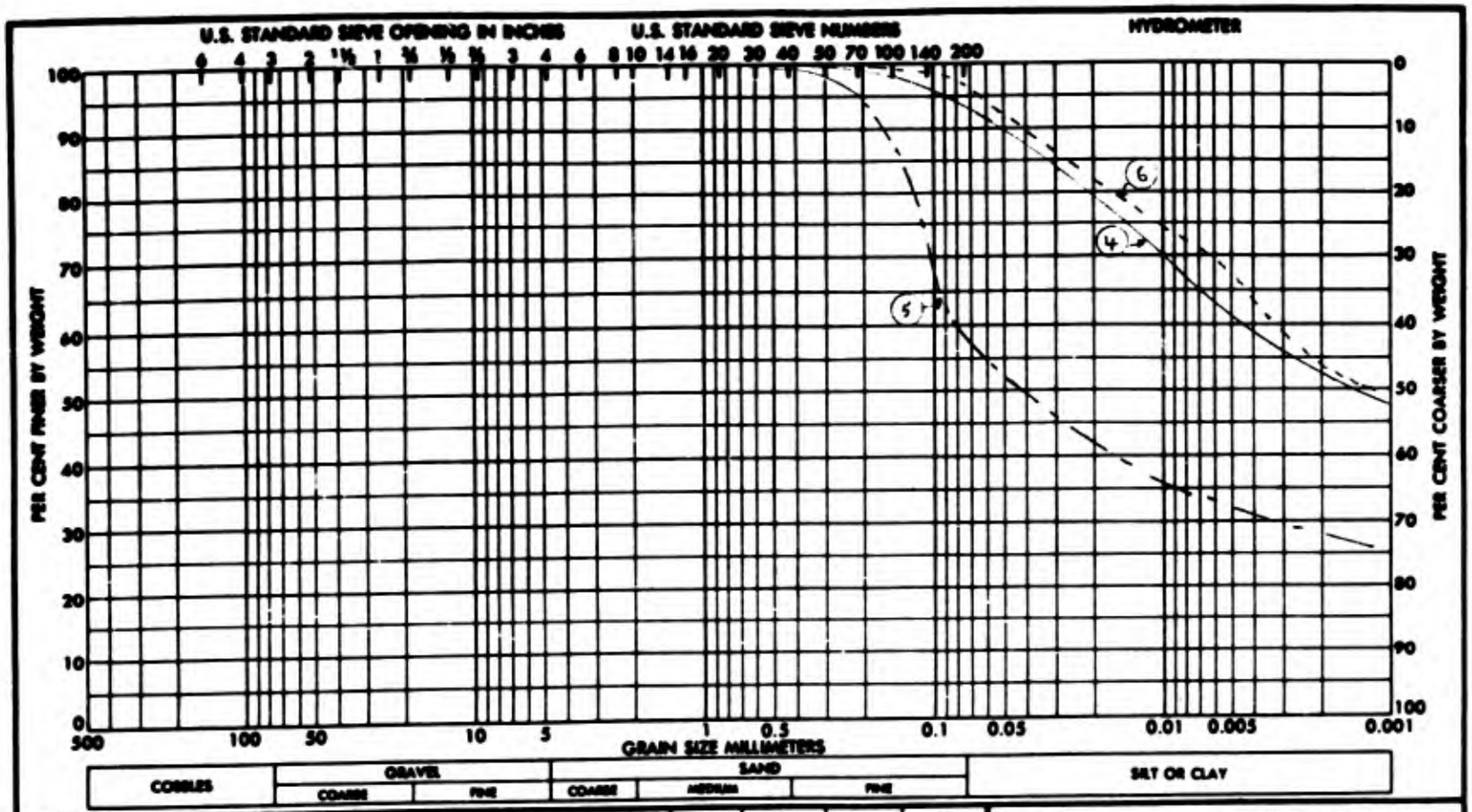

SAMPLE NO.	ELEV OR DEPTH	CLASSIFICATION	NAT WC	LL	PL	PI
4	3.5-3.85 M	CH with Sand, brown, G_s=2.74		59	21	38
5	5.0-5.35 M	CL, sandy clay, brown, G_s=2.72		28	15	13
6	7.0-7.5 M	CH, brown, G_s=2.79		60	22	38

GRADATION CURVES

PROJECT Foundations on Swelling Soils

AREA Sigonella, Sicily

BORING NO. U-4 to U-6

DATE 19 January, 1977

WES FORM 2087
1 MAY 63

REPLACES WES FORM NO. 1241, SEP 1962, WHICH IS OBSOLETE.

APPENDIX G: COMPUTER PROGRAM ULTRAT

Organization

1. The code ULTRAT is composed of a main program and two subroutines. The main program reads in input data and computes vertical overburden and surcharge pressures exerted by soils and the overlying foundation and superstructure. The first subroutine HSWAND computes heave and heave with time from results of laboratory swell tests using the mechanical swell model. The second subroutine HSUCT computes heave and heave with time from results of suction tests and permeability data using the soil suction model. The program is set with statement PARAMETER NL=10, NQ=81 where NL is the maximum number of soils NMAT and NQ is the maximum number of nodal points NNP. The capacity of the program may be increased by increasing NL and NQ.

Input Data

2. Input data are as follows:

STEP	DATA
1	The code will print = : A description of the problem is recommended
2A	The code will print after carriage return: NOPT,NPROB,NRATE,NSUCT,NBPRESS,NNP,NBX,NMAT,DX = Input the above variables, Table G1
2B	If NSUCT=1 and NRATE=1, the code will print after carriage return: DT,NTIME,(NOUT(I),I=1,NTIME) = Input the above variables, Table G1
3	The code will print after carriage return: M,G,WC,EO = Input the above variables, Table G1, for soil M=1
4A	If NSUCT=0, the code will print after carriage return step 3: M,ALL,EPO,ES,PO,SP,CVS,CC = Input the above variables, Table G1, for soil M=1
4B	If NSUCT=1, the code will print after carriage return step 3: M,A,B,ALPHA,AKO,PI,PERM = Input the above variables, Table G1, for soil M=1
	The code will repeat steps 3 and 4 until all soils from M=1 to M=NMAT are read into the computer

STEP	DATA
5	The code will print after carriage return: ELEMENT,NO. OF SOIL = 1,1 should be input = element, 2 should be input for elements in increasing order for each increase in soil number M = NEL,NMAT should be input as the last (deepest) element for soil M=NMAT
6	The code will print after carriage return up to NPROB: Q,BLEN,BWID,DGWT,IOPTION,IVOL,IK = Input the above variables, Table G1
7	The code will print after carriage return for rectangular (NBPRES=2) and long, continuous (NBPRES=3) foundations: LOCATION: CENTER=0, CORNER/EDGE=1 = 0 or 1 should be input for MRECT, Table G1

Steps 6 and 7 will be repeated following printout of the solution of the problem until the number of problems = NPROB

Output Data

Mechanical swell model

3. If NOPT=1 and NRATE=1 all computed data will be printed:

STEP	DATA
1	ELEMENT DEPTH,FT FRACTION HEAVE EXCESS PRESSURE,TSF Data of each element will be printed below the above heading
2	DELH = FEET Total heave will be printed below the above heading in feet
3	TIME,DAYS HEAVE,FT Time required to achieve 20, 40, 60, 80, and 90 percent of DELH will be printed below the above heading. Step 2 will be printed only if NOPT=0 and NRATE=0. Steps 2 and 3 will be printed if NOPT=0 and NRATE=1. The nomenclature for the output data is defined in Table G3.

Soil suction model

4. If NOPT=1 and NRATE=1 all computed data will be printed:

STEP	DATA
1	ELEMENT DEPTH,FT FRACTION HEAVE EXCESS PRESSURE,TSF Data of each element will be printed below the above heading

STEP	DATA
2	DELH = FEET
	Total heave will be printed above in feet
3A	DEPTH,FT FRACTION HEAVE EXCESS SUCTION,TSF
	Data of each element for each increase of time NOUT will be printed below the above heading
3B	TIME = DAYS HEAVE = FT FRACTION =
	Time required to achieve heave and fraction of DELH will be printed above for each increase in time NOUT. Step 2 will be printed only if NOPT=0 and NRATE=0. Steps 2 and 3B will be printed only if NOPT=0 and NRATE=1. The nomenclature for the output data is defined in Table G2.

Table G1

Nomenclature of Input Data

Symbol	Step	Description
NOPT	2A	Option for amount of output: =0 for heave beneath the foundation; =1 for depth, fraction heave, excess pressure (or suction for suction model) and heave beneath foundation
NPROB	2A	Number of loading cases using the same material properties and soil profile
NRATE	2A	Option for heave with time: =0 not used; =1 heave with time computed and printed
NSUCT	2A	Option for model: =0 for mechanical swell model; =1 for soil suction model
NBPRES	2A	Option for foundation: =1 for circular or pier; =2 for rectangular or slab; =3 for long, continuous or strip
NNP	2A	Total number of nodal points, NEL+1. NNP is set at the depth of the active zone X_a below which no changes in moisture are expected
NBX	2A	Number of nodal point at bottom of foundation
NMAT	2A	Total number of different soil layers
DX	2A	Increment of depth, ft. A DX of 0.5 is usually satisfactory
DT	2B	Increment of time, days for NSUCT=1 and NRATE=1. A DT of 1 is usually satisfactory
NTIME	2B	Total number of times that heaves are printed for various increases in time
NOUT(I)	2B	Number of time iterations; DT·NOUT(I) = time, days
M	3	Number of soil layer
G	3	Specific gravity of soil layer M , G_s
WC	3	Initial water content of soil layer M, w_o percent
EO	3	Initial void ratio of soil layer M , e_o
M	4A	Number of soil layer
ALL	4A	Liquid limit of soil layer M , LL percent
EPO	4A	Void ratio at PO following saturation of soil layer M , e_{po} , Figure 3, Table 3
ES	4A	Void ratio at 0.1 tsf following saturation of soil layer M , e_s , Figure 3, Table 3
PO	4A	Original overburden pressure of soil layer M , p_o tsf, Figure 3, Table 3
SP	4A	Swell pressure of soil layer M , p_s tsf, Figure 3, Table 3
CVS	4A	Coefficient of swell of soil layer M , c_{vs} sq ft/day
CC	4A	Compression index of soil layer M , C_c ; = 0.007(ALL-10) if set equal to 0 or a negative number

(Continued)

Table G1 (Concluded)

Symbol	Step	Description
M	4B	Number of soil layer
A	4B	Suction parameter of soil layer M , tsf
B	4B	Suction parameter of soil layer M , dimensionless
ALPHA	4B	Compressibility factor of soil layer M ; if Alpha= 0 or negative, alpha is given by Equation 32
AKO	4B	Ratio of total horizontal to vertical pressure of soil layer M , K_T
PI	4B	Plasticity index of soil layer M , percent
PERM	4B	Coefficient of saturated permeability k_s of soil layer M , ft/day
ELEMENT	5	Number of soil element, Figure 1
NO. OF SOIL	5	Number of soil layer M
NEL	5	Total number of soil elements, Figure 1
NMAT	5	Total number of soil layers
		The following are input up to NPROB for each of the above variables. This provision permits variation in structure loading pressure, foundation dimensions, water table depth, type of equilibrium moisture profile, use of volume parameter C and use of variable permeability for the soil suction model
Q	6	Foundation and superstructure pressure, tsf
BLEN	6	Radius of circular foundation (NBPRES=1); length of rectangular foundation (NBPRES=2); =0.0 for long, continuous foundation (NBPRES=3), ft
BWID	6	0.0 if circular foundation (NBPRES=1); width of rectangular foundation (NBPRES=2) and long, continuous footing (NBPRES=3), ft
DGWT	6	Depth to the water table, ft
IOPTION	6	Equilibrium moisture profile: =0 for saturation (Figures 4 and 5); =1 for negative hydrostatic head continuous to depth of water table (Figure 4); =2 only when NSUCT=1 for negative hydrostatic head continuous to depth of active zone (DGWT should be set to depth of active zone or deeper
IVOL	6	Option for volume parameter C of soil suction model: =0 not used; =1 if used
IK	6	Option for variable permeability of soil suction model: =0 for constant k; =1 for variable k
MRECT	7	Option for location: = 0 for center of rectangular (NBPRES=2) or long, continuous foundation (NBPRES=3); =1 for corner of rectangular foundation or edge of long, continuous foundation. Not used if NBPRES=1 where results are printed only for center of circular foundation

Table G2

Nomenclature of Output Data

Symbol	Step	Description
		Mechanical Swell Model
ELEMENT	1	Number of element
DEPTH, FT	1	Depth of center of element, ft
FRACTION HEAVE	1	$(e_f - e_o)/(1 + e_o)$ of the element, Equation 9
EXCESS PRESSURE, TSF	1	$p_s - \bar{p}_f$ of the element, Figure 3; a measure of the additional confining pressure needed to avoid swell for the assumed equilibrium moisture profile
DELH	2	Total heave ΔH , ft, Equation 9
TIME, DAYS	3	Accumulated time from start of heave, days
HEAVE, FT		Accumulated heave up to TIME, ft
		Soil Suction Model
ELEMENT	1	Number of element
DEPTH, FT	1	Depth of center of element, ft
FRACTION HEAVE	1	DELTA(I)/DX of the element, Equation 11
EXCESS PRESSURE, TSF	1	Difference between the calculated initial in situ suction τ_{mo} and assumed final in situ suction τ_{mf} , Equation 16, tsf; the initial in situ suction of the element if IOPTION=0
DELH	2	Total heave ΔH , ft, Equation 9
DEPTH, FT	3A	Depth of the element, ft
FRACTION HEAVE	3A	Accumulated DELTA(I)/DX of the element up to TIME
EXCESS SUCTION TSF	3A	Difference between initial and final in situ suction remaining at TIME, tsf
TIME	3B	Accumulated time from start of heave, days
HEAVE	3B	Accumulated heave up to TIME, ft
FRACTION	3B	Fraction of total heave DELH accumulated up to TIME

(Continued)

Table G2 (Continued)

Example Problem of Slab Foundation Above Water Table

Mechanical Swell Model

```
♦RUN
=LACKLAND ABOVE WATER TABLE                    8 FT                    SO TEST
NOPT,NPROB,NRATE,NSUCT,NBPRES,NNP,NBX,NMAT,DX
=1,2,0,0,2,17,1,2,.5
M,G,WC,EO
=1,2.69,31.6,.930
M,ALL,EPO,ES,PO,SP,CVS,CC
=1,60,.943,.951,.24,1.2,.01,.27
M,G,WC,EO
=2,2.78,34.5,1.044
M,ALL,EPO,ES,PO,SP,CVS,CC
=2,60,1.045,1.051,.29,.40,.01,.27
ELEMENT,NO. OF SOIL
=1,1
=11,2
=16,2
Q,BLEN,BWID,DGWT,IOPTION,IVOL,IK
=.072,100,100,8.,,1,1
LOCATION:  CENTER=0,CORNER/EDGE=1
=0
```

ELEMENT	DEPTH,FT	FRACTION HEAVE	EXCESS PRESSURE,TSF
1	0.25	0.01158	1.11367
2	0.75	0.01022	1.08501
3	1.25	0.00917	1.05640
4	1.75	0.00833	1.02852
5	2.25	0.00777	1.00702
6	2.75	0.00762	1.00078
7	3.25	0.00755	0.99775
8	3.75	0.00717	0.98124
9	4.25	0.00666	0.95562
10	4.75	0.00621	0.92758
11	5.25	0.00043	0.09908
12	5.75	0.00030	0.07052
13	6.25	0.00017	0.04194
14	6.75	0.00005	0.01336
15	7.25	-0.00214	-0.01522
16	7.75	-0.00596	-0.04380

DELH = 0.03755 FEET

(Continued)

Table G2 (Continued)

```
Q,BLEN,BWID,DGWT,IOPTION,IVOL,IK
=.072,100,100,8.,1,1,1
LOCATION:  CENTER=0,CORNER/EDGE=1
=0
```

ELEMENT	DEPTH,FT	FRACTION HEAVE	EXCESS PRESSURE,TSF
1	0.25	0.00542	0.87148
2	0.75	0.00526	0.85845
3	1.25	0.00510	0.84546
4	1.75	0.00496	0.83320
5	2.25	0.00489	0.82733
6	2.75	0.00500	0.83672
7	3.25	0.00515	0.84931
8	3.75	0.00514	0.84843
9	4.25	0.00502	0.83843
10	4.75	0.00488	0.82602
11	5.25	0.00005	0.01314
12	5.75	0.00000	0.00021
13	6.25	-0.00180	-0.01274
14	6.75	-0.00357	-0.02570
15	7.25	-0.00426	-0.03084
16	7.75	-0.00596	-0.04380

DELH = 0.01764 FEET

Soil suction model

```
♦RUN
=LACKLAND ABOVE WATER TABLE                    8 FT DEPTH
NOPT,NPROB,NRATE,NSUCT,NBPRES,NNP,NBX,NMAT,DX
=1,2,0,1,2,17,1,2,.5
M,G,WC,EO
=1,2.7,25.,.97
M,A,B,ALPHA,AKO,PI,PERM
=1,6.774,.25,.94,1.,40,.008
M,G,WC,EO
=2,2.75,30.,.95
M,A,B,ALPHA,AKO,PI,PERM
=2,5.044,.167,1.,1.,40,.008
ELEMENT,NO. OF SOIL
=1,1
=11,2
=16,2
```

(Continued)

Table G2 (Continued)

Q,BLEN,BWID,DGWT,IOPTION,IVOL,IK
=.072,100,100,8.,,1,1
LOCATION: CENTER=0,CORNER/EDGE=1
=0

ELEMENT	DEPTH,FT	FRACTION HEAVE	EXCESS PRESSURE,TSF
1	0.25	0.08346	3.26169
2	0.75	0.07735	3.23653
3	1.25	0.07257	3.21141
4	1.75	0.06873	3.18698
5	2.25	0.06622	3.16855
6	2.75	0.06570	3.16446
7	3.25	0.06556	3.16339
8	3.75	0.06390	3.14965
9	4.25	0.06145	3.12734
10	4.75	0.05902	3.10276
11	5.25	0.04929	0.79939
12	5.75	0.04575	0.77077
13	6.25	0.04251	0.74213
14	6.75	0.03954	0.71349
15	7.25	0.03679	0.68484
16	7.75	0.03423	0.65619

DELH 0.46603 FEET

Q,BLEN,BWID,DGWT,IOPTION,IVOL,IK
=.072,100,100,8.,1,1,1
LOCATION: CENTER=0,CORNER/EDGE=1
=0

ELEMENT	DEPTH,FT	FRACTION HEAVE	EXCESS PRESSURE,TSF
1	0.25	0.05233	3.01950
2	0.75	0.05168	3.00997
3	1.25	0.05105	3.00047
4	1.75	0.05048	2.99167
5	2.25	0.05030	2.98886
6	2.75	0.05105	3.00040
7	3.25	0.05202	3.01495
8	3.75	0.05215	3.01684
9	4.25	0.05169	3.01015
10	4.75	0.05110	3.00120
11	5.25	0.03954	0.71345
12	5.75	0.03826	0.70046
13	6.25	0.03703	0.68744
14	6.75	0.03584	0.67442
15	7.25	0.03468	0.66140
16	7.75	0.03356	0.64838

DELH = 0.36639 FEET

(Continued)

Table G2 (Continued)

Listing

```
27747 01  08-11-77   14,637

1000C  PREDICTION OF ULTIMATE AND RATE OF HEAVE-ULTRAT
1010C  BASED ON MECHANICAL SWELL AND SOIL SUCTION MODELS
1020C  DEVELOPED BY L. D. JOHNSON
1030   PARAMETER NL=10,NQ=8$
1040   COMMON A(NL),B(NL),G(NL),WC(NL),EO(NL),EPO(NL),ES(NL),PO(NL),
1050&  SP(NL),CVS(NL),ALL(NL),PI(NL),ALPHA(NL),PERM(NL),NOUT(NL),
1060&  CC(NL),AKO(NL),P(NQ),IE(NQ,1),NBX,NEL,DXX,DX,GAW,IOPTION,NRATE,
1070&  DT,NTIME,ANBX,NOPT,DGWT,IVOL,IK
1080   READ 3
1090   3   FORMAT(30H
1100   GAW=0.03125
1110   NP=1
1120   PRINT 5
1130   5   FORMAT(45HNOPT,NPROB,NRATE,NSUCT,NBPRES,NNP,NBX,NMAT,DX)
1140   READ,NOPT,NPROB,NRATE,NSUCT,NBPRES,NNP,NBX,NMAT,DX
1150   NEL=NNP-1
1160   IF(NSUCT.EQ.0.OR.NRATE.EQ.0)GO TO 14
1170   PRINT 7
1180   7   FORMAT(27HDT,NTIME,(NOUT(I),I=1,NTIME)
1190   READ,DT,NTIME,(NOUT(I),I=1,NTIME)
1200   14   PRINT 10
1210   10   FORMAT(9HM,G,WC,EO)
1220   READ,M,G(M),WC(M),EO(M)
1230   IF(NSUCT.EQ.1)GO TO 25
1240   PRINT 12
1250   12   FORMAT(25HM,ALL,EPO,ES,PO,SP,CVS,CC)
1260   READ,M,ALL(M),EPO(M),ES(M),PO(M),SP(M),CVS(M),CC(M)
1270   GO TO 20
1280   25   PRINT 8
1290   8   FORMAT(23HM,A,B,ALPHA,AKO,PI,PERM)
1300   READ,M,A(M),B(M),ALPHA(M),AKO(M),PI(M),PERM(M)
1310   IF(ALPHA(M).LE.0.)GO TO 16
1320   GO TO 20
1330   16   ALPHA(M)=.0275*PI(M)-.125
1340   IF(PI(M).LE.5.)ALPHA(M)=0.0
1350   IF(PI(M).GE.40.)ALPHA(M)=1.
1360   20   IF(NMAT-M)26,27,14
1370   26   PRINT 17,M
1380   17   FORMAT(20H  ERROR IN MATERIAL ,I5)
1390   STOP
1400   27   L=0
1410   PRINT 30
1420   30   FORMAT(19HELEMENT NO. OF SOIL)
1430   40   READ,N,IE(N,1)
1440   50   L=L+1
1450   IF(N-L)60,60,70
1460   70   IE(L,1)=IE(L-1,1)
1470   GO TO 50
1480   60   IF(NEL-L)80,80,40
1490   80   CONTINUE
1500   200   PRINT 90
1510   90 FORMAT(32HQ,BLEN,BWID,DGWT,IOPTION,IVOL,IK)
```

(Continued)

Table G2 (Continued)

Listing (Continued)

```
2774T 01  08-11-77   14.637

1520    READ,Q,BLEN,BWID,DGWT,IOPTION,IVOL,IK
1530    IF(NSUCT.EQ.0.AND.IOPTION.GT.1)IOPTION=1
1540    IF(NBPRES.EQ.2.OR.NBPRES.EQ.3)GO TO 92
1550    GO TO 94
1560    92 PRINT 96
1570    96 FORMAT(32HLOCATION: CENTER=0,CORNER/EDGE=1)
1580    READ,MRECT
1590C   CALCULATION OF SURCHARGE PRESSURE FROM SOIL
1600    94 DXX=DX
1610    P(1)=0.0
1620    DO 100 I=2,NNP
1630    MTYP=IE(I-1,1)
1640    WCC=WC(MTYP)/100.
1650    GAMM=G(MTYP)*GAW*(1.-WCC)/(1.+EO(MTYP))
1660    IF(DXX.GT.DGWT.AND.NSUCT.EQ.0)GAMM=GAMM-GAW
1670    P(I)=P(I-1)+DX*GAMM
1680    DXX=DXX+DX
1690    100   CONTINUE
1700C   CALCULATION OF SURCHARGE PRESSURE FROM STRUCTURE
1710    ANBX=NBX
1720    ANBX=ANBX+DX
1730    DXX=0.0
1740    BPRES=Q-P(NBX)
1750    DO 120   I=NBX,NNP
1760    IF(NBPRES.EQ.1)GO TO 122
1770    IF(NBPRES.EQ.3)GO TO 127
1780    IF(DXX.LT.0.01)GO TO 123
1790    IF(MRECT.EQ.1)GO TO 121
1800    BLEN=BLEN/2.
1810    BWID=BWID/2.
1820    121 VE2=(BLEN**2.+BWID**2.+DXX**2.)/(DXX**2.)
1830    VE=VE2**0.5
1840    AN=BLEN*BWID/(DXX**2.)
1850    AN2=AN**2.
1860    ENM=(2.*AN*VE/(VE2+AN2))*(VE2+1.)/VE2
1870    FNM=2.*AN*VE/(VE2-AN2)
1880    IF(MRECT.EQ.1)BPRES=BPRES/4.
1890    AB=ATAN(FNM)
1900    IF(FNM.LT.0.)AB=3.1416+AB
1910    P(I)=P(I)+BPRES*(ENM+AB)/3.1416
1920    GO TO 125
1930    122   IF(DXX.LT.0.01)GO TO 123
1940    PS=1.+(BLEN/DXX)**2.
1950    PS=PS**1.5
1960    P(I)=P(I)+BPRES*(1.-1./PS)
1970    GO TO 125
1980    127 DB=DXX/BWID
1990    PS=-.157-.22*DB
2000    IF(MRECT.EQ.0.AND.DB.LT.2.5)PS=-.28*DB
2010    PS=10.**PS
2020    P(I)=P(I)+BPRES*PS
2030    GO TO 125
```

(Continued)

Table G2 (Continued)

Listing (Continued)

```
2774T 01  08-11-77   14,637

2040    123   P(I)=P(I)+BPRES
2050    125   IF(IOPTION.EQ.1.AND.NSUCT.EQ.0)GO TO 130
2060    GO TO 140
2070    130   AI=I-1
2080    HN=(DGWT/DX)-AI
2090    ADXX=ANBX+DXX
2100    IF(ADXX.GE.DGWT)GO TO 140
2110    P(I)=P(I)+BN*DX*GAW
2120    140   DXX=DXX+DX
2130    120   CONTINUE
2140    IF(NOPT.EQ.0)GO TO 147
2150    PRINT 145
2160    145   FORMAT(/,33HELEMENT  DEPTH,FT  FRACTION HEAVE,
2170&   21H  EXCESS PRESSURE,TSF)
2180    147   DXX=ANBX+DX/2.
2190    IF(NSUCT.EQ.1)GO TO 150
2200C   CASES FOR MECHANICAL SWELL MODEL
2210    CALL HSTAND
2220    GO TO 160
2230C   CASES FOR SOIL SUCTION MODEL
2240    150   CALL HSUCT
2250    160   NP=NP+1
2260    IF(NP.GT.NPROB)GO TO 180
2270    GO TO 200
2280    180   STOP
2290    END
2300C
2310C
2320    SUBROUTINE HSTAND
2330    PARAMETER NL=10,NQ=81
2340    COMMON A(NL),B(NL),G(NL),WS(NL),EO(NL),EPO(NL),ES(NL),PO(NL),
2350&   SP(NL),CVS(NL),ALL(NL),PI(NL),ALPHA(NL),PERM(NL),NOUT(NL),
2360&   CC(NL),AKO(NL),P(NQ),IE(NQ,1),NBX,NEL,DXX,DX,GAW,IOPTION,NRATE,
2370&   DT,NTIME,ANBX,NOPT,DGWT,IVOL,IK
2380    DIMENSION AMV(NQ)
2390    DELH=0.0
2400    DO 10 I=NBX,NEL
2410    MTYP=IE(I,1)
2420    PR=(P(I)+P(I+1))/2.
2430    IF(PR.GT.SP(MTYP))GO TO 50
2440    IF(SP(MTYP).LT.PO(MTYP).AND.PR.LT.SP(MTYP))GO TO 25
2450    IF(PR.GT.PO(MTYP).AND.PO(MTYP).GT.0.1)GO TO 30
2460    IF(PR.LE.PO(MTYP).AND.PO(MTYP).GT.0.1)GO TO 40
2470    IF(PR.LE.0.1)GO TO 20
2480    25 C2=0.1/SP(MTYP)
2490    CS2=(ES(MTYP)-EO(MTYP))/ALOG10(C2)
2500    AMV(I)=-0.435*CS2/((1.+EO(MTYP))*PR)
2510    C=PR/SP(MTYP)
2520    E=EO(MTYP)+CS2*ALOG10(C)
2530    GO TO 60
2540    20    C1=PO(MTYP)/0.1
2550    CS1=(ES(MTYP)-EPO(MTYP))/ALOG10(C1)
```

(Continued)

Table G2 (Continued)

Listing (Continued)

```
2774T 01  08-11-77   14,037

2560    AMV(I)= 0,435*CS1/((1,+EO(MTYP))*PR)
2570    C=PR/0,1
2580    E=ES(MTYP)-CS1*ALOG10(C)
2590    GO TO 60
2600    30   C2=PO(MTYP)/SP(MTYP)
2610    CS2=(EPO(MTYP)-EO(MTYP))/ALOG10(C2)
2620    AMV(I)=-0,435*CS2/((1,+EO(MTYP))*PR)
2630    C=PR/SP(MTYP)
2640    E=EO(MTYP)+CS2*ALOG10(C)
2650    GO TO 60
2660    40   C1=0,1/PO(MTYP)
2670    CS1=(ES(MTYP)-EPO(MTYP))/ALOG10(C1)
2680    AMV(I)=-0,435*CS1/((1,+EO(MTYP))*PR)
2690    C=PR/PO(MTYP)
2700    E=EPO(MTYP)+CS1*ALOG10(C)
2710    GO TO 60
2720    50   CCC=CC(MTYP)
2730    IF(CCC.LE.0,00001)CCC=0,002*(ALL(MTYP)-10)
2740    AMV(I)=0,435*CCC/((1,+EO(MTYP))*PR)
2750    C=SP(MTYP)/PR
2760    E=EO(MTYP)+CCC*ALOG10(C)
2770    60   DEL=(E-EO(MTYP))/(1,+EO(MTYP))
2780    IF(NOPT,EQ,0)GO TO 75
2790    DELP=SP(MTYP)-PR
2800  PRINT 70,I,DXX,DEL,DELP
2810    70   FORMAT(I5,F10,2,F15,5,5X,F15,5)
2820    75   DELH=DELH+DX*DEL
2830    DXX=DXX+DX
2840    80   CONTINUE
2850    PRINT 80,DELH
2860    80 FORMAT(/,10H  DELH =  ,F10,5,7H   FEET,/)
2870    IF(NRATE,EQ,0)GO TO 200
2880  C  COMPUTE RATES OF HEAVE FROM OEDOMETER TESTS
2890    AKT=0,0
2900    BKT=0,0
2910    DO 100 I=NOX,NEL
2920    MTYP=IE(I,1)
2930    AKT=AKT+DX/(CVS(MTYP)*AMV(I))
2940    BKT=BKT+AMV(I)*DX
2950    100   CONTINUE
2960    AB=AKT*BKT
2970    T2=0.010*AB
2980    T4=0.050*AB
2990    T6=0.163*AB
3000    T8=0.435*AB
3010    T9=0.722*AB
3020    H2=0.2*DELH
3030    H4=0.4*DELH
3040    H6=0.6*DELH
3050    H8=0.8*DELH
3060    H9=0.9*DELH
3070    PRINT 110
```

(Continued)

Table G2 (Continued)

Listing (Continued)

```
2774T 01  08-11-77   14.637

3080    110   FORMAT(/,20H TIME,DAYS  WEAVE,FT)
3090    PRINT 120,T2,H2,T4,H4,T6,H6,T8,H8,T9,H9
3100    120   FORMAT(/,2E10.3,/,2E10.3,/,2E10.3,/,2E10.3,/,2E10.3,/)
3110    200   CONTINUE
3120    RETURN
3130    END
3140C
3150C
3160    SUBROUTINE HSUCT
3170    PARAMETER NL=10,NQ=81
3180    COMMON A(NL),B(NL),G(NL),WC(NL),EO(NL),EPB(NL),ES(NL),PO(NL),
3190&   SP(NL),CVS(NL),ALL(NL),PI(NL),ALPHA(NL),PERM(NL),NOUT(NL),
3200&   BC(NL),AKO(NL),P(NQ),IE(NQ,4),NBX,NEL,DXX,DX,GAW,IOPTION,NRATE,
3210&   DT,NTIME,ANBX,NOPT,DGWT,IVOL,IK
3220    DIMENSION UINIT(NQ),U(NQ),YY(NQ),DELTA(NQ),GEE(NQ),HSS(NQ)
3230    H=0
3240    NN=NEL+1
3250    N=NBX+1
3260    ANEL=NEL
3270    ANEL=ANEL*DX
3280    IF(IOPTION.EQ.2)GO TO 5
3290    GO TO 7
3300    5   MATNEL=IE(NEL,1)
3310    FNNP=(1.+2.*AKO(MATNEL))/3.
3320    SUCTI=A(MATNEL)-B(MATNEL)*WC(MATNEL)
3330    SUCTI=10.**SUCTI
3340    TFI=SUCTI-P(NN)*FNNP*ALPHA(MATNEL)
3350    7   DELH=0.0
3360    DO 10 I=NBX,NEL
3370    MTYP=IE(I,1)
3380    F=(1.+2.*AKO(MTYP))/3.
3390    I=I+1
3400    BN=(DGWT/DX)-AI
3410    BO=BN-1.
3420    TF=0.0
3430    IF(IOPTION.EQ.1.OR.DXX.GT.DGWT)TF=(BN+BO)*DX*GAW/2.
3440    IF(IOPTION.EQ.2)TF=TFI+(ANEL-DXX)*GAW
3450    PR=(P(I)+P(I+1))/2.
3460    ALP=ALPHA(MTYP)
3470    IF(DXX.GT.DGWT)ALP=1.0
3480    TAUF=TF+ALP*PR*F
3490    IF(TAUF.GT.0.000001)GO TO 15
3500    PRINT 20,TAUF,I
3510    20    FORMAT(31HNEGATIVE FINAL EFFECTIVE STRESS,
3520&   F10.5,12H  IN ELEMENT,I5)
3530    H=H+1
3540    GO TO 35
3550    15    TAUI=A(MTYP)-B(MTYP)*WC(MTYP)
3560    TAUI=10.**TAUI
3570    TI=TAUI+ALP*PR*F
3580    UINIT(I)=TI-TF
3590    GT=ALPHA(MTYP)*G(MTYP)/(100.*B(MTYP))
```

(Continued)

Table G2 (Continued)

Listing (Continued)

```
2774T 01  08-11-77   14.637

3600    CT=CT/(1.+EO(MTYP))
3610    RTAU=TAUI/TAUF
3620    DELTA(I)=CT*ALOG10(RTAU)
3630    IF(DELTA(I).LT.0.0.AND.DXX.GT.DGHT)DELTA(I)=DELTA(I)/ALPHA(MTYP)
3640    IF(DELTA(I).LT.0.0.AND.TI.LT.0.0)DELTA(I)=DELTA(I)/ALPHA(MTYP)
3650    IF(NOPT.EQ.0)GO TO 33
3660    PRINT 30,I,DXX,DELTA(I),UINIT(I)
3670    30   FORMAT(I5,F10.2,F15.5,5X,F15.5)
3680    33   DELH=DELH+DX*DELTA(I)
3690    35   DXX=DXX+DX
3700    20   CONTINUE
3710    IF(M.GT.0)GO TO 200
3720    PRINT 40,DELH
3730    40   FORMAT(/,10H  DELH =  ,F10.5,7H   FEET,/)
3740    IF(NRATE.EQ.0)GO TO 200
3750C   COMPUTE RATES OF HEAVE FROM PERMEABILITY DATA
3760    IF(IOPTION.EQ.1.OR.IOPTION.EQ.2)GO TO 45
3770    UINIT(NN)=UINIT(NEL)
3780    U(NBX)=0.0
3790    V(NBX)=0.0
3791    FTYP=IE(NBX,1)
3792    E=EO(FTYP)+(DELTA(NBX)*(1.+EO(FTYP)))
3793    GEE(NBX)=(E*(1.+EO(FTYP)))/(EO(FTYP)*(1.+E))
3794    TAUI=A(FTYP)-B(FTYP)*WC(FTYP)
3795    TAU=10.**TAUI=UINIT(NBX)
3796    HSS(NBX)=(A(FTYP)-ALOG10(TAU))*G(FTYP)/(100.*B(FTYP)*E)
3800    GO TO 47
3810    45   UINIT(NBX)=UINIT(NBX+1)
3820    U(NBX)=U(NBX+1)
3830    V(NBX)=U(NBX)
3840    UINIT(NN)=0.0
3841    FTYP=IE(NBX,1)
3842    GEE(NBX)=1.
3843    HSS(NBX)=WC(FTYP)*G(FTYP)/(100.*EO(FTYP))
3850    47   DO 50 I=N,NN
3860    U(I)=UINIT(I)
3870    V(I)=UINIT(I)
3880    50   CONTINUE
3890    NCT=0
3900    N1=0
3910    TIME=0.0
3920    100  NCT=NCT+1
3930    JJ=2*N1
3940    DO 80 J=N,NEL
3950    IF(JJ.EQ.NCT)GO TO 60
3960    I=J
3970    IF(U(I-1).LT.0.0.AND.U(I).GT.0.0)U(I)=0.0
3980    IF(U(I-1).GT.0.0.AND.U(I).LT.0.0)U(I)=0.0
3990    60 TO 70
4000    60   I=NEL+N-J
4010    IF(U(I+1).LT.0.0.AND.U(I).GT.0.0)U(I)=0.0
4020    IF(U(I+1).GT.0.0.AND.U(I).LT.0.0)U(I)=0.0
```

(Continued)

Table G2 (Continued)

Listing (Continued)

```
2774T 0$  08-11-77   14,637

4030    70 MTYP=IE(I,1)
4040    NTYP=IE(I-1,1)
4050    PR=(P(I-1)+P(I))/2.
4060   F=(1.+2.*AK0(MTYP))/3.
4070    ALP=ALPHA(MTYP)
4080    TAUI=A(MTYP)-B(MTYP)*WC(MTYP)
4090    TAUI=10.**TAUI
4100    IF(DXX.GT.DGWT)ALP=1.0
4110    TI=TAUI*ALP*PR*F
4120    TF=TI-UINIT(I)
4130    TAU=U(I)+ALP*PR*F+TF
4140   IF(TAU.LE.0.001)TAU=TAUI
4150    TEMP1=100.**(1.+EO(MTYP))-ALPHA(MTYP)*WC(MTYP)*G(MTYP)
4160    TEMP2=ALPHA(MTYP)*G(MTYP)*(A(MTYP)-ALOG10(TAU))
4170    IF(TI.LE.0.0)GO TO 65
4180    TEMP=(B(MTYP)*TEMP1+TEMP2)**2.
4190    GE=(SQRT(TEMP)-100.*B(MTYP))*(1.+EO(MTYP))
4200    GEE(I)=GE/(EO(MTYP)*SQRT(TEMP))
4210    HS=TEMP2/(ALPHA(MTYP)*(SQRT(TEMP)-100.*B(MTYP)))
4215    IF(HS.GT.1.)HS=1.
4220    HSS(I)=HS**3.
4225    PERR=PERM(NTYP)*GEE(I-1)*HSS(I-1)
4230    PER=PERM(MTYP)*GEE(I)*HSS(I)
4240    IF(IK.EQ.0)PER=PERM(MTYP)
4245    IF(IK.EQ.0)PERR=PERM(NTYP)
4250    DV=75.75*PER*TAU*TEMP/(G(MTYP)*B(MTYP)*TEMP1)
4260    GO TO 66
4270    65 DV=0.435*G(MTYP)/(100.*B(MTYP)*(1.+EO(MTYP))*TAU)
4280    DV=PERM(MTYP)/(GAW*DV)
4290    66  R=PERR/PER
4300    DR=DV*DT/(DX*DX)
4310    CONT=1.+TEMP2/(B(MTYP)*TEMP1)
4320    IF(IVOL.EQ.0)CONT=1.
4330    IF(R.GT.10000.)R=10000.
4340    FR=(1.-R)/(1.+R)
4350    IF(JJ.EQ.NCT)GO TO 75
4360    SI=U(I+1)*(U(I+1)-V(I-1))*FR
4370    U(I)=(DR*(U(I-1)-U(I)+SI)+U(I)*CONT)/(DR+CONT)
4380    GO TO 80
4390    75   SI=U(I-1)+(V(I+1)-U(I-1))*FR
4400    U(I)=(DR*(U(I+1)-U(I)+SI)+U(I)*CONT)/(DR+CONT)
4410    80   CONTINUE
4420    IF(JJ.NE.NCT)N1=N1+1
4430    IF(IOPTION.EQ.0)GO TO 85
4440    U(NBX)=U(NBX+1)
4450    V(NBX)=U(NBX)
4455    GEE(NBX)=GEE(NBX+1)
4456    HSS(NBX)=HSS(NBX+1)
4460    GO TO 87
4470    85   U(NN)=U(NEL)
4480    V(NN)=U(NN)
4490    87   TIME=TIME+DT
```

(Continued)

Table G2 (Concluded)

Listing (Concluded)

```
2774T 01  08-11-77   14,637

4500    DO 90 I=NBX,NN
4510    90   V(I)=U(I)
4520    DO 100 I=1,NTIME
4530    J=NOUT(I)
4540    IF(NCT.EQ.J)GO TO 110
4550    100   CONTINUE
4560    GO TO 150
4570    110   IF(NOPT.EQ.0)GO TO 125
4580    PRINT 120
4590    120 FORMAT(//,44HDEPTH,FT  FRACTION HEAVE  EXCESS SUCTION,TSF)
4600    125   DELHT=0.0
4610    DXX=ANBX-DX/2.
4620    DO 130 I=NBX,NEL
4630    MTYP=IE(I,1)
4640    TAUI=A(MTYP)-B(MTYP)*WC(MTYP)
4650    TAUI=10.**TAUI
4660    TAUF=TAUI-UINIT(I)
4670    TAU=TAUI+U(I)-UINIT(I)
4680    RTAU=TAUI/TAUF
4690    RTA=TAUI/TAU
4700    DEL=DELTA(I)*(ALOG10(RTA)/ALOG10(RTAU))
4710    DELHT=DELHT+DEL*DX
4720    IF(NOPT.EQ.0)GO TO 135
4730    PRINT 140,DXX,DEL,U(I)
4740    140 FORMAT(F7.2,F15.5,5X,F15.5)
4750    135   DXX=DXX+DX
4760    130   CONTINUE
4770    RATIO = DELHT/DELH
4780    PRINT 145,TIME,DELHT,RATIO
4790    145   FORMAT(/,5HTIME=,F8.2,14H DAYS   HEAVE=,F8.4,
4800&   15H FT   FRACTION=,F7.4)
4810    IF(NCT.EQ.NOUT(NTIME))GO TO 200
4820    GO TO 150
4830    200   CONTINUE
4840    RETURN
4850    END
```

APPENDIX H: NOTATION

NOTATION

A*	Soil suction parameter corresponding to the intercept on the ordinate of the soil suction-water content relationship, tsf
AKO*	Ratio of total horizontal to vertical stress in situ, K_T
ALPHA*	Compressibility factor, α
AREA	Area of base of pier, ft^2
B	Soil suction parameter corresponding to the slope of the soil suction-water content relationship
BLEN*	Length of foundation, ft
BWID*	Width of foundation, ft
$\bar{c}_{vs}$	Average coefficient of swell, ft^2/day
c_{vs},CVS*	Coefficient of swell, ft^2/day
C	Soil cohesion, tsf
$\bar{C}$	Dimensionless volume parameter
c_c,CC*	Compression index
C_s	Swell index
CVS	Constant volume swell test
C_τ	Suction index
D	Moisture diffusivity, ft^2/day
$\bar{D}$	Time parameter, days/ft
D_t	Dimensionless time parameter
D_T	Thermal diffusivity for liquid water, $ft^2/day \cdot deg\ C$
DELTA(i)	Potential volumetric swell of soil element i , fraction

---

* Capitalized symbols used in ULTRAT.

DGWT*	Depth to the ground water table from the ground surface, ft
DT*	Increment in time t, days
DX*	Increment of depth, ft
DXX*	Accumulative increments of depth from bottom of the foundation, ft
e	Void ratio
e_f	Final (equilibrium) void ratio
$e_f(i)$	Final void ratio of element i
$e_o(i)$	Initial void ratio of element i
e_o,EO*	Initial void ratio
e_{po},EPO*	Void ratio under the overburden pressure p_o when the pore water pressure is zero
e_s,ES*	Void ratio under the pressure 0.1 tsf when the pore water pressure is zero
e^t	Void ratio at time t
E	Microvolt output at temperature t
E_{25}	Microvolt output at 25 C
F	Fraction of total potential heave at some given time
$F(i, t + 1)$	Fraction of the potential volumetric swell of soil element i at time $t + 1$
G_e,GEE*	Void ratio factor, $(e^t/(1 + e^t))/e_o/(1 + e_o))$
G_s,G*	Specific gravity
H	Depth of soil, ft
$\bar{H}$	One-half of the thickness of the specimen for sorption from both top and bottom of the specimen, in.
HYD	Hydrostatic equilibrium moisture profile, $u_{wf} = u_{wa} + \gamma_w(DXX-X_a)$

* Capitalized symbols used in ULTRAT.

ISO	Improved simple oedometer test
k	Coefficient of vertical permeability, ft/day
k_s, PERM*	Initial coefficient of vertical permeability of saturated soil at void ratio e_o, ft/day
k^t	Coefficient of vertical permeability at time t, ft/day
k_n^t	Coefficient of vertical permeability of soil layer n at time t, ft/day
K_o	Ratio of intergranular pressure on horizontal and vertical planes, coefficient of earth pressure
K_T	Ratio of total horizontal pressure to total vertical pressure in situ
L	Vertical load applied at top of pier at ground surface, tons
LL*	Liquid limit, percent
m_v	Coefficient of volume change, tsf^{-1}
M	Gram-formula weight per 1000 grams of water
n	Thickness of soil layer
N	Fraction of volumetric swell that occurs as heave in the vertical direction
NBX*	Number of nodal point at bottom of the foundation
NEL*	Total number of elements
NPROB*	Number of problems
p	Total vertical applied pressure, tsf
p_b	Pressure at base of foundation, tsf
p_f	Final total vertical pressure including pressure from the foundation, tsf
p_{fo}	Final total soil vertical overburden pressure, tsf

---

* Capitalized symbols used in ULTRAT.

p_{fo}(NBX)	Total vertical overburden pressure of surrounding soils at bottom of the foundation, tsf
$\bar{p}_f$	Final vertical effective pressure, tsf
p_o,PO*	Initial total vertical pressure, tsf
p_s,SP*	Swell pressure, tsf
p_{st}	Vertical pressure due to the foundation and superstructure, tsf
PI*	Plasticity index, percent
PL	Plastic limit, percent
PVR	Potential vertical rise, ft
q,Q*	Total foundation and superstructure pressure, tsf
R	Ideal gas constant, 86.81 cc-tsf/mole·deg K
RAD	Radius of pier shaft, ft
RH	Relative humidity, fraction
S	Degree of saturation, fraction
SAT	Saturated equilibrium moisture profile, $u_{wf} = 0$
SO	Swell overburden test
S_p	Swell or potential heave, percent
t	Time, days
t_{90}	Time to complete 90 percent of primary swell, min
T	Absolute temperature, deg K
T_{90}	Time factor needed to complete 90 percent of primary swell, 0.848
T_s	Surface tension of liquid water, ton/ft
$\bar{T}$	Uplift forces, tsf

* Capitalized symbols used in ULTRAT.

u_w	Pore water pressure, tsf
u_{wa}	Pore water pressure at bottom of active zone, tsf
u_{wf}	Final (equilibrium) pore water pressure, tsf
u_{wo}	Initial pore water pressure, tsf
v	Volume of a mole of liquid water, 18.02 cc/mole
V	Total volume, ft^3
V_w	Volume of water, ft^3
V_T	Specific total volume, $(1 + e)/G_s$
V_{TO}	Initial specific volume, $(1 + e_o)/G_s$
w	Water content, percent dry weight
w_o,WC*	Initial water content, percent dry weight
x	Vertical coordinate or elevation head above a reference datum, ft
X_a	Depth below which no change in moisture occurs or volume changes are negligible, ft
α, ALPHA*	Volume compressibility factor
α_s	Volume compressibility factor for change in volume
α_σ	Compressibility factor for change in mean normal confining pressure
γ	Moist unit weight, $tons/ft^3$
γ_d	Dry density, $tons/ft^3$
γ_w	Unit weight of water, 0.0312 $tons/ft^3$
γ_T	Relationship between surface tension of water and temperature, deg C^{-1}
Δ	Change in; e.g., Δt

---

* Capitalized symbols used in ULTRAT.

ΔH	Potential vertical heave at the bottom of the foundation from swelling in soil of depth H , ft
ΔHT	Potential vertical heave at time t + 1 at the bottom of the foundation, ft
Δp_b	Increase in pressure at base of foundation, tsf
Δp_{st}	Increase in pressure due to the foundation and superstructure, tsf
ΔV_t	Change in specific total volume
Δw	Change in water content, percent dry weight
Θ	Volumetric water content, fraction
$\partial\Theta$	Partial derivative of volumetric water content, fraction
$\partial e/\partial t$	Partial derivative of volumetric water content with time
∂T_s	Partial derivative in surface tension of liquid water, ton/ft
∂x	Partial derivative of vertical coordinate or elevation head above a reference datum, ft
σ	Total mean normal confining pressure, tsf
σ_f	Final total mean normal confining pressure, tsf
$\bar{\sigma}_f$	Final effective mean normal confining pressure, tsf
σ_o	Initial total mean normal confining pressure, tsf
$\bar{\sigma}_o$	Initial effective mean normal confining pressure, tsf
τ	Total soil suction under surcharge pressure, tsf
τ_m	Matrix suction under surcharge pressure, tsf
τ_{mo}	Initial in situ matrix soil suction, tsf
τ_{mf}	Final (equilibrium) in situ matrix soil suction, tsf
τ_s	Osmotic suction, tsf
τ^o	Total soil suction without surcharge pressure, tsf
τ_m^o	Matrix suction without surcharge pressure, tsf

τ^{o}_{mo} Initial matrix soil suction without surcharge pressure, tsf

τ^{o}_{mf} Final (equilibrium) matrix soil suction without surcharge pressure, tsf

Φ Pore pressure potential, ft

ϕ Angle of internal friction, deg

In accordance with letter from DAEN-RDC, DAEN-ASI dated 22 July 1977, Subject: Facsimile Catalog Cards for Laboratory Technical Publications, a facsimile catalog card in Library of Congress MARC format is reproduced below.

Johnson, Lawrence D
Predicting potential heave and heave with time in swelling foundation soils / by Lawrence D. Johnson. Vicksburg, Miss. : U. S. Waterways Experiment Station ; Springfield, Va. : available from National Technical Information Service, 1978.
78, [116] p. : ill. ; 27 cm. (Technical report - U. S. Army Engineer Waterways Experiment Station ; S-78-7)
Prepared for Office, Chief of Engineers, U. S. Army, Washington, D. C.
References: p. 71-78.

1. Computer programs. 2. Heaving. 3. Permeability (Soils). 4. Soil suction. 5. Soil swelling. 6. ULTRAT (Computer program). I. United States. Army. Corps of Engineers. II. Series: United States. Waterways Experiment Station, Vicksburg, Miss. Technical report ; S-78-7.
TA7.W34 no.S-78-7